Molecular Characterization of Begomoviruses Causing Yellow Mosaic Disease in Mungbean and Disease Management Through Biotechnological Intervention

A Thesis

Submitted in partial fulfilment of the requirements for the award of the degree of

DOCTOR OF PHILOSOPHY

by

KIRAN VILAS DHOBALE

Roll no: 176106003

Department of Biosciences and Bioengineering

Indian Institute of Technology Guwahati

July 2024

DECLARATION

I do hereby declare that the matter embodied in this thesis entitled "**Molecular Characterization of Begomoviruses Causing Yellow Mosaic Disease in Mungbean and Disease Management Through Biotechnological Intervention**" is the result of work carried out in the Department of Biosciences and Bioengineering, Indian Institute of Technology Guwahati, India, under the supervision of **Prof. Lingaraj Sahoo**.

In keeping with the general practice of reporting of scientific observations, due acknowledgement has been made wherever the work described is based on the findings of other investigators.

Kiran Vilas Dhobale
Roll no. 176106003
Department of Biosciences and Bioengineering
Indian Institute of Technology Guwahati
Assam 781039, India

CERTIFICATE

It is certified that the work described in this thesis entitled "**Molecular Characterization of Begomoviruses Causing Yellow Mosaic Disease in Mungbean and Disease Management Through Biotechnological Intervention**" by Mr. Kiran Vilas Dhobale for the award of degree of Doctor of Philosophy is an authentic record of the results obtained from the research work carried out under my supervision in the Department of Biosciences and Bioengineering, Indian Institute of Technology Guwahati, India. The work embodied in this thesis has not been submitted elsewhere for a degree.

Prof. Lingaraj Sahoo
Thesis supervisor
Department of Biosciences and Bioengineering
Indian Institute of Technology Guwahati
Assam 781039, India

ACKNOWLEDGEMENT

I express my heartfelt gratitude to Prof. Lingaraj Sahoo, my thesis supervisor. His unwavering belief in my abilities and the invaluable opportunity to pursue a Ph.D. under his guidance have been pivotal in my academic journey. I consider myself fortunate to have been exposed to his wealth of knowledge, receiving guidance that extends beyond the confines of traditional academia. Working under his direction has not only enriched my understanding of our research field but has also provided diverse opportunities for interdisciplinary exploration.

I express my gratitude to my doctoral committee members, Assoc. Prof. Selvaraju Narayanasamy (Chairperson), Prof. Ajaikumar B. Kunnumakkara, and Prof. Vaibhav V. Goud, for their invaluable contributions in evaluating my research progress, providing unbiased opinions, and offering constructive suggestions.

My sincere thanks to Prof. Rakhi Chaturvedi, the Department of Biosciences and Bioengineering (BSBE), IIT Guwahati, for her support as the respected Head of the Department during my Ph.D. tenure. I am also thankful to Prof. Vishal Trivedi, Prof. Siddhartha S. Ghosh, and Prof. B. Anand for their teaching and valuable suggestions that shaped my research understanding. I extend my thanks to the BSBE Department and the Central Instrumentation Facility of IIT Guwahati for crucial research facilities and the staff for their support. Additionally, I acknowledge the financial assistance from IIT Guwahati, the Ministry of Human Resources Development, and the Department of Biotechnology, Government of India.

I express my sincere gratitude to all my lab members who played a pivotal role in boosting my confidence and providing continuous support throughout my Ph.D. journey. Special thanks to my seniors, Dr. Richa Srivastava, Dr. Muthuvel J, and Dr. Prabin Kumar Sharma, for their guidance. I am also thankful to Dr. Sanjeev Kumar for his guidance and support. I would like to acknowledge my lab mates Mahesh Das and Anurabh Chakravarty for their support and encouragement.

My gratitude extends to colleagues from the BSBE Department, Dr. Himanshu Sharma, Dr. Yoganand KNR, Dr. Sunanda Chhetry, Dr. Siddharth Nimkar, Manasasri Murlidharan, and Rohan Pal, for their continuous support and shared knowledge. Particularly, I am thankful to Pooja Rani Kuri, who has been by my side at IIT Guwahati. Her unwavering love and support during

both happy and challenging times have been invaluable, and I appreciate her encouragement throughout my journey.

I was fortunate to have a teacher like Asst. Prof. Sandip Asthana, who believed in my potential and encouraged me to pursue a Ph.D. during my master's degree. I extend my sincere gratitude to Dr. Narendra Kadoo, who provided me with an opportunity and introduced me to the world of research.

Finally, I express my heartfelt acknowledgment to my mother, Smt. Sangita Vilas Dhobale, for her unwavering support, love, encouragement, and everything she has provided. I recognize and appreciate her numerous sacrifices that have played a crucial role during my Ph.D. Additionally, I extend my gratitude to my siblings, Govinda and Mayuri, for their love and care throughout my journey.

Kiran Vilas Dhobale

TABLE OF CONTENTS

LIST OF TABLES

LIST OF FIGURES

LIST OF ABBREVIATIONS

AF -	Apoplast Fluid
AWF -	Apoplast Wash Fluid
BC1 -	Movement Protein
bp -	Base Pairs
BV1 -	Nuclear Shuttle Protein
CP -	Coat Protein
CR -	Common Region
DCL -	DICER LIKE
DiOC6 -	3,3'-Dioctadecyloxacarbocyanine Perchlorate (a fluorescent dye)
DLS -	Dynamic Light Scattering
DNA -	Deoxyribonucleic Acid
DNA-A–	Genomic component of begomovirus
DNA-B –	Genomic component of begomovirus
dpi -	Days Post-Infection / Days Post Infiltration
dsDNA -	Double-Stranded DNA
dsRNA -	Double-stranded RNA
EVs -	Extracellular Vesicles
GUs -	Genomic Units
HIGS -	Host-Induced Gene Silencing
IR -	Intergenic Region
MES -	2-(N-Morpholino) Ethanesulfonic Acid
MP -	Movement Protein
MVBs -	Multivesicular Bodies
MYMIV -	Mungbean Yellow Mosaic India Virus
MYMV -	Mungbean Yellow Mosaic Virus
NCBI -	National Center for Biotechnology Information
NMR -	Nuclear Magnetic Resonance
NSP -	Nuclear Shuttle Protein
OD600 -	Optical Density at 600 nm

ORF -	Open Reading Frame
ORI -	Origin of Replication
PCR -	Polymerase Chain Reaction
PD -	Plasmodesmata
PDA -	Percent Disease Incidence
PTGS -	Post-Transcriptional Gene Silencing
qRT-PCR -	Quantitative Real Time Polymerase Chain Reaction
RCA -	Rolling Circle Amplification
RCR -	Rolling Circle Replication
RISC -	RNA-induced silencing complex
RNA -	Ribonucleic Acid
RNA Pol II -	RNA Polymerase II
RNAi -	RNA interference
Semi qRT-PCR –	Semi Quantitative Reverse Transcription Polymerase Chain Reaction
SIGS -	Spray-Induced Gene Silencing
siRNA -	Small interfering RNA
sRNA -	Small RNA
ssDNA -	Single-Stranded DNA
SYBR Green -	Fluorescent dye used in real-time PCR
TEM -	Transmission Electron Microscope
TrAP -	Transcriptional Activator Protein
VIB -	Vesicle Isolation Buffer
VIC -	Vacuum-Infiltration-Centrifugation
YEP Medium -	Yeast Extract Peptone Medium
YMD -	Yellow Mosaic Disease
YMVs-	Yellow Mosaic Viruses

THESIS ABSTRACT

Yellow mosaic diseases (YMD), caused by Begomovirus, pose a significant threat to mungbean cultivation in the Indian subcontinent. This study investigates the epidemiology of begomovirus in three YMD hotspot regions, identifying *Mungbean Yellow Mosaic Virus* (MYMV) in Bihar and *Mungbean Yellow Mosaic India Virus* (MYMIV) in Assam and Orissa. The study explored the population structure and genetic diversity of MYMV and MYMIV isolates, revealing independent evolution of DNA-A and coevolution of DNA-B. To identify YMD-resistant mungbean genotypes, an agroinoculation-based genotype screening approach was employed. Using prepared infectious clones (MYMV and MYMIV) for screening YMD-resistant and susceptible mungbean genotypes, we identified genotypes highly susceptible to MYMV (cv. ML267) and MYMIV (cv. K851), as well as genotypes immune to MYMV (cv. PDM139, cv. SML668) and MYMIV (cv. Pusa Vishal). The study explores a non-transgenic approach for inducing resistance to YMD in mungbean. Two target regions within the viral genomes were identified for gene silencing using RNAi. We show that out of three intron hpRNAi constructs, namely hpTR-1: AC4/AC1, hpTR-2: AC2/AC3, and hpTR-1+2: AC4/AC1_AC2/AC3 (fusion construct), the hpTR-1+2 construct provided 100% protection, validated through a transient agroinfiltration assay. Subsequently, we show that in vivo synthesized hpRNA of hpTR-1+2 can persist and induce the generation of small interfering RNA (siRNA) in both local and systemic tissues for at least 12 days post-spray without viral inoculation, validated through semi-reverse transcription-PCR and northern blotting. Our data indicate that the naked hpRNA spray conferred resistance to MYMIV in mungbean, with the most significant inhibition of MYMIV replication observed when plants were treated on the same day, two days, and four days before viral inoculation. Furthermore, the study explored the role of the apoplast in Begomovirus infection. Importantly, we show the presence of genomic components of MYMIV in apoplastic fluid validated by molecular detection of viral genome through RCA and PCR analysis to enhance our understanding of the cell-to-cell movement of begomovirus via apoplast. Additionally, we have shown that virus infection induces elevated secretion of vesicles into the apoplast. NMR-based metabolomics analysis reveals altered metabolic profiles in both apoplast and symplast in response to MYMIV infection. Citrate downregulation and increased levels of valine, α-β-glucose, and pipecolic acid were observed in both compartments. Phenolic metabolites were absent in the apoplast and downregulated in the symplast, while proline exhibited contrasting levels in MYMIV-infected samples. Additionally, heightened aspartate levels were confined to the symplast. These findings provide insights into metabolites associated with stress and defense mechanisms triggered by MYMIV infection. In conclusion, our findings may help prevent an epidemic of YMD in *Vigna* species, and the study may contribute to enhancing disease management strategies in mungbean cultivation.

Chapter 1: Thesis Introduction

1.1 General Introduction

Mungbean (*Vigna radiata* L. Wilczek) is an important grain legume in Southeast Asia, ranking next to chickpea (*Cicer arietinum* L.), and pigeonpea [*Cqjanus cajan* (L.) Millsp.]. Mungbean serves as a cheap source of dietary protein for impoverished populations in developing countries (1). The seeds contain 24% protein, low flatulence factors, and high iron content (40–70 ppm), becoming the choice for source of balanced diets (2). Mungbean sprouts are highly valued in Asian cuisine due to their high vitamin C and folate content. The association of mungbean roots with *Rhizobium* sp. and *Bradyrhizobium* sp. bacteria enhances soil fertility through atmospheric nitrogen fixation, benefiting subsequent crops (1). Mungbean is primarily cultivated in tropical and sub-tropical regions, covering 7.3 million hectares globally, with an average yield of 721 kg/ha. India and Myanmar together contribute 30% to the global production (3). Within India, the states of Rajasthan and Maharashtra are the highest producers of mungbean. However, India's average mungbean productivity is very low, approximately 570 kg/ha, significantly lagging behind other pulse crops (3).

One of the significant challenges faced by mungbean cultivation is the yellow mosaic disease (YMD) caused by yellow mosaic viruses (YMVs) (4). The yield loss due to YMD in mungbean can go up from 10 to 100%, depending on the mungbean cultivar and the stage of infection. YMD has been reported worldwide, with heavy incidence primarily in countries like India, Bangladesh, and Pakistan. The disease is transmitted by the whitefly (*Bemisia tabaci* Gennadius) (5). Mungbean plants infected with YMD generally show yellowing or chlorosis of leaves followed by necrosis, shortening of internodes, and severe stunting of plants with no yield or few flowers and deformed pods produced with small, immature and shriveled seeds.

The YMVs belong to the genus *Begomovirus*, the largest genus within the family *Geminiviridae*, characterized by twinned quasi-icosahedral particles (6). The genome structure comprises bipartite (DNA-A and DNA-B) or monopartite configurations, with each circular single-stranded DNA (ssDNA) component around 2.7 kb. Additionally, some begomoviruses are associated with circular DNA satellites: betasatellites, alphasatellites, and deltasatellites (7). Begomovirus proteins play multifunctional roles crucial for disease development (6). DNA-A features six open reading frames (ORFs): two in the virion sense, where AV1 and AV2 encode capsid protein (CP) and pre-coat protein, respectively, and four in the complementary sense. AC1, AC2, and AC3 serve as replication initiator protein (Rep), transcription activator protein (TrAP), and replication enhancer protein (REn), respectively. AC4-encoded protein is essential for symptom production. DNA-B carries BC1 and BV1 ORFs, functioning as movement protein (MP) and nuclear shuttle protein (NSP), respectively.

Begomoviruses comprise nearly 450 species, infecting various economically important dicot crops. In pulses, YMD is caused by four distinct bipartite begomoviruses: Mungbean Yellow Mosaic Virus (MYMV), Mungbean Yellow Mosaic India Virus (MYMIV), Dolichos Yellow Mosaic Virus (DoYMV), and Horsegram Yellow Mosaic Virus (HgYMV), collectively known as YMVs. These viruses collectively contribute to significant challenges in mungbean cultivation (8). Legume-infecting begomoviruses, predominantly MYMIV and MYMV in India, exhibit a narrow but distinct and overlapping host range. MYMIV is more prevalent in northern, central, and eastern regions, while MYMV commonly occurs in southern and western India. However, recent reports

indicate the occurrence of MYMIV in south India and MYMV in north India. Horsegram yellow mosaic virus (HgYMV) has been reported to cause YMD in *Vigna* crops, including mungbean, in the Indian subcontinent (9).

YMD management employs pre-planting (cultivar selection, virus-free materials), in-season (vector management, roguing, biological control), and post-harvest (sanitation, host-free periods) strategies. Developing and utilizing YMD-resistant mungbean varieties is the most sustainable approach for disease management (10). However, progress in breeding for YMD resistance is hindered by challenges in identifying resistant and susceptible varieties under natural field conditions. The major limitation in hotspot screening is the influence of weather parameters on whitefly activity, impacting YMD outbreaks in open-field conditions. Variation in whitefly populations can lead to non-uniform disease development, and the efficacy of transmission depends on various factors. Using viruliferous whiteflies for screening genotypes is advantageous, although there is a lack of correlation between whitefly populations and disease severity. Since YMD transmission in legumes occurs only through the vector whitefly, agroinoculation-based genotype screening is considered advantageous for identifying YMD-resistant genotypes, creating uniform disease symptoms under controlled conditions. Therefore, agroinoculation-based screening, validated by molecular diagnosis, offer efficient identification of YMD-resistant mungbean genotypes independent of whiteflies (11–13). Numerous studies have employed agroinoculation to screen susceptible or resistant mungbean varieties (12–14).

Among various management strategies deployed, RNA interference (RNAi) stands out as a highly effective strategy for developing durable resistance against viral diseases in plant (15). Plants use post-transcriptional gene silencing (PTGS) to degrade viral RNA through small interfering RNA (siRNA) produced from double-stranded RNA (dsRNA). This siRNA, guided by argonaute (AGO) proteins, leads to RNA degradation, providing viral resistance. RNAi has been harnessed for transgenic resistance, but challenges like GMO concerns and regulatory issues exist. In India, only Bt cotton is approved for cultivation among GM crops, while others like chickpea, pigeonpea, corn, and sugarcane are undergoing research and field trials (Ministry of Environment, Forest and Climate Change, 2019). An alternative, non-GMO approach involves applying external double-stranded RNA (dsRNA), demonstrating efficacy against various plant viruses (16), including geminiviruses like MYMV. This approach offers a promising, efficient, and socially acceptable method for viral disease management (17).

Begomoviruses, functioning as intracellular parasitic pathogens, utilize a symplastic route via plasmodesmata for cell-to-cell movement (18). RNA viruses like turnip mosaic virus associate their RNA genome and proteins with multi-vesicular bodies (MVBs), releasing them into the leaf apoplast (19). In the case of potato virus X-infected plants, virus particles and RNAs are detected in the apoplast, although they are not associated with extracellular vesicles (EVs) (20). The presence of viral proteins, RNA, and virus particles in the plant apoplast highlights its crucial role in viral infection, particularly in the systemic spread of the virus within the host. However, the role of the apoplast and EVs in the cell-to-cell genome transmission in begomoviruses, is still not known.

The study aims to identify begomovirus species affecting mungbean in three YMD hotspots across India. The study involves screening of mungbean cultivars for YMD resistance through the agroinoculation method. The study assesses the effectiveness of exogenous dsRNA in controlling YMD in mungbean, exploring a non-transgenic approach. Further study is conducted to understand the role of the mungbean leaf apoplastic space in the cell-to-cell movement and infectivity of MYMIV.

1.2 Objectives and Thesis Outline

1.2.1 Thesis Objectives

- To detect and characterize YMVs infecting mungbean across diverse YMD hotspots in India.
- Screening of mungbean cultivars for YMD resistance through the agroinoculation method.
- To assess the effectiveness of exogenous dsRNA in controlling YMD in mungbean through a non-transgenic approach.
- To investigate the role of the mungbean leaf apoplastic space in the cell-to-cell movement and infectivity of MYMIV.

1.2.2 Thesis Outline

Chapter 1: Chapter 1 of the thesis reviews the DNA viruses of plants and particularly of geminiviruses. The evolutionary aspects of geminiviruses are highlighted, with a focus on the emergence of begomoviruses as highly destructive pathogens causing YMD in legume crops. The chapter further emphasizes the significance of the mungbean crop, providing insights into its distribution and the overall yield loss due to diseases, particularly YMD. Various techniques for the detection and diagnosis of begomoviruses are discussed, and the chapter concludes with an extensive exploration of YMD management strategies, giving special attention to the role of RNAi in disease control.

Chapter 2: In this chapter, we describe screening of YMVs affected mungbean through the molecular detection of viral genome, in three states (Bihar, Assam, and Orissa) of India. Subsequently, we study the sequence variability, phylogenetic relationships, recombination events, and population structure to enhance our understanding of the genetic distinctiveness of the identified YMVs mungbean isolates. We prepare agroinfectious constructs and screened a few mungbean cultivars for their response to YMVs infection by symptom analysis and molecular detection of viral genome through RCA and qRT-PCR analysis.

Chapter 3: In this chapter, we explore a non-transgenic approach for inducing resistance to YMD in mungbean. The study is based on the identification of viral target regions for gene silencing using RNAi. We evaluate their efficacy through transient expression analysis to pinpoint highly efficient target regions. Using these targets, we assess the effectiveness of exogenous dsRNA in controlling YMD in mungbean.

Chapter 4: In this chapter, we investigate the role of the apoplast in begomovirus infection. We study presence of MYMIV in apoplastic fluid by molecular detection of viral genome through RCA and PCR analysis to enhance our understanding of the cell-to-cell movement of begomovirus via apoplast. Further we investigate apoplastic and symplastic metabolites related to stress and defense in response to MYMIV infection using NMR-based metabolomics.

The conclusions drawn from the above-mentioned objectives and future perspectives of the work are discussed in the concluding section.

1.3 Review of Literature

1.3.1 Introduction

Multipartite DNA plant viruses, characterized by segmented, single-stranded DNA (ssDNA) genomes, pose a substantial threat to diverse agricultural crops, causing significant economic damage and raising food security concerns. These viruses exhibit an unconventional architecture, with their genomes divided into two or more distinct components, individually packaged into separate viral particles during transmission (21). This unique structure provides evolutionary advantages, enabling rapid adaptation, genome reassortment, and dynamic changes in gene copy numbers (22,23). Notable families with multipartite DNA genomes include *Geminiviridae* and *Nanoviridae*. Geminiviruses, characterized by circular ssDNA segments, have led to substantial economic losses globally, as witnessed in devastating outbreaks affecting tomato crops in India and the Dominican Republic, resulting in total yield losses (24). Similarly, geminivirus infections have inflicted a staggering $2 billion blow to African cassava production (25). These examples underscore the urgency of unraveling factors impacting geminivirus evolution, transmission, pathogenesis, detection, and management strategies (10,26,27).

This review provides a brief exploration of the evolutionary history and genomic organization of geminiviruses, with a specific focus on the *Begomovirus* genus, the largest within the virosphere. Begomoviruses are recognized for inducing severe symptoms associated with YMD in various plants. The impact of Begomoviruses extends globally, causing substantial losses in open-field vegetable, root, and fiber crops in tropical and subtropical regions, as well as greenhouse production systems (25,28–30). Within this context, the review delves into the nutritional values, economic importance, and geographic distributions of mungbean, a crucial leguminous crop. Furthermore, the review explores YMD detection and diagnosis methods, providing insights into technological approaches used to identify this viral disease. Finally, it addresses YMD management strategies, including innovative gene silencing-based approaches that show promise in reshaping disease control methodologies. This concise overview aims to contribute to the scientific understanding of geminiviruses, emphasizing the pivotal role of Begomoviruses, economic implications for mungbean cultivation, advancements in disease detection, and innovative strategies for disease management within the context of YMD.

1.3.2 Geminivirus Evolution and Diversity

A distinctive class of viruses known as multipartite viruses, a term introduced in the 1960s and alternatively referred to as coviruses, multicomponent, multiparticle, or multicompartment viruses in the literature (31). Multipartitism is prevalent, especially in plant viruses, accounting for 30–40% of plant virus genera and families (23). Viral genomes can be categorized into three primary configurations: non-segmented, segmented, and multipartite (32). Unlike non-segmented and segmented viruses, which encapsulate all genetic material required for completing the viral life cycle within a single viral particle, multipartite viruses possess segmented genomes distributed among two or more viral particles, necessitating co-infection for survival (33–36). The enigma surrounding multipartite viruses extends to a multitude of unanswered questions, with the overarching puzzle being why multipartite viruses exist in the first place (33). Despite their

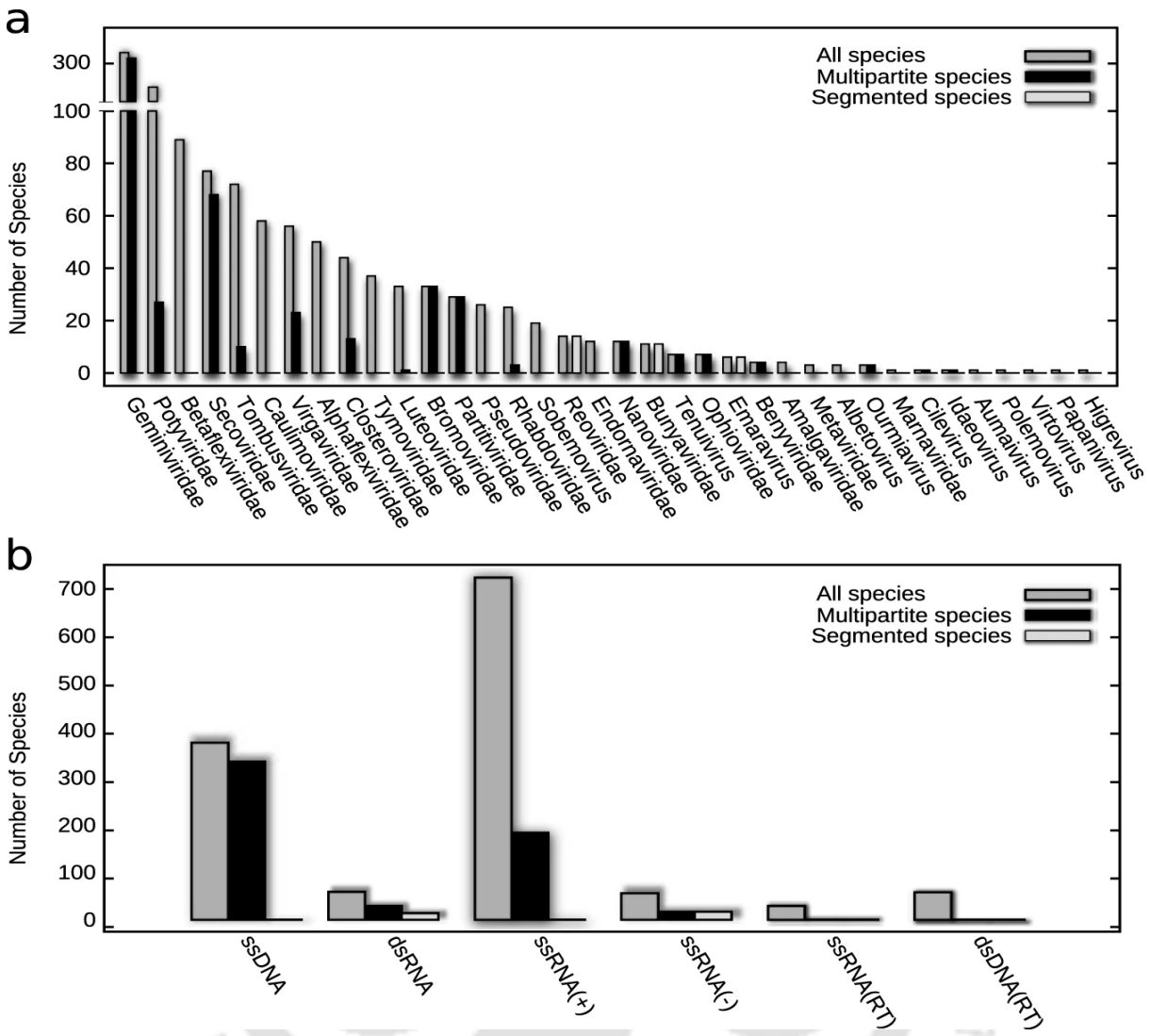

Figure 1 Histogram of the number of plant virus species.
a) per viral family and **b)** per genome type. (Image taken from Lucía-Sanz & Manrubia, 2017).

predominant association with plants, multipartitism has emerged recurrently in evolutionary history (37). Far from being incidental or a frozen evolutionary anomaly, multipartitism is presumed to represent a stable and intentional evolutionary strategy (21). However, the exact mechanisms conferring adaptive advantages to multipartite viruses, which ostensibly offset their seemingly unconventional and resource-intensive lifestyle, remain elusive. While bipartite or segmented viruses may emerge from monopartite viruses, both rarely originate from the same virus (38,39). However, there has been a recent resurgence of interest in this class of viruses, as evidenced by several recent reviews (22,23,32,34,40). Amongst crucial plant viruses, the *Geminiviridae* family stands out for hosting the highest number of multipartite viral species which underscores its significance (Figure 1).

Single-stranded DNA (ssDNA) viruses exhibit high diversity and abundance across various environments (41–43). Presently, they are categorized into four prokaryotic virus families and nine eukaryotic virus families including *Geminiviridae*. Most ssDNA viruses possess small circular genomes that replicate through the rolling circle mechanism (44,45). Those with circular genomes

Figure 2 Genomic organization of geminiviruses.
The long intergenic region (LIR), short intergenic region (SIR), common region (CR), capsid protein (cp), movement protein (mp), nuclear shuttle protein (nsp), regulatory gene (reg), replication enhancer (ren), replication-associated protein (rep), symptom determinant (sd), silencing suppressor (ss), and trans-activator protein (trap). (Source: Roumagnac et al., 2022).

encoding a replication initiator protein (Rep), found in families like *Bacilladnaviridae, Circoviridae, Geminiviridae, Genomoviridae, Inoviridae, Microviridae, Nanoviridae, Pleolipoviridae, Smacoviridae*, and several unclassified viruses, are collectively termed circular Rep-encoding single-strand (CRESS)-DNA viruses (46,47). The Reps of CRESS-DNA viruses are closely related to those of small, rolling circle-replicating bacterial plasmids, suggesting evolution from plasmids on multiple independent occasions (48).

The International Code of Virus Classification and Nomenclature (ICVCN) provisionally proposes six taxa, including *Shotokuvirae*, a member of the kingdom *Shotokuvirae* defined by encoding a Rep protein with a characteristic N-terminal endonuclease domain and a C-terminal superfamily 3 helicase domain (6). The name "Shotokuvirae" is derived from Japanese Empress Shōtoku, this choice is in recognition of her composition of a poem describing a plant disease, likely caused by a geminivirus. This poem stands as one of the earliest written records of a plant virus disease and a disease caused by a CRESS-DNA virus (49). The suffix "*-virae*" for kingdom taxa. Geminiviruses, belonging to the family *Geminiviridae* within the *Shotokuvirae* kingdom, are a family of small, non-enveloped viruses characterized by genomes consisting of one or two circular ssDNA ranging from 2.5 to 5.2 kb (Figure 2) (6). These viruses infect a broad spectrum of plant species (50,51) and are transmitted by various insects from four homopteran families, including whiteflies, leafhoppers, aphids, and treehoppers (52).

1.3.2.1 Geminivirus: Taxonomy and Genomic Organization

The International Committee on Taxonomy of Viruses (ICTV) currently recognizes more than 500 species of geminiviruses, establishing them as the largest and one of the most diverse virus families (6). Presently, within the family *Geminiviridae*, 14 distinct genera are acknowledged, namely *Becurtovirus, Begomovirus, Capulavirus, Citlodavirus, Curtovirus, Eragrovirus, Grablovirus, Maldovirus, Mastrevirus, Mulcrilevirus, Opunvirus, Topilevirus, Topocuvirus,* and *Turncurtovirus*, each distinguished by insect vectors, host range, genome structure, and phylogeny (6) (Figure 2). The familial relationships within the *Geminiviridae* family are elucidated through phylogenetic analysis of complete genome sequences (Figure 3). The comprehensive analysis reveals distinct clustering patterns, forming cohesive groups corresponding to the 14 genera within the *Geminiviridae* family.

***Becurtovirus*:** The *Becurtovirus* genus, consisting of three species—*Beet curly top Iran virus*, *Exomis microphylla latent virus*, and *Spinach curly top Arizona virus*—is characterized by monopartite viruses infecting dicot plants. Notably, they exhibit a unique 5′-TAAGATTCC-3′ nonanucleotide at the origin of virion strand replication, setting them apart from other geminiviruses (53).

Begomovirus: Taxonomic lineage of this genus is: Viruses > Monodnaviria > Shotokuvirae > Cressdnaviricota > Repensiviricetes > Geplafuvirales > Geminiviridae > Begomovirus > species (Example: *Mungbean yellow mosaic virus*). With 445 distinct species, this genus stands as the largest within the entire virosphere (Figure 4) (6). New World (NW) begomoviruses possess bipartite genomes, while Old World (OW) begomoviruses can exhibit both monopartite and bipartite genome configurations (54). The genome structure varies, existing as either bipartite

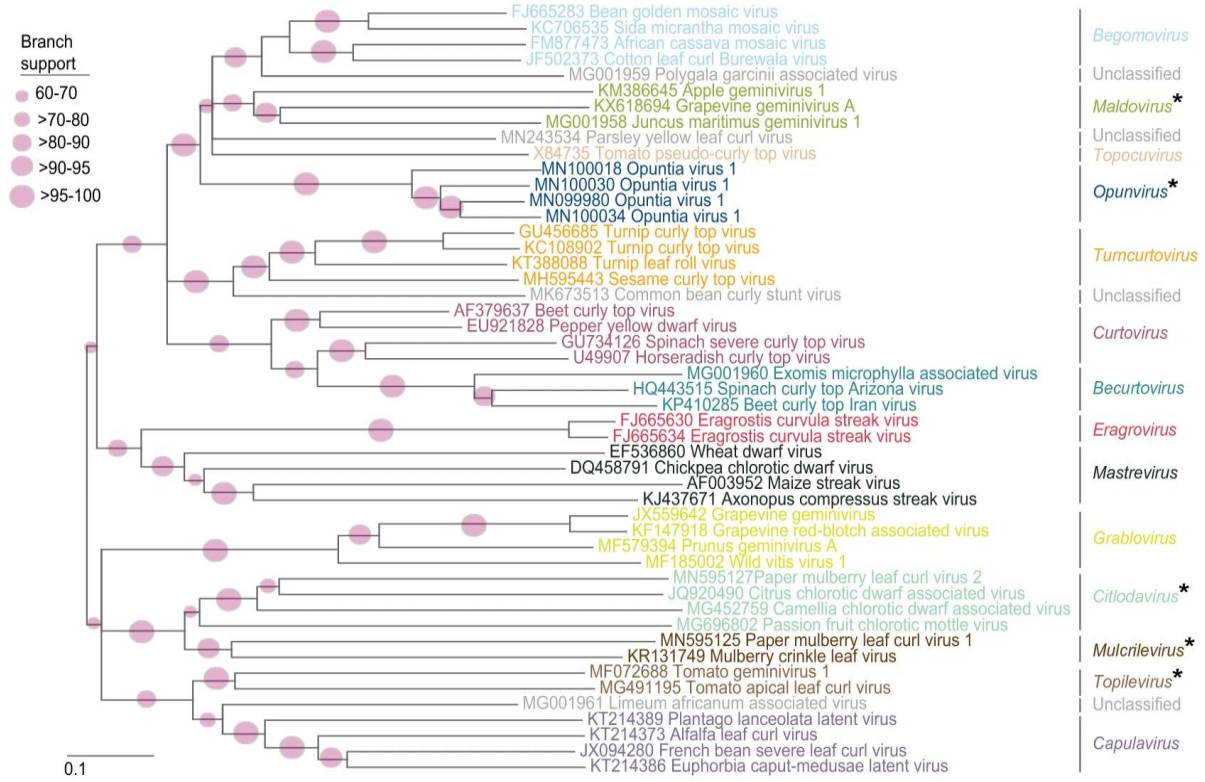

Figure 3 Phylogenetic analysis of fourteen genera in the family Geminiviridae.
Unrooted neighbor-joining tree inferred from aligned complete genome sequences of representative isolates from the various geminivirus genera. The five new genera are indicated by asterisks. Branches with less than 60% bootstrap support have been collapsed with TreeGraph2. (Image taken from Roumagnac et al., 2022).

(consisting of two circular ssDNA molecules, DNA-A and DNA-B, each of 2.5–2.7 kb) or monopartite (a single circular ssDNA molecule around 2.7 kb) configurations. The genomes of monopartite begomoviruses exhibit a resemblance to the DNA-A component of bipartite. *Chilli leaf curl virus* (ChiLCV) is an example of a monopartite begomovirus, while *Pepper golden mosaic virus* (PepGMV), MYMV, MYMIV, and *Pepper huasteco yellow vein virus* (PHYVV) are notable examples of bipartite.

Furthermore, previous studies documented begomoviruses are associated with three classes of circular DNA satellites: betasatellites, alphasatellites, and deltasatellites (55–57). Begomovirus infects dicot plants and weeds and is transmitted by whiteflies belonging to the *Bemisia tabaci* cryptic species complex (58). Begomoviruses commonly elicit severe symptoms in vast number of plants, such as mosaics, mottles, yellowing, leaf curling, deformation, reduced plant growth, and a decreased number of fruits (25). The impact of these viruses is substantial, often leading to a total loss of production, particularly affecting open-field vegetable, weeds, root, and fiber crops in tropical and subtropical regions, as well as greenhouse production systems (29,59,60). Among the devastating pathogens within this genus are the *African cassava mosaic virus*, *Bean golden mosaic virus*, *Cotton leaf curl Multan virus*, MYMV, and *Tomato yellow leaf curl virus*. Remarkably, research on the tomato yellow leaf curl virus has shown that its replication extends beyond host plants, occurring in the salivary glands of the insect vector (Figure 5) (61).

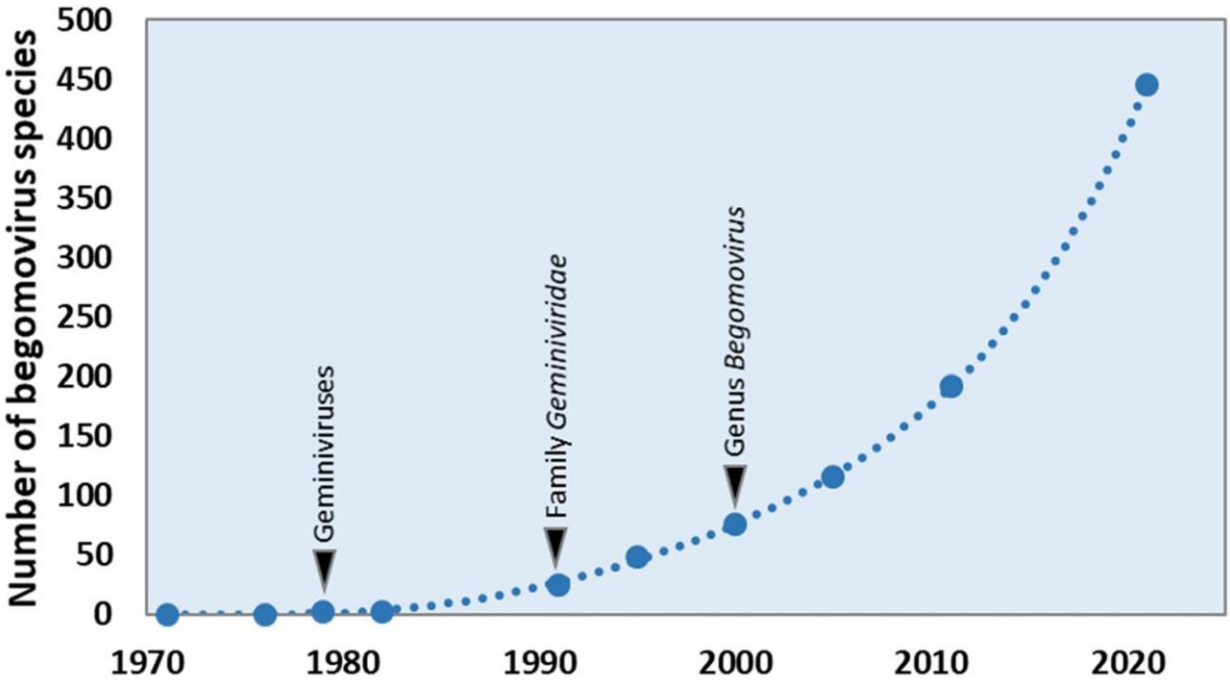

Figure 4 The evolution of the number of officially accepted begomovirus species by the ICTV. Blue circles represent the count of species documented in the ICTV Reports on Virus Taxonomy (1st to 10th). Arrowheads denote significant milestones, including the introduction of 'geminiviruses' in the 3rd report, the recognition of the family Geminiviridae in the 5th report, and the acknowledgment of the genus Begomovirus in the 7th report. (Image taken from Fiallo-Olivé & Navas-Castillo, 2023).

Primarily, this genus is responsible for inducing economically significant diseases in numerous crucial crops, forming the central focus of this study (25,28,62,63).

Capulavirus: It includes four species: *Alfalfa leaf curl virus*, *Euphorbia caput-medusae latent virus*, *French bean severe leaf curl virus* and *Plantago lanceolata latent virus*. Three of these species are transmitted by aphids. Capulavirus genomes exhibit a unique arrangement of movement protein-encoding ORFs and have a monopartite structure with the 5′-TAATATTAC-3′ nonanucleotide at the v-ori (64).

Citlodavirus: This genus comprises four species: *Camellia chlorotic dwarf-associated virus*, *Citrus chlorotic dwarf associated virus*, *Paper mulberry leaf curl virus 2*, and *Passion fruit chlorotic mottle virus*. These viruses have been identified in symptomatic dicot host plants, including trees and shrubs. Citlodaviruses have monopartite genomes with the 5′-TAATATTAC-3′ nonanucleotide at the v-ori (65).

Curtovirus: This genus encompasses three acknowledged species: *Beet curly top virus*, *Horseradish curly top virus*, and *Spinach severe curly top virus*. These viruses infect dicot plants and are transmitted by leafhoppers. Beet curly top virus, a well-studied member of this genus, is an economically significant pathogen in North America and Iran, exhibiting a broad host range (66).

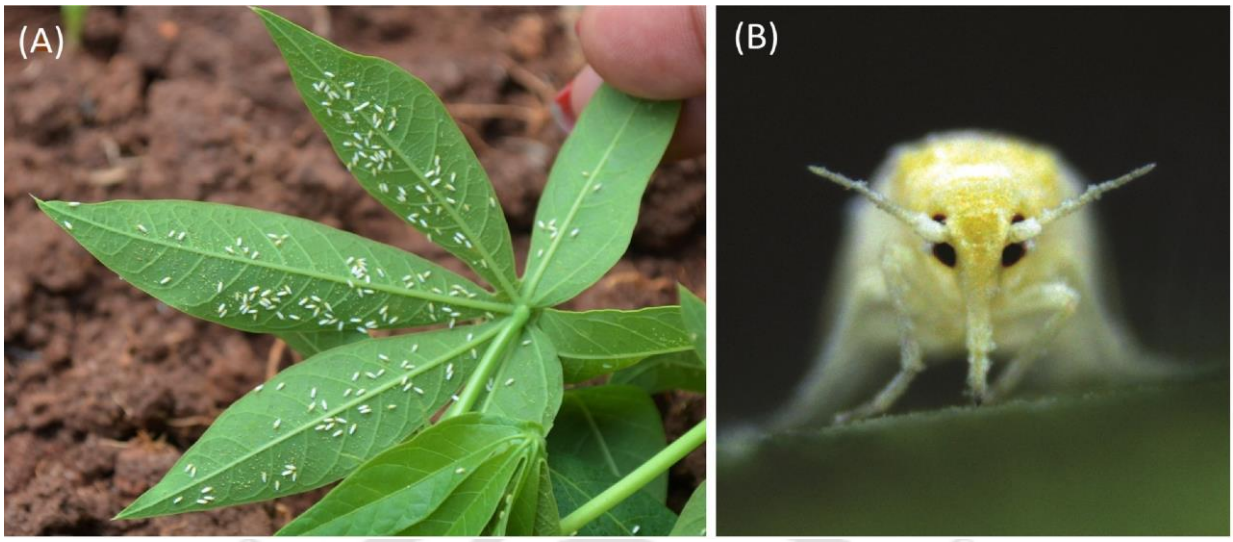

Figure 5 *Bemisia tabaci* sensu lato.
(A) Depiction of *Bemisia tabaci* adults on the underside of a cassava leaf. **(B)** Close-up view of a *B. tabaci* adult engaged in feeding on a tobacco leaf. (Image taken from Fiallo-Olivé & Navas-Castillo, 2023).

Eragrovirus: This genus comprises the single species, *Eragrostis curvula streak virus*, with monopartite genomes. Isolates of this virus exclusively infect the monocot plant *Eragrostis curvula* in the Kwa-Zulu Natal region of South Africa. Similar to becurtoviruses, eragroviruses feature a 5′-TAAGATTCC-3′ nonanucleotide sequence at the v-ori (53).

Grablovirus: This genus, consisting of *Grapevine red blotch virus*, *Prunus latent virus*, and *Wild Vitis latent virus*, is transmitted by a treehopper and primarily infects dicot plants (64).

Maldovirus: This genus, including *Apple geminivirus 1*, *Grapevine geminivirus A*, and *Juncus maritimus geminivirus 1*, is known to infect both dicot (e.g., apple, grapevine) and monocot (e.g., *Juncus maritimus*) plants. All maldovirus genomes share the conserved origin of replication (5′-TAATATTAC-3′) found in most geminiviruses (65).

Mastrevirus: This genus with monopartite genomes, primarily infect monocots, and are transmitted by leafhoppers (67). Notable species include *Maize streak virus* cause severe maize disease in Africa (68) and *Wheat dwarf virus* cause disease in wheat (69). *Wheat dwarf India virus* associates with alphasatellites and betasatellites (70).

Mulcrilevirus: This genus comprises two species: *Mulberry crinkle leaf virus* and *Paper mulberry leaf curl virus 1*. These viruses have monopartite genomes with a conserved origin of replication (5′-TAATATTAC-3′). Mulcrileviruses are associated with symptomatic plants (*Morus alba or Broussonetia papyrifera*) in China, and one isolate, mulberry crinkle leaf virus, is transmitted by the leafhopper *Tautoneura mori* (65).

Opunvirus: This genus is represented by a single member, *Opuntia virus 1*, described from asymptomatic New World Cactaceae plants (involving 20 different cactus species from the subfamilies *Cactoideae* and *Opuntioideae*) and cactus-feeding cochineal insects (*Dactylopius* sp.).

Genomes of Opuntia virus 1 are monopartite and feature the conserved geminivirus nonanucleotide (5′-TAATATTAC-3′) (65).

Topilevirus: It comprises two species, *Tomato apical leaf curl virus* and *Tomato geminivirus 1*. These species feature monopartite genomes with the conserved geminivirus nonanucleotide (5′-TAATATTAC-3′). Both viruses exhibit infection in the common host plant, tomato, and Tomato geminivirus 1 has additionally been identified in *Cleome* sp. plants (65).

Topocuvirus: *Tomato pseudo-curly top virus*, a lone species within its genus, is transmitted by a treehopper (71). The virus genome exhibits similarities with that of curtoviruses.

Turncurtovirus: This genus comprises three species: *Turnip curly top virus*, *Turnip leaf roll virus*, and *Sesame curly top virus*. All members exhibit a monopartite genome. Isolates of turnip curly top virus and turnip leaf roll virus have been exclusively identified in Iran, with transmission facilitated by the leafhopper *Circulifer haematoceps*. Sesame curly top virus isolates have been detected in sesame (*Sesamum indicum*) in Pakistan and Iran, with the leafhopper *Circulifer haematoceps* serving as a vector in Iranian sesame plants (53).

1.3.2.2 Geminivirus Virion

Virions from the *Geminiviridae* family, characterized by their distinctive twinned or "geminate" structure, exhibit varying morphologies across genera (Figure 6). For instance, the *Maize streak virus* (MSV) within the *Mastrevirus* genus displays virions with dimensions of approximately 22×38 nm, composed of two incomplete icosahedra (T=1) and organized into 22 pentameric capsomers, totaling 110 coat protein subunits (72). Meanwhile, the *Ageratum yellow vein virus* (AYVV) from the *Begomovirus* genus presents unique structural features. The virion structure of *African cassava mosaic virus* (ACMV) was resolved at 4.2 Å resolution using electron cryo-microscopy and image processing (73). At a resolution of 3.3 Å, the N-terminus of its single coat protein adopts three conformations crucial for building the interface between geminate halves (74). *Tobacco curly shoot virus* (TbCSV) particle structure, resolved at 3.57 Å using single-particle cryo-electron microscopy, confirms the geminate architecture with single-strand DNA binding to each coat protein (CP) (75). Virions physicochemical and physical properties include a sedimentation coefficient (S20, w) of approximately 70S (76). Twinned virions encapsulate a singular circular single-stranded DNA (ssDNA) copy, ranging from 2.5 to 3.2 kb. In the case of viruses with bipartite genomes, infection necessitates two virions, each containing different genomic components, resulting in a cumulative genome size of about 5.2 kb (77). Furthermore, half-size defective components and ssDNA satellites may also be encapsidated in these virions (7). The proteinaceous composition of virions is notably minimal, with a single structural protein, the coat protein (CP), having a molecular weight of about 28–34×10^3. No other associated proteins have been discerned within the virion structure (76).

1.3.3 Begomovirus

1.3.3.1 Gene Functions

As obligate parasites, begomoviruses rely entirely on host cellular machinery to establish successful pathogenesis. These viruses encode a limited set of multifunctional proteins capable of

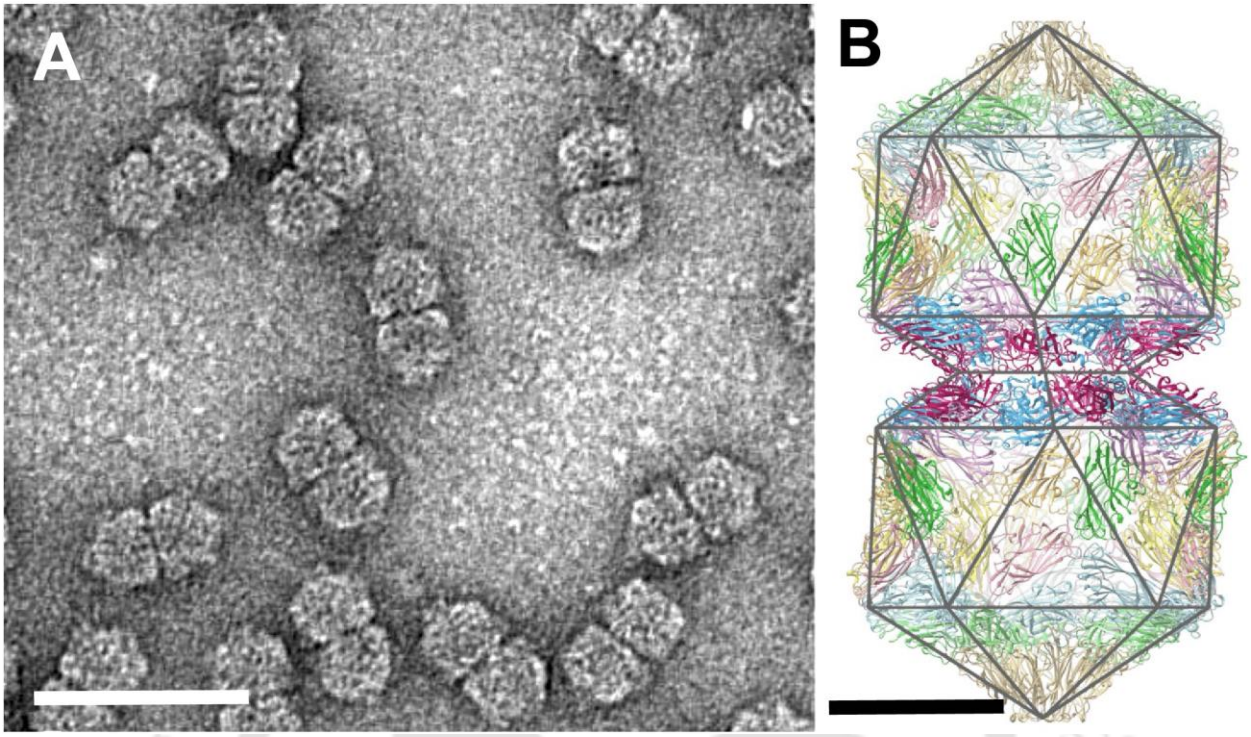

Figure 6 Geminivirus structure.

effectively modulating the expression profiles of numerous host factors (78). Through interactions with these factors, these proteins mediate various aspects of the viral life cycle, including replication, transcription, and movement. The hijacking of host factors plays a crucial role in rewiring the host cellular environment, ultimately subverting host antiviral defenses. The multifunctional roles executed by the proteins encoded in the open reading frames (ORFs) of begomoviruses are pivotal for the development of disease.

The transcription of geminivirus DNA occurs bidirectionally from promoters located within the Intergenic Region (IR), orchestrated by RNA Pol II. The IR houses divergent promoters for early and late genes. In the case of begomoviruses, the DNA-A features six ORFs, encompassing two in the virion sense (AV1 and AV2) and four in the complementary sense (AC1, AC2, AC3, and AC4) (Figure 2). DNA-B comprises two ORFs, the virion-sense BV1 and complementary-sense BC1 (Figure 2). The presence of the AV2 ORF is a distinctive trait of Old World bipartite begomoviruses, while it is absent in New World viruses. The AV1 and AV2 ORFs encode the capsid protein (CP) and pre-coat protein, respectively (76,79).

Meanwhile, AC1, AC2, and AC3 serve as the replication initiator protein (Rep) (80–87), transcription activator protein (TrAP) (88–94), and replication enhancer protein (REn) (95–98), respectively. The AC4-encoded protein is essential for symptom production (99,100). On the other hand, the DNA-B molecule carries the BC1 and BV1 ORFs, functioning as the movement protein (MP) (101–103) and nuclear shuttle protein (NSP) (104–107), respectively. Monopartite begomoviruses' ORFs consist of the virion-sense V1 and V2 genes, along with the complementary-sense C1, C2, C3, and C4 genes (Figure 2**)**. The comprehensive details of ORFs and their respective functions is outlined in (Table 1) (78).

Table 1 Begomovirus ORFs functions.

Protein Names	Function	Reference
Replication-associated protein; AC1, AL1	Essential for the replication of viral single-stranded DNA (ssDNA), Rep plays a crucial role in converting the closed circular ssDNA genome into superhelical double-stranded DNA (dsDNA). By binding to a specific region at the genome origin of replication, Rep introduces an endonucleolytic nick within the conserved sequence 5'-TAATATTAC-3' in the intergenic region shared by all geminiviruses. This action initiates rolling circle replication (RCR). Following cleavage, Rep binds covalently to the 5'-phosphate of DNA in the form of a tyrosyl ester. The cleavage event produces a free 3'-OH, serving as a primer for cellular DNA polymerase. The polymerase then synthesizes the positive strand DNA through the rolling circle mechanism. Upon completion of one replication round, Rep catalyzes a nucleotidyl transfer reaction, releasing a circular single-stranded virus genome and thereby terminating the replication process. Notably, Rep exhibits activities such as origin-specific DNA cleavage, nucleotidyl transferase, ATPase, and helicase.	Akbar Behjatnia, 1998; Bagewadi et al., 2004; Castillo et al., 2003; Fontes et al., 1994; Horváth et al., 1998; Ilyina & Koonin, 1992; Kong, 2000; Koonin & Ilyina, 1992; Kushwaha et al., 2017; Luque et al., 2002; Sánchez-Durán et al., 2011; Steinfeldt et al., 2006; Wawrzyniak et al., 2017; Wu et al., 2021; L. Zhao et al., 2019.
Transcriptional activator protein; AC2, AL2	Strong activator of the late viral genes' promoters. Enhances the expression of the capsid protein and nuclear shuttle protein. Acts as a suppressor of RNA-mediated gene silencing, also known as post-transcriptional gene silencing (PTGS). Suppresses the host RNA silencing by inhibiting adenosine kinase 2 (ADK2), a kinase involved in a general methylation pathway. Also suppresses the host basal defense by interacting with and inhibiting SNF1 kinase, a key regulator of cell metabolism implicated in innate antiviral defense. Determines pathogenicity (By similarity)	Babu et al., 2018; Castillo-González et al., 2015; Guerrero et al., 2020; L. Liu et al., 2014; Lozano-Duran & Bejarano, 2011; Rajeswaran et al., 2007; Sun et al., 2020
Capsid protein; AR1, AV1	Encapsidates the viral DNA into characteristic twinned ('geminate') particles. Binds the genomic viral ssDNA and shuttles it into and out of the cell nucleus. The CP of bipartite geminiviruses is not required for cell-to-cell or systemic movement.	Oda et al., 2000; B. V. V. Prasad & Schmid, 2012; B. V Prasad et al., 1999; Rojas et al., 1998; Liu et al., 2001
Protein AC4; AC4, AL4	Symptom development, cell cycle regulation, suppression of RNA silencing, disruption of host disease resistance signaling, virus movement in infected cells, and viral DNA accumulation.	K. Chen et al., 2019; Fondong, 2019, 2022; Jupin et al., 1994; H. Li et al., 2018; Mei et al., 2023
Replication enhancer protein; AC3, AL3	Increases viral DNA accumulation. Enhances infectivity and symptom expression.	Pasumarthy et al., 2011; Pedersen & Hanley-Bowdoin, 1994; Settlage et al., 1996; Wijaya et al., 2023
Movement protein BC1; BC1, BL1	Transports viral genome to neighboring plant cells directly through plasmosdesmata, without any budding. The movement protein allows efficient cell to cell propagation, by bypassing the host cell wall barrier. Begomovirus genome is shuttled out of nucleus by nuclear shuttle protein (NSP) and the movement protein transports the DNA-NSP complex to cell plasmodesmata and facilitates further movement across the cell wall.	Aberle et al., 2002; Frischmuth et al., 2004, 2007a; Kleinow et al., 2008; Padidam et al., 1996; Qin et al., 1998; Rojas et al., 1998b, 2001a; S. C. Zhang et al., 2001, 2002

Nuclear shuttle protein; BR1, BV1	Binds to the genomic viral ssDNA, shuttles it into and out of the cell nucleus. Begomoviruses use 2 proteins to transport their DNA from cell to cell. The nuclear shuttle protein (NSP) shuttles it between nucleus and cytoplasm and the movement protein (MP) probably transports the DNA-NSP complex to the cell periphery and facilitates movement across the cell wall.	Florentino et al., 2006; E. P. B. Fontes et al., 2004; Frischmuth et al., 2007; Happle et al., 2021; Mariano et al., 2004; Martins et al., 2020; Sanderfoot et al., 1996; Yu et al., 2019; Y. Zhou et al., 2011

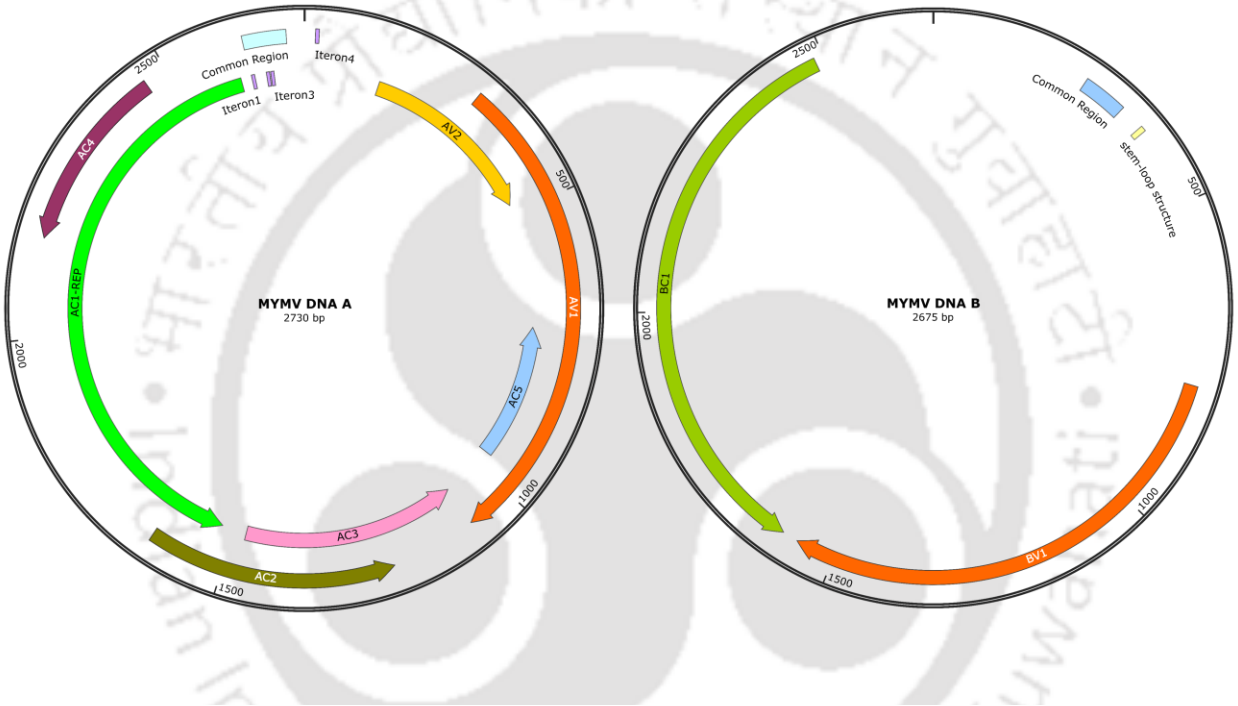

Figure 7 Genomic organization of bipartite begomoviruses.
A representative schematic of *Mungbean yellow mosaic virus* (MYMV) DNA A and B along with their open reading frames (ORFs). **DNA A**: AC1, AC2, AC3, AC4, AC5; **DNA B**: BV1, and BC1.

Recent investigations have brought attention to the presence of additional ORFs in geminiviral genomes (108,109). Example: *Tomato yellow leaf curl virus* (TYLCV), have unveiled additional ORFs. The largest of these newly discovered ORF, designated as V3, exhibits specific subcellular localizations, predominantly in the Golgi apparatus, and plays a vital role in ensuring the success of the viral infection process by serving as an effective RNA silencing suppressor (110). Another noteworthy ORF, C5, has been identified as a pathogenicity determinant and an additional RNA silencing suppressor, highlighting the multifunctional nature of these viral proteins (Figure 7) (111).

1.3.3.2 Transcription Regulation

Geminiviruses share common features in their genomic organization and transcriptional regulation. The coding regions on both virion-sense and complementary-sense strands diverge from an intergenic region (IR), initiating bi-directional transcription with independently controlled transcripts within the IR (112). Geminiviruses known to employ multiple overlapping transcripts and may utilize transcript splicing for gene expression regulation (113,114). A thorough analysis and review is available regarding the regulation of geminivirus transcription (115).

The replication initiator protein (Rep) in geminiviruses undergoes auto-regulation by binding to the iteron between the TATA box and the Rep transcription start site, leading to down-regulation of its own expression (87,116,117). This auto-regulation, specific to the homologous Rep protein, involves the C2 terminus domain, which contains a trans-activation domain in *Mastrevirus* Rep (118). Importantly, auto-regulation is not dependent on a functional viral ori, suggesting an independent action of the Rep binding site during both transcription and replication (117).

In the case of TGMV, the AL4 protein plays a role in repressing the AL1 promoter, involving elements such as a TATA box and a G-box upstream of the Rep binding site. Mutations affecting these motifs underscore the G-box's significance as the primary Rep transcriptional activating sequence. Both the TATA box and G-box elements contribute to replication and transcription, potentially facilitated by a host G-box transcription factor (119). In various geminiviruses, the AC2 protein serves as a recognized trans-activator for viral-sense promoter transcription (120,121). Geminivirus transcription sees early Rep activity, followed by repression upon Rep and AC4 accumulation, likely limiting interference with downstream TrAP promoters. TrAP and MP promoters activate midway, regulating virion sense genes as late genes in the infectivity cycle (122–124).

1.3.3.3 Replication

In host plants, geminivirus replication unfolds in three distinct phases: initiation, elongation, and termination (44). The replication processes have been thoroughly documented, with detailed mechanisms reviewed comprehensively (27,125–127). Geminiviruses lack a DNA polymerase and depend entirely on host factors recruited during the early stages of replication (86). These processes occur through double-stranded replicative intermediates, employing both recombination-dependent and rolling circle mechanisms (128–130). The mechanism of rolling circle replication (RCR) is depicted (Figure 8). Complementary-sense DNA synthesis on the virion-sense (encapsidated) strand, leading to dsDNA production, relies solely on host factors (131). Within the nuclei of infected cells, virus ssDNA synthesis is initiated by cleavage of the virion-sense strand by the virus-encoded Rep (132). This cleavage takes place immediately

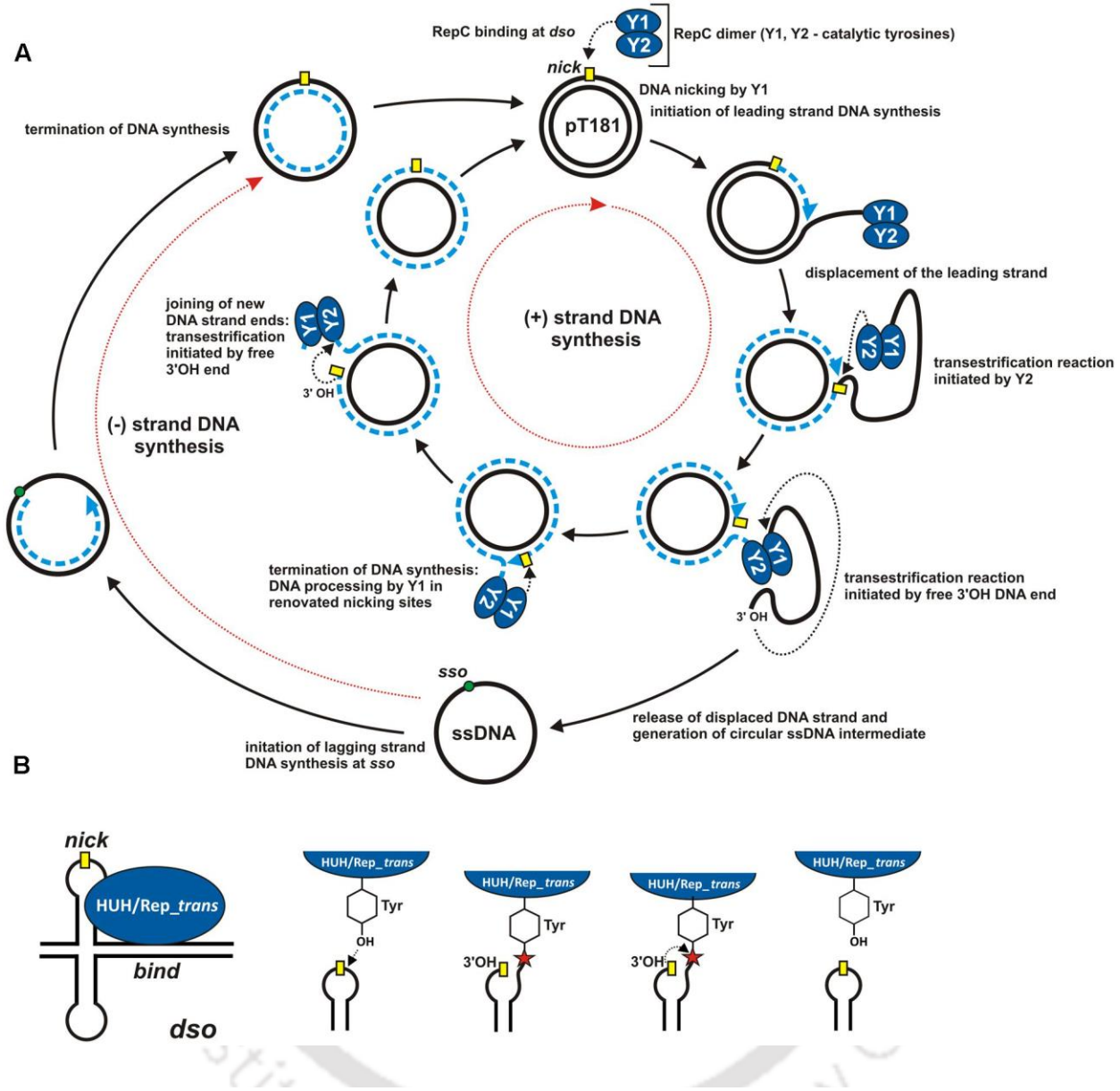

Figure 8 Mechanism of rolling-circle replication.
(**A**) The model illustrates rolling circle replication (RCR) based on the study of plasmid pT181. Leading (+) and lagging (–) DNA strand synthesis cycles, initiated at the dso and sso origins, respectively, are depicted with red dotted arrows. The RCR initiation protein (RepC) initiates (+) strand replication at the nick site (highlighted by a yellow rectangle). Nascent DNA strands are indicated by dashed blue lines, and the direction of synthesis is denoted by blue arrows. Black dotted arrows represent nucleophilic attacks during the synthesis process. (**B**) ssDNA breakage and joining reactions at the dso catalyzed by HUH and Rep_trans endonucleases. The yellow rectangle indicates the nick site in a hairpin-like structure. The red star marks the phosphotyrosine bond between the enzyme and the 5′-end of the DNA. The HUH/Rep_trans catalyzed reaction is reversible, as the released 3′-OH DNA end can act as a nucleophile on the phosphotyrosine bond (Image taken from Wawrzyniak et al., 2017).

downstream of the 3′-thymidine residues in a conserved 5′-TARTATT↓AC-3′ sequence located in the loop of a potential stem-loop structure within the IR (133). RCR generates large amounts of heterogenous sub- and extra-genome length geminivirus DNA (hDNA) (44,84,134). The viral REn, also referred to as C3, plays a significant role in enhancing the accumulation of DNA in begomovirus and curtovirus (135). It is presumed to be a component of the viral replisome. Both Rep and REn have the ability to bind to proliferating cell nuclear antigen (PCNA), which serves as the processivity factor for host DNA polymerase-δ (82,83,85).

An alternative mode of replication termed recombination dependent replication (RDR) has been identified for certain begomoviruses, their satellites, and curtoviruses complexes (128,130,136). Unlike traditional replication mechanisms, RDR does not depend on a specific origin of replication. Instead, it utilizes any available free 3′ end of ssDNA or ssDNA overhangs in a dsDNA to initiate replication within a homologous stretch of supercoiled master DNA. The direct involvement of geminiviral proteins in RDR, excluding the necessity of AC2 and AC3, requires further investigation. TYLCSV Rep's helicase activity, as described earlier, aligns with this model, akin to the RecBCD helicase in bacterial recombination. Consequently, extended 3′ ends of viral ssDNA can potentially invade homologous dsDNA with the assistance of host recombination enzymes, such as the RecA-like eukaryotic protein Rad51 in plants (137,138). This mechanism allows for the repair of geminiviral DNA fragments resulting from incomplete synthesis or nucleolytic attack with high fidelity. Furthermore, RDR may facilitate recombination in cases where two partially related viruses coexist in the same nucleus, providing insights into the recombinogenic potential of geminiviruses.

1.3.3.4 Infection Cycles

The initial phase of the infection cycle involves the introduction of viral ssDNA into a plant cell by an insect vector such *B. tabaci* while feeding on plant leaf (Figure 5). Geminiviruses undergo replication through a dsDNA intermediate within the nucleus of infected cells. Upon entering a host cell, the virus relies on the CP for movement to the nucleus, exploiting the host's transport mechanism. The mechanism by which the virus moves to the nucleus, either as an encapsulated virion or a decapitated nucleoprotein complex, is not entirely clear. CP is thought to play a role in this transport stage, likely through interactions with the host transport network (139,140).

Once inside the nucleus, the viral ssDNA transforms into a transcriptionally active dsDNA intermediate, serving as a template for both transcription and replication. Complementary DNA synthesis is entirely facilitated by host proteins. The resulting viral dsDNA associates with histones and forms mini-chromosomes. Similar to other viral systems, the expression of geminiviral genes follows a precisely regulated temporal sequence. It is hypothesized that genes encoding proteins involved in replication and transcription (e.g., Rep, TrAP, and REn) are expressed earlier than virion sense genes (e.g., CP and NSP genes).

After the expression of early viral genes, the virus genome multiplies through a RCR mechanism, generating new viral ssDNA molecules from the dsDNA intermediate. The final stage of the cycle involves the acquisition of virions by the insect vector. The CP and likely virus particles are essential for insect transmission in this phase. The viral ssDNA genome replicates in the nucleus using dsDNA templates through a rolling-circle mechanism. The viral-encoded NSP binds to progeny ssDNA genomes and facilitates their transportation between the nucleus and cytoplasm. The viral cell-to-cell movement protein (MP) traps NSP-genome complexes in the cytoplasm and directs them to and across the cell wall via modified plasmodesmata. In adjacent

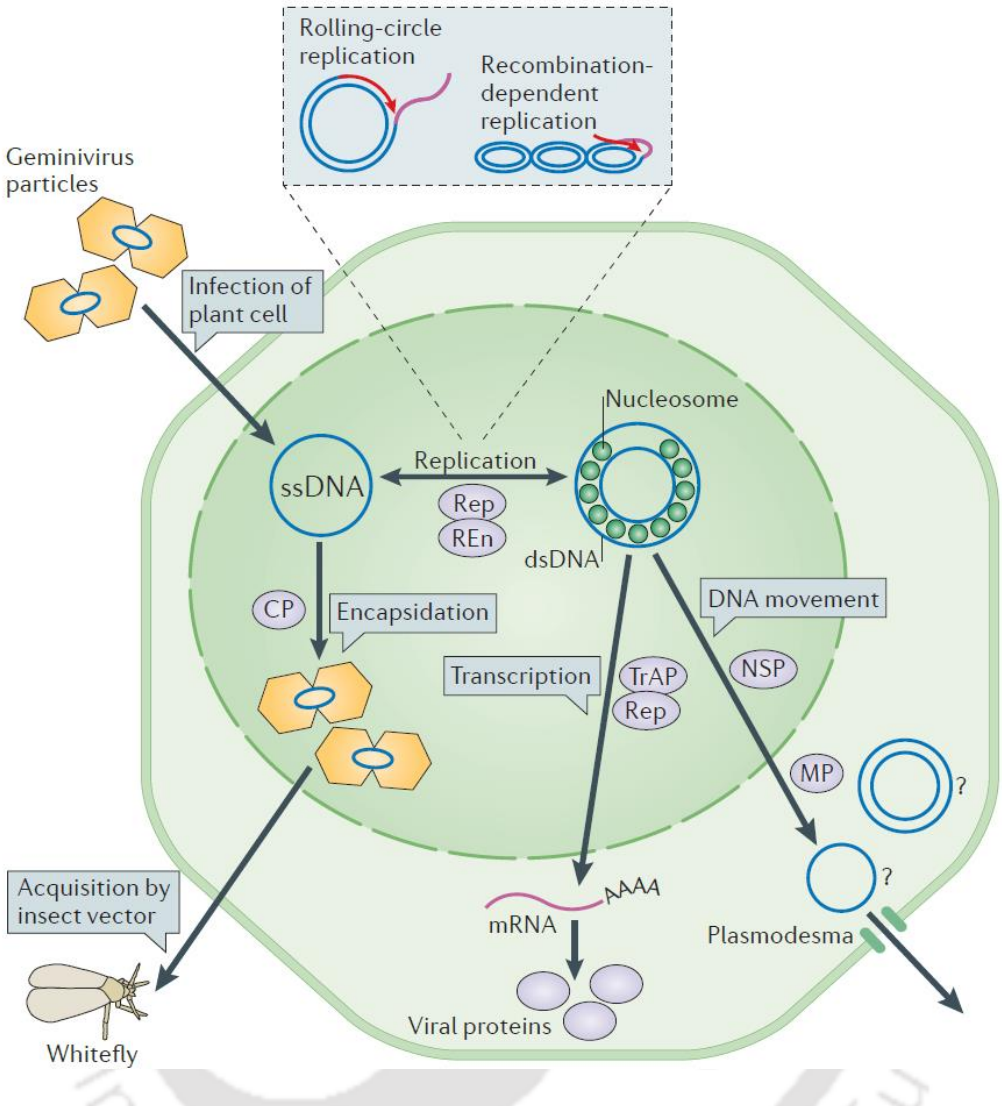

Figure 9 The begomovirus life cycle.
The infection process in plant cells initiates with the release of viral single-stranded DNA (ssDNA) from virions, followed by its conversion into double-stranded DNA (dsDNA). The assembled dsDNA, associated with nucleosomes, undergoes transcription by host RNA polymerase II, leading to the production of the replication initiator protein (Rep). Rep induces rolling-circle replication by introducing a nick into a viral dsDNA molecule, creating a free 3′-hydroxyl end that primes ssDNA synthesis. This process displaces the parental strand (inset). The liberated ssDNA is then converted back to dsDNA, re-entering the replication cycle. Subsequently, viral replication shifts to recombination-dependent replication, initiated by homologous recombination between a partially replicated ssDNA and a closed, circular dsDNA. This forms a looped molecule acting as a template for both ssDNA and dsDNA synthesis (inset). Later in infection, Rep suppresses its own transcription, leading to the activation of transcriptional activator protein (TrAP) expression. TrAP, in turn, activates the expression of coat protein (CP) and nuclear shuttle protein (NSP). Circular ssDNA is encapsidated by CP into virions, available for whitefly acquisition. NSP binds to viral DNA, facilitating its movement across the nuclear envelope, with the movement protein (MP) transporting it through a plasmodesma. The mode of viral DNA movement, whether as ssDNA versus dsDNA or as a linear versus a circular molecule, remains unknown.

uninfected cells, NSP-genome complexes are released, and NSP targets the viral ssDNA to the nucleus, initiating new rounds of replication and infection, same has been shown in Figure 9 (27).

1.3.3.5 Movement

To replicate within the nucleus, spread between cells, and disseminate between plants, geminiviruses and their satellites have developed a coordinated network of movement-associated proteins. Various proteins, such as V1, V2, AV1, C4, BV1 (NSP), BC1 (MP), and BetaC1, play roles in geminivirus movement functions (139,141,142). A proposed movement model for bipartite begomoviruses involves the coordinated actions of NSP and MP, where NSP shuttles ssDNA from the nucleus to the cell periphery's plasma membrane, and MP transfers the viral DNA to adjacent cells through plasmodesmata (143–145). The viral DNA movement complex in begomoviruses can bind both ssDNA and dsDNA, facilitating transport to neighboring cells (146). While BC1 and BV1 have specific limitations in binding viral DNA, their interaction is crucial for virus movement. For monopartite begomoviruses like TYLCV, CP and C4 proteins act similarly to BV1-BC1 interaction, contributing to virus movement. The MP encoded by MSV (AV2) interacts with CP for viral DNA movement, and both localize in the nucleus, resembling the NSP of begomoviruses (147). This coordination emphasizes the interaction of nuclear-targeting and cell membrane trafficking proteins for geminivirus movement. Recent studies suggest that BetaC1, encoded by betasatellites, can serve as an alternative to DNA-B components. However, more experimental evidence is needed to determine whether the coordinated action of CP and BetaC1 or BetaC1 alone facilitates viral DNA movement. BetaC1, like other geminivirus DNA-binding MPs, can bind to both dsDNA and ssDNA in a sequence-independent manner and localizes in the nucleus (148). The current model depicting the intra- and intercellular movement of the bipartite begomovirus is illustrated in Figure 10**.**

1.3.4 Geminivirus Diagnosis

Geminiviruses, pose significant threats to global food security, causing substantial economic damage to crops. Unfortunately, there is no practical method for curing infected plants. Early detection is essential for effective management and disease spread reduction (10). Recognizing distinctive foliar symptoms like golden mosaic, leaf curling, and vein discoloration helps identify geminivirus-induced diseases. Involvement of vectors like leafhoppers and whiteflies underscores potential geminivirus etiology. However, acknowledging similar symptoms from alternative viral sources emphasizes the need for precise virus identification. Relying solely on symptomatology is insufficient, necessitating diagnostic tests to conclusively confirm geminivirus infections (149). Today, disease estimation is crucial for management decisions, plant breeding, and crop protection. In this context, the development of rapid, specific, and innovative techniques for virus detection is crucial (Figure 11) (150). Practical application depends on factors like cost, sensitivity, speed, instrument availability, and disease stage (151,152). Prior reviews have primarily focused on comprehensive plant virus detection and diagnosis, spanning i) biochemical, serological, and molecular methods (151,153), ii) Next-generation technology-based techniques (151,154,155), iii) remote sensing (RS) techniques (156,157), and precision farming technologies which includes machine learning, artificial intelligence, deep learning etc. (Figure 11) (158–164). The development of farmer-friendly, point-of-care diagnostic tools designed to offer high-sensitivity and rapid diagnosis of plant viruses (165,166).

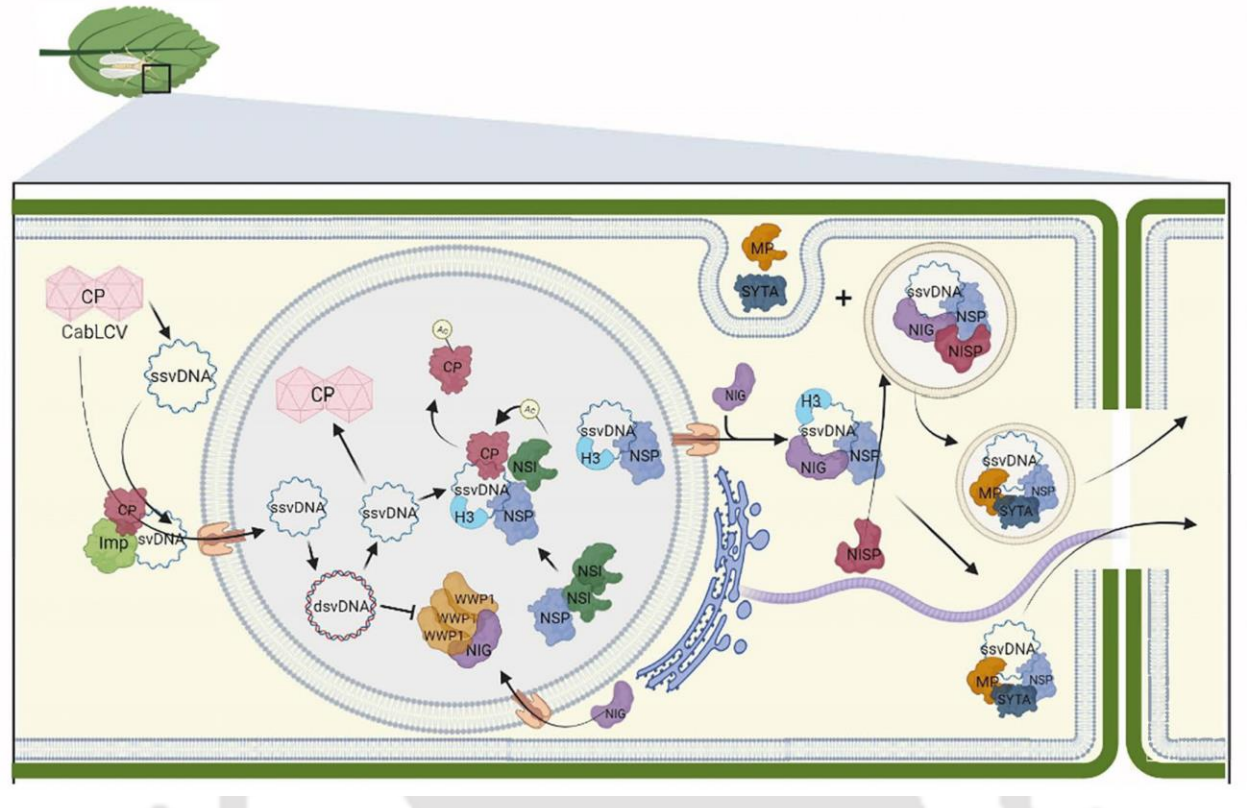

Figure 10 The intra- and intercellular movement of begomovirus.
The insect vectors deliver the viral particle into the cytoplasm upon cell infection. Importin-like proteins aid in translocating disassembled CP-bound single-stranded viral DNA (ssvDNA) to the nucleus, where host polymerases convert it to double-stranded DNA (dsDNA). NSP within the nucleus binds to both ssvDNA and dsvDNA, with the exported vDNA form remaining unclear. CP binds to synthesized ssvDNA for packaging, and NSP recruits NSI to prevent packaging by acetylating CP, causing its dissociation from vDNA. This NSP-mediated nuclear export of vDNA occurs through nuclear pores. In the cytosol, NSP interacts with NIG, releasing the vDNA-NSP complex from the nuclear pore. NSP and NIG interact with endosomal NISP, directing the vDNA-NIG-NSP complex to early endosomes. MP interacts with endocytosis regulator SYTA in the endosome and moves to the endoplasmic reticulum-plasma membrane (ER-PM) junctions via SYPT. From the endosome, the nucleoprotein complex utilizes the SYTA-mediated endocytic recycling pathway to reach plasmodesmata for cell-to-cell vDNA-NSP movement. CabLCV MP can relocate SYPT-induced ER-PM junctions to plasmodesmata for efficient cell-to-cell transport of vDNA. An alternative route may involve the secretory pathway along microtubules and microfilaments for trafficking to plasmodesmata. The antiviral protein WWP1 sequesters NIG in nuclear bodies to prevent its proviral function. Nascent vDNA disrupts WWP1 nuclear bodies, restoring NIG's cytosolic localization and proviral function. (Breves et al., 2023; Silva et al., 2022).

A single-tube duplex and multiplex PCR assay was devised to concurrently detect four cassava mosaic begomoviruses—African cassava mosaic virus (ACMV), East African cassava mosaic Cameroon virus (EACMCV), East African cassava mosaic Malawi virus (EACMMV), and East African cassava mosaic Zanzibar virus (EACMZV). In a study TYLCV-specific primers were

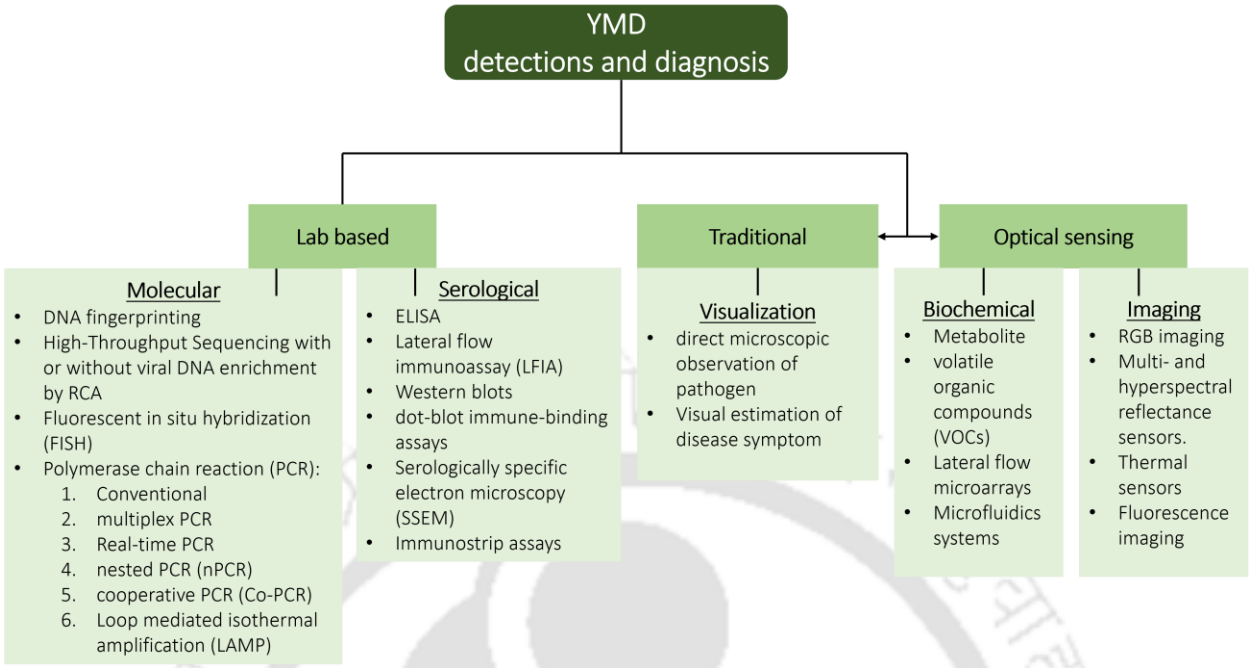

Figure 11 Geminivirus disease diagnosis and detection methods.

developed, enabling the creation of a duplex PCR method (167,168). This method allows for rapid and large-scale diagnostics, distinguishing between two species of Tomato yellow leaf curl virus—TYLCV-Israel (TYLCV-Is) and TYLCV-Sardinia (TYLCV-Sar)—directly from infected leaf extracts. Londoño et al., (2016) evaluated the Recombinase Polymerase Amplification (RPA) assay for the specific detection of three begomoviruses—Bean golden yellow mosaic virus, Tomato mottle virus, and Tomato yellow leaf curl virus (TYLCV). The study explored the potential of RPA as a cost-effective and rapid tool for begomovirus detection in plant diagnostic clinics. Seepibam et al. (2017) developed triple antibody sandwich enzyme-linked immunosorbent assays (TAS-ELISAs) for the detection of various begomoviruses, including Tomato yellow leaf curl Thailand virus (TYLCTHV) (170). These assays provide sensitive and high-throughput detection, offering valuable tools for virus surveillance and screening virus-resistant cultivars.

Mahas et al., (2021) introduced a loop-mediated isothermal amplification (LAMP)-coupled Cas12-based assay for the rapid and highly sensitive detection of Tomato yellow leaf curl virus (TYLCV) and Tomato leaf curl New Delhi virus (ToLCNDV). This method provides easy-to-interpret visual readouts, making it suitable for point-of-use applications. Lavanya et al. (2021) reported the development of a visual detection method based on functionalized gold nanoparticles (AuNP assay) (172). This assay demonstrated effectiveness in detecting begomoviral infection across various plants, showcasing its utility and versatility. Studies have shown the efficacy of rolling-circle amplification (RCA)-enrichment coupled with RFLP, conventional (Sanger) sequencing (173), and high-throughput sequencing with bioinformatic analysis (174,175) for selectively amplifying and identifying new geminiviruses (176–179).

Hossain et al., (2023) utilized spectral reflectance analysis with a handheld spectrometer, coupled with machine learning, for accurate prediction of Turnip yellows virus content in *Nicotiana benthamiana* plants (175). This approach demonstrates the potential for non-destructive and informative monitoring of virus spread in greenhouse or field settings. A handheld active multispectral imaging (A-MSI) device, integrated with machine learning algorithms, was

developed for the early and real-time detection of *Cassava Brown Streak Disease* (CBSD) (181). Prabhakar et al., (2013) employed hyperspectral remote sensing, utilizing optimal spectral reflectance ratios, for the rapid and non-destructive estimation of leaf chlorophyll and severity of YMD in blackgram (177). Raji et al., (2016) demonstrated the application of photochemical reflectance index (PRI) imaging for detecting and assessing varying levels of Cassava Mosaic virus Disease (CMD) infection in cassava plants (178). Feng et al., (2023) investigated the application of reflectance spectroscopy with preprocessing methods like 3SV for detecting Wheat Yellow Mosaic Disease (179). The study employed spectral indices and machine learning models, such as SVM, achieving high accuracy in disease prediction during field validation. Uke et al., (2019) monitored the spread of CMD in Southeast Asia using the AGRIBUDDY smartphone app (180). Farmers uploaded CMD photos and location data, enabling the identification of Sri Lankan cassava mosaic virus (SLCMV) in Cambodia. These advanced diagnostic methods collectively contribute to a comprehensive toolkit for efficient geminivirus detection, enabling precise disease management and surveillance strategies in diverse agricultural settings.

1.3.5 Mungbean and Begomoviruses: Economic importance and distribution

Mungbean (*Vigna radiata* (L.) Wilczek) is a self-pollinated, short-duration grain legume crop, ranking third in importance after chickpea and pigeonpea. It is recognized by various names such as greengram, greenbean, mashbean, goldengram, and greensoy (186). Mungbean boasts a relatively small genome size of 579 Mb with 22 chromosomes (2n) (187). The seeds, with 24% protein, low flatulence factors, and high iron content (40–70 ppm), are an ideal choice for a balanced diet (1,188,189). Particularly in Asia, it plays a crucial role in alleviating protein malnutrition, catering to impoverished populations (2,190). Growing consumer preference for plant-based proteins, such as pea, soybean, and mungbean, is reflected in the rising U.S. sales of plant-based meats, exceeding $1 billion in 2020 (191). Notably, mungbean features prominently in popular products like Beyond Meat's burger substitute, Eat JUST's vegan egg, and McPlant was also developed for McDonald’s contributing to a broader shift towards sustainable plant-derived alternatives of meat products (191). In Asian cuisine, mungbean sprouts are widely enjoyed for their high vitamin C and folate content, while the foliage serves as fodder, feed, and hay. Mungbean roots' association with *Rhizobium* and *Bradyrhizobium* bacteria enhances soil fertility via atmospheric nitrogen fixation, providing benefits to subsequent crops. Mungbean cultivation spans a wide range of latitudes, covering tropical and sub-tropical regions globally and adapting well to various cropping systems (192). Cultivated over 7.0 million hectares worldwide, mungbean production exceeds 3.5 million tons, primarily in Asia, with major producers including India, China, Pakistan, Bangladesh, and others (3). India leads in global mungbean production, yielding 2.17 million tons from around 4.32 million hectares (3). However, the average productivity of mungbean in India remains relatively low at approximately 502 kg/ha (193,194).

Mungbean faces various globally recognized diseases, with foliar diseases standing out as the main culprit for yield loss (191). Among foliar diseases, fungal and bacterial pathogens are prevalent (195). Notably, viruses which cause YMD emerge as the most impactful biotic constraint, exerting a significant impact on overall mungbean yield (8). YMD in legumes is caused by four distinct species of bipartite begomoviruses (family *Geminiviridae*) and it was first reported from western India (9,51,196,197). This disease poses a significant threat to mungbean crops, particularly in South and Southeast Asia (59,62), causing yield losses ranging from 10 to 100%,

depending on the mungbean genotype and the stage of infection (10,198). YMD spreads through the whitefly (*Bemisia tabaci* Gennadius), serving as an insect vector for YMVs (58,199,200).

The genus name *Begomovirus* is derived from Bean Golden Mosaic virus (BGMV), the causative agent of golden mosaic disease in beans. The identified begomoviruses, including *Mungbean yellow mosaic virus* (MYMV) (14,201,202) and *Mungbean yellow mosaic India virus* (MYMIV) (203,204), are prevalent across the Indian subcontinent, with overlapping host ranges affecting various legume crops (204–207). *Dolichos yellow mosaic virus* (DoYMV) has a narrow host range, primarily infecting Dolichos (*Lablab purpureus*) (208), while *Horsegram yellow mosaic virus* (HgYMV) is the least characterized among the four viruses. The virus enters the phloem cells of the host through the whitefly proboscis, leading to visible symptoms such as scattered yellow spots on young leaves, progressing into a yellow mosaic pattern. This ultimately results in complete yellowing, drying, leaf curling, and withering of leaves, accompanied by reduced pod size and decreased photosynthetic efficiency, leading to severe yield penalties (Figure 12) (209). These four begomovirus species responsible for legume YMD and will be referred to as legume yellow mosaic viruses (LYMVs) (9).

MYMV particles were first identified and purified in the leaf cells of mungbean by (209) and (210), respectively. The genomes of MYMV isolates from Thailand (79) and North India (211) displayed less than 89% similarity (212), leading to their classification as a distinct species, subsequently named MYMIV. A comprehensive historical perspective on YMD in *Vigna* species is provided by Mishra et al., (2020). For a detailed understanding of *Begomovirus* genome architecture (Figure 2), replication (Figure 8), transmission (Figure 9), and systemic movement (Figure 10), please refer to previous sections.

1.3.6 Yellow Mosaic Disease (YMD) Management

Geminivirus disease management adopts a comprehensive strategy throughout the growing season (10). Pre-planting involves cultivar selection, obtaining virus- and vector-free planting materials, and strategic farming. During the season, key strategies include vector management, roguing, and biological control. Post-harvest practices encompass sanitation and host-free periods. The integrated approaches such as conventional, molecular, insecticides, and disease-free planting aims to effectively control YMD in mungbean and mitigate economic losses (8,63,193). However, it is important to note that these approaches do not guarantee complete success (213). Consequently, YMD management heavily relies on utilizing resistant cultivars and use of innovative biotechnological strategies.

1.3.6.1 Identification of YMD Resistant Cultivars

The evaluation of germplasm entries for disease resistance is a crucial step in managing plant diseases through host plant resistance (214). Routine screening procedures, including germplasm evaluation, play a vital role in identifying genes that confer resistance to a certain extent. While the impracticality of mechanically transmitting YMV has led to the predominant screening of mungbean for YMD resistance in YMV hot spots, there is a growing trend towards more precise screening methods using viruliferous whiteflies and agroinoculation techniques (215).

1.3.6.1.1 Screening of Genotypes at YMV Hot-Spots

The assessment of mungbean resistance to YMD in hot-spot conditions employs the infector-row technique within a specific standard statistical experimental design. Typically, a row of the most susceptible spreader genotype in that region is sown after every two, three, or 10 rows of the test genotypes (26). To encourage the whitefly population for sufficient infection and YMD spread, insecticide spraying is not recommended. Since whiteflies begin infecting the plants soon after germination, and YMD symptoms become visible during the 2nd to 6th week after planting, constant monitoring is essential. The assessment of YMD severity involves visually scoring the infected plants (216,217).

One limitation of hot-spot screening is the unknown identity of the causative viruses and whitefly biotypes (218). Moreover, non-uniform disease development may occur due to variations in whitefly populations, dependent on planting locations and seasons (219). Field conditions reveal that whitefly buildup is higher at elevated temperatures, while increased rainfall and humidity negatively impact whitefly populations (220). Additionally, a negative correlation between high-altitude regions with low humidity and YMD incidence underscores the influence of various environmental factors on YMD severity (221). Hence, the development of an efficient artificial inoculation technique using specific virus(es) at an early stage will prove more useful in phenotyping plant materials against the specific virus and breeding for enhanced resistance. Genotype evaluations in field or natural condition have been documented in various studies (222–227).

1.3.6.1.2 Screening Genotypes Using Viruliferous Whiteflies

Utilizing net-houses for screening genotypes against YMD using viruliferous whiteflies proves to be an effective method (218). Whiteflies are made viruliferous through force-feeding on YMV infected mungbean plants during a 24-hour acquisition access period (AAP). Subsequently, these whiteflies are used for inoculating healthy plants during a 24-to-48-hour inoculation access period (IAP). Whiteflies, being highly efficient vectors, can transmit YMV within 24 hours of AAP and IAP, with even a single viruliferous adult causing transmission (201). Transmission efficiency is reported to be 70.50% with 10 viruliferous adult whiteflies after 24 hours each of AAP and IAP, increasing to 85% with 20 viruliferous whitefly adults after 48 hours of AAP and 24 hours of IAP (5). Genotype evaluations using viruliferous whiteflies have been documented in various studies (24,228–231). Despite low densities of adult whiteflies effectively spreading YMD, no correlation has been established between the number of whiteflies and YMD severity (232). Therefore, efficient artificial inoculation techniques using specific viruses was developed to phenotype plant materials against the targeted virus.

1.3.6.1.3 Screening Genotypes Using Agroinfection

In 1986, the groundbreaking technique of Agroinoculation was developed, employing *Agrobacterium*-based binary vectors for the efficient delivery of viral genomes into plants (233–236). By circumventing the reliance on unpredictable insect vectors, agroinoculation ensures highly efficient and reproducible infections, revolutionizing the study of plant viruses (237). Its versatility is evident in its broad host range, encompassing diverse plant species that were previously inaccessible (238). The technique provides unprecedented control over the viral inoculum, allowing researchers to dissect viral functions meticulously (239,240). In the laboratory, agroinoculation establishes a controlled environment, emancipating research from field condition vagaries. This confined landscape ensures consistent disease development, facilitating rigorous experimentation and hypothesis testing (241).

The agroinoculation-based germline screening methodology is depicted in Figure 13. Briefly, the process begins by extracting total plant DNA from symptomatic tissues (242,243). The viral genome is then amplified through polymerase chain reaction (PCR) (244) or rolling circle amplification (RCA) (245), leading to the formation of multimers (246) or full-length viral genomes (247) with tandem repeats or concatemers with two viral origins of replication (248,249). These multimers are linearized, ligated into plasmids, and transformed into *Agrobacterium tumefaciens* using methods like electroporation, freeze/thaw, or triparental mating (250). The *A. tumefaciens* containing the infectious clone is introduced into host plants through leaf infiltration techniques such as syringe or vacuum infiltration (251) providing a cost-effective alternative to biolistic methods (252). Agroinfection based screening of resistant genotypes have been documented in various plants such as mungbean (11,13,14,252–255), blackgram (211,223,256,257), tomato (206,258–261), soyabean (262), *N. benthamiana* (263,264), and rice (265).

Additionally, agroinoculation serves as a method for strong transient protein expression in targeted plant tissues using virus-based vectors (266) and as a tool for mutational and gene function analysis (267–270). It has also emerged as a trending method for precise and efficient genome editing in plants when coupled with CRISPR/Cas technology (241). Furthermore, agroinoculation is widely employed for delivering VIGS (Virus-Induced Gene Silencing) vectors into plants through vacuum-infiltration (271) or agrodrench (272) methods, facilitating RNA silencing and functional genomic studies (273–275).

1.3.6.2 Biotechnology-based Approaches to Control YMD

Facing the limitations of traditional virus control methods in plants, genetic engineering emerges as a powerful tool. Our deepening understanding of viral biology and host-pathogen interactions has given rise to two main strategies: pathogen-derived resistance (PDR) and host genetic resistance. PDR introduces viral sequences like coat protein, AC1 (Rep) (276,277), AC2 (TrAP), AC3 (REn) (278), and AC4 (gene silencing suppressor) into the plant genome, triggering a defensive response (279). This concept, pioneered by Sanford & Johnston, led to the successful CP-mediated resistance (CPMR) approach, culminating in the first commercially available virus-resistant squash in the 1990s (280–282). Furthermore, genome editing tools like clustered regularly interspaced short palindromic repeats/CRISPR-associated (CRISPR/Cas) technologies (283–287) and RNA interreference (RNAi) technology (288–295) enabled the creation of genome edited geminivirus resistant crops (296,297). These advancements hold immense potential, even as traditional methods like resistant cultivars and integrated management remain crucial. However, concerns about chemical pesticides and the limitations of genetically modified organisms (GMOs) (298,299), despite their benefits like pest and pathogen resistance, spurred the search for environmentally sustainable and alternative innovative solutions (300,301). Enter non-GMO dsRNA-based strategy: a novel technology utilizing RNAi or RNA silencing to target pests and pathogens without modifying plant genomes (302). This approach holds promise in addressing both conventional limitations and GMO challenges (303,304).

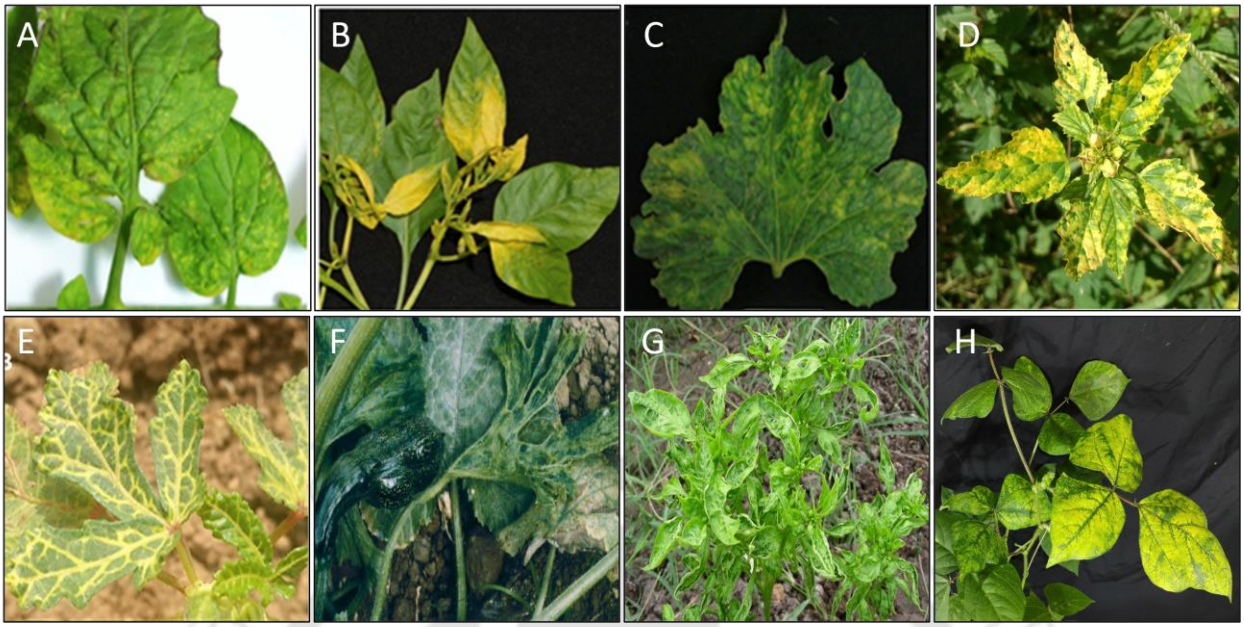

Figure 12 Typical YMD symptoms induced by begomoviruses on different crops.
A) tomato plants infected with Tomato yellow leaf curl Thailand virus (TYLCTHV), B) Pepper plants infected with Pepper yellow leaf curl Thailand virus (PepYLCTHV), C) Cucurbits plant infected with Squash leaf curl China virus (SLCCNV), D) Weeds from *Malvastrum* genus infected with Sida chlorotic leaf virus, E) Okra plants infected with Bhendi yellow vein mosaic virus (BYVMV), F) Cucurbits plants infected with Zucchini yellow mosaic potyvirus (ZYMV), G) *Capsicum annuum* infected with chilli leaf curl virus (ChiLCV), H) Mungbean infected with Mungbean yellow mosaic virus (MYMV). A), B), C) Photograph was obtained from Charoenvilaisiri et al., 2020; D) Photograph was obtained from Navas-castillo, 2016; E) Photograph was obtained from Shuja et al., 2022; F) Photograph was obtained from Desbiez & Lecoq, 1997; G) Photograph was obtained from Bhatt et al., 2016; H) Photograph was obtained from Dhobale et al., 2023.

1.3.6.3 Gene Silencing Strategies

Gene silencing processes within plant cells orchestrate the downregulation of transcript levels through two distinct mechanisms. The first, known as transcriptional gene silencing (TGS), operates at a transcriptional level. In contrast, the second, post-transcriptional gene silencing (PTGS) or RNAi, involves the degradation of accumulated mRNA (Figure 14) (305).

- **Transcriptional Gene Silencing (TGS):**
  TGS, an epigenetic gene silencing form, is characterized by the methylation of promoter DNA sequences. This initiates the formation of a heterochromatin region surrounding the gene, resulting in the repression of gene transcription (306,307).

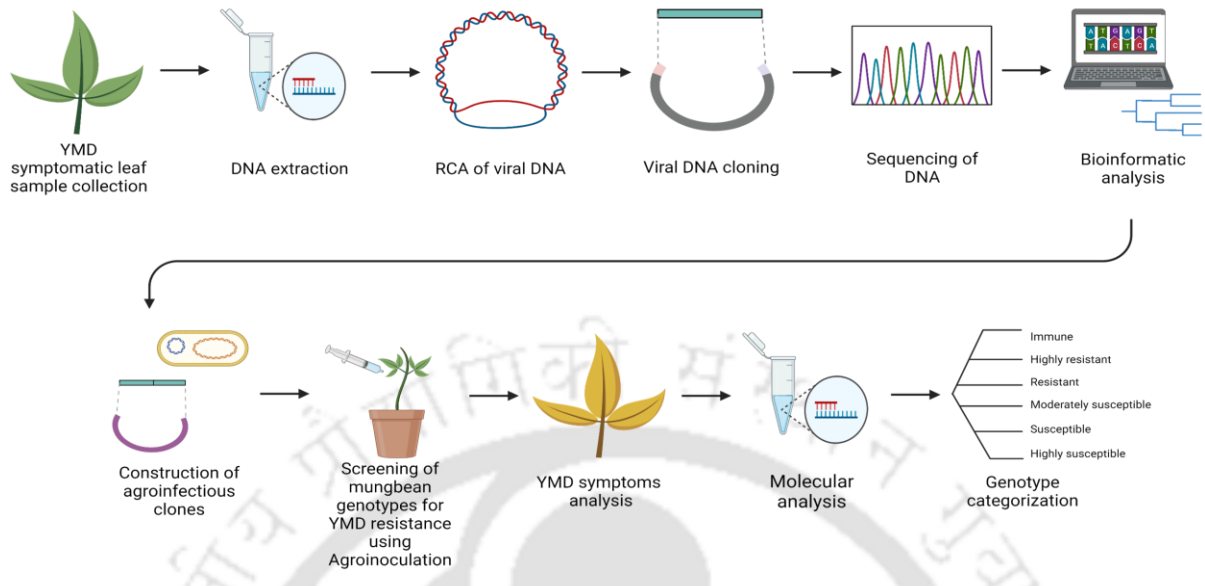

Figure 13 The agroinoculation-based screening for YMD-resistant germlines.

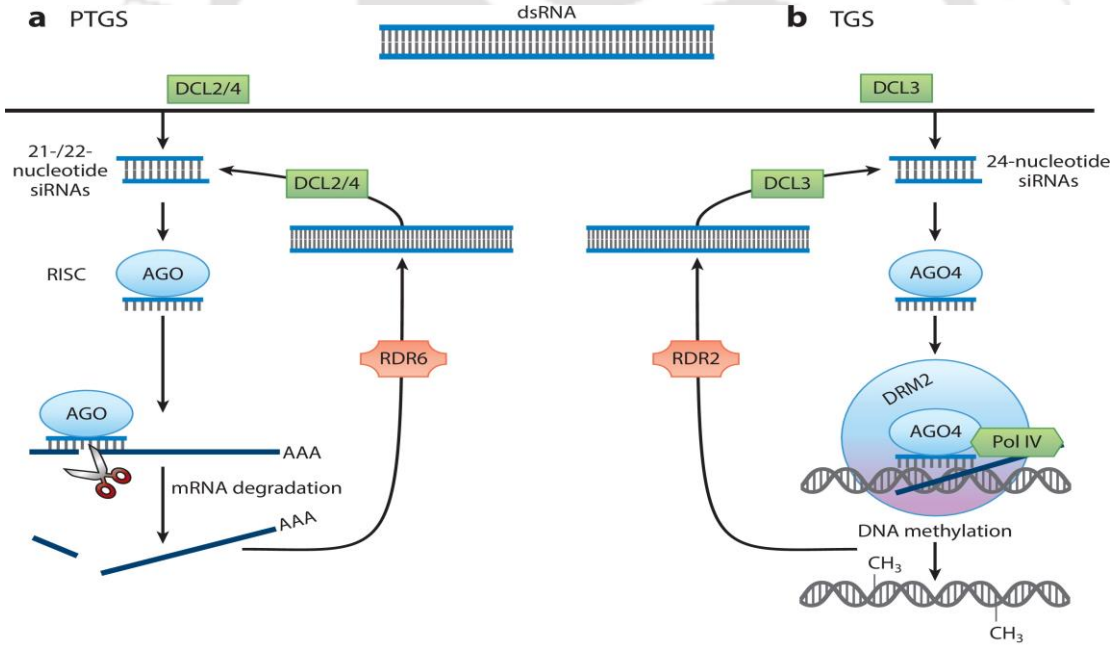

Figure 14 The two primary mechanisms of gene silencing in plants.
The figure provides a schematic representation of gene silencing, illustrating **(a)** Post-Transcriptional Gene Silencing (PTGS) and **(b)** Transcriptional Gene Silencing (TGS). It emphasizes the interconnected nature of PTGS and TGS, focusing on these mechanisms while excluding the pathway of translation inhibition for simplicity. Notably, the mechanistic strategy predominantly derives from animal studies. Abbreviations used include AGO (argonaute), DCL (Dicer-like), DRM2 (DNA methyltransferase 2), dsRNA (double-stranded RNA), mRNA (messenger RNA), Pol (polymerase), PTGS (post-transcriptional gene silencing), RDR (RNA-dependent RNA polymerase), RISC (RNA-induced silencing complex), siRNA (small interfering RNA), and TGS (transcriptional gene silencing). Image source: Voloudakis et al., 2022.

- **Post-transcriptional Gene Silencing (PTGS)/RNAi:**
  Its molecular mechanism and applications, has been thoroughly reviewed in several literature sources (308–311). Briefly, the initiation of this mechanism involves two types of small RNAs: microRNAs (miRNAs) and small interfering RNAs (siRNAs) (312,313). These are produced from various precursor elements, including hairpin RNAs (hpRNAs), double-stranded RNAs (dsRNAs), artificial microRNAs (amiRNAs), and small RNAs (15). Both siRNA and miRNA silencing pathways converge in a unified biochemical pathway within plant cells (314). In plant cell cytoplasm, this intricate mechanism relies on Dicer-like proteins (DCLs) to process dsRNAs, whether endogenously expressed (host-induced gene silencing; HIGS) or exogenously introduced (spray-induced gene silencing; SIGS), into small interfering RNA (siRNA) duplexes (315–317). These siRNA duplexes then associate with ARGONAUTE proteins (AGOs), leading to the degradation of the passenger strand. The resulting multiprotein complex, guided by AGOs, forms the RNA-induced silencing complex (RISC) with the remaining guide strand. Subsequently, the RISC binds to complementary transcripts, facilitating their cleavage and consequent downregulation of gene expression (318,319). Furthermore, the number of siRNA molecules are amplified through the action of RNA-dependent RNA polymerase (RDR) enzymes (320,321). This finely orchestrated process highlights the sophisticated machinery plants employ to regulate gene expression through PTGS/RNAi (322).

1.3.6.3.1 Different Types of Gene Silencing

Virus-Induced Gene Silencing (VIGS): In VIGS, the viral genome is modified by removing disease-causing genes and inserting the modified viral genome cDNA into a binary vector (323). Viruses lacking strong gene silencing suppressors serve as potential VIGS vectors (324). The vector includes multiple cloning sites (MCS) for inserting targeted gene fragments. The recombinant virus enters plant cells through Agrobacterium-mediated transformation or DNA bombardment eventually triggering PTGS against target molecules (325). The commonly used VIGS vector is *Tobacco rattle virus* (TRV), known for its wide host range infection and systemic transmission (326,327). VIGS serves as a crucial tool for understanding gene functions (328,329).

Host Induced Gene Silencing (HIGS): It exploits the natural immune system of plants through biotechnological applications of RNA interference (RNAi) to combat viral infection (330). Initially, HIGS has proven effective against nematodes (331). The most efficient induction of HIGS involves transgene constructs that produce dsRNA, commonly in the form of hpRNA (332). Plant viruses, equipped with silencing suppressors, are effectively countered by HIGS, achieving an average control rate of 90%, particularly against intracellularly replicating viruses accessible to plant RNAi. Numerous studies have applied HIGS in crops to confer resistance against diverse plant pathogens and diseases (333–342). Various review papers, summarize current knowledge about the molecular mechanisms underlying HIGS and its applications in disease control (342–346).

Strategies involve target gene identification, aiming for RNAi-mediated knockdown with high lethality, durability, low resistance risk, and minimal off-target effects. Advances in sequencing and bioinformatics aid target selection, but broader applications heighten the risk of off-target effects. Effective RNAi trigger design considers dsRNA sequence complementarity and

length, emphasizing the need for integrating molecular knowledge and pathogen-specific RNAi mechanisms in successful HIGS strategies. Following the identification of the target sequence, the subsequent step involves the construction of RNAi vectors. This entails cloning the sense and antisense sequences (332), separated by a spacer sequence (347), and subsequently sub-cloning them into suitable plant binary vectors such as pHANNIBAL, pKANNIBAL, pHELLSGATE, pANDA, pSAT, and pSH (346). The resulting RNAi vector is then transformed into *Agrobacterium tumefaciens*. The transfer of RNAi constructs to plants is facilitated using *A. tumefaciens*. Efficient induction of PTGS against geminiviruses can be achieved through stable transgene integration in host plants (288,348–352), expressing self-complementary hpRNA, or by transient expression within the plant (353–355). However, the broader adoption of HIGS faces challenges, including limited transformation protocols in various crop species, time-consuming processes, high costs, public concerns about GMOs, and the instability of engineered RNA silencing traits.

Exogenous dsRNA (hpRNA)-Induced Gene Silencing: The limitations associated with HIGS and other transgenic approaches for achieving virus or pathogen resistance may find potential solutions in the exploration of non-transgenic pathogen resistance derived from RNAi. This resistance can be induced by topically or foliarly applying environmental dsRNA molecules (356). Previous work has shown that fungal pathogens, such as *Botrytis cinerea* and *Fusarium graminearum*, can efficiently take up environmental dsRNAs, which are then processed into siRNA and induce the silencing of pathogen genes with complementary sequences (357,358). These discoveries have led to the development of an innovative crop protection strategy known as spray-induced gene silencing (SIGS) (Figure 15). Serving as a non-GMO alternative to HIGS, SIGS inhibits pathogen infection by topically applying dsRNA or small RNA (sRNA) molecules onto plants to silence pathogen virulence-related genes (359). Various reviews papers explore the challenges, risks, and successes of non-transformative RNAi application, specifically exogenous dsRNAs-induced RNAi, in managing pest insects, viruses, and plant diseases in agriculture (17,304,360–368). Methods for producing exogenous dsRNA without genetic transformation include in vitro transcription (IVT) (369), microbial expression in bacteria or fungi, and cell-free synthesis. Conversely, transformative methods involve creating transgenic plants (GM crops) (360). dsRNA synthesis can be accomplished by transforming the *Escherichia coli* HT115 (DE3) with a suitable vector, such as L4440 and pGEM/IR 54, designed to express a dsRNA/hpRNA. This bacterial strain is recognized for its capacity to generate significant quantities of dsRNA in vivo due to the absence of the dsRNA-specific RNase III enzyme (370,371). The choice of delivery system for dsRNA varies depending on the target organism and crop, including options such as foliar spray (362), irrigation, trunk injection, baits, and others (366). The selection of appropriate delivery strategies plays a crucial role in achieving effective control results and determines the success of the technology. Hoang et al, reviewed the uptake of dsRNA molecules by plants through foliar and cellular processes, addressing key barriers and potential overcoming methods (372). Recently, a study demonstrated that loading RNAi-inducing dsRNA into layered double hydroxide (LDH) nanoparticles (BioClay) and applying it to plant surfaces through spraying facilitated sustained release of the dsRNA, leading to increased protection compared to applying naked dsRNA (367,373). Ongoing efforts in nanotechnology have explored various innovative approaches to efficiently deliver nanoparticle composite dsRNA into plants.

The application of dsRNA vaccination has been well-established against various plant RNA viruses (374–381), but limited studies have explored its efficacy against plant DNA viruses,

particularly begomoviruses. Recently, a study demonstrates the effectiveness of a single dsRNA molecule in conferring protection against two tomato-infecting viruses: the bipartite geminivirus *Tomato leaf curl virus* (ToLCV) and the tripartite RNA virus CMV (382). Notably, topical application of dsRNA has shown promise against monopartite geminiviruses as well, such as *Tomato yellow leaf curl virus* (TYLCV) (383) and *Chilli leaf curl virus* (ChiLCV) (384). The study by Rego-Machado et al. revealed the failure of resistance against *Tomato severe rugose virus* (ToSRV), a Begomovirus, in tomato plants (385). In a similar investigation, Delgado-Martín et al. explored whether exogenously applied dsRNAs could confer protection against *Tomato leaf curl New Delhi virus* (ToLCNDV), resulting in the failure to elicit protection in ToLCNDV infections (378).

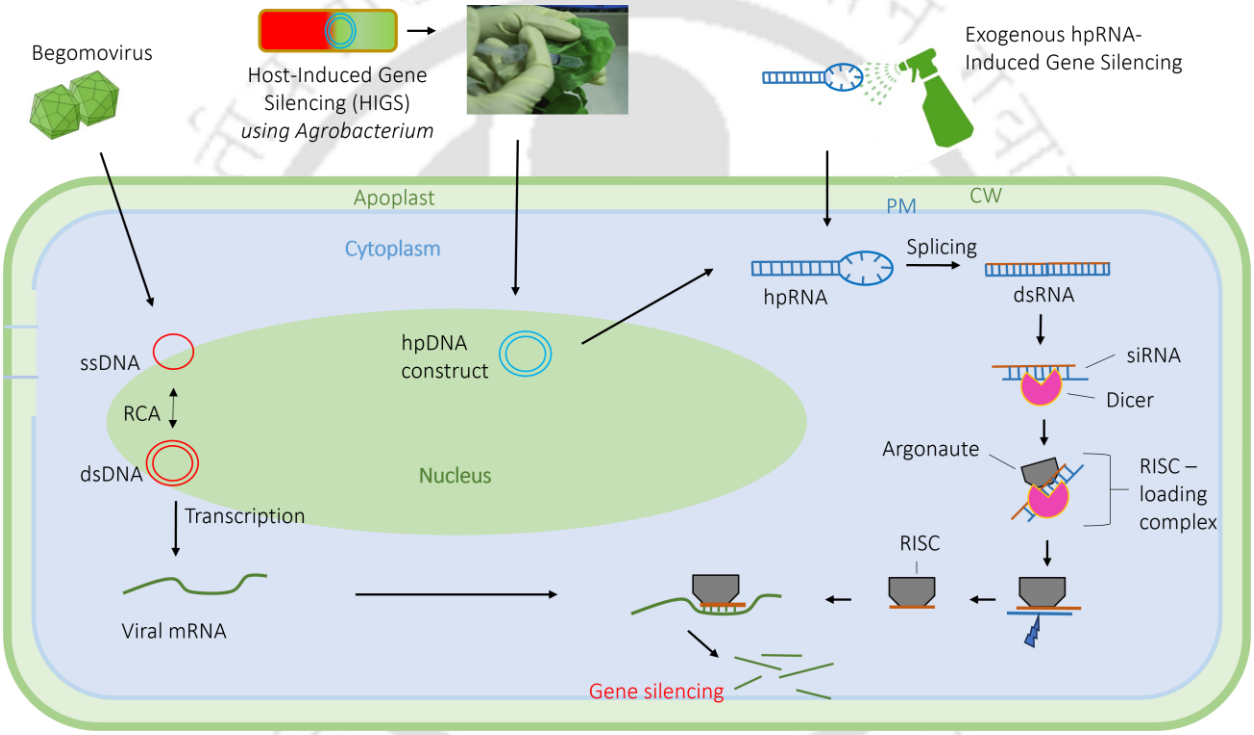

Figure 15 The RNAi activation by HIGS and SIGS.
The siRNA pathway begins with Dicer's cleavage of double stranded (dsRNA) or hairpin RNA (hpRNA) of exogenous or nuclear origin. The resulting siRNA duplex is loaded onto Argonaute by the RISC-loading complex, which comprises Dicer, a dsRBP protein such as TRBP, and an Argonaute protein. The passenger strand (blue) is cleaved and ejected. The guide strand (brown) remains bound to Argonaute, forming the RISC. The RISC binds to complementary target sequences (green) and silences them via the slicing activity of Argonaute.

https://doi.org/10.1007/s12010-023-04402-3

Chapter 2: Molecular Epidemiology of Begomoviruses Infecting Mungbean from Yellow Mosaic Disease Hotspot Regions of India

2.1 Abstract

Yellow Mosaic Disease (YMD), induced by Begomoviruses with bipartite genomes (DNA-A and DNA-B), poses a significant threat to mungbean (*Vigna radiata* L.) cultivation in the Indian subcontinent. This study addresses the epidemiology of begomoviruses affecting mungbean in YMD hotspot regions of India. Full-length genomic components from symptomatic leaves were cloned using rolling circle amplification (RCA) and sequenced. Mungbean Yellow Mosaic Virus (MYMV) was identified in Bihar, while Mungbean Yellow Mosaic India Virus (MYMIV) was found in Assam and Orissa. The population structure and genetic diversity of MYMV and MYMIV isolates from *Vigna* species in India were examined. Phylogenetic analysis revealed independent evolution of DNA-A and coevolution of DNA-B in MYMV and MYMIV. This observation was supported by a high mutation rate and recombination events in DNA-B, particularly in BV1 and BC1 genes over DNA-A, with a notable transition/transversion bias (R) for DNA-A over DNA-B. To assess the impact of Begomovirus infection, infectious clones (MYMV and MYMIV) were constructed and agroinfiltrated into eight mungbean genotypes, cowpea (*Vigna unguiculata* L.), and tobacco (*Nicotiana benthamiana*). The infected plants exhibited varying degrees of YMD symptoms. Mungbean genotypes were categorized based on disease severity score and viral titre, with cv. ML267 highly susceptible to MYMV, cv. K851 to MYMIV, and cv. PDM139 and cv. SML668 showing immunity to MYMV, and cv. Pusa Vishal to MYMIV. In conclusion, this study provides insights into the molecular characteristics, evolution, and population structure of begomoviruses affecting *Vigna* species in India. The identified genotypic variations in susceptibility to MYMV and MYMIV could contribute to breeding programs aimed at developing mungbean genotypes resistant to YMD, thereby aiding in the prevention of YMD epidemics in *Vigna* species.

Keywords: Agroinoculation · Begomovirus · Epidemiology · Mungbean · RCA · qRT-PCR

https://doi.org/10.1007/s12010-023-04402-3

2.2 Introduction

Mungbean, the third most important grain legume crop in the Indian subcontinent, provides a cheap source of high-quality dietary protein and essential nutrients (386). Despite India's position as the world's largest producer and consumer of mungbean, it faces challenges with a low average yield of 0.5 to 1.5 t/ha (3). Yellow Mosaic Disease (YMD) caused by mungbean yellow mosaic virus (MYMV) and mungbean yellow mosaic India virus (MYMIV) contributes to yield losses ranging from 10% to 100%, prevalent globally, especially in India, Bangladesh, and Pakistan (3). Transmitted by whiteflies, YMD exhibits symptoms like leaf yellowing, necrosis, stunted growth, and deformed pods with small, immature seeds (58). The bipartite genome of begomoviruses consists of two components, DNA-A and DNA-B, each approximately 2.8 kb in length. The DNA-A component encompasses seven overlapping genes that encode proteins responsible for transcriptional regulation, replication, and packing. Meanwhile, the DNA-B component encodes two proteins facilitating inter- and intracellular movement of the virus (6).

Legume-infecting begomoviruses MYMIV and MYMV in India show a specific and overlapping host range, with MYMIV more prevalent in the north, central, and east, and MYMV in the south and west (232,387). Recent reports indicate a shift in this pattern. Horsegram yellow mosaic virus (HgYMV) is reported to cause YMD in *Vigna* crops, including mungbean, in the Indian subcontinent.

YMD management utilizes pre-planting, in-season, and post-harvest strategies, with a focus on developing resistant mungbean varieties as the most sustainable approach (10). Breeding progress faces challenges in identifying resistant varieties under natural conditions, particularly due to weather-dependent whitefly activity in hotspot screening (202). Variation in whitefly populations impacts disease development, and using viruliferous whiteflies for screening has limitations. Agroinoculation-based genotype screening is advantageous, offering efficient identification of YMD-resistant mungbean genotypes independently of whiteflies (11). This approach, validated by molecular diagnosis, proves effective in numerous studies, screening for susceptibility or resistance (254).

The present study aims to (i) identify begomovirus species infecting mungbean through molecular detection in various YMD hotspot regions of India, (ii) explore sequence variability and phylogenetic relationships, (iii) investigate recombination events and population structure for understanding genetic distinctiveness of YMVs *Vigna* isolates, and (iv) identify mungbean cultivars resistant to both MYMV and MYMIV using agroinoculation, combining symptom analysis with molecular detection of viral genome accumulation through RCA and qRT-PCR expression analysis.

2.3 Materials & Methods

2.3.1 Sample Collection, DNA Isolation and RCA

A field survey was conducted during the 2018 and 2019 cropping seasons in mungbean hotspot regions of Bihar, Assam, and Odisha, India. Mungbean leaf samples, exhibiting YMD symptoms and containing whiteflies, were collected from 5 to 10 distant fields (approximately 10 km apart). Samples were frozen with liquid nitrogen and stored at -80˚C. Genomic DNA (gDNA) was extracted using the HiPurA Plant Genomic DNA Purification Kit. Rolling circle amplification (RCA) was performed on 100 ng of gDNA to amplify the begomoviral genomes. The RCA

https://doi.org/10.1007/s12010-023-04402-3

product, containing concatemers of viral DNA, was monomerized through separate restriction with EcoRI, HindIII, BamHI, PstI, and SacI. The restricted DNA fragments were cloned into pUC18 vector using respective enzymes, transformed into *Escherichia coli* strain DH5α and sequenced (AgriGenome Labs Pvt. Ltd. Kerala, India).

2.3.2 Phylogeny and Recombination Analysis

The nucleotide sequences from the samples were compared to NCBI database using BLASTn (https://blast.ncbi.nlm.nih.gov/BLAST). In silico analyses, including restriction digestion, PCR, cloning, primer design, and amino acid sequence analysis, were performed using SnapGene software (Insightful Science). All identified full-length nucleotide sequences were either deposited in NCBI GenBank or DDBJ database. For bioinformatic analysis, a total of 129 sequences, including 6 newly characterized ones, were employed in this study. These sequences were specifically chosen based on their association with begomoviruses causing YMD in *Vigna* species. The dataset consists of 68 full-length DNA-A sequences and 68 DNA-B sequences linked with MYMV and MYMIV reported in India as of March 2022. Utilizing the ClustalW algorithm in MEGA X (388), a multiple sequence alignment was conducted. Subsequently, a phylogenetic tree for DNA-A and DNA-B of MYMV and MYMIV was constructed using the MEGA X program, applying 1000 bootstrap replicates and the maximum likelihood algorithm.

2.3.3 Population Structure and Substitution Rate Estimation

Transitional and transversional substitution rates, along with transition/transversion bias (R), were calculated for DNA-A and DNA-B using Mega X software. Sequence Demarcation Tool (SDT v1.2) assessed pairwise sequence diversity, and a heat map was generated for both genomes with a 70% homogeneity threshold. Recombination events were screened using seven algorithms (CHIMERA, RDP, GENECONV, BOOTSCAN, MaxChi, SISCAN, and 3Seq) in the RDP 4.1 program with default settings (389), controlling for multiplicity using Bonferroni adjustment (with *p* values cut off of 0.05) and considering a minimum of three algorithms (390).

Genetic variability among the virus population was determined using DNA Sequence Polymorphism Software (DnaSPv.6.12). Parameters such as total mutations (η), nucleotide diversity (π), average nucleotide difference between sequences (k), total segregating sites (s), and Watterson's estimate of population mutation rate based on total mutations (θ–η) were assessed (391). Hypotheses, including Tajima's D and Fu & Li's D*, Fu & Li's F*, were evaluated to estimate neutral mutation under the DNA polymorphism framework.

2.3.4 Construction of Agroinfectious Clones of MYMV and MYMIV

To generate head-to-tail tandem repeats of MYMV Begusarai isolate and MYMIV Odisha isolate in mungbean, the DNA-B and DNA-A were amplified using a high-fidelity PCR-based method. The agroinfectious dimer clone construction is schematically represented in Figure 18. For MYMV DNA-A amplification from the template Beg-MYMV-A_pUC18 (Acc. No. OK431081), forward primer 5′-GTAAAACGACGGCCAGT-3′ and reverse primer 5′-GGCATGCGAGCTCTACGCATAATG-3′ (containing SacI restriction sites) were used. PCR conditions included denaturation at 95 °C for 3 min, followed by 30 cycles of 95 °C for 1 min, 60 °C for 1 min, and 72 °C for 3 min, with a final extension at 72 °C for 10 min. The resulting ~2.7 kb PCR products were cloned into the plant binary vector pCambia3300, creating the monomeric clone named Beg-MYMV-A_pCam. Subsequently, the 2.7 kb HindIII viral DNA fragment from "Beg-MYMV-A_pUC18" was re-cloned into Beg-MYMV-A_pCam, generating a complete

https://doi.org/10.1007/s12010-023-04402-3

DNA-A dimer in tandem (named Beg-MYMV-2A_pCam). The orientation of the dimeric clones was confirmed by HindIII digestion and sequencing. Similar procedures were followed for the preparation of agroinfectious dimeric clones of MYMV DNA-B (Beg-MYMV-2B_pCam), MYMIV DNA-A (Bhu-MYMIV-2A_pCam), and MYMIV DNA-B (Bhu-MYMIV-2B_pCam) (Table 2). All dimeric clones were transferred into *Agrobacterium tumefaciens* strain EHA105 through electroporation (25 μF, 200 Ω, 2500 V) using a Gene Pulser XCell (Bio-Rad, USA).

2.3.5 Agroinoculation

The extensively cultivated high-yielding or resistant mungbean varieties in India were carefully chosen and subjected to YMD resistance screening using infectious clones of MYMV and MYMIV. To assess the infectivity of these clones, non-host plants (Cowpea and tobacco) were also subjected to agroinfiltration. The agroinfectious clones, including MYMIV DNA-A (Bhu-MYMIV-2A_pCam) and DNA-B (Bhu-MYMIV-2B_pCam), as well as MYMV DNA-A (Beg-MYMV-2A_pCam) and DNA-B (Beg-MYMV-2B_pCam), were cultured separately in YEP medium containing antibiotics (50 μg/ml kanamycin and 20 μg/ml rifampicin) overnight at 28 °C until reaching OD600 = 0.8. The cells were harvested, resuspended in a buffer with 10 mM 2-(N-morpholino) ethanesulfonic acid (MES) and 10 mM MgCl2 at pH 5.8, and 200 μM acetosyringone. After agitation at 90 rpm at 28 °C for 1 h, the resuspended cells were infiltrated into the abaxial surface of young trifoliate leaves of 3-4 weeks-old mungbean plants (eight varieties: cv. K851, cv. Pusa Vishal, cv. Pusa Ratna, cv. Pusa-105, cv. OUM 11-5, cv. PDM139, cv. SML-668, and cv. ML267), 4-week-old cowpea plants (cv. Pusa Komal), and non-host tobacco plants (cv. *Nicotiana benthamiana*) using a 5 ml needleless syringe. The plants were then kept in a greenhouse at 25 ± 2°C with a 16/8 h light/dark cycle. Agroinoculation was performed in three combinations: 1) Beg-MYMV-2A_pCam + Beg-MYMV-2B_pCam, 2) Bhu-MYMIV-2A_pCam + Bhu-MYMIV-2B_pCam, and 3) empty pCambia3300 as a negative control.

2.3.6 Visual Symptoms and Molecular Analysis-based Detection

Based on the occurrence and intensity of typical YMD symptoms, the disease scoring of mungbean genotypes was done using the standard 0–5 scale (202). The scoring is based on the percent area of leaf symptomatic due to YMD, where 0 denotes no visible symptoms or completely immune, 1 denotes less than 5% leaf area infected (Highly resistant; HR), 2 denotes 6–10% leaf area infected (Resistant; R), 3 denotes 11–20% leaf area infected (Moderately susceptible; MS), 4 denotes 21–50% leaf area infected (Susceptible; S) and 5 denotes >51% leaf area infected (Highly Susceptible; HS). Total gDNA was isolated from the leaves of agroinoculated plants exhibiting YMD symptoms, and RCA was performed to amplify the begomoviral genome. In order to detect virus accumulation in the inoculated test plants, the RCA products were monomerized by restriction digestion with unique cutter PstI. The RCA products were also subjected to diagnostic conventional PCR analysis using DNA A specific primer set (Table 3).

2.3.7 Viral Titer Quantification by qRT-PCR

For quantification of virus titre in the inoculated plants of each genotype, quantitative real-time polymerase chain reaction (qRT-PCR) was employed. Standard curves facilitating the absolute quantification of MYMV or MYMIV were established using plasmids containing the cloned full-length Beg-MYMV-A or Bhu-MYMIV-A genomic components, following the methodology outlined by (392). Plasmids underwent serial tenfold dilution, covering a range from 10^2 to 10^8 copies of the viral genome per sample. DNA extracted from uninfected mungbean plants served

https://doi.org/10.1007/s12010-023-04402-3

Figure 16 Mungbean leaf samples collected from several YMD-hotspot fields.

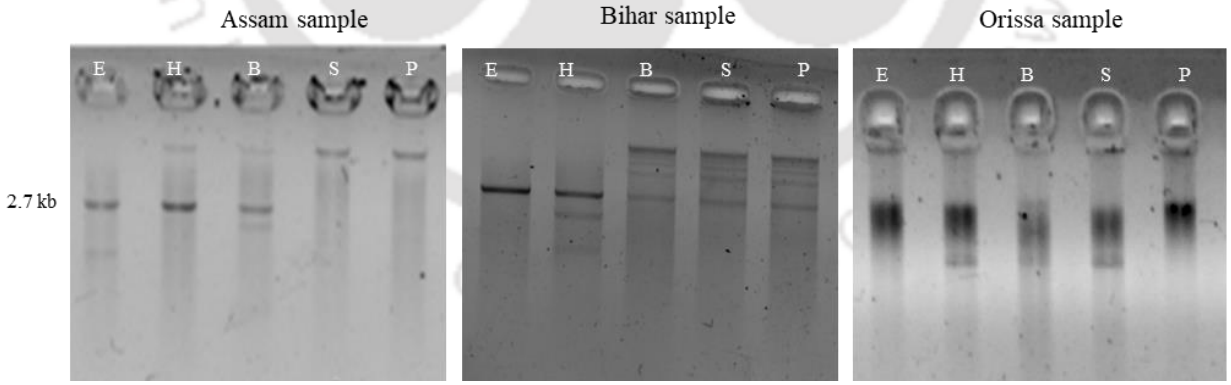

Figure 17 RCA-based amplification of begomoviruses.

https://doi.org/10.1007/s12010-023-04402-3

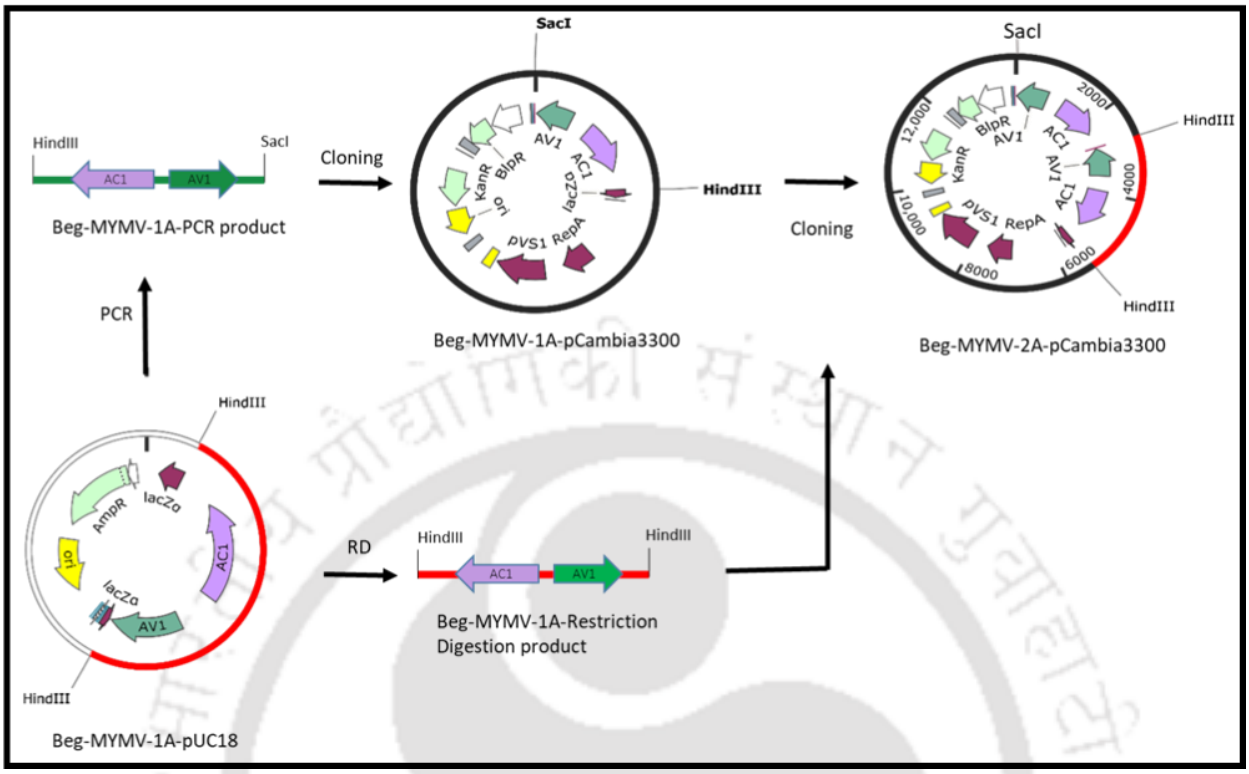

Figure 18 Schematic representation of cloning strategy followed for infectious dimeric clone preparation.

Infectious dimeric clone preparation of MYMV DNA-A. Similar strategy followed for MYMV DNA-B as well as for MYMIV DNA-A & DNA-B components in pCambia3300 plant binary vector. RD: restriction digestion.

Table 2 Set of primers used to construct agroinfectious dimeric clones.

PCR Template plasmid	Forward primer 5'-3'	Reverse primer* 5'-3'	Intermediate monomeric clone	Final Dimeric clone
Beg-MYMV-A_pUC18	tgtaaaacgacggccagt	ggcatgcgagctctacgcataatg	Beg-MYMV-A_pCam	Beg-MYMV-2A-pCam
Beg-MYMV-B_pUC18	tgtaaaacgacggccagt	cgtcgcctgcagccttctggcataagtaag	Beg-MYMV-B_pCam	Beg-MYMV-2B-pCam
Ori-MYMIV -A_pUC18	tgtaaaacgacggccagt	gagtcgacgagctctgatgctctc	Ori-MYMIV-A_pCam	Ori-MYMIV-2A-pCam
Ori-MYMIV-B_pUC18	tgtaaaacgacggccagt	cccggggctgcagctggagattcag	Ori-MYMIV-B_pCam	Ori-MYMIV-2B-pCam

https://doi.org/10.1007/s12010-023-04402-3

Table 3 Primers used to detect viral DNA in agroinfected plants via conventional PCR.

Template	Forward primer 5'-3'	Reverse primer 5'-3'
RCA product of MYMV infected samples	ctatcgccttcaatcacaatg	cattcgacatcggggtag
RCA product of MYMIV infected samples	cgtccatccataccttacccg	gtatgcgtcgttggcagattg

Table 4 Primers used for qRT-PCR to calculate viral copy number in agroinfected plants.

Template	AC1 gene specific forward primer 5'-3'	AC1 gene specific reverse primer 5'-3'
Total gDNA of MYMV infected leaf	agtgctgtgttatcagcctcg	ggcagtctaacgtcaagtacgg
Total gDNA of MYMIV infected leaf	ctaataggtctatctggccgcg	cggatattcacagagcctgtcc

as standards. Each qRT-PCR reaction comprised a 20 µl volume, incorporating 10 µl SYBR Green mix (PowerUp™ SYBR™ Green Master Mix, Applied Biosystems™), 1.6 µl (0.5 µM) of Rep (AC1) gene-specific primers (Table 4), and 1 µl of template DNA. Optimization of qRT-PCR reactions for both primer sets involved initial denaturation at 95 °C for 2 min, followed by 40 cycles of 95 °C for 15 s and 60 °C for 30 s, conducted in a Rotor-Gene® Q (QIAGEN). Standard curves were generated through linear regression analysis of Ct values over the log of total DNA content in each dilution. All reactions were performed with three technical replicates and three biological replicates.

2.4 Results

2.4.1 Cloning of Begomoviruses Associated with Mungbean YMD Hotspots in India

Leaf samples exhibiting characteristic yellow spots and leaf curling symptoms were systematically collected from mungbean hotspot regions in Bihar, Assam, and Odisha, India (Figure 16). Symptomatic plants displayed reduced pod numbers and stunted growth in comparison to their healthy counterparts. A total of 17 begomovirus clones were successfully obtained using RCA. Subsequent restriction digestion and sequencing of RCA products revealed distinctive bands of ~2.7 kb for DNA-A and ~2.6 kb for DNA-B, characteristic of begomovirus genomes (Figure 17). Notably, samples from asymptomatic plants in close proximity showed consistently negative results, indicating the absence of RCA products. The genomic sequences of DNA-A and DNA-B encoded the anticipated ORFs typical of New World begomoviruses. Detailed information on viral genomic sequences, including accession numbers and sequence identity, is provided in Table 5.

https://doi.org/10.1007/s12010-023-04402-3

Table 5 Viral components identified in mungbean collected from YMD hotspot.

Geographic Location	Isolate	DNA Type	Accession Number	Genome Size (bp)	Cloning approach, Unique cloning site	% Identity	NCBI sequence Identity with
Bihar	MYMV	DNA-A	OK431081	2730	RCA, *HindIII*	98.42%	JQ398669
	MYMV	DNA-B	OK431082	2675	RCA, *EcoRI*	96.20%	JQ398670
Orissa	MYMIV	DNA-A	OK431083	2746	RCA, *PstI*	98.03%	KU950430
	MYMIV	DNA-B	OK431084	2655	RCA, *EcoRI*	98.46%	KU950431
Assam	MYMIV	DNA-A	OK431079	2746	RCA, *PstI*	98.73%	KU950430
	MYMIV	DNA-B	OK431080	2654	RCA, *BamHI*	98.00%	KU950431

Table 6 Recombination analysis for DNA-A (1 to 13) and DNA-B (14-33).

S. No	Recombination Sequence	Breakpoint Position			Putative Major Parent	Putative Minor Parent	Methods (¥)	p value (£)
		Begin	End	Loci				
1	**OK431081**	378	984	AV1	KC911721	KX363947	RGBMCST	$8.277*10^{-50}$
2	MN698289	412	1188	AV1	MN698280	Unknown	RGMST	$5.707*10^{-42}$
3	KC911723	516	1048	AV1	KC911723	Unknown	RGBMCST	$7.353*10^{-17}$
4	MT671430	2746	1739	AC1	MT232629	Unknown	RBMCST	$8.358*10^{-10}$
5	KC911722	1185	2827	AV1	MW436692	KC911717	MST	$1.491*10^{-08}$
6	AJ416349	2464	695	AC1, AC2	KP779630	KX363947	MCT	$2.189*10^{-07}$
7	MN698295	2678	2087	AC1	AY271896	MN602422	GBMCS	$1.112*10^{-16}$
8	**OK431083**	1809	203	AV1, AC3	MT312254	KU950430	MCST	$2.345*10^{-10}$
9	MT312254	1433	41	AV1	KP313758	Unknown	MCT	$1.185*10^{-05}$
10	MW600934	674	780	AV1	NZ235792	MN698280	RGT	$2.548*10^{-05}$
11	MH324445	1599	2742	AC1	MT232629	MW917145	MCS	$1.532*10^{-09}$
12	AY271893	2351	1059	AC2, AC1	LC271790	KC911720.1	MCS	$9.967*10^{-05}$
13	DQ400847	1385	2744	AC1	Unknown	KP779630	MCST	$3.869*10^{-05}$
14	MN698290	499	1906	BV1, BC1	KP319017	MW917146	RGBMCST	$1.970*10^{-28}$
15	MZ356197	369	2501	BV1, BC1	MN020536	KP319017	RGBMCST	$7.020*10^{-18}$
16	KP828155	2102	162	BV1, BC1	EU523.46	MT232630	RMCT	$2.880*10^{-14}$
17	MT027039	371	2666	BV1, BC1	Unknown	MN698283	RGMCST	$3.828*10^{-15}$
18	**OK431080**	179	2286	BV1, BC1	AY939925	KC911729	MCST	$3.382*10^{-07}$
19	MN020536	189	285	A - rich	KC911730	**OK431082**	RGMCT	$4.150*10^{-09}$
20	**LC651663**	2505	2620	CR	MN698292	**OK431082**	RGBMCST	$1.488*10^{-07}$
21	KC911725	765	2184	BC1	DQ400849	KC911730	RGMCST	$1.472*10^{-08}$
22	MW659820	758	863	BV1	MW659819	KC911730	RGT	$1.810*10^{-08}$
23	KC911729	226	2302	BV1, BC1	KC911730	KC911724	MCST	$1.162*10^{-07}$
24	MF693402	2200	552	BV1, BC1	KP7796331	KX363948	RMS	$6.599*10^{-09}$
25	MW659820	2371	2601	CR	MF693402	KC911729	RGMCST	$9.733*10^{-06}$
26	KC911730	33	178	A - rich	Unknown	KC911729	MCST	$3.007*10^{-05}$

https://doi.org/10.1007/s12010-023-04402-3

27	LC271793	1279	2039	BC1	MT232630	LC271791	MCT	$1.185*10^{-06}$
28	MT232630	189	274	A - rich	KC911730	**OK431082**	RGT	$1.650*10^{-06}$
29	KX36398	2161	2317	CR	MT671431	AY271894	GMS	$8.626*10^{-06}$
30	KP779634	1416	2236	BC1	MW659820	EU523046	RGMST	$4.514*10^{-06}$
31	KC911729	2488	2644	CR	Unknown	KC911730	GBST	$1.755*10^{-04}$
32	MW917146	1428	2159	BC1	MW659820	AY939925	MCST	$9.078*10^{-05}$
33	KC911726	20	2575	BV1, BC1	Unknown	KP319017	MCST	$1.370*10^{-04}$

* CR, a common region of a begomovirus genome; Methods (¥): R, RDP; G, GeneConv; B, Bootscan; M, MaxChi; C, Chimaera; S, SiScan; £, The lowest P-value calculated for the underlined method in the column

Table 7 Substitution rate of MYMV and MYMIV isolates of *Vigna* species.

Virus componant	Transitional substitution rate	Transversional substitution rate	Transition / Transversion bias (R)
DNA-A	10.71-18.61	4.72-6.65	1.21
DNA-B	9.42-17.90	4.77-7.83	0.99

Table 8 Genetic structure of MYMV and MYMIV isolates of *Vigna* species.

Virus component*	S	η	π	k	θ–η
DNA-A	493	616	0.091	137.3	0.085
DNA-B	992	1440	0.127	268.5	0.142

*, virus components of all known up-to-date MYMV/MYMIV of Vigna isolate from India; π, the total number of mutations; k, the average number of nucleotide differences; η, the total number of mutations.

Table 9 Neutrality tests of MYMV and MYMIV isolates of *Vigna* species.

	Neutrality tests		
Virus componant	Tajima's D	Fu & Li's D	Fu & Li's F
DNA-A	0.23823	-0.75845	-0.25674
DNA-B	-0.37852	-0.62215	-0.39384

2.4.2 Viral DNA Sequence Analysis

The BLAST analysis and pairwise sequence comparison revealed a sequence similarity of 96–98% with other begomovirus isolates, indicating that the isolated strains are variants of previously reported begomoviruses (393). The MYMV mungbean isolate of Bihar [DNA-A OK431081: DNA-B OK431082] exhibited the highest sequence identity (96.20-98.42%) with the MYMV urdbean isolate of New Delhi [DNA-A JQ398669, DNA-B JQ398670]. The MYMIV mungbean isolates of Assam [DNA-A OK431083; DNA-B OK431084] and Orissa [DNA-A OK431079; DNA-B OK431080] showed ~98% sequence identity with the MYMIV mungbean isolate of Meghalaya (Table 5). The DNA-A component encodes seven ORFs, including two (capsid protein AV1 and pre-coat protein AV2) in the virion sense strand (5'–3') and five (Rep protein AC1, transcriptional activator protein AC2, replication enhancer AC3, pathogenicity determinant AC4 and AC5 gene) in the complementary sense strand (3'-5'). The DNA-B component encodes two predicted ORFs (nuclear shuttle protein BV1 and movement protein BC1), one in each orientation.

https://doi.org/10.1007/s12010-023-04402-3

The MYMV mungbean isolate of Bihar contains three iterons (ATCGGTGT) and a stem-loop structure (TAATATTAC) within the common region (CR) of 132 bp, whereas the MYMIV mungbean isolates of Assam and Orissa have four iterons (ATCGGTGT) and a stem-loop structure (TAATATTAC) in the CR (124 bp). Additionally, the pairwise nucleotide identity matrix suggests ~85% sequence similarity among DNA-A of MYMV and MYMIV and ~75% sequence similarity for DNA-B.

2.4.3 Phylogenetic Analysis

Phylogenetic analysis of complete DNA-A sequences of begomovirus isolates, including reported YMD-associated viruses, is presented in (Figure 19). MYMIV DNA-A sequences are categorized into three groups: Group I include isolates from soybean, urdbean, and pigeonpea from Jabalpur, Akola, and Raichur, respectively; Group II contains isolates from french bean and dolichos; and Group III includes sequences from tomato and soybean isolates from Bengal and Chitrakoot. MYMIV isolates from Assam (OK431079) and Orissa (OK431083), grouped with MYMIV sequences from Meghalaya (KU950430), Chirtakoot, and Tirupati in Group III, show a maximum sequence identity of ~98%, indicating that these are isolates of MYMIV. The phylogenetic analysis segregates MYMV DNA-A components into two groups. The majority of the viruses are clustered in Group I, containing sequences from Dharwad, Belgaum, Namakkal, and Hyderabad, while Haryana and Tirupati isolates are distantly related within the same group. In Group II, the MYMV isolate of Bihar (OK431081) shares the highest nucleotide identity (~98%) with the MYMV-Urdbean isolate from New Delhi (JQ398669).

Similarly, DNA-B components form three major groups, as shown in (Figure 20). In Group I, except for the MYMV black gram isolate (MZ235793) of Guntur, all sequences belong to MYMIV of french bean, soybean, urdbean, and pigeon pea isolates from Aligarh, Varanasi, Jabalpur, and Bhopal. Group II consists of two clusters: one contains the newly characterized MYMIV isolates of Assam (OK431080) and Orissa (OK431084), closely related to the MYMIV isolates of Meghalaya and Chitrakoot, while the other cluster contains MYMV black gram and mungbean isolates of Coimbatore, Namakkal, and Vamban. This group likely occurred due to reassortment between MYMV DNA-B and MYMIV DNA-B [62]. Group III is also segregated into two clusters: the larger cluster consists of MYMV isolates from Belgaum, Raichur, Dharward, and Hyderabad, and the other cluster includes two sequences, MYMV isolate of Begusarai (OK431081) and MYMV Urdbean isolate of New Delhi. This newly identified DNA-B component of MYMV isolate of Bihar is basal to and distinct from all other MYMV DNA-Bs.

2.4.4 Recombination Analysis

Within the populations of DNA-A or DNA-B, evidence of intertwined evolution suggests attribution to recombination events. The investigation focused on identifying putative recombination breakpoints and determining minor and major parental viruses for the sequence datasets of MYMV and MYMIV. Upon analysis, twenty-four breakpoints were found in sixty-eight DNA-A sequences, with only 13 breakpoints meeting the minimum threshold. A recombination breakpoint was observed in the AV1 gene of the MYMV isolate of Bihar (OK431081) at nucleotide positions 378 to 984, and one event for the MYMIV isolate of Orissa (OK431083) indicated a potential recombinant in the AC3 and AC1 genes (nucleotide positions 1806 to 203).

https://doi.org/10.1007/s12010-023-04402-3

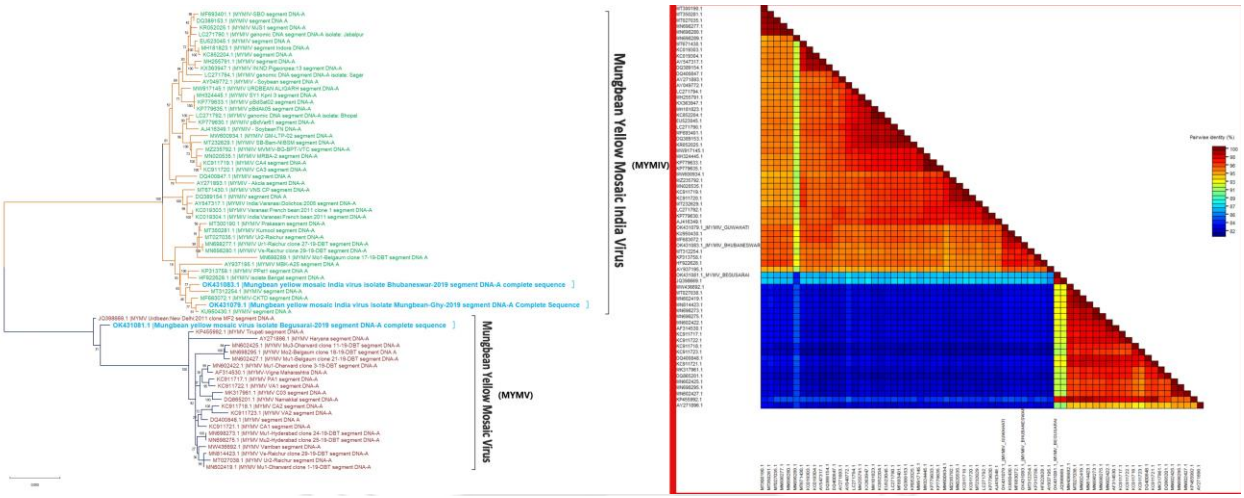

Figure 19 Phylogenetic and pairwise nucleotide identity matrix analysis of DNA-A. Phylogenetic analysis of DNA-A using maximum likelihood tree algorithm with bootstrap values of 1000 replicate (at nodes) using MEGA X software. Color pairwise nucleotide identity matrix performed using Sequence Demarcation Tool version 1.2 (SDTv1.2). **A**) Phylogenetic tree of 68 DNA-A grouped into two clades, i.e. MYMV and MYMIV, where MYMIV further segregated into 3 major groups; **B**) Color pairwise nucleotide identity matrix of the full length of DNA-A

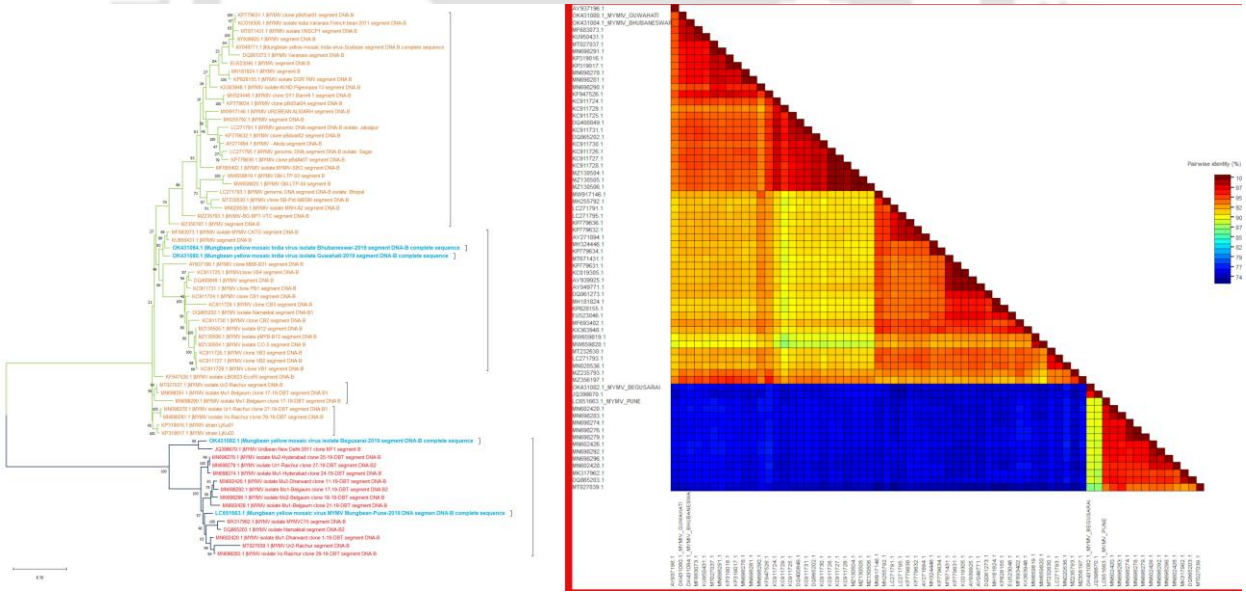

Figure 20 Phylogenetic and pairwise nucleotide identity matrix analysis of DNA-B. Phylogenetic analysis of DNA-B using maximum likelihood tree algorithm with bootstrap values of 1000 replicate (at nodes) using MEGA X software. Color pairwise nucleotide identity matrix performed using Sequence Demarcation Tool version 1.2 (SDTv1.2). **A**) Phylogenetic tree of 68 DNA-B is categorized majorly into three groups; **B**) Color pairwise nucleotide identity matrix of the full length of DNA-B.

https://doi.org/10.1007/s12010-023-04402-3

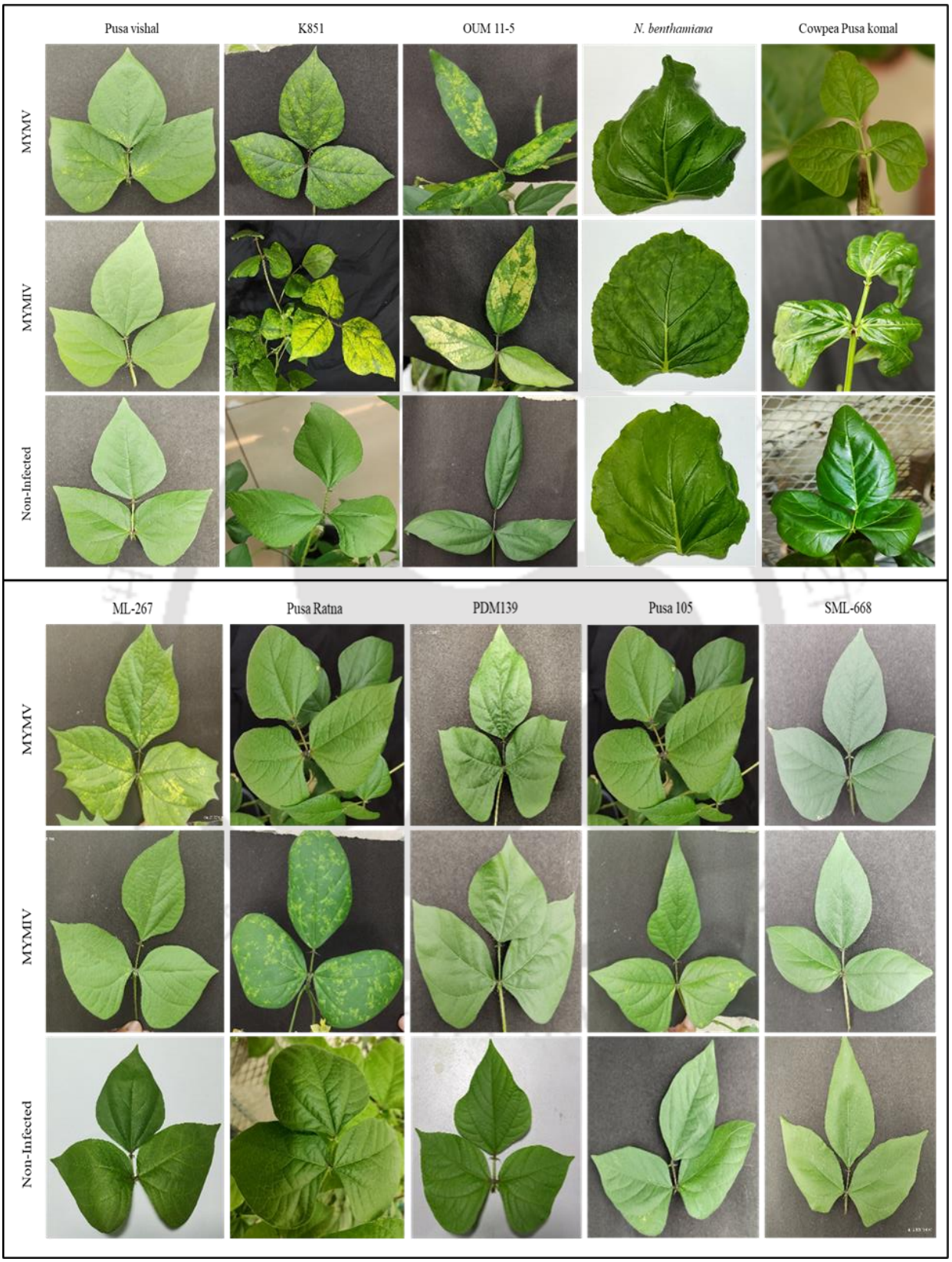

Figure 21 Systemic infection of MYMV and MYMIV in mungbean and non-host plants.

https://doi.org/10.1007/s12010-023-04402-3

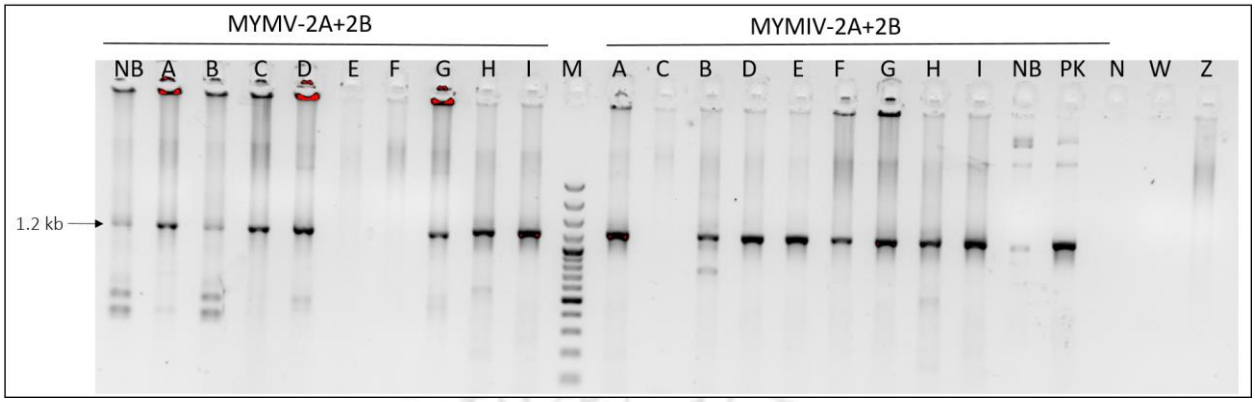

Figure 22 PCR-based confirmatory analysis of agroinoculated plants.
Conventional PCR confirmatory analysis of agroinoculated plants performed using internal primer set which is specific either to Beg-MYMV-A or Ori-MYMIV-A. (NB) N. benthamiana; (A) K851; (B) Pusa Ratna; (C) Pusa Vishal; (D) PDM139; (E) SML668; (F) Pusa 105; (G) ML267; (H) OUM 11–5; (I) positive control; (M) 100 bp DNA ladder; (PK) cowpea Pusa Komal; (N) no template, negative control; (W) noninfected mungbean cv. K851; (Z) mock inoculated by pCambia3300 in mungbean.

Table 10 Infectivity analysis of MYMV and MYMIV infectious dimeric clones.

	Host Plant Variety	Virus strain	Avg. infect -ivity	Types Symptoms (21 dpi) *	Severity grade (0-5)	PCR (¥)	RCA /R.D. (£)	GUs /100 ng DNA	Disease rating
1	PDM139	MYMV	0/10	No	0	-	-	75.33	Immune
		MYMIV	2/10	MY	1	+	+	47.33	H. resistant
2	Pusa Vishal	MYMV	9/10	YM, St	4	+	+	171208.67	Susceptible
		MYMIV	0/10	No	0	-	-	36	Immune
3	Pusa Ratna	MYMV	8/10	MY	2	+	+	12848.67	Resistant
		MYMIV	10/10	YM,St	4	+	+	174478.33	Susceptible
4	Pusa 105	MYMV	8/10	MY	2	+	+	8371.67	Resistant
		MYMIV	8/10	YM	3	+	+	21163.33	M. susceptible
5	K851	MYMV	10/10	YM, SL, LC	4	+	+	130.33	Susceptible
		MYMIV	10/10	YM,St, LC, SL	5	+	+	696069.33	H. susceptible
6	ML 267	MYMV	10/10	YM,St, LC, SL	5	+	+	689031.01	H. susceptible
		MYMIV	8/10	MY, LC	3	+	+	26796.33	M. susceptible
7	SML 668	MYMV	0/10	No	0	-	-	43	Immune
		MYMIV	3/10	MY	1	+	+	47.33	H. resistant
8	OUM 11-5	MYMV	10/10	YM, LC, SL	4	+	+	395148.33	Susceptible
		MYMIV	9/10	MY, LC	2	+	+	5865.33	Resistant

*Days Post Inoculation (dpi); LC, leaf curling; SL, small leaves; MY, mild yellowing; St, stunting; YM, yellow mosaic; + indicates the presence of viral components; ¥ Primers specific for MYMV or MYMIV DNA-A; £, RCA restriction digestion using unique site generating 2.7 kb specific to DNA-A

https://doi.org/10.1007/s12010-023-04402-3

Similarly, for DNA-B, out of twenty-five recombination breakpoints among sixty-eight DNA-B sequences, five breakpoints did not satisfy the threshold. A total of four breakpoints were detected in the isolates identified in this study. The MYMIV isolate of Bihar (OK431082) is the putative minor parent in three breakpoint events, and the MYMIV isolate of Assam (OK431080) is the potential recombinant in the other event (Table 6).

2.4.5 Genetic Structure and Demographic Analysis

Rates of different transitional substitutions of DNA-A ranged from 10.71 to 18.61, and transversional substitutions ranged from 4.72 to 6.65, with an estimated transition/transversion bias (R) of 1.21. Similarly, transitional substitutions of DNA-B ranged from 9.42 to 17.90, transversional substitutions from 4.77 to 7.83, and the estimated transition/transversion bias (R) was 0.99 (Table 7). The mutation rate plays a vital role in genetic variability to adapt to changing environments. Here, we calculated the total number of mutations (π) for DNA-A to be 0.091, and for DNA-B, it was 0.127, whereas the average number of nucleotide differences (k) of DNA-A was 136.3, and for DNA-B sequences, it was 268.5. For DNA-B, the total number of mutations (η) is higher than that of DNA-A, i.e., 1440 and 616, respectively (Table 8). Statistical deviations were calculated using neutrality tests (Tajima's D, Fu & Li's D*, and Fu & Li's F*) for sequence datasets of DNA-B and DNA-A. These tests indicated negative values for both datasets, confirming purifying selection and the conserved nature of a gene for MYMV and MYMIV in India (Table 9).

2.4.6 Infectivity Analysis of Cloned MYMV and MYMIV

The mungbean genotypes were classified based on disease severity determined by percent disease incidence (PDA), RCA-PCR method, and viral titre quantification. Agroinfectious clones of MYMV and MYMIV mungbean isolates, constructed using DNA-A and DNA-B dimers, were employed to assess their infectivity in selected mungbean, cowpea (Pusa Komal), and tobacco (*N. benthamiana)* genotypes. Typical YMD symptoms, such as yellow mosaic spots and leaf curling, were observed in infiltrated mungbean plants at 22 days post-infiltration (dpi), tobacco plants at 20 dpi, and cowpea plants at 40 dpi (Figure 21). Symptomatic plants were confirmed by PCR using AC1 and AC2–specific primers (Figure 22). Additionally, absolute quantification of MYMV and MYMIV was performed using qRT-PCR, with total DNA from agroinoculated mungbean genotypes as the template. The standard curve equation was derived by plotting Ct values against log viral DNA-A (conc= 10^ (-0.385*CT + 11.138) [R2= 0.99843] for MYMV, and conc= 10^ (-0.293*CT + 9.240) [R2= 0.99783] for MYMIV).

Among the mungbean varieties, PDM 139 and SML 668 exhibited immunity to MYMV, with a severity score of 0, an absence of viral DNA, and an insignificant viral titre (Table 10). Pusa Vishal was found to be immune to MYMIV. PDM 139 and SML 668 showed high resistance against MYMIV, with a severity score of 1, detectable viral DNA, and viral copies/Genomic Units (GUs). Immune and highly resistant varieties had <100 copies/100 ng of DNA. Resistant varieties, with 100 – 15,000 copies/100 ng of DNA and a severity score of 2, included Pusa Ratna and Pusa 105 against MYMV and OUM 11-5 against MYMIV. The MYMIV-infected Pusa 105 and ML 267 exhibited moderate susceptibility (15,000-100,000 copies/100 ng of DNA and a severity score of 3). The mungbean varieties Pusa Vishal, K851, and OUM 11-5 were susceptible to MYMV, and Pusa Ratna was susceptible to MYMIV, with 100,000-400,000 copies/100 ng of DNA and a severity score of 4. The highly susceptible varieties to MYMV and MYMIV were ML 267 and

https://doi.org/10.1007/s12010-023-04402-3

K851, respectively, with a corresponding viral titre of > 400,000 copies/100 ng of DNA and a maximum severity score of 5 (Table 10).

2.5 Discussion

Mungbean serves as a crucial grain legume, contributing significantly to the dietary protein supply in India and other South-Asian nations (394,395). However, it faces various diseases, such as Bacterial leaf blight (*Xanthomonas phaseoli*), Cercospora leaf spot (*C. canescens, C. cruenta*), powdery mildew (*Erysiphe polygoni*), and yellow mosaic disease (Viral). Yellow mosaic disease is attributed to begomoviruses, specifically MYMV, MYMIV, DoYMV, and HgYMV (9). The impact of YMD caused by MYMV and MYMIV is significant, negatively affecting mungbean seed quality and overall plant growth. Visible symptoms include yellow mosaic spots on leaves, leaf curling, and reduced pod size, ultimately leading to a substantial yield penalty (396). The first reported YMD-associated MYMV infection in mungbean and blackgram occurred in India, as documented by Nariani et al. (196). Prevalence of MYMV and MYMIV in mungbean crops has been reported in various districts of Karnataka, Tamilnadu, and Andhra Pradesh (397,398). In North India, MYMV isolates were identified as the most active strain (399), while MYMIV was prevalent in central and northeast India (400,401). This extensive survey conducted in three different Indian states aimed to identify begomoviruses responsible for YMD in mungbean.

Our study confirms the presence of MYMIV and MYMV in mungbean YMD in the Eastern (Bihar and Odisha) and North-Eastern regions (Assam) of India. Multipartite begomoviruses exhibit rapid evolution through recombination and mutation, emphasizing the need for continuous surveillance and characterization of virus populations (27). Using RCA for amplification, cloning, and sequencing, we isolated and characterized variants of MYMIV and MYMV mungbean isolates from these regions. RCA of 17 symptomatic samples identified 6 DNA components (~2.7 kb), representing DNA-A and DNA-B of MYMV and MYMIV. Comparative analysis revealed distinct relationships, with the Bihar MYMV isolate closely related to the New Delhi MYMV-Urdbean isolate, and newly identified MYMIV isolates from Bhubaneshwar and Guwahati showing similarity to a Meghalaya MYMIV isolate. Our finding aligns with previous consistent observations, indicating the sustained presence of a MYMV strain genetically most akin to a MYMV-Urdbean isolate in North India over the years. Similarly, the prevalence of the MYMV isolate of Vigna is notable in South India, while MYMIV has been documented in East India (402). Notably, the newly identified MYMIV mungbean isolates from Bhubaneshwar and Guwahati both exhibit ~98% identity with the MYMIV mungbean isolate from Meghalaya (401). Based on DNA sequence identity, we highlight new variants of MYMV and MYMIV isolates in mungbean, currently predominant in mungbean cultivation fields across India.

Phylogenetic analysis unveiled two distinct groups of DNA-A, each associated with various legume plants across diverse regions of India, confirming the independent evolution of their genomes. In contrast, DNA-B was observed to co-evolve with MYMV and MYMIV genomes, likely due to a high rate of mutation and genetic recombination events. The calculated transitions/transversions bias (R) was greater than one for DNA-A and almost equal to one for DNA-B, indicating a frequent occurrence of transitions compared to transversions in the selected viral DNA sequences. This bias is crucial for accurately inferring phylogeny, genome evolution, and divergence analysis (403). Genetic recombination and a high mutation rate are pivotal factors contributing to significant genetic variation in geminiviruses (404–406). Mixed infections may

https://doi.org/10.1007/s12010-023-04402-3

contribute to virus evolution through recombination events occurring throughout the genomic sequence in begomoviruses (401,407,408). Our recombination analysis suggests that the AC1 and AV1 regions could be recombination hotspots in DNA-A, while the BC1 and BV1 regions hold potential in DNA-B (Table 6). The A-rich and Common region of DNA-B in the MYMV mungbean isolate from Begusarai (OK431082) were identified as the putative minor parent for MYMIV mungbean isolates from Pune and Raipur. Similarly, the DNA-A component of the MYMIV mungbean isolate from Bhubaneswar (OK431083) is a potential recombinant at AV1 and AC3 genes (1809 to 203), with the MYMIV black gram isolate from Tirupati (MT312254) as the major parent and the MYMIV mungbean isolate from Meghalaya (KU9504430) as the minor parent. Detailed genetic variability and the population of other begomoviruses were analyzed to understand begomovirus evolution (59,406,407,409). Newly identified isolates share 90 to 93% sequence similarity with MYMV isolates reported until 2015 in India. In contrast, MYMV sequences reported after January 2015 (available as per the NCBI database) share more than 97% sequence similarity, potentially due to recombination events during that period. No similar pattern was observed in the case of MYMIV, as they share a close range of 95±2% sequence similarity. Genomic structure analysis predicted DNA-B to have encountered more mutations than DNA-A, with double the number of mutations and nucleotide differences observed in DNA-B. Such genetic variability evades the plant defense mechanism from time to time. Hence, periodic screening of genotypes and varieties against newly emerging viruses is crucial for identifying resistance sources against YMV.

Researchers employ a promising strategy to identify MYMV-resistant sources in mungbean. Initially, a large number of mungbean germplasms undergo screening under natural field conditions, and selected resistant genotypes are subsequently re-evaluated under controlled conditions using the agroinoculation method (410–413). Field screening, dependent on whiteflies, initially identifies 28 mungbean genotypes as resistant, but when subjected to agroinoculation, only three genotypes are confirmed as MYMV resistant (254). The agroinoculation method has recently been optimized to achieve maximum MYMV infection efficiency in mungbean plants (11). Various studies involve the development of infectious clones for MYMV and MYMIV mungbean isolates using complete dimeric viral DNA in a plant binary vector (11,13,413–416). In the present study, co-infiltration of DNA-A and DNA-B clones on host mungbean and susceptible non-host cowpea and tobacco produces typical yellow mosaic symptoms, satisfying Koch's postulates (254). Confirmation of the viral components' accumulation is achieved through the digestion of RCA products for size confirmation, followed by PCR with DNA-A specific primers, validating the virulence of the constructed clones. These clones are then utilized to assess the susceptibility of eight mungbean genotypes based on the manifestation of typical YMD symptoms.

In 2013, Paul et al. identified mungbean genotypes PDM-139 and SML-668 as moderately resistant, while Pusa-105, Pusa Vishal, and Pusa Ratna were classified as moderately susceptible to MYMV in the agro-ecological conditions of West Bengal (417). A previous report categorized PDM-139 as immune after screening it for resistance against begomoviruses with isolates from Tirunelveli, Pusa, and Ludhiana (402). Under natural field conditions, mungbean genotypes displayed diverse responses to MYMV, ranging from highly susceptible (Pusa Vishal and K851) to resistant (PDM-139) (418). Consistent with earlier findings, we confirm PDM-139 and SML-668 as immune to MYMV but highly resistant to MYMIV. While Pusa Vishal exhibited susceptibility to MYMV, as reported by Paul et al. in 2013, it surprisingly displayed immunity to MYMIV. Consequently, future studies may use the Pusa Vishal genotype as a model plant to explore its distinct response mechanisms against MYMV and MYMIV infections, contributing to

https://doi.org/10.1007/s12010-023-04402-3

a deeper understanding of plant defense mechanisms. ML-267 and K-851 were highly susceptible to MYMV and MYMIV, respectively, with altered susceptibility upon infiltration.

Pathogen detection methods based on real-time PCR offer superior sensitivity and accuracy compared to other approaches. Real-Time PCR assays utilizing SYBR Green chemistry rely on the binding of SYBR Green dye to double-stranded amplified DNA, enabling the quantification of target sequences (419). Numerous studies have demonstrated the efficacy of qRT-PCR assays in quantifying viral titers, coupled with disease symptom severity-scoring methods, to categorize plant genotypes based on their disease resistance responses (392,420,421). In this study, resistance screening was further supported by the absolute quantification of viral titers. Highly susceptible genotypes ML267 and K851 against MYMV and MYMIV, respectively, exhibited viral titers of approximately 6.5*10^5 GUs per 100 ng of genomic DNA. Immune and highly resistant genotypes showed insignificant virus titers for quantification, i.e., less than 50 GUs per 100 ng of genomic DNA. These cloned sequences can be further employed in resistance screening for various leguminous crops. Thus, this study provides a comprehensive survey of the genetic diversity of YMD-associated begomoviruses linked with MYMV and MYMIV isolates of *Vigna* species in India, along with resistance screening of eight mungbean genotypes using newly characterized sequences.

2.6 Summary

In this chapter, we conducted an epidemiological study on Yellow Mosaic Viruses (YMVs), the causative agents of Yellow Mosaic Disease (YMD) in mungbeans. Symptomatic mungbean leaf samples from YMD hotspot regions in Bihar, Orissa, and Assam, India, were assessed for the presence of YMV. Molecular analysis utilizing PCR and RCA confirmed the presence of viruses in the collected samples. Viral DNA sequence analysis revealed the presence of the MYMIV isolate in Assam and Orissa samples, while MYMV was found to be associated with samples collected from Bihar. Furthermore, phylogenetic, recombination, and mutation analysis showed differences in the ancestry of DNA-A and DNA-B. The analysis indicated a higher number of recombination events in DNA-B compared to DNA-A, resulting in increased genetic variability in DNA-B.

Additionally, we prepared agroinfectious clones of MYMV and MYMIV to screen YMD-resistant and susceptible mungbean cultivars. Our findings showed that cultivars PDM-139 and SML-668 are immune to MYMV but highly resistant to MYMIV. On the other hand, cultivar Pusa Vishal exhibited susceptibility to MYMV but immunity to MYMIV. In contrast, cv. K851 was highly susceptible to both MYMV and MYMIV. Based on these observations, we proceeded to develop resistance in cv. K851 using RNAi.

https://doi.org/10.1101/2024.03.15.585278

Chapter 3: Hairpin-RNA Spray Confers Resistance to Mungbean Yellow Mosaic India Virus in Mungbean

3.1 Abstract

Mungbean yellow mosaic India virus (MYMIV) poses a severe threat to mungbean crops, necessitating sustainable, non-transgenic control strategies. This study investigates the effectiveness of double-stranded RNA (dsRNA) for RNA interference (RNAi)-based resistance against MYMIV. Among three intron hairpin RNAi (hpRNAi) constructs - hpTR-1: AC4/AC1, hpTR-2: AC2/AC3, and hpTR-1+2: AC4/AC1_AC2/AC3 (fusion construct) - the hpTR-1+2 provided 100% protection against MYMIV in mungbean, as demonstrated by a transient agroinfiltration assay. Consequently, the hpTR-1+2 cassette was chosen for in vivo dsRNA production. Spraying of plants with dsRNA resulted in siRNA (ranging from 21 to 24 nt in length) formation in treated and nontreated distal tissues validated by semi-reverse transcription-PCR and northern blotting. Importantly, naked hpRNA spray conferred resistance to MYMIV in mungbean, with the most significant inhibition of MYMIV replication observed when plants were treated on the same day, two days, and four days before viral inoculation. This resulted in disease ratings of immune, highly resistant, and resistant, respectively, providing valuable insights for optimizing treatment scenarios.

Keywords: Mungbean yellow mosaic India virus (MYMIV), RNA interference (RNAi), Double-stranded RNA (dsRNA), Mungbean

https://doi.org/10.1101/2024.03.15.585278

3.2 Introduction

Mungbean (*Vigna radiata* L. Wilczek) is a crucial legume crop in India and South Asian countries, providing an affordable source of high-quality dietary nutrients (217,422). Cultivated in tropical and sub-tropical regions globally, India is a prominent producer and consumer of mungbean (3). Despite its significance, the average productivity of mungbean in India remains low (3). Yellow mosaic disease (YMD) poses a major challenge to mungbean cultivation worldwide (62,193). Caused by yellow mosaic viruses (YMVs) transmitted by the whitefly (5,228), YMD leads to crop yield losses ranging from 10 to 100% (8). The disease is prevalent in countries like India, Bangladesh, and Pakistan (193). YMD is caused by four distinct begomoviruses, collectively known as yellow mosaic viruses (YMVs) (9), including *Mungbean Yellow Mosaic Virus* (MYMV) (201), *Mungbean Yellow Mosaic India Virus* (MYMIV) (257), D*olichos Yellow Mosaic Virus* (DoYMV) (208), and *Horsegram Yellow Mosaic Virus* (HgYMV), all belonging to the genus *Begomovirus* within the family *Geminiviridae* (6).

The begomovirus genus, comprising 445 distinct species, is the largest in the virosphere (6). It induces economically significant diseases in crucial crops like mungbean (62). New World (NW) begomoviruses have bipartite genomes, while Old World (OW) begomoviruses exhibit both monopartite and bipartite configurations. The genome structure includes bipartite (DNA-A and DNA-B) or monopartite configurations, each circular single stranded DNA (ssDNA) components being around 2.7 kb (75). Additionally, begomoviruses are associated with circular DNA satellites: betasatellites, alphasatellites, and deltasatellites (7,55,142). Begomovirus proteins, play multifunctional roles crucial for disease development. DNA-A features six open reading frames (ORFs): two in the virion sense (AV1 and AV2) and four in the complementary sense (AC1, AC2, AC3, and AC4). DNA-B comprises two ORFs: BV1 and BC1. AV2 is unique to Old World bipartite begomoviruses, absent in New World viruses. AV1 and AV2 encode capsid protein (CP) and pre-coat protein, respectively (140). AC1, AC2, and AC3 serve as replication initiator protein (Rep) (45,132), transcription activator protein (TrAP) (88,91), and replication enhancer protein (REn) (85,98,423), respectively. AC4-encoded protein is essential for symptom production (424,425). DNA-B carries BC1 and BV1 ORFs, functioning as movement protein (MP) and nuclear shuttle protein (NSP) (107), respectively (101,106).

Among various YMD management strategies deployed, RNA interference (RNAi) is a highly effective strategy for developing durable resistance against viral diseases in plants (314). Plants employ post-transcriptional gene silencing (PTGS) to silence or knock down the expression of specific viral genes, conferring resistance (333). This mechanism involves the sequence-specific degradation of viral RNA, achieved by processing double-stranded RNA (dsRNA)/hairpin RNA (hpRNA) or partial overlapping transcripts of DNA viruses into small interfering RNA (siRNA) of approximately 21–24 nucleotides. Dicer-like enzymes facilitate this process (15). The processed siRNA binds to argonaute (AGO) protein and incorporates into the RNA-induced silencing complex (RISC), leading to the degradation of target RNA or viral transcripts with sequence similarity to the siRNA (315–317). Additionally, complementary guide RNA can serve as a primer for RNA-dependent RNA polymerase (RDR), generating secondary siRNA and ensuring the amplification of the siRNA signal (321).

The principle of RNAi has been extensively used to engineer transgenic resistance in plants against viruses (218,288,291,350,352,426). This involves genetically modifying plants with a segment of nucleotide sequence from the viral genome. Transgenic technology has successfully produced begomovirus-resistant cultivars in various legume crops, including mungbean (288).

https://doi.org/10.1101/2024.03.15.585278

While stable transgene integration allows efficient RNAi induction against geminiviruses, the broader adoption of Host-Induced Gene Silencing (HIGS) faces challenges such as limited transformation protocols, time-consuming processes, high costs, public concerns about genetically modified organisms (GMOs), stringent regulatory laws, and engineered RNA silencing trait instability (299). To address these challenges, an alternative approach has emerged, involving the induction of RNAi in plants against viruses through the external or topical application of dsRNA/hpRNA derived from the viral genome (15). This non-GMO approach is promising, efficient, and socially acceptable for viral disease management (303).

The use of externally applied naked dsRNA to prevent infection by various plant viruses was first reported by Tennellado and Diaz Ruiz in 2001 (377). Subsequent studies confirmed the efficacy of dsRNA vaccination against several plant RNA viruses (374–376,378–381). Although limited, there are reports of RNA-based vaccination against DNA viruses like begomoviruses (15). For instance, Namgiala et al. utilized RNA-based vaccination to confer protection against the bipartite geminivirus *Tomato leaf curl virus* (ToLCV) and the tripartite RNA virus *Cucumber mosaic virus* (CMV) (382). Recently, the approach was successfully employed in blackgram plants against MYMV (427). Topical dsRNA application also shows promise against monopartite geminiviruses such as Tomato yellow leaf curl virus (TYLCV) (383) and Chilli leaf curl virus (ChiLCV) (384).

In the present study, a non-transgenic approach was employed to induce resistance to YMD in mungbean. Initially, three hpRNAi constructs were transiently expressed in the MYMIV-susceptible mungbean cultivar K851, akin to previous studies (288,428), to evaluate their efficacy in providing protection against MYMIV infection. The most efficient hpRNAi clone was then selected, and from this single construct, highly efficient in vivo-produced hpRNA molecules were derived. The study revealed that the spray application of hpRNA derived from DNA A genes significantly provides protection against MYMIV in mungbean. Importantly, this research represents the first demonstration of the effectiveness of exogenously applied hpRNA against YMD in mungbean crops.

3.3 Materials & Methods

3.3.1 Biological Materials and Target Region (TR) selection

Mungbean cultivar (cv.) K851, highly susceptible to MYMIV, was cultivated in plastic pots filled with vermiculite and soil under greenhouse conditions (~25°C, 16 hours light/8 hours darkness) was used throughout the study. Infectious clones of MYMIV mungbean isolates of Orissa (GenBank Accessions: DNA-A, OK431083 and DNA-B, OK431084) were utilized to induce YMD in the mungbean plants (14).

To achieve broad-spectrum resistance against YMD, a total of 25 representative MYMV and MYMIV DNA-A components, originating from 10 different host plants in 6 countries were selected for multiple sequence alignment using the ClustalW algorithm. The sequences were obtained from the NCBI Viral RefSeq database, ensuring a comprehensive representation of the YMD causing begomovirus diversity. Two RNAi target regions (TRs) were carefully selected based on multiple criteria, including the functional significance of viral proteins, overlapping regions of ORFs, sequence length, and sequence conservation. TR-1, spanning 239 base pairs (bp), and TR-2, also 239 bp in length, encompass highly conserved regions within the viral genome.

https://doi.org/10.1101/2024.03.15.585278

TR-1 includes the overlapping section of the AC4 and AC1 genes, while TR-2 encompasses the overlapping region of the AC2, AC3, and AC1 genes.

3.3.2 Development of hpRNAi Constructs

Three hpRNAi constructs (hpTR-1_pART27, hpTR-2_pART27, and hpTR-1+2_pART27) were prepared using high fidelity PCR based method. Plasmid DNA containing a full-length DNA-A genomic component of MYMIV mungbean isolate of Orissa (Acc. No. OK431083) was used as a template for the amplification of the viral RNAi target regions using primer set with cloning restriction site (Table 11). To prepare hpRNAi cassettes, for TR-1 and TR-2 the PCR amplified target fragments were cloned in sense orientation (XhoI and KpnI) and in antisense orientation (XbaI and ClaI) on either side of PDK-intron of the intermediate vector, pKannibal (CSIRO, Plant Industry, Canberra, Australia). The constructed clones were named as hpTR-1_pKannibal and hpTR-2_pKannibal respectively. For construction of hpTR-1+2 stack RNAi cassette, the sense fragments of TR-1 (XhoI and EcoRI) and TR-2 (EcoRI and KpnI) interrupted by 8 nt gap, and antisense fragments of TR-1 (XbaI and BamHI) and TR-2 (BamHI and ClaI) interrupted by 8 nt gaps were cloned on either side of the PDK intron of pKannibal and prepared construct labelled as hpTR-1+2_pKannibal. To prepare the agroinfectious hpRNAi constructs, each hpRNAi cassette (from hpRNAi_pKannibal clones) under the control of CaMV35S promoter and OCS terminator (as NotI fragments) were subcloned into the plant binary vector, pART27. The hpRNAi clones of pART27 were finally transformed into *Agrobacterium tumefaciens* strain EHA105 by electroporation (25 µF, 200 Ω, 2500 V) in a Gene Pulser XCell (Bio-Rad, USA).

3.3.3 Efficacy Validation of hpRNAi Constructs Using Transient Assay

Agrobacterium strain EHA105 harboring hpRNAi_pART27 constructs was used against MYMIV infection in mungbean cv. K851. For transient bioassay about 5-6 plants were infected and three biological replicates were performed. Briefly, the *A. tumefaciens* strain EHA105 harboring respective clones were cultured separately in YEP medium containing antibiotics (50 µg/ml kanamycin and 20 µg/ml rifampicin) overnight at 28 °C to reach the OD_{600} = 0.6. Cells were harvested and resuspended in a buffer containing 10 mM 2-(*N*- morpholino) ethanesulfonic acid (MES) and 10 mM $MgCl_2$, pH 5.8, and 200 µM acetosyringone. The resuspended cells were agitated at 90 rpm at 28 °C for 1 h before infiltrating the abaxial surface of two trifoliate leaves of 3-4 weeks-old mungbean cv. K851 plants using a 5 ml needleless syringe and the plants were kept in greenhouse at 25 ± 2°C and a 16/8 h light/dark.

For the efficacy validation of three hpRNAi_pART27 clones, the co-infiltration of viral infectious clones (MYMIV 2A + 2B DNA components) and hpRNAi clones was performed, i.e., an equal volume of each *A. tumefaciens* cultures were mixed prior to agroinoculation. The plants were agroinoculated in five combinations, i.e., 1) MYMIV + hpTR-1_pART27, 2) MYMIV + hpTR-2_pART27, 3) MYMIV + hpTR-1+2_pART27, 4) MYMIV + empty pART27, and 5) empty pART27.

3.3.4 In vivo Production of hpRNA in *E. coli* HT115

To produce hairpin RNA (hpRNA) molecules, the hpRNAi cassette was obtained as an XhoI and XbaI fragment from the hpTR-1+2_pART27 clone. Subsequently, the L4440 vector, harboring T7 promoters at both ends, was chosen as the recipient vector for subcloning. The hpTR-1+2 cassette was ligated into the L4440 vector, creating the recombinant vector labelled as hpTR-1+2_L4440 clone. This recombinant vector was then transformed into *E. coli* HT115 (DE3) cells, which

https://doi.org/10.1101/2024.03.15.585278

possess an IPTG-inducible T7 RNA polymerase gene and lack RNAse III activity due to disrupted gene by a Tn*10* transposon (429).

Following the methodology described by (430) with minor modifications (431), single colonies of *E. coli* HT115 transformants carrying the hpTR-1+2_L4440 plasmid were cultured at 37°C with shaking for 16 hours in LB medium supplemented with tetracycline (12.5 µg/mL) and ampicillin (100 µg/mL). Each culture was then diluted 1:100 in a final volume of 0.5 L of LB medium supplemented with the same antibiotics and incubated at 37°C until reaching an OD600 of 0.5. Subsequently, 0.4 mM IPTG was added to induce T7 polymerase expression for an additional 3-4 hours. The cells were harvested by centrifugation, lysed using a lysis buffer (0.1% SDS in 1x PBS), and treated with RNaseA solution (1 µg of RNase enzyme in 5 mM EDTA, 300 mM sodium acetate, 10 mM Tris–Cl pH 8) at 37°C for 30 minutes to degrade single-stranded RNAs. Finally, dsRNA was extracted using TRIzol™ reagent (Invitrogen, USA, Cat. No. 15596026) following the manufacturer's protocol. The double stranded nature of RNA was validated by incubating hpRNA molecules with DNase I and RNase A.

3.3.5 Life Span and Systemic Movement of hpRNA and siRNA

In order to evaluate the life-span of hpRNAs and siRNA in the plants, that were not infected with MYMIV, 30 µg of hpRNAs (hpTR-1+2) was mixed with 1 ml of sterile water and syringe-inoculated in abaxial surface of trifoliate leaves without any abrasives (1 ml per plant). Five plants were used for each time point. Just before sampling, leaves were washed with Triton X-100 (0.05%) and water to eliminate residual hpRNAs present on the leaf surface. Treated plants were kept in the growth chamber as mentioned above. Trifoliate leaves from treated (local) (at time points 3, 6, 9, 12 dpi) and from non-treated (systemic) leaves (at time points 3, 6, 9, 24 dpi) were collected from all plants.

To assess the internalization of hpRNA within plant cells and its subsequent systemic movement, semi-quantitative reverse transcriptase PCR (semi-qRT-PCR) was performed. Total RNA was isolated from collected leaves using TRIzol reagent, and its quality and concentration were assessed. cDNAs were generated from 50 ng of total RNA using gene-specific primer pair AC2_S2_xhoI_FP and AC4_S2_kpnI_RP (Table 11). This same primer pair was employed to identify the presence of hpRNA (for hpTR_1+2) via PCR in both local and systemic leaves.

For the detection of hpRNA conversion to siRNA and its systemic movement, a northern blot analysis was carried out. Total RNA was isolated using TRIzol extraction and enriched for low molecular weight (LMW) RNAs in line with the procedure described by Peng et al. (432). Subsequently, 15 µg of LMW RNA samples underwent electrophoresis in an 18% polyacrylamide (19:1) gel containing 7 M urea and buffered with 0.5 X TBE using an SE600 standard dual-cooled gel electrophoresis unit (GE Healthcare, USA) until the bromophenol blue dye reached the bottom of the gel. Blots were transferred using a trans-blot SD semi-dry electrophoretic transfer unit (Bio-Rad, Cat. No. 170-3940) onto a Hybond–N membrane (Roche). The membrane was auto-crosslinked at 120,000 µJ in a Stratalinker 1800 (Agilent Technologies, Belgium). Following prehybridization in DIG Easy Hyb hybridization solution (Roche Diagnostics, Belgium) at 65°C for 30 minutes, the membrane was hybridized with a DIG-labeled TR-1+2 RNA probe (spanning 479 nucleotides) at 65°C for 12 hours in a hybridization oven. The DIG-labeled RNA probe was prepared through PCR amplification with M13-FP and AC4-S2-KpnI-RP primers (Table 11) using the hpTR-1+2_L4440 plasmid DNA as the template. After purification, 1 µg of the PCR product was used for RNA probe labeling with T7 RNA polymerase as per the DIG Northern Starter Kit's Instruction Manual (Roche). Post-hybridization washes and immuno-chemiluminescent detection

https://doi.org/10.1101/2024.03.15.585278

of the bound probe were conducted following the instructions provided in the DIG Northern Starter Kit manual (Roche). To assess siRNA size via northern blot analysis, three oligos (24 nt, 22 nt, and 20 nt) with sequences complementary to the hpRNA probe were commercially synthesized and used as an RNA ladder (Figure 26A).

Table 11 Primers used for amplification of virus sequences for the production of hpRNAi constructs.

hpRNAi Clone	Fragment	Primers	Sequence* 5' to 3'	Cloning site
hpTR-1_pART27	TR-1 sense	AC4-S-XhoI-FP	tatattctcgagcctcatctccatgttct	XhoI
		AC4-S-kpnI-RP	taggaaggtaccgcataagcgtcgttg	KpnI
	TR-1 antisense	AC4-AS-XbaI-FP	taggaatctagacctcatctccatgttct	XbaI
		AC4-AS-ClaI-RP	tattggatcgatgcataagcgtcgttg	ClaI
hpTR-2_pART27	TR-2 sense	AC2-S-XhoI-FP	tatattctcgagttctcctccgtcgat	XhoI
		AC2-S-KpnI-RP	tattaaggtaccggaccctgcttgaat	KpnI
	TR-2 antisense	AC2-AS-XbaI-FP	tatacctctagattctcctccgtcgat	XbaI
		AC2-AS-ClaI-RP	tattggatcgatggaccctgcttgaat	ClaI
hpTR-1+2_pART27	TR-2 sense	AC2-S2-XhoI-FP	atgcttctcgagtttctcctccgtcgat	XhoI
		AC2-S2-EcoRI-RP	tagtaagaattcggaccctgcttgaat	EcoRI
	TR-1 sense	AC4-S2-EcoRI-FP	tatattgaattcatcctcatctccatgttct	EcoRI
		AC4-S2-KpnI-RP	gcgcttggtaccgcataagcgtcgttg	KpnI
	TR-1 antisense	AC4-AS2-BamHI-FP	taatggggatccctcatctccatgttct	BamHI
		AC4-AS2-ClaI-RP	acagaaatcgatgcataagcgtcgttg	ClaI
	TR-2 antisense	AC2-AS2-XbaI-FP	taataatctagatttctcctccgtcgat	XbaI
		AC2-AS2-BamHI-RP	tactggggatccttggaccctgcttgaat	BamHI

* The restriction sites included in primers are underlined.

Table 12 List of primers used to detect MYMIV genome and qRT-PCR.

Template	Forward Primer (5' to 3')	Reverse Primer (5' to 3')	Purpose
RCA product of MYMIV infected samples	cgtccatccataccttaccg	gtatgcgtcgttggcagattg	To detect viral DNA in agroinoculated plants via conventional PCR (1.2 kb)
Total gDNA of MYMIV infected leaf	ctaataggtctatctggccgcg	cggatattcacagagcctgtcc	To calculate viral copy number (GUs) in Agroinfected plants by qRT-PCR

https://doi.org/10.1101/2024.03.15.585278

Table 13 TR-1 and TR-2 sequence percent Identity.

Virus	Accession	TR-1 Percent Identity	Virus	Accession	TR-2 Percent Identity
MYMV	OK431081.1	100	MYMV	OK431081.1	100
MYMV	JX244176.1	99.16	MYMV	MW736042.1	99.16
MYMV	KC911721.1	98.74	MYMV	MW736054.1	98.74
MYMV	MN814423.1	98.33	MYMV	AY738104.1	98.33
MYMV	OM106038.1	97.91	MYMV	MW792466.1	98.32
MYMV	MN698275.1	97.49	MYMV	MN698295.1	97.91
MYMV	MN602427.1	97.07	MYMV	KP784665.1	99.12
MYMV	MW736048.1	96.23	MYMV	AB017341.1	98.68
MYMV	FM242701.1	95.82	MYMV	KP455992.1	97.07
MYMV	MW814714.1	95.4	MYMV	MW736046.1	98.67
MYMV	OM106037.1	94.98	MYMV	AJ421642.1	96.65
MYMV	AM932429.1	88.8	MYMV	OM106037.1	95.82
MYMV	KP752088.1	88.38	MYMV	JQ004982.1	95.87
MYMV	MW816837.1	87.97	MYMV	AY271896.1	95.82
MYMIV	MW814709.1	87.92	MYMV	FM242701.1	95.4
MYMIV	MT027035.1	87.5	MYMV	MN885479.1	94.98
MYMIV	KP313758.1	87.08	MYMV	D14703.1	96.49
MYMIV	OK431079.1	87.14	MYMV	MW792462.1	99.02
MYMIV	HF922628.1	87.19	MYMV	MW792465.1	99
MYMIV	MT300190.1	87.08	MYMV	MW792463.1	98.99
MYMIV	KX363947.1	86.25	MYMIV	AY049772.1	91.18
MYMIV	MH255791.1	85.83	MYMIV	MW814710.1	90.79
TYLCV	MN842307.1	83.9	MYMIV	MN885468.1	98.74
CLCKV	AH013913.2	82.08	MYMIV	MN885463.1	98.33
TLCBV	AF428255.1	82.08	HgYMV	MW816839.1	93.72
TLCBV	KP164858.1	81.67	HgYMV	KR053204.1	92.05
VBSMV	FN543425.1	81.03	HgYMV	MN698287.1	91.63
TLCBV	DQ887537.1	80.33	HgYMV	KP752088.1	93.24
TYLCKV	MK946454.1	77.69	HgYMV	AM932425.1	91.21
TiCV-2	MK087038.1	78.06	HgYMV	MW816837.1	92.79

(Abbreviations: Mungbean yellow mosaic virus (MYMV), Mungbean yellow mosaic India virus (MYMIV), Cotton leaf curl Kokhran virus (CLCKV), Tomato yellow leaf curl virus (TYLCV), Tomato leaf curl Bangalore virus (TLCBV), Velvet bean severe mosaic virus (VBSMV), Tomato yellow leaf curl Kanchanaburi virus (TYLCKV), Tomato interveinal chlorosis virus-2 (TiCV-2), and Horsegram yellow mosaic virus

https://doi.org/10.1101/2024.03.15.585278

3.3.6 hpRNA Spray Assay

The study aimed to evaluate the effectiveness of hpTR-1+2 against MYMIV through five treatment combinations. These treatments (T1-T5) comprised: (T1) positive control involving MYMIV agroinoculation into three-week-old mungbean cv. K851 plants without hpRNA; (T2) mock inoculation with *A. tumefaciens* carrying empty pCambia3300, followed by a spray (5 ml perfume spray bottle) of 30 µg of hpTR-1+2; (T3) MYMIV infection, immediately followed by hpTR-1+2 spray on the same day; (T4) topical spray after MYMIV agroinoculation, with hpTR-1+2 sprayed at 2 days post-inoculation (dpi) and 4 dpi; and (T5) pre-inoculation treatments, where hpTR-1+2 was sprayed 2 days and 4 days before virus infection (Table 15).

3.3.7 Detection of MYMIV and Disease Severity Analysis

The progression of YMD symptoms in the inoculated plants was monitored on a daily basis. Disease severity scoring was performed according to a standardized 0-5 scale, as described in previous studies (14,202). Genomic DNA was isolated from the agroinoculated leaves (local) at 7 dpi and from the systemic leaves at 22 dpi. Rolling circle amplification (RCA) was conducted to amplify the MYMIV genomes. Subsequently, the size of the viral genome, indicative of geminivirus size (2.7 kb), was determined by monomerizing the RCA products containing MYMIV genomic DNA through restriction digestion using PstI, a unique cutter. To detect the presence of the virus in the inoculated test plants, diagnostic conventional PCR analysis was performed using a specific primer set targeting the MYMIV DNA A region (Table 12).

To quantify the virus titre in the inoculated plants, an absolute quantification real-time PCR (qRT-PCR) experiment using the standard curve method was conducted. Standard curves were generated by utilizing plasmid containing the cloned full-length MYMIV DNA A genomic component, following the method described by (14,433,434). Tenfold serial dilutions of these plasmid, ranging from 10^2 to 10^8 copies of the viral genome per sample, were prepared in DNA extracted from non-infected mungbean plants and used as standards. Each qPCR reaction was performed in a 20 µl reaction volume, consisting of 10 µl of SYBR Green mix (PowerUp™ SYBR™ Green Master Mix, Applied Biosystems™), 1.6 µl of Rep (AC1) gene-specific primers (Table 12), and 1 µl of template DNA. The reaction conditions were optimized for primer pair, involving an initial denaturation at 95 °C for 2 minutes, followed by 40 cycles of denaturation at 95 °C for 15 seconds and annealing/extension at 60 °C for 30 seconds, using a Rotor-Gene® Q instrument (QIAGEN). The standard curve was generated by performing linear regression analysis of the Ct values plotted against the log of total DNA content in each dilution. To ensure accuracy and reproducibility, all reactions were performed with three technical and biological replicates.

Finally, viral gene expression analysis carried out using semi quantitative reverse transcriptase-PCR. Briefly, total RNA extracted from the systemic leaves (22 dpi) using Invitrogen™ TRIzol™ Reagent (Catalog number, 15596026). Then cDNA synthesis performed using Thermo Scientific™ RevertAid™ H Minus First Strand cDNA Synthesis Kit (Catalog number, #K1632) in a 20 µl reaction volume containing random hexamer primer. The reaction mixture was incubated for 5 min at 25°C followed by 60 min at 42°C. Next, PCR was performed using 2X G9 Taq PCR Master Mix (Catalog number, #G7117) with the (Rep) or AC1 gene specific primer to detect target viral gene expression and with the *Vigna radiata* tubuline gene (*vr*Tubulin) specific primer as an internal housekeeping gene control.

https://doi.org/10.1101/2024.03.15.585278

3.3.8 Statistical Analysis

The statistical analysis of the experimental data followed a rigorous methodology to ensure robust and reliable results. Mean values with standard error bars were utilized for clear data presentation. Statistical comparisons between mean values were conducted using both the Student T-test and ANOVA F-test, depending on the nature of the analysis. All statistical tests were conducted using Graph Prism 9.0 analytical software (La Jolla, CA). For qRT-PCR analysis, all treatment combinations were treated as independent experiments, and statistical analysis was performed by ANOVA, considering a p-value < 0.05 as indicative of significance.

3.4 Results

3.4.1 Identification of Conserved Target Regions (TRs) in Begomoviruses

The study aimed to establish broad spectrum resistance against YMD in mungbean by identifying highly conserved genomic regions associated with MYMV and MYMIV. Analysis of these viruses involved in-depth examination of their complete genome sequences to identify potential targets for Host-Induced Gene Silencing (HIGS). Multiple sequence alignment analysis unveiled two conserved target regions, TR-1 (286 to 524 bp, orange color) and TR-2 (1141 to 1379 bp, green color), situated at distinct positions within the MYMIV DNA A genome (Figure 23). TR-1 and TR-2 were selected based on their exceptional sequence conservation across various begomoviruses. TR-1 displayed a high sequence percent identity with MYMV (95 to 100%), HgYMV (~88%), MYMIV (~86 to 88%), TYLCV (~84%), and Tomato leaf curl virus (TLCV, ~81%) (Table 13). Similarly, TR-2 exhibited robust sequence conservation with MYMV (97-100%), MYMIV (90-98%), and HgYMV (91-94%) (Table 13).

3.4.2 Differential Inhibition of MYMIV by Three hpRNAi Constructs in Mungbean

An evaluation was conducted to determine the efficacy of various constructs targeting MYMIV in the mungbean-MYMIV pathosystem. Response assessment and virus content monitoring were performed at 7 days post-inoculation (dpi) for inoculated leaves and at 22 dpi for systemic leaves, utilizing PCR and RCA-based restriction digestion analysis.

When mungbean plants were agroinoculated with MYMIV and hpTR-1 (AC4/AC1 hpRNAi construct), an average infection rate of 1 out of 10 was observed, without any visible symptoms (Table 14). The infection had a severity grade of 1, and though viral DNA was detected in local tissue at 7 dpi, it was notably absent in systemic leaves at 22 dpi. The qRT-PCR based quantification assays indicated a viral titre of less than 100 genomic units (GUs), indicating a highly resistant condition (Figure 25). In another scenario involving MYMIV and hpTR-2 (AC2/AC3/AC1 hpRNAi construct) agroinoculation, the infection rate was 2 out of 10, accompanied by mild yellow mosaic symptoms with a severity grade of 2. Both PCR and RCA-based analyses confirmed viral presence in both local and systemic leaves, with a viral titre between 1000 and 8000 GUs, suggesting this construct's ability to impart resistance against MYMIV. Utilizing hpTR-1+2 resulted in no observed infection among the 10 plants. No visible symptoms were recorded, and both PCR and RCA analyses displayed the absence of viral DNA in local and systemic leaves at 7 and 22 dpi, with negligible viral titre (Figure 24). Notably, it was found that hpTR-1+2 effectively restricts the systemic movement of MYMIV and its viral gene expression (Figure 25C). This illustrated the robust immunity conferred by hpTR-1+2_pART27 construct. Conversely, agroinoculation with MYMIV and an empty vector led to infections in all plants, exhibiting severe YMD symptoms with a severity grade of 5 (Table 14). Both PCR and

https://doi.org/10.1101/2024.03.15.585278

RCA analyses revealed the presence of viral DNA in both local and systemic leaves, with a viral titre surpassing 30000 GUs, indicating high susceptibility.

3.4.3 Selection and Synthesis of hpRNA

The mungbean-MYMIV pathosystem, coupled with agrobacterium-mediated transient expression assays, pinpointed the highly effective hpTR-1+2 construct. This transient assay revealed varied inhibition levels of MYMIV in mungbean leaves, with the hpTR-1+2 clone demonstrating superior effectiveness in impeding MYMIV accumulation and systemic movement compared to individual hpTR-1 and hpTR-2 constructs. Consequently, the hpTR-1+2 cassette was selected for hpRNA production. The cassette was obtained as an XhoI and XbaI fragment from the hpTR-1+2_pART27 clone and subcloned into the L4440 vector. The resulting plasmid, hpTR-1+2_L4440, was then transformed into *E. coli* strain HT115 for *in vivo* expression (Figure 26A). In the *in vivo* experiment, 1 to 1.5 mg of hpRNA was obtained from a 50 ml bacterial culture after RNase A digestion. The quality of hpTR-1+2 was assessed on a 1.5% agarose gel, and its concentration was measured using a nanodrop. Purified hpTR-1+2 underwent nuclease treatments to confirm its double-stranded nature (Figure 26B). Finally, sequence confirmation was achieved through semi-qRT-PCR analysis, using the AC2-S2-XhoI-FP and AC4-S2-kpnI-RP primer pair, amplifying a 500 bp fragment of the sense strand of hpTR-1+2 (Figure 26A and B).

3.4.4 Cellular Uptake, Systemic Movement, and siRNA Induction by hpRNA

Hairpin RNA (hpTR-1+2) was externally applied to trifoliate of 2-3-week-old mungbean plants without MYMIV infection to explore its cellular uptake, stability, and systemic movement. Purified naked hpTR-1+2 at a concentration of 30 µg/ml was sprayed onto the mungbean plants (Figure 26D). The abundance of hpRNA was assessed at various time points (3, 6, 9, and 12 days-post-spray) from both local (treated) and systemic (non-treated) trifoliate using semi-quantitative reverse transcription-polymerase chain reaction (RT-PCR) analysis (performed same as above). The results demonstrated the presence of hpTR-1+2 in both local and systemic tissues up to 12 days post-spray (Figure 26C).

To assess the potential of exogenously applied hpRNA molecules to generate siRNAs in planta, their detection was attempted through northern blot analysis. Its presence was monitored in treated (local) leaves at 3, 6, 9, and 12 days-post-spray, as well as in systemic leaves at 12 days post-spray in mungbean. Northern blot analysis utilized both sense and antisense strands of hpTR-1+2 as a DIG-labeled hybridization probe for siRNA detection. The northern blot data suggested the presence of siRNAs ranging from 24 to 22 nucleotides in length, with the intensity of siRNA signals markedly increasing from 6 days post-spray in local tissues (Figure 26E). In systemic tissues at 12 days post-spray, a lower intensity of a similar siRNA pattern was observed.

https://doi.org/10.1101/2024.03.15.585278

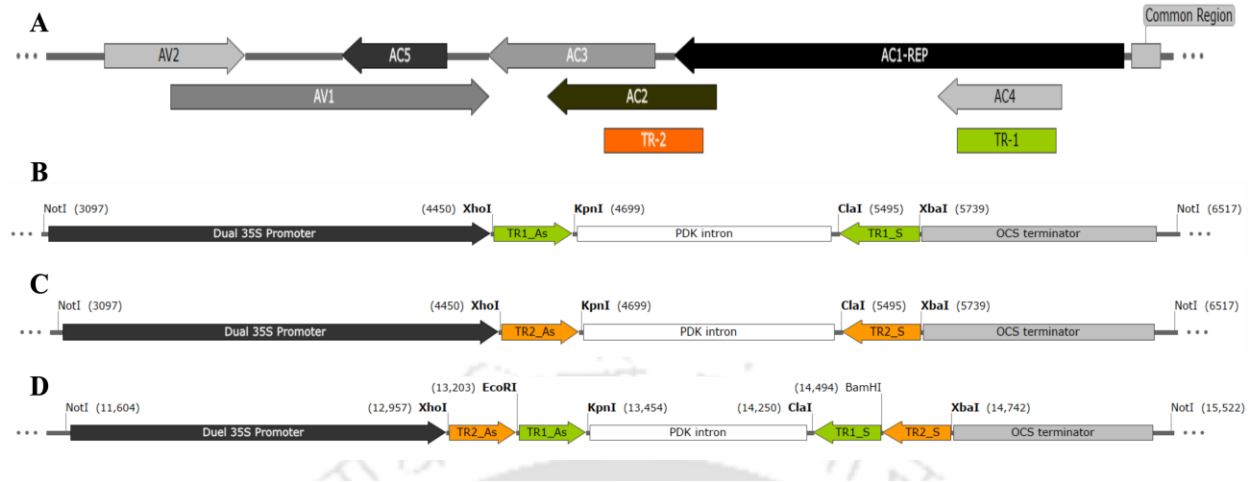

Figure 23 Schematic of MYMIV DNA A and three hpRNAi constructs.
A) A complete MYMIV DNA A genome (GenBank Accessions: OK431083) showcasing various ORFs (AC1, AC2, AC3, AC4, AC5, AV1, and AV2) and the two selected target regions (TRs): TR-1 (AC4/AC1 genes; green color) and TR-2 (AC2/AC3/AC1 genes; orange color) position is shown. Schematic T-DNA map of pART27 RNAi cassettes of TR-1 (**B**), TR-2 (**C**), and TR-1+2 (**D**) in sense (S) and antisense (As) orientation. Abbreviations: Dual 35S Promoter: Cauliflower mosaic virus 35S promoter; OCS terminator: octopine synthase terminator, PDK intron: pyruvate dehydrogenase kinase intron, Restriction enzyme NotI were used for cloning of all the three RNAi cassettes from the intermediate RNAi vector pKannibal into the plant transformation binary vector pART27.

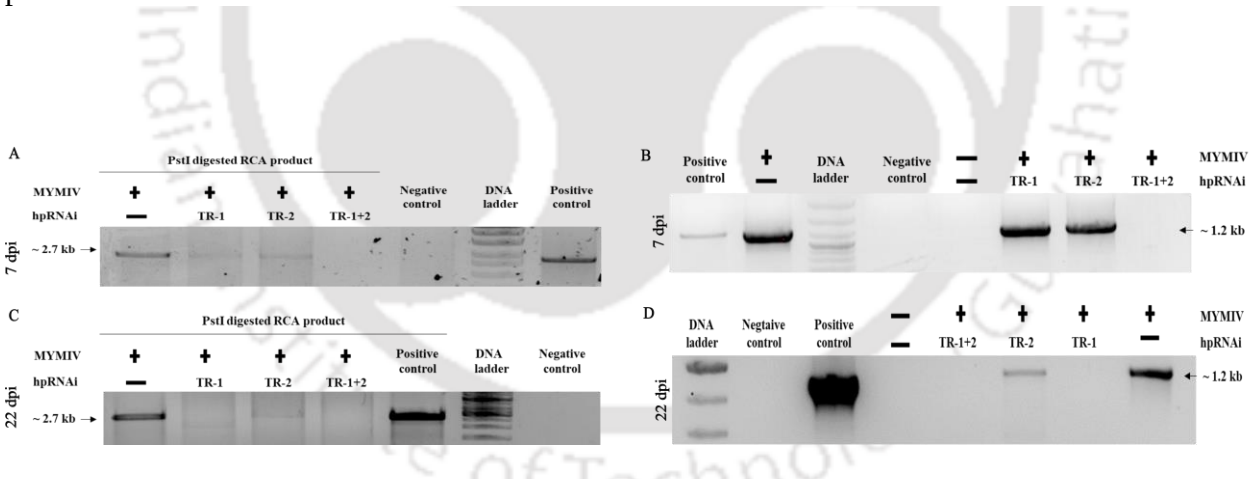

Figure 24 Resistance imparted by three hpRNAi constructs against MYMIV.
RCA analysis: RCA product generated from total genomic DNA of mungbean leaf collected at local leaves at 7 dpi **(A)** and systemic leaves at 22 dpi **(C)** from hpRNAi transient assay. RCA product subjected to restriction digestion using a unique cutter (pstI). Appearance of a 2.7 kb fragment indicates the presence of MYMIV DNA A components; Conventional PCR analysis: Detection of viral DNA using a MYMIV DNA-A specific primer. Genomic DNA extracted from mungbean leaf collected at local leaves at 7 dpi **(B)** and systemic leaves at 22 dpi **(D)** from hpRNAi transient assay.

https://doi.org/10.1101/2024.03.15.585278

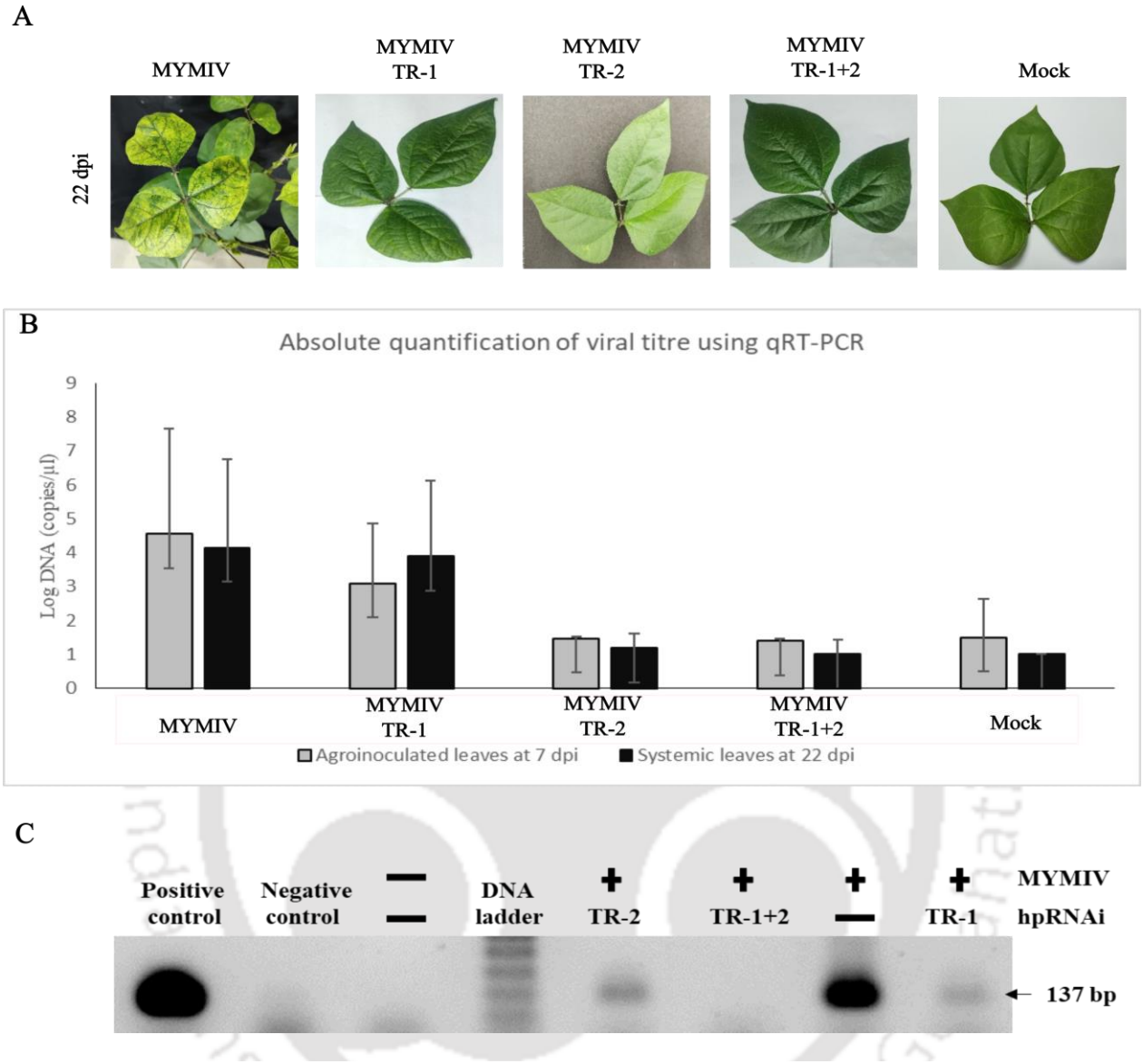

Figure 25 Efficacy of three hpRNAi constructs against MYMIV infection in mungbean.
A) Systemic symptom analysis: Evaluation at 22 dpi on mungbean plants treated with hpTR-1, hpTR-2, and hpTR-1+2 transient expression and agroinoculated with MYMIV; **B)** Viral titre measurement by qRT-PCR: Quantification in local leaves at 7 dpi and systemic leaves at 22 dpi. Data points represent means of triplicate measurements, and vertical lines on each bar indicate standard deviations. Statistically significant difference indicates ($p < 0.05$, ANOVA); **C)** Viral gene expression analysis by semi-quantitative RT-PCR: Utilizing AC1 gene-specific primer. Detection of a 137 bp fragment in systemic leaves at 22 dpi indicates the presence of viral mRNA.

https://doi.org/10.1101/2024.03.15.585278

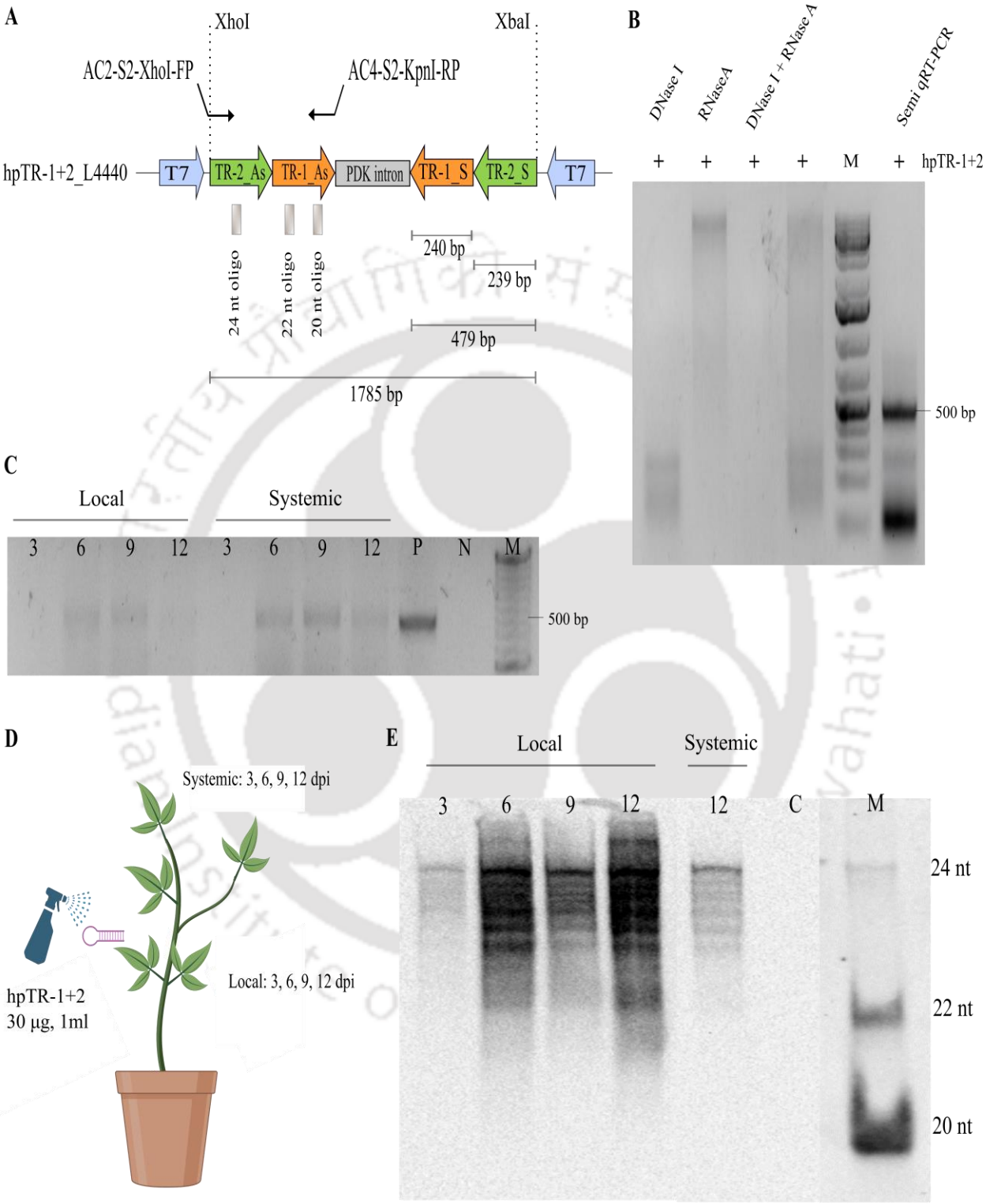

https://doi.org/10.1101/2024.03.15.585278

Figure 26 In vivo production of hpRNA, persistence, systemic movement, and induction of siRNA formation.

A) Schematic representation illustrates hpTR-1+2_L4440 plasmid: The highly efficient hpRNA cassette (hpTR-1+2) is subcloned into the L4440 plasmid, a vector with two T7 promoters. This plasmid construction is achieved through the utilization of XhoI and XbaI restriction sites. The resulting plasmid, designated hpTR-1+2_L4440, is subsequently transformed into *E. coli* strain HT115 to facilitate in vivo expression; **B)** In vivo production of hpRNA in bacteria: In this step, the *E. coli* strain HT115, hosting the hpTR-1+2_L4440 construct, is induced with 0.4 mM IPTG to initiate the in vivo expression of hpTR-1+2. Post-induction, total RNA was isolated and subjected to DNase I and RNase A treatment to confirm the double-stranded nature of the RNA. The hpRNA sequence was verified through semi-quantitative reverse transcriptase PCR (semi-qRT-PCR) using the AC2-S2-XhoI-FP and AC4-S2-kpnI-RP primer pair, amplifying a 500 bp fragment of the sense strand of hpTR-1+2. The resulting hpRNAs were electrophoresed through a 1.5% agarose gel and visualized by staining with ethidium bromide. Lane M represents 1 kb Plus DNA Ladder (Invitrogen); **C)** Detection of hpTR1+2 in local (treated) and systemic (non-treated) leaves of mungbean plants by semi-qRT-PCR analysis: This phase involves the validation of hpRNA internalization into plant cells and the assessment of its persistence and systemic movement. Leaf samples obtained from both local and systemic regions undergo semi-qRT-PCR analysis. Positive (P) and negative (N) controls are included for reference, and a DNA ladder (M); **D)** Treatment of mungbean plants and sample collection: A comprehensive schematic diagram outlines the treatment procedure of three-week-old mungbean plants. These plants are sprayed with a solution containing 30 µg/ml of hpRNA on leaves without MYMIV infection. Subsequent leaf sample collected at various time points, spanning 3, 6, 9, and 12 days-post-spray, from both local and systemic trifoliate. These samples are destined for further semi-qRT-PCR and northern blot analyses; **E)** Detection of hpTR1+2-derived small interfering RNAs (siRNAs) in local and systemic leaves of mungbean plants by northern blot analysis: This final step involves assessing the ability of hpRNA to initiate RNA interference (RNAi) in plant cells, leading to the induction of small interfering RNA (siRNA) formation. The northern blot analysis meticulously examines siRNA size, persistence, and systemic movement. Lane C represents non-treated control plants, while lane M consists of three oligomers (each with lengths of 24 nt, 22 nt, and 20 nt), serving as siRNA size references.

https://doi.org/10.1101/2024.03.15.585278

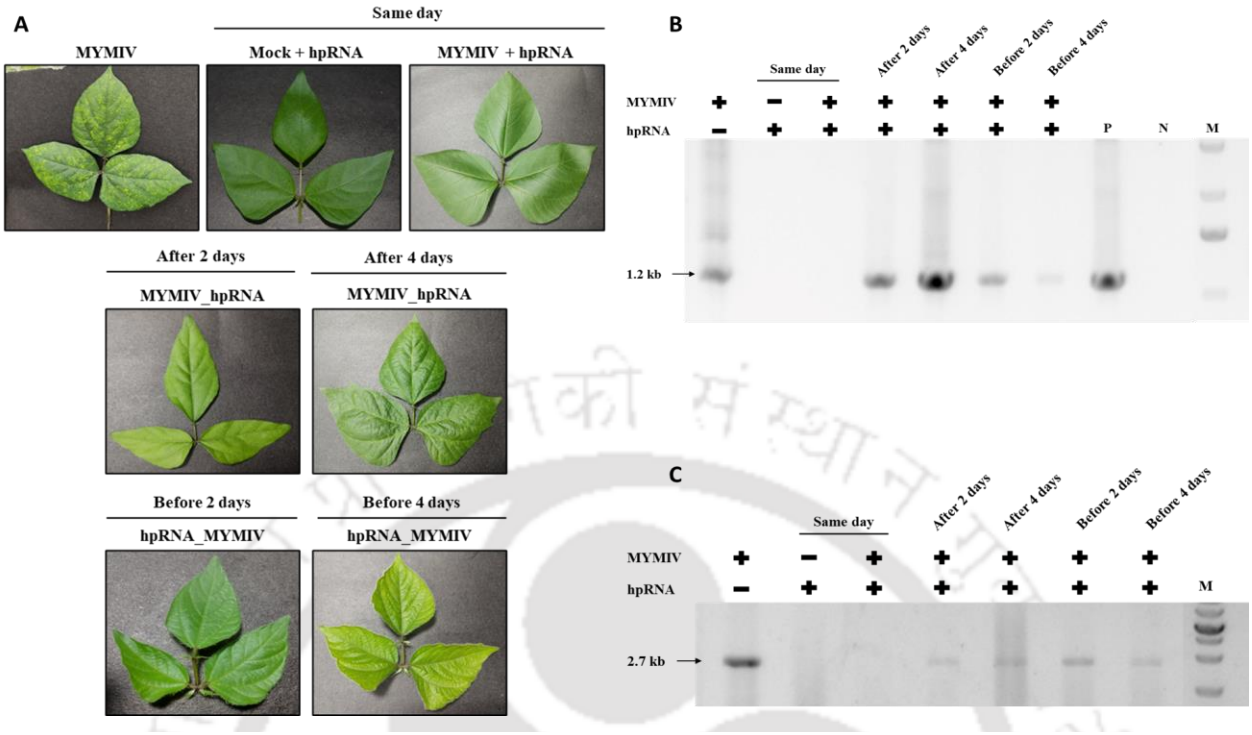

Figure 27 In vivo-produced hpRNA confers resistance to MYMIV in mungbean.
A) Phenotypic response of mungbean plants to MYMIV agroinoculation with in vivo-produced hpRNA. Inoculation scenarios: MYMIV agroinoculation without hpRNA (positive control); mock inoculation followed by 30 µg hpTR-1+2 spray; MYMIV infection, with immediate hpTR-1+2 spray; topical hpTR-1+2 spray at 2 and 4 dpi after MYMIV agroinoculation; pre-inoculation hpTR-1+2 spray 2 and 4 days before virus infection. Systemic symptoms were photographed at 24 dpi; **B)** Conventional PCR analysis: Detection of viral DNA using MYMIV DNA-A specific primer. Genomic DNA extracted from mungbean leaf collected at systemic leaves at 24 dpi from hpRNA spray assay. N, negative control (water); P, positive control (pCambia 3300 harboring MYMIV DNA A); and M, DNA Ladder; **C)** RCA analysis: RCA product generated from total genomic DNA of mungbean leaf collected at systemic leaves at 24 dpi from hpRNA spray assay. RCA product subjected to restriction digestion using a unique cutter (PstI). Appearance of a 2.7 kb fragment indicates the presence of MYMIV DNA A components.

3.4.5 Efficacy of Spray-Induced Gene Silencing Against MYMIV in Mungbean

To optimize the efficacy of hpRNA-based vaccination, five treatment combinations (refer to Table 15) were employed with MYMIV inoculation. Disease incidence was assessed at systemic leaves 24 days post-MYMIV inoculation using PCR and RCA-based restriction digestion analysis.

Mungbean plants inoculated with MYMIV without hpRNA spray exhibited typical YMD symptoms at 18 dpi, consistent with the expected timeframe for symptom appearance (Figure 27A). All plants in this treatment displayed 100% disease incidence, as confirmed by conventional PCR analysis, revealing the anticipated 1.2 kb fragment (Figure 27B). Additionally, RCA-based restriction digestion identified a characteristic 2.7 kb band (Figure 27C), affirming the infectious nature of the MYMIV inoculum and suitable environmental conditions for symptom development on mungbean plants. In contrast, mock-inoculated plants treated with hpRNA spray, using an

https://doi.org/10.1101/2024.03.15.585278

empty pCambia3300 vector instead of the vector carrying the infectious dimeric clone of MYMIV, remained healthy without exhibiting any symptoms.

Despite the topical application of single hpRNA molecules with sequence homology to key genes of MYMIV, variable levels of protection against MYMIV infection were observed in three repeated experiments. The co-application of in vivo produced hpTR-1+2 together with MYMIV on plants provided 100% protection, as evident by absence of DNA fragments in PCR and RCA based analysis and complete lack of YMD symptoms. Notably, this data suggests that spraying hpRNA on the same day as infection provides highest protection (Table 15).

The protective efficacy of hpRNA was further assessed by topical spray of hpRNA after MYMIV agroinoculation, performed at 2 dpi and 4 dpi. In this treatment, at 2 dpi, 30% of plants exhibited a disease severity of scale 3 out of 5, indicating moderate susceptibility to MYMIV. Conversely, when hpRNA was sprayed after MYMIV inoculation at 4 dpi, even less protection activity was observed. Nevertheless, hpRNA spray delayed the onset of YMD symptoms by six days, and viral DNA was detected by PCR and RCA-based analysis in systemic leaves at 24 dpi instead of 18 dpi.

The hpRNA-based vaccination activity of hpTR-1+2 was validated by topical spray of hpRNA before MYMIV agroinoculation, administered at 2 and 4 days before virus infection. Interestingly, spraying hpRNA two days before virus infection increased plant's ability to significantly restrict viral accumulation and decreased disease severity by many folds in this treatment, only 10% of the plants were infected, exhibiting high resistance to MYMIV., viral DNA was detected by molecular analysis after delayed symptom appearance at 24 dpi. More interestingly 4 days before hpRNA spray also provided help combat virus infection showed MYMIV resistance with an average infectivity of 40% and disease severity of scale 2 out of 5. Viral DNA was detected by molecular analysis after delayed symptom appearance at 24 dpi. From these results, it can be inferred that the hpRNA spray treatment before virus infection provided a certain level of protection against MYMIV infection in mungbean (Table 15).

Intriguingly, spraying hpRNA two days before virus infection significantly enhanced the plant's ability to restrict viral accumulation and decreased disease severity by many folds. In this treatment, only 10% of the plants were infected, exhibiting high resistance to MYMIV, with viral DNA detected after a delayed symptom appearance at 24 dpi. Similarly, spraying hpRNA 4 days before virus infection provided moderate protection, resulting in an average infectivity of 40% and a disease severity of scale 2 out of 5. Viral DNA was detected after delayed symptom appearance at 24 dpi. These results collectively suggest that hpRNA spray treatment before virus infection confers a certain level of protection against MYMIV infection in mungbean.

3.5 Discussion

RNA interference, triggered by dsRNA molecules, is a potent method for controlling plant viruses in transgenic plants (332). However, global approval of transgenesis is lacking, and concerns about potential adverse effects on the natural environment exist. As an alternative, a non-transgenic approach utilizing RNAi, known as 'RNA-based vaccination,' has been developed for the control of plant viruses (377). Tenllado and Díaz-Ruíz, 2001 were pioneers in reporting antiviral protection through the topical application of homologous dsRNA (377). Since then, various studies have reported the effectiveness of directly applying dsRNA to confer resistance against a broad spectrum of RNA viruses (376,377,379,381,382,435–439).

https://doi.org/10.1101/2024.03.15.585278

Table 14 Infectivity analysis of MYMIV in hpRNAi transient expression assay in mungbean.

Virus strain	hpRNAi_ pART27	Avg. infectivity	Types Symptoms (22 dpi) *	Severity grade (0-5)	Viral GUs /100 ng DNA 7 dpi	Viral GUs /100 ng DNA 22 dpi	Disease rating
MYMIV	hpTR-1	1/10	No	1	15	29	H. resistant
MYMIV	hpTR-2	2/10	MY	2	7,617	1,192	Resistant
MYMIV	hpTR-1+2	0/10	No	0	10	24	Immune
MYMIV	-	10/10	YM, St, LC, SL	5	13,979	34,731	H. susceptible
Mock	-	0/10	-	-	10	31	N/A

*Days post inoculation (dpi); LC, leaf curling; SL, small leaves; MY, mild yellowing; St, stunting; YM, yellow mosaic.

Table 15 Overview of hpRNA spray treatment combinations and YMD incidence.

Treatments	Treatment combinations	Time of hpRNA spray	Avg. infectivity	Disease rating	Disease severity score (0-5)	Symptom appearance (dpi)*
T1	MYMIV	N/A	10/10	H. susceptible	5	18
T2	Mock + hpRNA	Same day	-	-	-	-
T3	MYMIV + hpRNA	Same day	0/10	Immune	0	-
T4	MYMIV_hpRNA	After 2 days	3/10	M. Susceptible	3	24
		After 4 days	8/10	Susceptible	4	24
T5	hpRNA_MYMIV	Before 2 days	1/10	H. resistant	1	24
		Before 4 days	4/10	Resistant	2	24

*Days post inoculation: dpi

https://doi.org/10.1101/2024.03.15.585278

In the context of DNA viruses, the first study came from Namgial et al. (2019), they reported protection against a bipartite geminivirus, ToLCV in tomato plants through the direct application of dsRNAs. Their study demonstrated significant protective effects, with 45%, 60%, and 50% reductions in disease incidence when dsRNAs targeting AC1/AC4, AV1/AV2, and AC1/AC4_AV1/AV2, respectively, were applied directly (382). On the other hand, Melita et al. 2021 provided the first report on monopartite geminivirus protection. In their study, dsRNAs were synthesized in vitro, targeting the C4 and V2 genes of TYLCV. When these dsRNA molecules were topically applied onto tomato plants along with the virus (via agroinfiltration), they observed a significant reduction in disease incidence to 23% and 46%, respectively, against TYLCV (383). Spray application of a in vivo produced dsRNA cocktail targeting suppressor genes C2, V2, and C4 reduced ChiLCV (a monopartite begomovirus) incidence by up to 66.7% in *Nicotiana benthamiana* (384). In a recent study (Krishnamoorthy et al., 2023), in vitro synthesized dsRNA targeting the coat protein gene (CP) and replication initiator protein gene (Rep) of MYMV was exogenously applied (2.5 µg of dsRNA) to blackgram plants showing MYMV symptoms. This treatment led to a reduction in disease severity for several days. Among plants treated with dsRep, 80% exhibited symptom remission at the 21st day post dsRNA treatment, while for dsCP treatment, 73% of plants showed symptom remission at the 15th day (427). Though, exogenously applied dsRNA presents a promising tool for virus control, its efficacy may vary across different viruses. For DNA viruses like the begomoviruses Tomato Severe Rugose Virus (ToSRV) in tomatoes (385) and Tomato Leaf Curl New Delhi Virus (ToLCNDV) in zucchini squash (378), the application of exogenous dsRNA has shown limited effectiveness. Considering the existing research gap, this study aimed to assess the effectiveness of exogenously applied hpRNA for the control of a bipartite begomovirus, MYMIV, in economically significant mungbean plants.

In this study, two RNAi target regions for HIGS in the MYMIV genome were identified: TR-1, targeting AC4/AC1 genes, and TR-2, targeting AC3/AC2/AC1 genes (Figure 23A). In most studies, these regions were selected due to their high conservation within the viral genome (Table 13), as demonstrated in previous studies that achieved effective resistance against begomoviruses through both transgenic and transient HIGS approaches (288,353,440–445). Three hairpin RNA interference (hpRNAi) constructs were prepared using these two target regions to evaluate their efficacy against MYMIV in a transient HIGS assay (Figure 23B, C, and D). The data indicated that the hpTR-1+2 clone (a stacked clone of AC4/AC1_AC3/AC2/AC1) was the most effective, providing immunity against MYMIV in mungbean compared to individual clones (Figure 24), (Figure 25), and (Table 14). Consequently, the hpTR-1+2 clone was selected for in vivo hpRNA synthesis for the spray induced gene silencing (SIGS) assay.

In the process of inducing RNAi through topical application, the preparation of dsRNA is a crucial step. The dsRNA can be efficiently produced in vivo using bacterial expression systems (446,447), which offer convenience and economic advantages compared to in vitro methods involving RNA polymerase (448). Here, we employed a *E. coli* HT115 expression system to generate hpRNA (hpTR-1+2) in large quantities. The dose of exogenous dsRNA varied across studies: 40 to 60 µg against Zucchini Yellow Mosaic Virus (ZYMV) (379), almost 200 µg/plant against Tobacco Mosaic Virus (TMV) (376), 2.5 µg/plant against MYMV (427), 250 µg/plant against Tomato Spotted Wilt Virus (TSWV) (439), 60 µg/plant against Cucumber Green Mottle Mosaic Virus (CGMMV) (378), 15 µg/plant against ChiLCV (384), 100 µg/plant against Pepper Mild Mottle Virus (PepMoV) (375), 12 to 16 µg/plant against Cucumber Mosaic Virus (CMV) (381), 10 µg/plant against TSWV (437), and 20 to 30 µg/plant against ToLCV (382). Machado et al. (2020) found a threshold, with concentrations below 16 µg/plant providing no protection in

https://doi.org/10.1101/2024.03.15.585278

Tobacco Mosaic Virus (ToMV)-dsRNA tests, and a dose-dependent response ranging from 50 to 400 µg/plant (380). Given this context, we utilized 30 µg/plant of hpRNA against MYMIV in mungbean (Figure 26D).

To optimize the effectiveness of hpRNA in suppressing MYMIV multiplication, the timing of virus and dsRNA application is crucial. In this study, mungbean cv. K851 was treated with the virus and hpRNA separately to determine the optimum treatment scenario. The most significant inhibition of MYMIV replication occurred when plants were treated with hpRNA on the same day, two days, and four days before viral inoculation, resulting in disease ratings of immune, highly resistant, and resistant, respectively (Figure 27) and (Table 15). These treatments demonstrated higher protection efficiency compared to post-treating plants at two or four days after virus inoculation. The earlier introduction of hpRNA proved more effective, suggesting that prior treatment allows for the generation of siRNAs and the formation of RISC in advance, facilitating an immediate response upon virus infection. This underscores the importance of a certain period for hpRNA processing within cells to observe the RNAi effect of exogenous hpRNA treatment. This observation is consistent with findings from previous studies on other viruses treated with dsRNA (375).

The uptake mechanisms of exogenously applied dsRNAs remain partially understood, with absorption capacity varying among plant organs. Overcoming physical barriers like the wax layer, cuticle, cell wall, and cell membrane, successful external application of dsRNA in plants for inducing RNAi involves methods such as mechanical rubbing, pressure spray, infiltration, injection, root or petiole absorption, and nano-carrier conjugation (449). Here, leaf spraying was chosen as the method for its recognized effectiveness in inducing RNAi (450). The cellular mechanism of dsRNA-induced RNA interference (RNAi) in plants involves several steps: Cellular uptake of dsRNAs, followed by rapid cleavage by DICER-LIKE (DCL) endonucleases into 20 to 25-nucleotide siRNAs with 2-nt 3´ overhangs at both ends. Subsequently, one strand of siRNAs is incorporated into an ARGONAUTE (AGO) protein to form an RNA-induced silencing complex (RISC). Finally, the siRNA molecules guide the RISC to scan the cytoplasm for recognition and cleavage/degradation of complementary transcripts, leading to post-transcriptional gene silencing (PTGS) (451,452).

Despite the transient nature of protection, both hpRNA and siRNA molecules (21 to 25 nucleotides long) remained detectable on local and systemic leaves for at least 12 days, as shown in (Figure 26C and E). This observation suggests that a significant portion of hpRNA may have entered the leaf apoplast through spray application as it is the first barrier before entering inside cells, facilitating systemic transport to other parts of the plants. Microscopic analyses have demonstrated the presence of spray-applied dsRNAs in various plant structures, including the apoplast (453). Subsequently, this transport might have triggered RNAi in receiving plant cells, leading to the formation of siRNA from hpRNA. Our results indicate the need for a gradual and continuous introduction of dsRNA/hpRNA into the cells or the implementation of a sustained amplification mechanism for specific RNA processing machinery to achieve durable and efficient resistance in plants.

In this study, we report a short protection window with the use of naked hpRNAs spray approach. This limitation could be addressed by exploring alternative delivery methods, such as high-pressure spraying, and investigating nanoparticle-based delivery approaches (454). These methods have the potential to enhance the stability and efficacy of exogenously applied dsRNAs when compared to naked dsRNA delivery (455,456).

https://doi.org/10.1101/2024.03.15.585278

3.6 Summary

In this chapter, we explore a non-transgenic approach to induce resistance against YMD in mungbean. Multiple viral target regions were identified for gene silencing using RNAi. Transient expression analysis identified the hpTR-1+2 stack clone (AC4/AC1_AC2/AC3) as an efficient target construct against MYMIV. In vivo-synthesized hpRNA (hpTR-1+2) was found to induce RNAi in planta, as validated by siRNA detection. The study reveals a protective window with the naked hpRNA spray approach, demonstrating significant inhibition of MYMIV replication when applied on the same day, two days, or four days prior to viral inoculation.

https://doi.org/10.1007/s00299-024-03247-2

Chapter 4: Identification of Mungbean Yellow Mosaic India Virus and Susceptibility-associated Metabolites in the Apoplast of Mungbean Leaves

4.1 Abstract

The apoplast, an extracellular space surrounding plant cells, is integral in plant-microbe interactions, influencing signaling, defense mechanisms, and nutrient transport. While the involvement of the apoplast and extracellular vesicles (EVs) in RNA virus infection is well-documented, the role of the apoplast in plant DNA viruses remains uncertain. This study investigates the apoplast's involvement in Mungbean yellow mosaic India virus (MYMIV) infection. Our results reveal the presence of MYMIV genomic components in apoplastic fluid, suggesting potential cell-to-cell movement of begomoviruses through the apoplast. Additionally, MYMIV infection induces heightened secretion of EVs into the apoplast. Metabolomic analysis using NMR indicates altered metabolic profiles in both apoplast and symplast in response to MYMIV infection, with notable changes in metabolites associated with stress and defense responses. Elevated levels of α- and β-glucose in both apoplast and symplast suggest a shift in glucose utilization. Surprisingly, this increase in glucose does not correlate with the synthesis of phenolic compounds, potentially impacting mungbean susceptibility to MYMIV. Fructose levels increase in the symplast, while apoplastic sucrose levels rise significantly. Symplastic aspartate levels rise, and apoplastic proline concentration increases while cytosolic levels decrease, indicating a potential role in triggering a hypersensitive response. These findings underscore the significant role of the apoplast in begomovirus infection and offer insights for targeted viral disease management strategies.

Keywords: Apoplast, Exosomes, Mungbean yellow mosaic India virus (MYMIV), NMR, Metabolomics

https://doi.org/10.1007/s00299-024-03247-2

4.2 Introduction

Geminiviruses (*Geminiviridae*), a plant-infecting virus family, pose a substantial threat to crucial agricultural crops (10), including mungbean, an important legume crop (3). Within this family, the *Begomovirus* genus is the largest, comprising over 450 species (6), with a particular emphasis on mungbean yellow mosaic India virus (MYMIV) in this study. These viruses encapsulate their single-stranded DNA (ssDNA) genomes into twin icosahedral particles [dimensions of approximately 18 to 22 × 38 nm, composed of two incomplete icosahedra (T=1)], with mono- or bipartite (DNA A and DNA B) genomes ranging from 2.5 to 3 kb each (27,136). These viruses are transmitted by the whitefly (*Bemisia tabaci*), in a circulative and persistent manner (200). Because of their limited coding capacity, they heavily rely on the host's cellular machinery for replication and other essential processes (457). Replication of their ssDNA genomes occurs by rolling circle replication, and recombination-dependent replication via double-stranded intermediates (122,127,458,459). Viral movement proteins (MPs) and nuclear shuttle proteins (NSPs) play multiple roles by of begomoviruses interacting with host factors to facilitate both intra- and intercellular viral movement (460).

Plant viruses, functioning as intracellular parasitic pathogens, utilize a symplastic route via PD for cell-to-cell movement. Whereas, RNA viruses like turnip mosaic virus associate their RNA genome and proteins with multi-vesicular bodies (MVBs), releasing them into the leaf apoplast (19). In the case of potato virus X-infected plants, virus particles and RNAs are detected in the apoplast, although they are not associated with extracellular vesicles (EVs) (20). The presence of viral proteins, RNA, and virus particles in the plant apoplast highlights its crucial role in viral infection, particularly in the systemic spread of the virus within the host. However, the role of the apoplast and EVs in the cell-to-cell genome transmission in begomoviruses, is still not known.

The apoplast, situated beyond the plasma membrane, is a pivotal extracellular space in plant physiology, hosting dynamic apoplastic fluid (AF) with a diverse composition, including EVs (461–464). The plants' secretome comprises proteins (465,466), RNA (467,468), metabolites (469), antimicrobial molecules (470), antioxidants (471,472), reactive oxygen species (473,474), and enzymes (475,476) exported from the symplast. This apoplastic components plays essential roles in growth regulation (477), cell wall maintenance (465), stress protection (478), transportation, cell signaling (478–480), and gas exchange. Proteomics approaches have identified roles for secreted proteins in the AF (479,481–484), while metabolomic investigations in the plant apoplast face challenges due to lower abundance compared to intracellular components. The vacuum-infiltration-centrifugation (VIC) method is commonly used to extract AF from in planta systems (485).

The primary objective of the study is to investigate the role of the mungbean leaf apoplast in MYMIV infection. We aim to study the presence of MYMIV in AF through the molecular detection of the viral genome using RCA and PCR analysis. We explore whether MYMIV infection induces vesicle formation by employing TEM, dynamic light scattering, and fluorescent quantification using $DiOC_6$ dye. In addition, we investigate apoplastic and symplastic metabolites related to stress and defense in response to MYMIV infection using NMR-based metabolomics.

4.3 Materials & Methods

https://doi.org/10.1007/s00299-024-03247-2

4.3.1 Plant Selection and Agroinoculation

Agro-infectious clones MYMIV DNA-A and DNA-B (Acc. no. OK431083 and OK431084) were used to agroinoculate mungbean cv. K851 (susceptible host) plants from our previous study (14). The abaxial surface of young trifoliate leaves of 3–4-week-old mungbean plants were virus inoculated. Three biological replicates were maintained in an insect-free greenhouse and monitored for the appearance of YMD symptoms. After 30 days post-infection (dpi), symptomatic leaf samples were collected and total genomic DNA (gDNA) was isolated using HiPurA plant Genomic DNA Purification Kit (HiMedia). To confirm viral infection, we employed rolling circle amplification (RCA) using TempliPhi™ DNA amplification kit (GE Healthcare). The RCA products were then monomerized through restriction digestion using the unique cutter PstI. Additionally, PCR was conducted to validate the presence of MYMIV DNA-A, utilizing a DNA-A specific primer set (Table 17).

4.3.2 Recovery of Apoplast Wash Fluid (AWF) and Leaf Without Apoplast (LWA)

To obtain apoplastic wash fluid (AWF), leaves from MYMIV-infected and uninfected mungbean plants were collected at the same time of day after 30 days post-infection (dpi). The isolation of AWF followed the protocol outlined by Rutter et al. (2017) with slight modifications (486). Leaves were initially rinsed with double-distilled water, tap-dried, and subsequently placed in a 60 mL syringe. Infiltration was carried out using vesicle isolation buffer (VIB) containing 20 mM 2-(N-morpholino) ethanesulfonic acid (MES) at pH 6, 2 mM CaCl2, and 0.1 M NaCl. After infiltration, the samples were blotted dry, transferred to a 30 mL syringe, and then centrifuged in a 50 mL falcon tube at 1800 x g for 15 minutes at 4 °C. The flow-through was carefully transferred to a fresh tube and subjected to centrifugation at 10,000 x g for 30 minutes at 4 °C to eliminate any remaining large particles from the AWF. This step was executed assuming the extraction of the majority of apoplastic fluid, designated as the "apoplastic fraction." The residual leaf tissue, labeled as leaf without apoplast (LWA), represented plant intracellular components and is now referred to as the “symplast fraction”. The AWF and LWA were immediately frozen with liquid nitrogen and stored at -80 °C for future use (487).

4.3.3 NMR Sample Preparation and Experiment

For metabolite extraction from the AWF, 1 mL of AWF was rapidly frozen using liquid nitrogen, lyophilized, and dried. The AWF sample was resuspended in an equal volume of aqueous methanol solution (80% v/v) and vortexed for 20 seconds (488). After centrifugation at 12,000 x g for 30 minutes at 4 °C, the supernatant was transferred to a fresh tube, evaporated using a SpeedVac concentrator (Eppendorf AG) at room temperature for 9 hours. The dried sample was dissolved in 600 µl of D2O with TMS and immediately transferred to a 5 mm NMR tube (Sigma-Aldrich). In contrast, for metabolite extraction from LWA samples, 100 mg of LWA tissue was homogenized with liquid nitrogen in a sterile mortar and pestle. The powder was suspended in a 1.5 mL aqueous methanol solution (80% v/v), vortexed for 20 seconds, and further extracted by ultrasonication for 5 minutes (Pulse ON: 20 sec; Pulse OFF: 10 sec) in ice-cold conditions. The extracted LWA sample was then prepared following the same protocol as the AWF sample. All experiments were conducted in triplicate.

The NMR spectroscopy analysis performed as previously described by Maravi et al. (2022) and Chen et al. (2019) (489). Briefly, the prepared metabolite samples were tested on Bruker Avance III 600 MHz spectrometer ((BrukerBiospin) operating at 600.17 MHz at 25 °C temperature (acquired data: free induction decay (FID) files; acquisition time: 3 sec.; spectral

https://doi.org/10.1007/s00299-024-03247-2

width: 16.0 ppm). The metabolite signals were analyzed using ^{1}H spectrum, 2D COSY (homonuclear correlation spectroscopy), ^{1}H-^{13}C HMBC, and 2D HSQC (^{1}H-^{13}C, heteronuclear single quantum coherence spectrometry) (490).

4.3.4 Spectra Processing and Statistical Analysis

The acquired ^{1}H-NMR spectrum was phase- and baseline- corrected, normalized and referenced at TMS peak (0.00 ppm) using MestReNova software (Version 9.0.1, Mestrelab Research). Then performed region binning with a bin width of 0.02 ppm ranging from 0.5 to 10.0 ppm based on sum intensities method. The methanol (3.29–3.32 ppm) and water (4.80–4.92 ppm) regions were excluded from binned dataset prior to multivariate data analysis (MVDA). The SIMCA software (version 17.0, Umetrics) was used to analyze the ^{1}H NMR binned dataset, which was normalized by Pareto scaling and log-transformation. The classification methods such as principal component analysis (PCA) and partial least squares discriminant analysis (PLS-DA) were used to explore class differences and highlight explanatory metabolites in MYMIV-infected and uninfected samples. Orthogonal partial least squares discriminant analysis (OPLS-DA) was employed to obtain the maximum class separation and verify the results with R^2X and Q^2 values. The MVDA methods were validated with 100 permutations analysis and Tukey's test was used to identify statistically significant differences ($P < 0.05$) between metabolites.

4.3.5 Metabolite Identification and Pathway Analysis

The metabolites corresponding to the peaks were identified using 1D ^{1}H and 2D ^{1}H–^{13}C NMR spectra, referencing the ChenomX NMR Suite (ChenomX Inc.), human metabolome database (https://hmdb.ca/) and consulting relevant literatures (491–499). The list of significant metabolites identified by multivariate data analysis was then used to study the differences in metabolic pathways by utilizing MetaboAnalyst 6.0 (https://www.metaboanalyst.ca/).

4.3.6 AWF DNA Extraction and Molecular Analysis

To detect viral DNA presence in the AWF solution obtained from both MYMIV-infected and uninfected mungbean leaves, total apoplastic DNA samples were extracted using the phenol/chloroform extraction method with slight modifications (500). The extracted AWF DNA underwent RCA using the TempliPhi™ DNA amplification kit (GE Healthcare) to amplify the circular DNA genomes of MYMIV. Subsequently, the resulting RCA product, consisting of concatemers of viral DNA, was utilized as a template for another RCA reaction to enrich viral genomes. After enrichment, the RCA products were monomerized through restriction digestion using the unique cutter PstI for MYMIV DNA A detection and MfeI for DNA B detection. Additionally, conventional PCR analysis was conducted on the enriched RCA products. PCR reactions employed MYMIV DNA-A and DNA-B specific primer sets (refer to Table S1) to target and amplify the respective regions of viral DNA. To identify any potential genomic DNA contamination, PCR reactions included a mungbean (*Vigna radiata*) tubulin gene-specific primer pair (Table 17).

4.3.7 Extracellular Vesicles Extraction

The AWF solution was passed through a 0.2 µm membrane and then subjected to centrifugation at 10,000 x g for 30 minutes at 4°C. The EVs were isolated from the AWF using successive ultracentrifugation steps. The ultracentrifugation was performed using a rotor (F50L-24 x 1.5) and

https://doi.org/10.1007/s00299-024-03247-2

1.5 mL ultra-microtube (Thermo Scientific) in the Thermo Scientific™ Sorvall™ WX+ ultracentrifuge series at 4°C. The two populations of EVs were obtained by centrifuging the AWF at 50,000 x g for 60 minutes at 4 °C (P50) and 100,000 x g for 60 minutes at 4 °C (P100). After centrifugation, the pellets were resuspended in vesicle isolation buffer (VIB) for further analysis (501).

4.3.8 Transmission Electron Microscopy (TEM)

To investigate the shapes and sizes of EVs, TEM was conducted using a JEM-2100 transmission electron microscope (JEOL) (501). In brief, the AWF solution was diluted 100-fold in VIB buffer and applied to a 300-mesh carbon-coated copper grid (Ted Pella, Inc.). Subsequently, the grids were negatively stained with 50 µl of 2% uranyl acetate, air-dried, and imaged at 80-100 kV. The resulting TEM images were subjected to analysis using ImageJ software.

4.3.9 Dynamic Light Scattering (DLS)

The hydrodynamic diameter and zeta potential of the isolated EVs were measured using the Litesizer 500 Particle Analyzer (Anton Paar) (502). Each retained EVs pellet (P50 and P100) was resuspended in 700 µl of a 50 mM Tris-Cl pH 7.5 solution for DLS analysis. The particle size measurement was carried out in a polystyrene 10 x 10 x 45 mm cuvette, using the default settings for exosome analysis. The analysis allows for the determination of the hydrodynamic diameter of the EVs, which provides information about their size.

4.3.10 Fluorometric Quantification of EVs

The isolated EVs (P50 and P100) were quantified using a fluorometric dye ($DiOC_6$) to assess total lipid membrane content (503). The EVs were resuspended in 100 µl of 100 µM $DiOC_6$ (Invitrogen) diluted in 50 mM Tris-Cl pH 7.5. The resuspended fractions were then incubated at 37 °C for 10 minutes, washed with 2 mL of the same buffer, pelleted using an ultracentrifuge at the respective speed, and the resulting pellet was resuspended in 52 µl of fresh buffer. Next, 50 µl of each sample was transferred to a 96-well, black, clear, polystyrene plate (Corning). The fluorescence of the $DiOC_6$ was then recorded using Tecan i-control (Infinite 200Pro), with an excitation wavelength of 485 nm, an emission wavelength of 535 nm, and a total of 25 flashes.

4.4 Results

4.4.1 MYMIV Genomic Components are Present in The Leaf Apoplast

To authenticate the infectivity and specificity of MYMIV infectious clones, total genomic DNA was extracted from newly emerged leaf tissues of agroinoculated plants. Consistent with our prior observations (14), typical YMD symptoms such as yellow mosaic patches and leaf curling were noted in plants agroinoculated with MYMIV infectious clones. Furthermore, the presence of viral DNA in leaf tissues was confirmed through both PCR and RCA. PCR revealed the presence of a ~1.2 kb band, while RCA demonstrated a ~2.7 kb band, characteristic of the typical size of the begomovirus genome. Hence, these plant trifoliates were denoted as "MYMIV-infected" in this study. Conversely, plants subjected to mock treatment and water only remained healthy, devoid of YMD symptoms, and showed no presence of viral DNA, as confirmed by both PCR and RCA. Therefore, these samples collectively termed as "Uninfected" in this study.

https://doi.org/10.1007/s00299-024-03247-2

We aimed to investigate the presence of viral genomic components in the extracellular space of MYMIV-infected plant leaves using AWF as a sample source. We extracted total DNA from the collected AWF, but its concentration was found to be very low, likely due to limited DNA circulation in AF. To overcome this challenge, we utilized the RCA technique, which generated only a few copies of viral DNA. We then used the RCA product as a template for further amplification to obtain a higher concentration of RCA product that could be used for subsequent experiments. Restriction digestion of the RCA product using the MYMIV DNA A specific PstI enzyme and DNA B specific MfeI enzyme revealed the presence of a ~2.7 kb band, which is indicative of the begomovirus genome size (Figure 28D). To identify the presence of both genomic components of MYMIV, i.e., DNA-A and DNA-B, we performed PCR analysis using specific primer pairs. We detected MYMIV DNA-A using two sets of primer pairs, namely DNA-A_Mid primer (PCR-I) and AC1 primer (PCR-II), both of which generated 1.2 kb and 137 bp fragments, respectively, in infected AWF samples (Figure 28E). We also identified MYMIV DNA-B using the DNA-B_Mid primer (PCR-III), which generated a 1.2 kb fragment that produced the expected size of an amplicon, as confirmed by gel electrophoresis (Figure 28E). To rule out any possibility of host genomic DNA contamination in AWF DNA samples, we used a housekeeping gene, tubulin-specific primer pair, which did not show any amplification in AWF samples but showed an expected band of 308 bp in the positive control (VP) i.e., total plant leaf genomic DNA sample (Figure 28D).

4.4.2 MYMIV Infection Enhanced EVs Secretion, and Geminivirus-like Structures are Detected in Apoplast

TEM analysis of AWF from MYMIV-infected and uninfected mungbean leaves revealed the presence of numerous circular vesicles. The size and number of vesicles were measured using ImageJ software, revealing an increase in both the total number and size of vesicles in MYMIV-infected AWF compared to uninfected AWF (Figure 29). To isolate potential complete virus particles, the AWF solution underwent ultracentrifugation at 40,000 x g for 60 minutes at 4 °C, resulting in a pellet (P40). The pellet was then resuspended in VIB buffer and subjected to TEM analysis. The objective was to identify twinned quasi-icosahedral virus particles with expected dimensions of approximately 18 x 30 nanometers (74). However, no exact sized virus particles were observed. Instead, geminivirus-like structures in a different size range of approximately 35 x 60 nm were detected (Figure 30). Furthermore, we employed fluorometric assays and DLS analysis to study the concentration and hydrodynamic diameter of different populations of secreted EVs (P50 and P100). The P50 fraction of MYMIV-infected and uninfected showed an increased population of EVs in terms of their elevated size and concentration (Figure 31A and D). Interestingly, the P100 EVs population showed a lowered concentration in infected compared to uninfected AWF (Figure 31B). However, the MYMIV-infected AWF had two separate populations of EVs in the range of 70-90 and 120-140 nm, while the uninfected AWF had only single population of EVs (70-90 nm) (Figure 31E). These findings suggest that MYMIV infection could have a significant impact on the population and characteristics of EVs.

4.4.3 Untargeted Metabolomics Detected Apoplastic and Symplastic Metabolites

The representative ^{1}H NMR spectra of AWF of MYMIV-infected and uninfected mungbean leaf is presented in (Figure 32A and B). Similarly, ^{1}H NMR spectra of LWA of MYMIV-infected and uninfected mungbean is shown in ((Figure 32C and D). The comprehensive comparative ^{1}H NMR spectra indicated significant variation in metabolite composition between the AWF and LWA in

https://doi.org/10.1007/s00299-024-03247-2

MYMIV- infected samples. In both virus-infected and uninfected plants, approximately 21 identifiable metabolites were detected within the apoplast fraction. These included compounds such as α-glucose, β-glucose, sucrose, alanine, asparagine, fucose, 4-aminobutyrate, isoleucine, leucine, thionine, valine, proline, citric acid, formic acid, trigonelline, fumaric acid, betaine, ethanolamine, D-ribose, pipecolic acid, and 2-hydroxybutyrate (Table 16). Moreover, in the infected AWF samples, various unidentified yet distinct metabolite signals or peaks were detected at specific chemical shift values, including 1.46 (s) ppm, 1.92 (s) ppm, 2.13 (s) ppm, 2.17 (s) ppm, 2.21 (s) ppm, 2.34 (s) ppm, 2.42 (s) ppm, 2.98 (s) ppm, 3.17 (s) ppm, 3.25 (d) ppm, 3.26 (s) ppm, 3.61 (s) ppm, and 3.87 (s) ppm. Furthermore, a higher number of metabolites were identified in the symplast fraction, which included the aforementioned 21 metabolites as well as additional compounds such as tyrosine, phenylalanine, threonine, glutamate, tryptophan, myo-inositol, caffeoylquinic acid, iso-butyrate, adenine, cytidine, shikimic acid, β-galactose, succinate, chlorogenate, acetic acid, and chlorine (Table 16). These findings indicate a substantial disparity between the metabolomic profiles of the plant leaf symplast and their extracellular space, highlighting the distinct metabolic landscapes of these regions.

4.4.4 Apoplastic and Symplastic Metabolites Change in Response to MYMIV Infection

To study metabolic differences between MYMIV-infected and uninfected mungbean plants, a statistical modeling tools like PCA, PLS and OPLS-DA were employed. Two sets of samples were analyzed: one set included the AWF of infected and uninfected plants, while the other set comprised of LWA of infected and uninfected plants. The unsupervised method, PCA score plot of apoplast fraction of MYMIV-infected and uninfected mungbean leaf showed good separation of the groups based on PC 1 = 37.5%, PC 2 = 22.8%, and PC 3 = 16.9 %. Further separation between the pair was confirmed via OPLS-DA model with statistical values of $R^2X = 0.755$, $R^2Y = 0.996$, and $Q^2 = 0.928$ (Figure 34A). The OPLS-DA model was validated by 200 permutations values of $R^2 = (0.0, 0.984)$, $Q^2 = (0.0, 0.557)$. Whereas, OPLS-DA loadings S-plot was used to identify important features of the spectra that drive pair separation (Figure 34C). Then we employed univariate analysis using the fold change (FC) analysis, which discriminates potentially significant peak region under study. The up-regulated metabolites in the infected apoplast were valine, 2-hydroxybutyrate, α-glucose, β-glucose, sucrose, pipecolic acid and the rest of the peaks were unknown. The PCA model of symplast fraction from MYMIV-infected and uninfected mungbean groups were separated based on PC 1 = 58.4 %, PC 2 = 22.2%, PC 3 = 17.4 %. The OPLS-DA model with statistical values of $R^2X = 0.921$, $R^2Y = 0.997$, and $Q^2 = 0.965$ shown to aggregate uninfected samples and dispersed samples of infected (Figure 34D). The OPLS-DA model was validated by 200 permutations values of $R^2 = (0.0, 0.836)$, $Q^2 = (0.0, 0.148)$ (Figure 34E). Whereas, important features of spectra identified using OPLS-DA loadings S-plot (Figure 34F). To discriminate potentially significant peak region the FC analysis was carried out. The up-regulated metabolites in the infected symplast were valine, threonine, aspartate, alanine, 4-aminobutyrate, myo-inositol, trigonelline, acetic acid, ethanolamine, α-glucose, β-glucose, sucrose, fructose, fucose, pipecolic acid and the downregulated metabolites were 2-hydroxybutyrate, citrate, proline, and succinate.

The affected metabolic pathways in AWF were citrate cycle (TCA cycle), glyoxylate and dicarboxylate metabolism, arginine and proline metabolism, glycolysis / gluconeogenesis, starch and sucrose metabolism, and galactose metabolism based on the statistically significant values of ($p < 0.05$) and an impact factor threshold > 0 (Figure 33A and Table 18). Whereas, 12 metabolic pathways were found to be affected in LWA sample i.e., inositol phosphate metabolism,

https://doi.org/10.1007/s00299-024-03247-2

phosphatidylinositol signaling system, glycine, serine and threonine metabolism, glyoxylate and dicarboxylate metabolism, glycerophospholipid metabolism, glycolysis/gluconeogenesis, sulfur metabolism, pyruvate metabolism, arginine and proline metabolism, butanoate metabolism, TCA cycle, and alanine, aspartate and glutamate metabolism (Figure 33B).

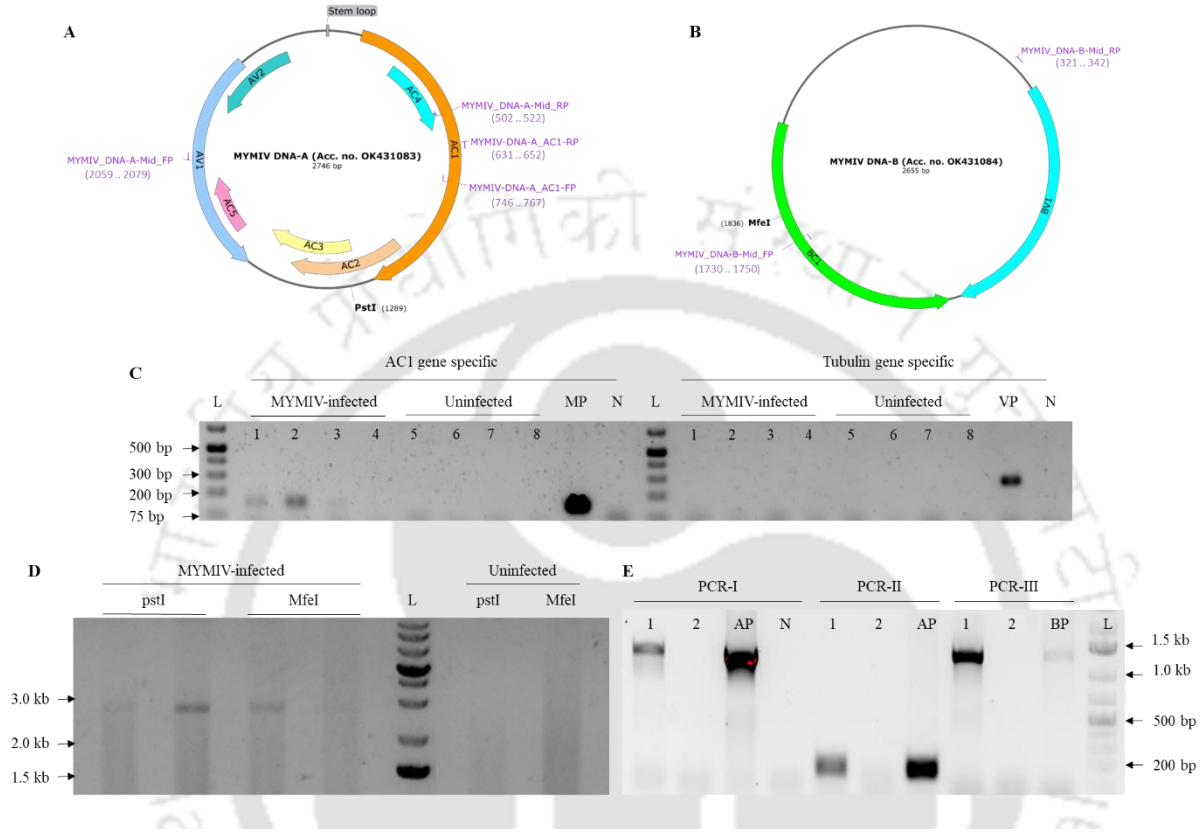

Figure 28 Identification of viral genomic components in the mungbean leaf apoplast.
A: Schematic representation of MYMIV DNA-A genome along with two sets of primer pairs (denoted as DNA-A_Mid and AC1_gene) for PCR detection. The unique cutter of MYMIV DNA A, PstI, is indicated; **B:** Schematic representation of MYMIV DNA-B genome along with a primer pair (denoted as DNA-B_Mid) for PCR detection; The unique cutter of MYMIV DNA B, MfeI, is indicated; **C:** Detection of viral DNA and host gDNA contamination in the apoplast of MYMIV-infected and uninfected leaf samples using PCR analysis. To specifically detect viral DNA, a primer specific to the AC1 gene of MYMIV was used. To check for any potential contamination of cytoplasmic DNA in AWF, a mungbean (*Vigna radiata*) tubulin gene-specific primer was used. PCR with the AC1 gene-specific primer produced a 137 bp fragment, while PCR with the tubulin-specific primer produced a 308 bp fragment. The following samples were used: four biological replicates (MYMIV-infected AWF sample no. 1, 2, 3, 4) and (Uninfected AWF sample no. 5, 6, 7, 8), L: Thermo Scientific GeneRuler 1 kb Plus DNA ladder, MP: MYMIV DNA-A_pCambia3300, N: water (negative control), VP: total gDNA extracted from a healthy mungbean leaf; **D:** Confirmation of MYMIV DNA-A and DNA-B genome sizes in AWF samples from MYMIV-Infected and Uninfected leaf samples. For both treatments, two biological replicative samples were analyzed. MYMIV DNA-A genome size was confirmed using unique cutter (PstI) restriction digestion analysis, whereas MYMIV DNA-B genome size was confirmed using unique cutter (MfeI) restriction digestion analysis. Each separate reaction yielded a ~2.7 kb band, indicative of the begomovirus genome size. In contrast, AWF from uninfected samples showed the absence of DNA bands, indicating the absence of viral DNA in control plants.; **E:** Identification of MYMIV DNA-A and DNA-B in AWF samples of MYMIV-infected and uninfected leaf samples using PCR analysis. Three sets of primer pairs (PCR-I, PCR-II, and PCR-III) were used to detect MYMIV DNA-A and DNA-B in the RCA product of AWF samples. PCR-I amplified MYMIV DNA-A mid-region (1210 bp), PCR-II amplified MYMIV DNA-A AC1 gene region (137 bp), and PCR-III amplified MYMIV DNA-B mid-region (1430 bp). The following samples were used: 1: RCA product of AWF extracted from MYMIV-infected leaf, 2: RCA product of AWF extracted from uninfected leaf, AP: MYMIV-DNA-A_pCambia3300, BP: MYMIV-DNA-B_pCambia3300.

https://doi.org/10.1007/s00299-024-03247-2

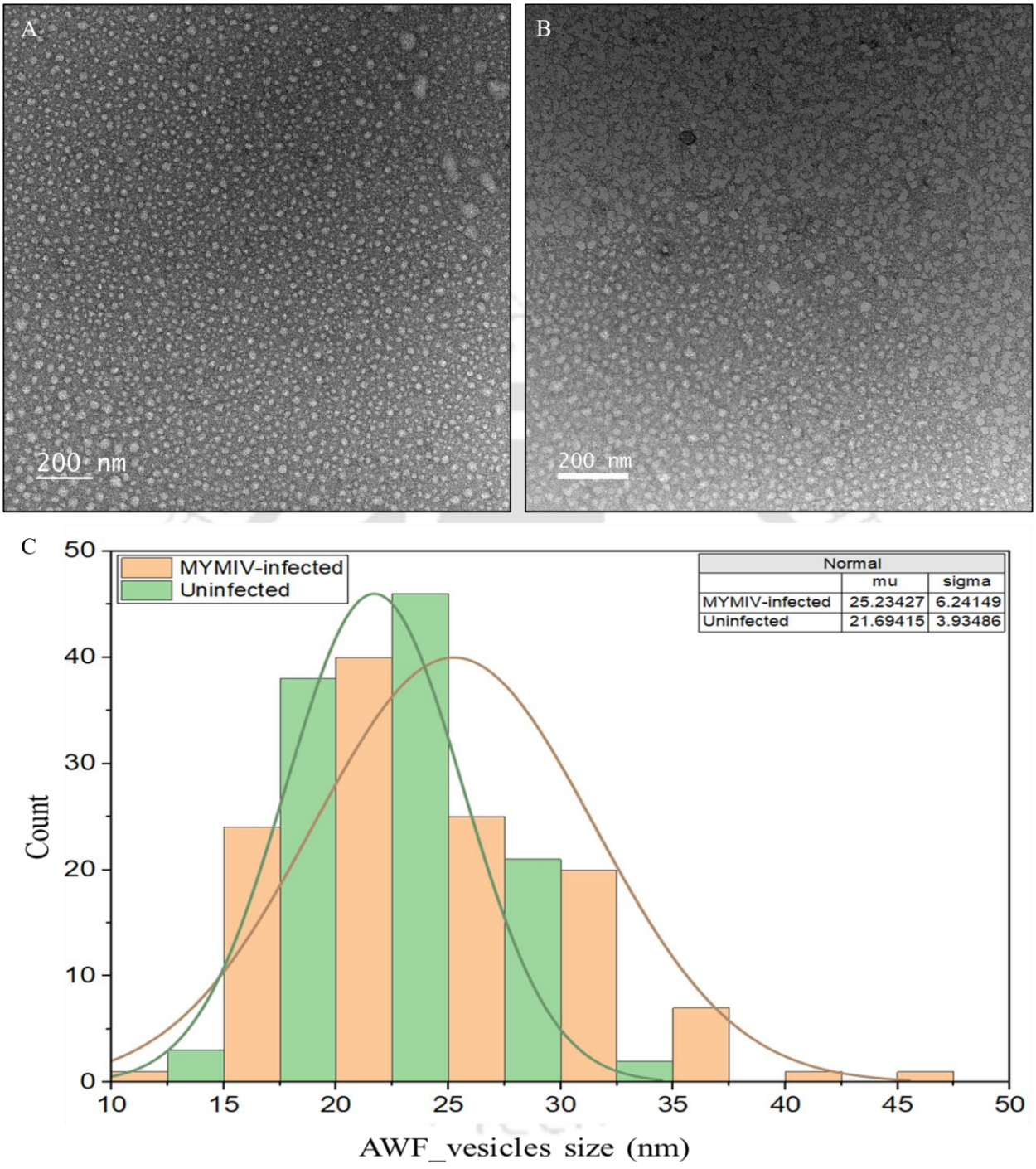

Figure 29 Vesicle-like structures seen in MYMIV-infected and uninfected AWF.
Transmission electron microscopy (TEM) image analysis revealed the presence of circular shaped extracellular vesicles in the apoplast fluid. **a:** MYMIV-infected AWF; **b**: uninfected AWF; **c:** vesicles size distribution graph analysis carried out using ImageJ and OriginPro software. Mu: mean size, sigma: standard deviation.

https://doi.org/10.1007/s00299-024-03247-2

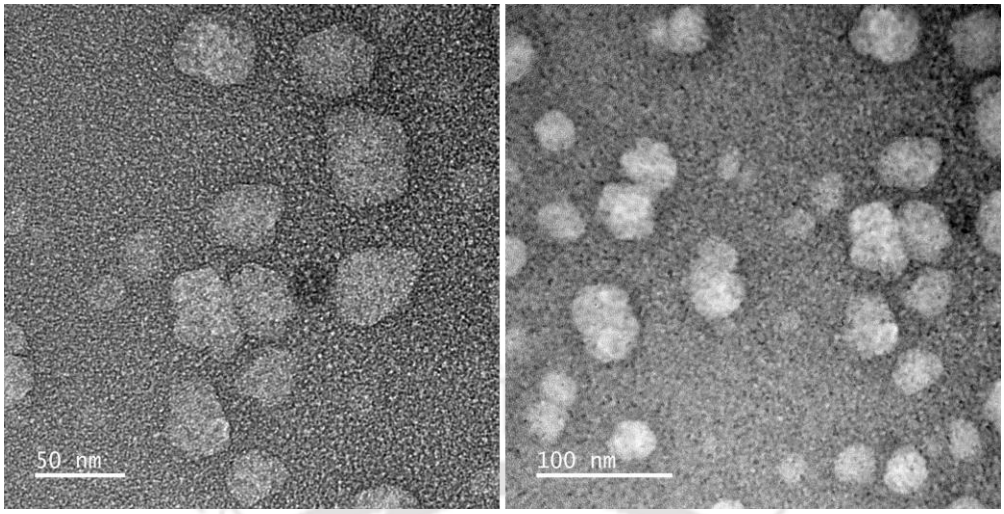

Figure 30 Geminivirus-like structures seen in mungbean apoplastic fluid.
TEM analysis of P40 fraction extracted from AWF of MYMIV-infected mungbean leaf.

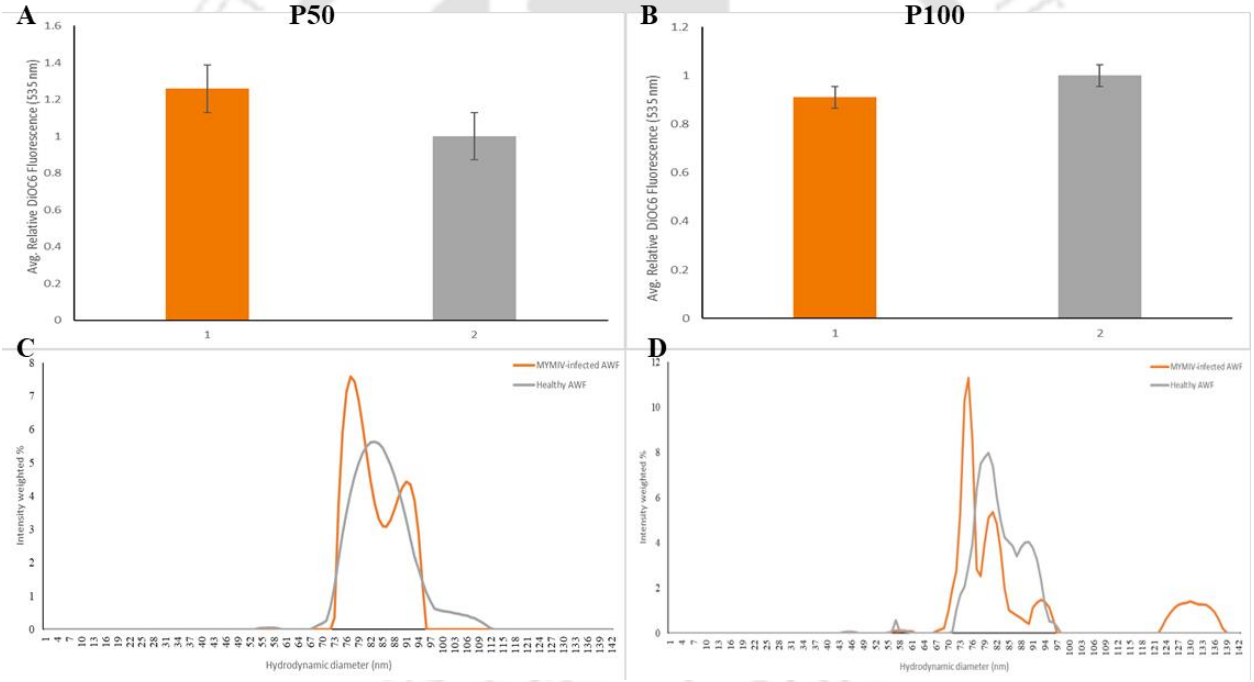

Figure 31 EVs secretion enhanced during MYMIV infection in mungbean plants.
The histograms and graphs depict the presence of EVs in MYMIV-infected (orange color) and uninfected (gray color) samples. The quantification of DiOC6 fluorescence in different EV fractions is represented in histograms, with **(A)** indicating the P50 fraction and **(B)** indicating the P100 fraction. The data for this analysis are derived from three biological replicates, each with three technical replicates. Fluorescence intensity measurements are shown, and error bars represent the standard deviation (sd). Statistical analysis was conducted using a two-tailed unpaired Student's t-test with a significance level of $P < 0.001$ (n = 3). The hydrodynamic diameter of EVs in the P50 and P100 fractions is depicted in the graph (**C** and **D**, respectively) and was determined using dynamic light scattering (DLS).

https://doi.org/10.1007/s00299-024-03247-2

Table 16 Metabolites identified in the apoplast and symplast of MYMIV-infected samples.

Metabolites	Chemical shifts (ppm), multiplicity, J (Hz)	Apoplast_ log2FC	Symplast_ log2FC
Isoleucine	1.01 (d, J=7)	NSC	NSC
Valine	0.99 (d, J=7.23), 1.05 (d, J=7)	2.737 (↑)	1.688 (↑)
Leucine	1.71 (m), 0.94 (m)	NSC	NSC
Tyrosine	6.9 (d, J=8.62), 7.17 (d, J=8.65)	Absent	NSC
Phenylalanine	7.36 (s), 7.43 (s)	Absent	NSC
Threonine	1.33 (d)	NSC	3.376 (↑)
Glutamate	2.13 (p, J=6.86 7.29), 2.37 (dt, J=5.10, 7.92)	Absent	NSC
Aspartate	2.67 (d, J=8.68), 2.81 (d, J=3.64), 2.84 (d, J=3.8)	Absent	1.141 (↑)
Tryptophan	7.63 (d, J=8.29)	Absent	NSC
Alanine	1.48 (d, J=7.4)	NSC	1.120 (↑)
Proline	2.07 (m), 3.31 (m)	1.040 (↑)	-1.05 (↓)
4-Aminobutyrate	1.91 (s), 2.31 (t, J=7.30), 3.02 (t, J=7.60)	NSC	1.009 (↑)
Myo-inositol	3.31 (t)	NSC	1.391 (↑)
Trigonelline	9.13 (s), 8.84 (t, J=7.19, 7.19), 8.08 (t, J=7.11), 4.44 (s)	NSC	1.624 (↑)
Isobutyrate	1.08 (s)	NSC	NSC
Adenine	8.25 (s)	Absent	NSC
Cytidine	7.96 (d, J=8.25)	Absent	NSC
Adenosine	6.07 (d)	NSC	NSC
β-galactose	4.57 (d, J=19.2)	NSC	NSC
Succinate	2.48 (s)	NSC	-1.054 (↓)
Formic acid	8.46 (s)	NSC	NSC
Fumaric acid	6.57 (s)	NSC	NSC
2-Hydroxybutyrate	1.37 (s)	2.433 (↑)	-1.911 (↓)
Chlorogenate	7.73 (d, J=15.8), 6.96 (d, J=8.1), 7.25 (s), 7.17 (d, J=8.3)	Absent	NSC
Citrate	2.57 (d, J=17.3)	-2.772 (↓)	-1.597 (↓)
Caffeoylquinic acid	6.53 (d, J=5.65)	Absent	NSC
Acetic acid	1.94 (s)	NSC	1.388 (↑)
Ethanolamine	3.13 (t, J=9.44, 9.44)	NSC	1.816 (↑)
Betaine	3.28 (s)	NSC	NSC
Choline	3.2 (s)	NSC	NSC
Sucrose	5.42 (d, J=3.8), 4.22 (d, J=8.8), 4.06 (t, J=8.5), 3.6 (s)	1.130 (↑)	NSC
β-Glucose	4.65 (d, J=7.95)	2.237 (↑)	2.933 (↑)
α-Glucose	5.24 (d, J=3.7), 3.9 (dtt, J=3.43, 3.43, 7.44, 7.44, 9.59)	2.237 (↑)	3.222 (↑)
Fructose	4.11 (d, J=3.8), 4 (t, J=11.74), 3.57 (q, J=1.99, 2.20)	NSC	1.975 (↑)
Fucose	1.24 (d, J=7.47), 1.17 (d, J=7.11)	NSC	1.790 (↑)
D-Ribose	2.2 (s)	NSC	NSC
Malic acid	2.44 (d, J=11.5), 4.33 (d, J=8.1), 2.71 (d, J=17.4)	NSC	NSC
Shikmic acid	2.78 (d, J=5.6), 2.75 (d, J=5.5), 6.45 (s)	Absent	NSC
Pipecolic acid	3.56 (dd)	1.479 (↑)	1.237 (↑)

↑: up regulated; ↓: down regulated; NSC: no significant change in metabolite; s: singlet; d: doublet; t: triplet; dd: doublet of doublets; m: multiplet; AWF: apoplast washing fluid; LWA: leaf without AWF; log2FC: log2 fold change.

https://doi.org/10.1007/s00299-024-03247-2

Table 17 List of primers used to detect apoplastic MYMIV.

Primer label	Primer pair	Sequence (5'-3')	Length	Amplicon
tubulin primer	*Vr*. tubulin_FP	aacttatcgattccgtcttggatg	24 nt	308 bp
	Vr. tubulin_RP	gaagggaaaacggaaaacgtcatca	25 nt	308 bp
DNA-B_primer	MYMIV_DNA-B-Mid_FP	ggactccaatgtgatcgacgg	22 nt	1430 bp
	MYMIV_DNA-B-Mid_RP	gctatacgcactatgtcgttcg	21 nt	1430 bp
DNA-A_ primer	MYMIV_DNA-A-Mid_FP	cgtccatccataccttacccg	21 nt	1210 bp
	MYMIV_DNA-A-Mid_RP	gtatgcgtcgttggcagattg	21 nt	1210 bp
AC1 primer	MYMIV-DNA-A_AC1-FP	ctaataggtctatctggccgcg	22 nt	137 bp
	MYMIV-DNA-A_AC1-RP	cggatattcacagagcctgtcc	22 nt	137 bp

4.5 Discussion

Understanding the strategies employed by pathogens and hosts in the apoplast can potentially improve specific characteristics and enhance protection for plant cells against pathogens and various stressors (467,504). This study unveils a significant role of the apoplast, shedding light on its previously unexplored involvement in DNA virus infection, particularly in begomovirus infection. The findings are substantiated by the identification of viral DNA and the induction of EVs. Utilizing NMR-based metabolomics, specific biomarkers associated with MYMIV infection were identified in both the apoplast (AWF) and symplast (LWA). Notably, this study represents a pioneering exploration of the leaf apoplast of mungbean in response to MYMIV.

Plant viruses, traditionally recognized for utilizing a symplastic route via plasmodesmata (PD) for cell-to-cell movement, have recently been implicated in the apoplast and the induction of vesicles. EVs in plants share physical and chemical characteristics with viruses, and their biogenesis pathways show similarities (505). For instance, RNA viruses like turnip mosaic virus (TuMV) associate viral RNA and protein with multivesicular bodies (MVBs), leading to the release of intraluminal vesicles into the apoplast (19). In potato virus X-infected plants, virus particles and RNAs are present in the apoplast but are not associated with vesicles (20). Ongoing studies emphasize the role of EVs in virus transmission. For example, Rice dwarf virus (RDV) employs the exosomal release pathway for horizontal transmission to leafhopper vectors (506). Cross-transmission of plant RNA viruses to fungi and the association of fungal viruses with EVs underscore the importance of extracellular virus transfer (507,508). Certain fungi efficiently absorb virus particles and viroid RNAs from the apoplast, highlighting their role in the uptake of secreted macromolecules (509). Our data indicate an increased size and number of EVs in the MYMIV-infected apoplast (Figure 29), suggesting that these vesicles may carry additional cargo from the cytoplasm under virus infection. This observation is consistent with previous findings demonstrating that plants produce EVs, particularly in response to pathogen infection (19,466,510).

https://doi.org/10.1007/s00299-024-03247-2

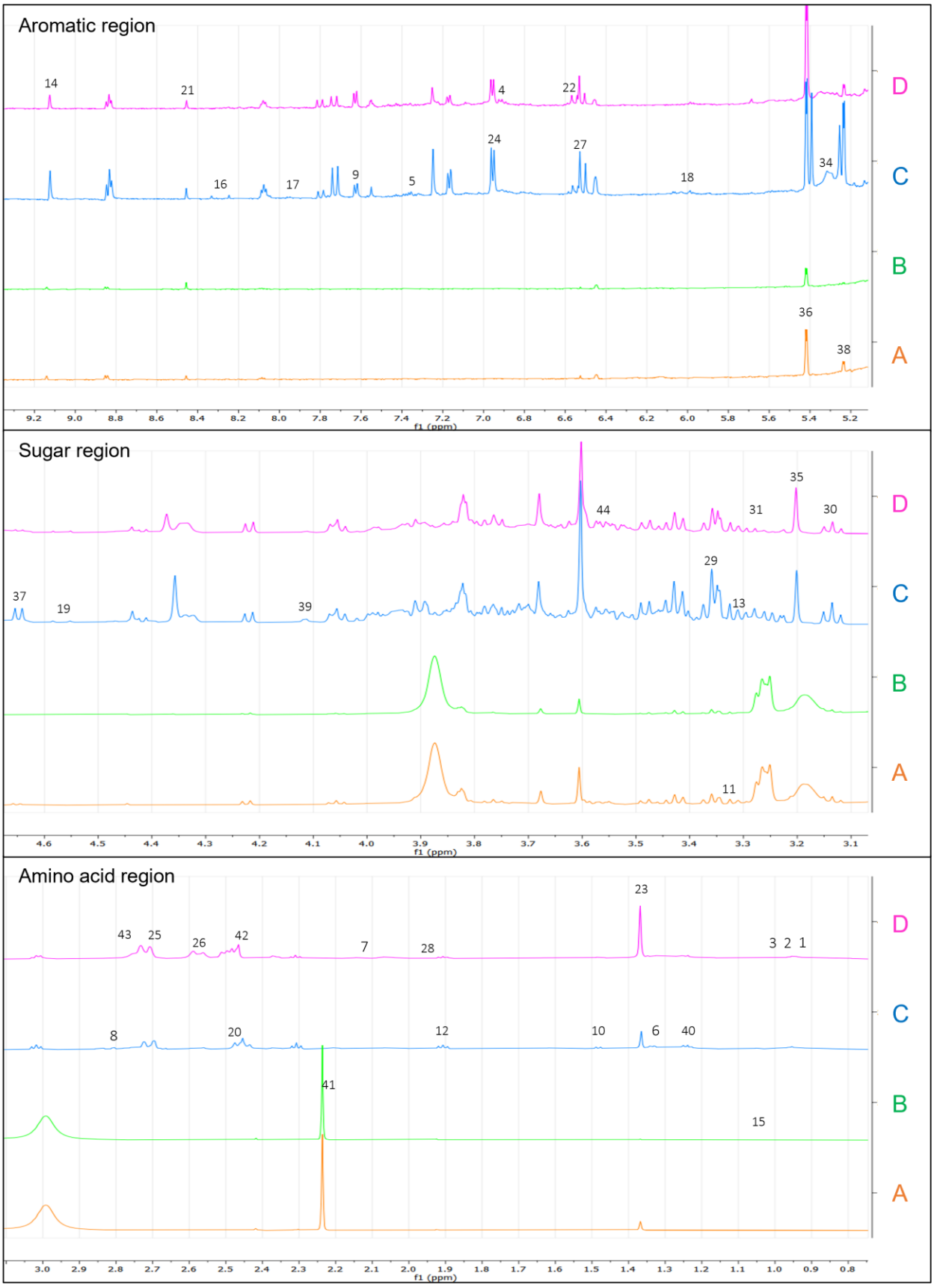

https://doi.org/10.1007/s00299-024-03247-2

Figure 32 Comparative 1H NMR spectrum of MYMIV-infected and uninfected leaf tissue. The spectra obtained at 600 MHz, were scaled in accordance with TSP used as internal standard. **A**: infected apoplast; **B:** uninfected apoplast; **C:** infected symplast; **D:** uninfected symplast. The NMR graph, ranging from 0.8 to 9.2 ppm, is categorized into three regions, namely amino acids, sugars, and the aromatic region. Identified amino acids include Isoleucine (1), Valine (2), Leucine (3), Tyrosine (4), Phenylalanine (5), Threonine (6), Glutamate (7), Aspartate (8), and Tryptophan (9). Organic acids such as Succinate (20), Formic acid (21), Fumaric acid (22), α-Hydroxyisobutyric acid (23), Chlorogenate (24), Citric acid (25), and Citrate (26) are present. Various sugars, including β-galactose (19), β-Glucose (37), α-Glucose (38), Fructose (39), Sucrose (36), and Fucose (40), were also detected. Additionally, D-Ribose (41), Malic acid (42), Shikmic acid (43), and Pipecolic acid (44) were identified. Other compounds comprise myo-Inositol (13), Trigonelline (14), Isobutyrate (15), Adenine (16), Cytidine (17), Adenosine (18), caffeoylquinic acid (27), Acetic acid (28), Methanol (29), Ethanolamine (30), Betaine (31), and Choline (35).

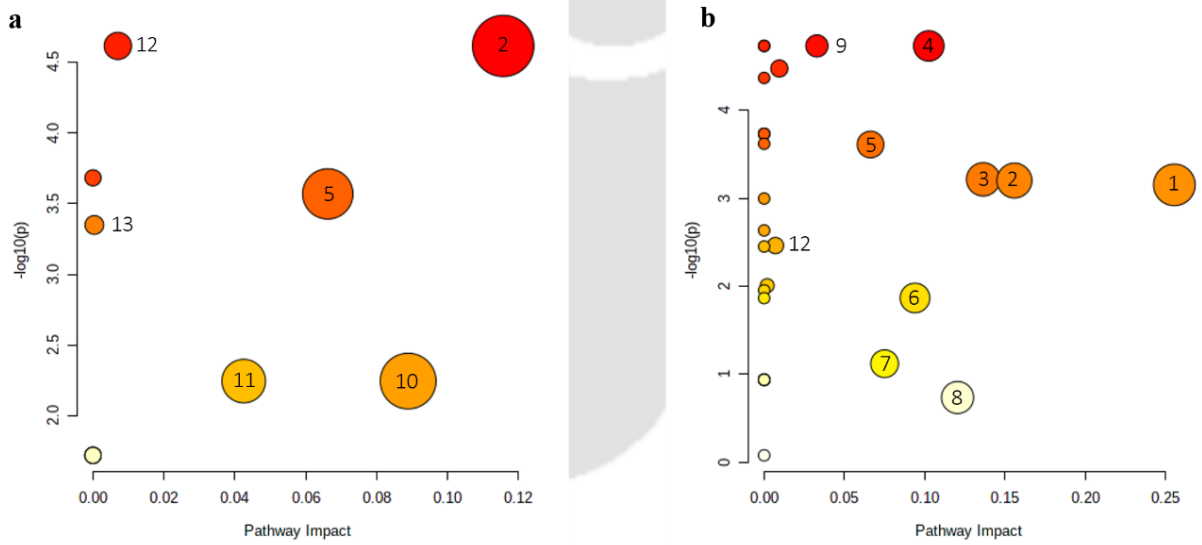

Figure 33 Metabolic pathways analysis of apoplast and symplast from MYMIV-infected mungbean.
Analysis carried out using MetaboAnalyst 5.0. Differences were considered statistically significant with P values < 0.05 and an impact factor threshold > 0. **A:** Altered metabolic pathways of AWF samples; **B:** Altered metabolic pathways of LWA samples. 1) Alanine, aspartate and glutamate metabolism, 2) Citrate cycle (TCA cycle), 3) Butanoate metabolism, 4) Inositol phosphate metabolism, 5) Arginine and proline metabolism, 6) Sulfur metabolism, 7) Pyruvate metabolism, 8) Glycine, serine and threonine metabolism, 9) Phosphatidylinositol signaling system, 10) Starch and sucrose metabolism, and 11) Galactose metabolism, 12) Glyoxylate and dicarboxylate metabolism, 13) Glycolysis / Gluconeogenesis.

https://doi.org/10.1007/s00299-024-03247-2

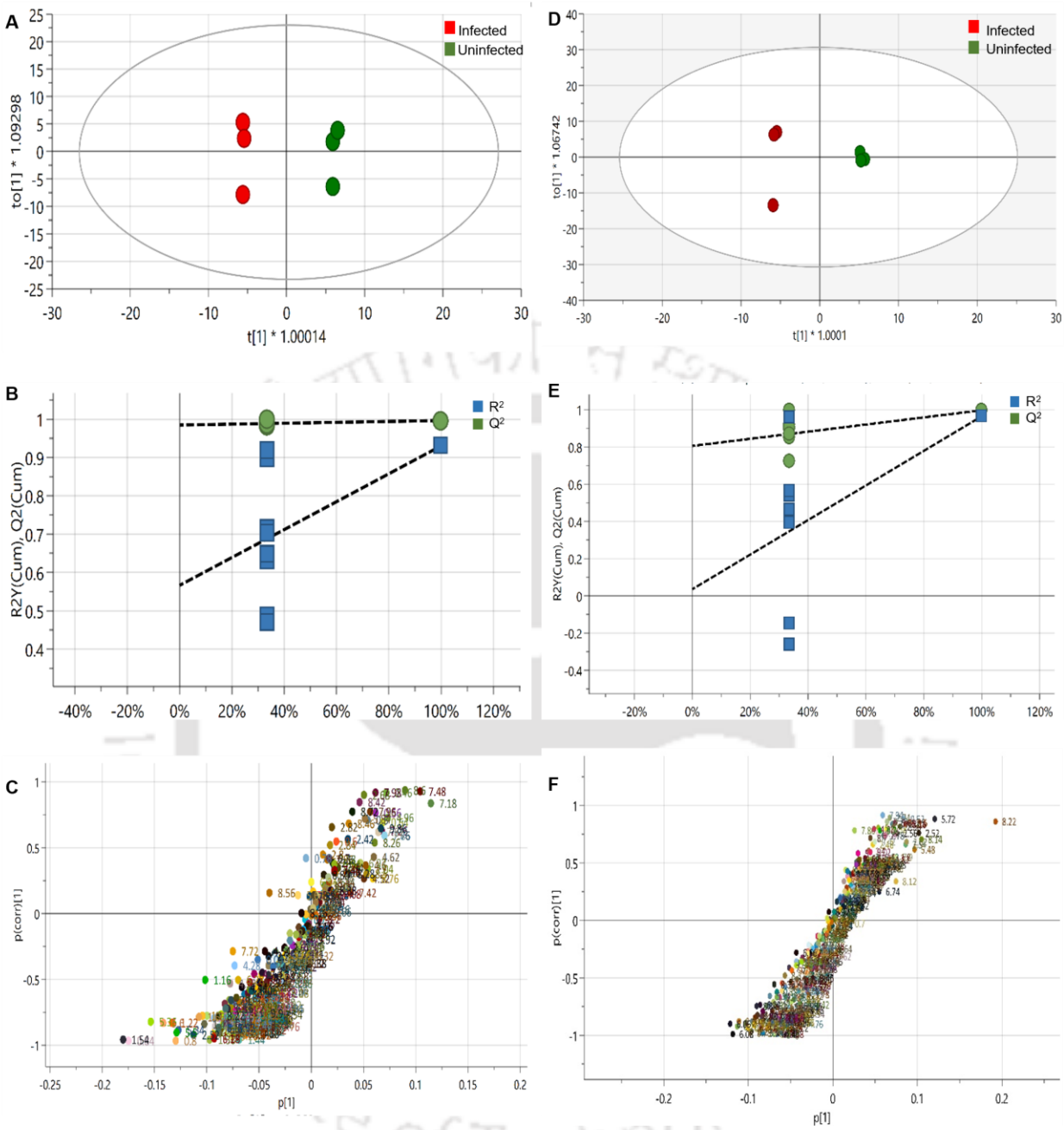

Figure 34 Statistical analysis of MYMIV-infected and uninfected samples.
OPLS-DA score plot, statistical validation by permutation analysis and loadings S-plot for discrimination of MYMIV-infected and uninfected samples. **A:** Score plot of AWF samples; **B:** Validation by 200 permutations, R2 = (0.0, 0.985), Q2 = (0.0, 0.566) of AWF samples; **C:** Loadings S-plot of AWF samples; **D:** Score plot of LWA samples; **E:** Validation by 200 permutations, R2 = (0.0, 0.806), Q2 = (0.0, 0.0361) of LWA samples**; F:** Loadings S-plot of LWA samples.

https://doi.org/10.1007/s00299-024-03247-2

Table 18 Metabolite pathways majorly affected by MYMIV infection in apoplast and symplast regions of mungbean leaf.

	AWF Metabolic Pathway	Total Cmpd	Hits	Raw p	-log10 (*P*)	Holm adjust	FDR	Impact
1	Citrate cycle (TCA cycle)	20	1	2.43E-05	4.6144	0.00026732	0.00013366	0.11571
2	Glyoxylate and dicarboxylate metabolism	29	1	2.43E-05	4.6144	0.00026732	0.00013366	0.00702
3	Arginine and proline metabolism	34	1	0.0002703	3.5682	0.0021624	0.00074332	0.06623
4	Glycolysis / Gluconeogenesis	26	1	0.00044789	3.3488	0.0031352	0.00098536	0.00038
5	Starch and sucrose metabolism	22	1	0.0056876	2.2451	0.034126	0.0089377	0.0889
6	Galactose metabolism	27	1	0.0056876	2.2451	0.034126	0.0089377	0.04252
	LWA Metabolic Pathway							
1	Inositol phosphate metabolism	28	1	1.87E-05	4.7271	0.0005999	0.00014997	0.10251
2	Phosphatidylinositol signaling system	26	1	1.87E-05	4.7271	0.0005999	0.00014997	0.03285
3	Glycine, serine and threonine metabolism	33	2	0.18328	0.73689	1	0.18919	0.1204
4	Glyoxylate and dicarboxylate metabolism	29	3	0.0034586	2.4611	0.055337	0.006303	0.00702
5	Glycerophospholipid metabolism	37	1	3.38E-05	4.4706	0.00094738	0.00021654	0.00947
6	Glycolysis / Gluconeogenesis	26	2	0.0098468	2.0067	0.13786	0.016584	0.00189
7	Sulfur metabolism	15	2	0.013598	1.8665	0.16317	0.019868	0.09392
8	Pyruvate metabolism	22	1	0.075791	1.1204	0.75791	0.10545	0.075
9	Arginine and proline metabolism	34	2	0.00024644	3.6083	0.0055597	0.00071693	0.06623
10	Butanoate metabolism	17	2	0.00061265	3.2128	0.012866	0.0015569	0.13636
11	Citrate cycle (TCA cycle)	20	2	0.00063249	3.1989	0.012866	0.0015569	0.15581
12	Ala, Asp and Glut metabolism	22	4	0.00070787	3.15	0.01345	0.001618	0.2554

https://doi.org/10.1007/s00299-024-03247-2

The detection of viral proteins, RNA, and virus particles in the plant apoplast emphasizes its critical role in viral infection, particularly in the systemic spread of the virus within the host. In bipartite begomoviruses, two crucial proteins cooperate to mediate cell-to-cell movement of the virus: the nuclear shuttle protein (NSP) and the movement protein (MP) encoded by DNA-B (144,145,511). In the presence of MP, NSP was observed to be associated with early endosomes, while MPs were demonstrated to be located at the plasma membrane, plasmodesmata, and in motile vesicles. These vesicles assist viral DNA complex to move into the next cell, either along the plasma membrane or via the endoplasmic reticulum (ER) spanning the PD (102,106,512–515). This report suggests that DNA viruses, such as begomovirus, might exploit the apoplast and/or EVs for systemic spread. Consistent with previous findings, we report the presence of both viral genomic components, i.e., DNA A and DNA B, in the apoplast of MYMIV-infected mungbean leaves (Figure 28). Based on structural observations from TEM, we speculate on the presence of geminivirus-like structures in the apoplast of MYMIV-infected leaves, as the size of the particles deviated from that typically reported for geminiviruses. However, further investigations are needed to confirm this speculation (Figure 30).

The most widely employed method for AF extraction with negligible intracellular contamination is the VIC method, involving vacuum infiltration with an appropriate extraction buffer and subsequent centrifugation (485,487). The VIC method is proven effective for AF protein recovery (465,479,484) and is suitable for apoplast proteomic analyses under various stresses, including biotic factors like bacterial (516) or fungal (517) infections and abiotic (481,518,519) or nutritional (520,521) stresses. However, investigating apoplastic metabolites poses challenges due to their relatively low abundance compared to intracellular or symplastic components (522). Currently, extracting AF metabolites from in planta systems is commonly performed using the VIC method. Variations in apoplastic metabolic components have been observed in response to biotic stresses caused by fungi (517,523) and bacteria (524–527), as well as abiotic stresses (528,529). Witzel et al. (2011) employed the VIC method to extract proteins from maize leaf apoplast and symplast, highlighting differential compositions of proteins in their respective fractions and minimal contamination of symplastic proteins in the apoplast fraction (530). However, under virus infection, region-specific alterations of metabolite composition in the apoplast and symplast have not been studied yet.

NMR metabolomics fingerprinting and profiling are highly pertinent for studying plant-pathogen systems (490,531–533). Recently, metabolomic studies have extensively investigated the metabolic changes in whole symptomatic plant leaves during virus infections (534–538), including those involving mungbean and MYMIV (539).

Phenolic acids, a diverse class of plant polyphenols, are primarily synthesized through the shikimic acid pathway in the phenylpropanoid pathway (540). This process converts simple carbohydrates into aromatic amino acids (phenylalanine, tyrosine, and tryptophan), serving as key precursors for phenolic acid and protein synthesis. The shikimic acid pathway is also associated with the synthesis of various secondary metabolites, including chlorogenic acids and caffeoylquinic acids (541). These polyphenols play a crucial role in stress protection in plants, offering antioxidant properties that enhance defense mechanisms and provide biomedical benefits (542–545). Chlorogenic acids and caffeoylquinic acids are widely distributed secondary metabolites known for their plant antioxidant properties, bolstering defense mechanisms and exhibiting biomedical benefits (546–549). While previous studies, based on whole tissue extracts, associate elevated chlorogenic phenolics with disease resistance (550,551), our investigation reveals the absence of these metabolites in the leaf apoplast of MYMIV-susceptible mungbean cv.

https://doi.org/10.1007/s00299-024-03247-2

K851 (Table 16), consistent with findings in viroid-infected tomatoes and tobacco or potato studies (552,553). Tomato curly stunt virus (ToCSV) infection significantly impacts the phenylpropanoid pathway, particularly chlorogenic acids, exhibiting distinct responses in resistant and susceptible tomato lines linked to chlorogenic acid depletion (537). Upon virus infection, our data reveal an upregulation of α- and β-glucose in the overall plant cell, encompassing both apoplast and symplast. However, these glucose molecules do not appear to be involved in the synthesis of phenolic acids, as indicated by the absence of key precursors like phenylalanine, tyrosine, tryptophan, shikimic acid, caffeoylquinic acid, and chlorogenic acid in the apoplast (Table 16). Additionally, there was no significant change in their symplastic concentration upon MYMIV infection. This suggests that, upon virus infection, glucose molecules may be utilized for other purposes within the plant cell. From these findings, we hypothesize that the susceptibility of mungbean cv. K851 may be attributed to this metabolic profile. Elevating the levels of these metabolites might potentially contribute to developing disease resistance (554,555), necessitating further validation through comprehensive examinations.

Previous studies have documented elevated sugar levels in virus-infected plants (556). In this study, we report upregulated levels of α- and β-glucose in both the apoplast and symplast. Furthermore, there is an increase in fructose levels within the symplast but not in the apoplast, while we observe a significant increase in apoplastic sucrose levels but not in the symplast (Table 16). We speculate that intracellular fructose is potentially involved in the upregulation of the abscisic acid (ABA)- and ethylene-signaling pathway, primarily associated with the defense mechanism (557). Overall, this data indicates that under MYMIV infection, plant cells intracellularly cleave sucrose into glucose and fructose, which may explain the lack of a significant change in intracellular sucrose levels. Sucrose, a recognized signaling molecule, constitutes a major component of phloem sap, typically loaded through the symplastic route. However, in CMV-infected melon plants, Shalitin et al. (2000) proposed a shift from symplastic to apoplastic phloem sap loading of sucrose, supported by increased levels of radioactive sucrose (558). Additionally, the phloem-feeding whitefly *Bemisia tabaci*, which primarily feeds on phloem sap containing sucrose, can detect apoplastic sucrose concentrations using the sugar receptor BtabGR1 (559). It is reported that elevated sucrose concentrations suppress callose deposition in *Arabidopsis thaliana* cells (560). Consistent with previous findings, our data reveal a significant increase in sucrose levels, particularly in the apoplast of MYMIV-infected plants compared to uninfected ones. This suggests that plant cells synthesize and secrete elevated quantities of sucrose into the apoplast to suppress callose formation on plasmodesmata, facilitating the unrestricted cell-to-cell spread of the virus and potentially aiding in the nutrition of insect vectors such as whiteflies.

The amino acid composition in the apoplast undergoes variations based on the plant's physiological state and in response to both abiotic and biotic stresses (477,561). We report an increase in symplastic aspartate levels with its absence in the apoplast. Aspartate is a crucial amino acid used to synthesize many other essential amino acids (562). The elevated cytosolic aspartate may assist the plant in meeting the heightened demand for other amino acids during virus infection. Apoplastic proline and GABA act as chemotactic signals, guiding bacterial pathogens into the tomato apoplast (526). Additionally, proline acts as a crucial osmoprotectant, balancing cytosolic osmolarity (563). Local proline accumulation during pathogen infection can act as an apoptotic signal, triggering a hypersensitive response (564). The proline metabolizing pathway plays a crucial role in providing resistance to begomovirus infection in black gram cultivars (554). Our findings reveal the upregulation of proline in the apoplast and its downregulation in the cytosol,

https://doi.org/10.1007/s00299-024-03247-2

suggesting proline transport out of cells in response to virus infection to trigger a hypersensitive response (Table 16).

4.6 Summary

In this chapter, we sought to reveal a role for the apoplast in MYMIV infection. Using a standard method, we extracted AF from MYMIV-infected and uninfected mungbean leaves. Our data suggest the exploitation of the foliar apoplast by DNA viruses, as we detected MYMIV genomic DNA, potentially facilitating their systemic movement via the apoplast and inducing alterations in EVs size and numbers. Furthermore, the metabolic analysis of isolated apoplasts and symplast revealed distinctive metabolic profiles for both compartments, identifying metabolites associated with disease susceptibility. These identified metabolites play pivotal roles in stress responses and defense, emphasizing the importance of apoplast in begomovirus infection.

Chapter 5: Conclusion and future perspectives

5.1 Conclusion

Legumes, particularly mungbean, emerge as crucial components among essential human food crops. As the second most substantial human food crop after cereals, legumes, often referred to as "the poor man's meat," provide abundant sources of proteins, bioactive compounds, minerals, and vitamins (1). Mungbean, cultivated over 7 million hectares, primarily in Asia, plays a significant role in global agriculture. Despite India's prominence in mungbean production, yielding 2.17 million tons from around 4.32 million hectares, the productivity of mungbean remains relatively low due to notable constraints such as YMD caused by begomoviruses (3,8,193).

The genus *Begomovirus*, a highly successful and emerging group of plant viruses within the family *Geminiviridae*, poses a substantial threat to mungbean and other dicotyledonous plants. These viruses thrive due to their remarkable ability to recombine easily, generating novel variants and species. Leveraging DNA satellites as pathogenicity determinants and exploiting a broad range of cultivated and wild hosts, begomoviruses continue to expand globally. This expansion is facilitated by factors like global plant trade and climate change. Effectively addressing this viral infection necessitates a comprehensive understanding of its epidemiology, screening for resistant genotypes, and developing resistance through sustainable agricultural practices.

Our data indicate the prevalence of MYMIV in Assam and Orissa, in contrast to the dominance of MYMV in Bihar. This underscores significant regional variations in mungbean crops concerning begomovirus species. Additionally, our investigation into the evolutionary dynamics of these viruses, employing phylogenetic, recombination, and mutational analyses, has uncovered notable differences in the ancestry of DNA-A and DNA-B, particularly higher recombination events and genetic variability occurring in DNA-B. This provides valuable insights into the intricate genomic variations that drive the evolution of begomoviruses. Further, we screened several mungbean cultivars for resistance and susceptibility to YMD. The preparation of agroinfectious clones of MYMV and MYMIV facilitated the identification of the highly resistant (cv. PDM139) and highly susceptible (cv. K851) mungbean cultivars.

Prompted by this identification, our research took a crucial step towards developing a non-GMO and sustainable approach to manage YMD in mungbean. Leveraging RNAi technology, we topically applied hpRNA to trigger RNAi within plant cells against MYMIV. We identify two target regions to induce RNAi, resulting in the preparation of three hpRNAi clones (TR-1: AC4/AC1, TR-2: AC3/AC2/AC1, and TR-1+2: AC4/AC1_AC3/AC2/AC1). Transient expression assays, revealed stack clone i.e., hpTR-1+2_pART27 as a highly efficient construct to counter MYMIV. In vivo synthesized hpRNA (hpTR-1+2) spray assay, shown to induce formation of siRNA with life span of at least 12 days in systemic leaves. Further we conclude naked hpRNA spray can provide a short but potent protection window against MYMIV. Specifically, spraying hpRNA on the same day, two days, or four days prior to viral inoculation resulted in the highest resistance.

Finally, we explore the role of the apoplast under begomovirus infection. Our data indicate the presence of MYMIV genomes in the apoplast fluid. Additionally, we observe an increase in both size and numbers of EVs in the apoplast under begomovirus infection, suggesting a potential role in carrying extra cargo under viral stress conditions. Furthermore, our NMR-based metabolic analysis of apoplast and symplast reveals distinctive metabolic profiles for both compartments. This analysis identifies metabolites associated with disease susceptibility, particularly noting low levels of phenolic compounds and increased levels of apoplastic proline and sucrose. These identified metabolites play pivotal roles in stress responses and defense, highlighting the significant involvement of the apoplast in plant defenses against begomoviruses.

5.2 Future perspectives

- **Global Surveillance and Predictive Modeling:**
  Conducting a pan-India or international survey can provide a more comprehensive understanding of begomovirus prevalence and evolution. In-depth analysis of geographical distribution and genetic diversity of mungbean-infecting begomoviruses, coupled with exploration of ecological factors like climate and insect vectors, is essential.

- **Expanded Application of Agroinfectious Clones:**
  The prepared MYMV and MYMIV mungbean isolate agroinfectious clones, offer their utility beyond their natural host (i.e., mungbean). Testing their infectivity on other legume crops such as cowpea and blackgram may facilitate a comprehensive host range analysis and broader resistance screening.

- **Advanced Delivery Methods for hpRNA:**
  While hpTR-1+2 demonstrated efficacy in conferring resistance to MYMIV, refining the delivery method is crucial. Exploring advanced strategies such as nanoparticle carriers and viral vectors holds promise for enhancing the stability and efficiency of hpRNA within plant cells. These innovations could potentially extend the protective window, providing long-lasting protection. Furthermore, the success of hpTR-1+2 suggests possibilities for employing single hpRNA constructs against other begomovirus species, particularly those causing mixed infections in important crops, leading to broad-spectrum resistance.

- **Unraveling the Mechanism of MYMIV Secretion:**
  Though we detect MYMIV genomic DNA in the apoplast, the mechanism of its secretion remains a major unanswered question. Understanding how viruses exploit this pathway may allow the disruption of their entry point, effectively hindering infection and spread.

- **Exploring EVs Dynamics:**
  The observed increase in the size and number of EVs during begomovirus infection presents an intriguing avenue for further exploration. Investigating whether exosomes play a role in the secretion of begomovirus and, if so, whether they encapsulate virions or virus particles could provide valuable insights into how the virus evades the host immune system. While our study demonstrates the secretion of EVs, a more comprehensive understanding of their types and potential recipient cells is crucial. Recent research has uncovered the presence of mRNA in exosomes, suggesting that transcriptomics of exosomes could help elucidate their RNA cargos, including siRNA, long non-coding RNA, and more. This exploration would contribute to a deeper understanding of the complex interactions between begomoviruses and their host cells.

- **Comprehensive Metabolomic Analysis:**
  While NMR analysis provided valuable insights into metabolomes in the apoplast and symplast, unidentified metabolites present opportunities for further exploration. Employing complementary approaches like mass spectrometry can unlock the identities of these unknown players, potentially revealing novel defense pathways or susceptibility

factors. This deeper understanding of plant-virus metabolic interactions will guide future research and disease management strategies.

REFERENCES

1. Pataczek L, Zahir ZA, Ahmad M, Rani S, Nair R, Schafleitner R, et al. Beans with Benefits—The Role of Mungbean (Vigna radiate) in a Changing Environment. Am J Plant Sci. 2018;09(07):1577–600.
2. Nair RM, Yang R, Easdown WJ, Thavarajah D, Thavarajah P, Hughes J d'A, et al. Biofortification of mungbean (Vigna radiata) as a whole food to enhance human health. J Sci Food Agric. 2013 Jun 5;93(8):1805–13.
3. Nair R, Schreinemachers P. Global Status and Economic Importance of Mungbean. In 2020. p. 1–8.
4. Karthikeyan A, Shobhana VG, Sudha M, Raveendran M, Senthil N, Pandiyan M, et al. Mungbean yellow mosaic virus (MYMV): a threat to green gram (*Vigna radiata*) production in Asia. Int J Pest Manag. 2014 Oct 2;60(4):314–24.
5. Govindan K, Nagarajan P, Angappan K. Molecular studies on transmission of mung bean yellow mosaic virus (MYMV) by Bemisia tabaci Genn. in mungbean. Afr J Agril Res. 2014;9(38):2874–9.
6. Fiallo-Olivé E, Lett JM, Martin DP, Roumagnac P, Varsani A, Zerbini FM, et al. ICTV Virus Taxonomy Profile: Geminiviridae 2021. Journal of General Virology. 2021 Dec 23;102(12).
7. Zhou X. Advances in Understanding Begomovirus Satellites. Annu Rev Phytopathol. 2013 Aug 4;51(1):357–81.
8. Mishra GP, Dikshit HK, Ramesh S V, Tripathi K, Kumar RR, Aski M, et al. Yellow Mosaic Disease (YMD) of Mungbean (Vigna radiata (L .) Wilczek): Current Status and Management Opportunities. 2020;11(June):1–24.
9. Qazi J, Ilyas M, Mansoor S, Briddon RW. Legume yellow mosaic viruses: Genetically isolated begomoviruses. Mol Plant Pathol. 2007 Jul;8(4):343–8.
10. Rojas MR, Macedo MA, Maliano MR, Soto-Aguilar M, Souza JO, Briddon RW, et al. World Management of Geminiviruses. Annu Rev Phytopathol. 2018 Aug 25;56(1):637–77.
11. Sivalingam PN, Dokka N, Mahajan MM, Sahu B, Marathe A. Achieving maximum efficiency of Mungbean yellow mosaic India virus infection in mungbean by agroinoculation. 3 Biotech [Internet]. 2022;12(1):1–9. Available from: https://doi.org/10.1007/s13205-021-03088-w
12. Jacob SS, Vanitharani R, Karthikeyan AS, Chinchore Y, Thillaichidambaram P, Veluthambi K. Mungbean yellow mosaic virus -Vi Agroinfection by Codelivery of DNA A and DNA B From One Agrobacterium Strain. Plant Dis. 2003 Mar;87(3):247–51.
13. Karthikeya A, Sudha M, Pandiyan M, Senthil N, Shobana VG, Nagarajan P. Screening of MYMV Resistant Mungbean (Vigna radiata L. Wilczek) Progenies through Agroinoculation. Int J Plant Pathol. 2011 Jun 15;2(3):115–25.
14. Dhobale KV, Murugan B, Deb R, Kumar S, Sahoo L. Molecular Epidemiology of Begomoviruses Infecting Mungbean from Yellow Mosaic Disease Hotspot Regions of India. Appl Biochem Biotechnol. 2023;
15. Voloudakis AE, Kaldis A, Patil BL. RNA-Based Vaccination of Plants for Control of Viruses. Annu Rev Virol [Internet]. 2022 Sep 29;9(1):521–48. Available from: https://doi.org/10.1146/annurev-virology-091919-073708

16. Borah M, Nath PD, Chaudhury SP, Biswas KK, Patil BL, Voloudakis A. Topical application of dsRNAs targeting Citrus tristeza virus (CTV) reduces its titer in the CTV infected sweet orange (Citrus sinensis). Eur J Plant Pathol. 2023 Aug 28;
17. Fletcher SJ, Reeves PT, Hoang BT, Mitter N. A Perspective on RNAi-Based Biopesticides. Front Plant Sci. 2020 Feb 12;11.
18. Zhao S, Gong P, Liu J, Liu H, Lozano-Durán R, Zhou X, et al. Geminivirus C5 proteins mediate formation of virus complexes at plasmodesmata for viral intercellular movement. Plant Physiol. 2023 Aug 31;193(1):322–38.
19. Movahed N, Cabanillas DG, Wan J, Vali H, Laliberté JF, Zheng H. Turnip mosaic virus components are released into the extracellular space by vesicles in infected leaves. Plant Physiol. 2019 Jul 1;180(3):1375–88.
20. Hu S, Yin Y, Chen B, Lin Q, Tian Y, Song X, et al. Identification of viral particles in the apoplast of Nicotiana benthamiana leaves infected by potato virus X. Mol Plant Pathol. 2021 Apr 1;22(4):456–64.
21. Lucía-Sanz A, Manrubia S. Multipartite viruses: adaptive trick or evolutionary treat? Vol. 3, npj Systems Biology and Applications. Nature Publishing Group; 2017.
22. Michalakis Y, Blanc S. The Curious Strategy of Multipartite Viruses. Annu Rev Virol. 2020 Sep 29;7(1):203–18.
23. Sicard A, Michalakis Y, Gutiérrez S, Blanc S. The Strange Lifestyle of Multipartite Viruses. PLoS Pathog. 2016 Nov 3;12(11):e1005819.
24. Picó B, Díez MaJ, Nuez F. Evaluation of whitefly-mediated inoculation techniques to screen Lycopersicon esculentum and wild relatives for resistance to Tomato yellow leaf curl virus. Euphytica. 1998;101(3):259–71.
25. Leke WN, Mignouna DB, Brown JK, Kvarnheden A. Begomovirus disease complex: emerging threat to vegetable production systems of West and Central Africa. Agric Food Secur. 2015 Dec 21;4(1):1.
26. Mishra GP, Dikshit HK, S. V. R, Tripathi K, Kumar RR, Aski M, et al. Yellow Mosaic Disease (YMD) of Mungbean (Vigna radiata (L.) Wilczek): Current Status and Management Opportunities. Front Plant Sci. 2020 Jun 24;11.
27. Hanley-bowdoin L, Bejarano ER, Robertson D. Geminiviruses : masters at redirecting and reprogramming plant processes. Nature Publishing Group [Internet]. 2013;11(11):777–88. Available from: http://dx.doi.org/10.1038/nrmicro3117
28. Charoenvilaisiri S, Seepiban C, Phironrit N, Phuangrat B, Yoohat K, Deeto R, et al. Occurrence and distribution of begomoviruses infecting tomatoes, peppers and cucurbits in Thailand. Crop Protection. 2020 Jan;127:104948.
29. Naresh M, Abdeen Z, Rohit K, Sumit K. Occurrence and variability of begomoviruses associated with bhendi yellow vein mosaic and okra enation leaf curl diseases in south-western India. Virusdisease [Internet]. 2019;30(4):511–25. Available from: https://doi.org/10.1007/s13337-019-00551-4
30. Rocha CS, Castillo-urquiza GP, Lima ATM, Silva FN, Xavier CAD, Hora-júnior BT. Brazilian Begomovirus Populations Are Highly Recombinant , Rapidly Evolving , and Segregated Based on Geographical Location. 2013;87(10):5784–99.
31. Van Kammen A. Purification and properties of the components of cowpea mosaic virus. Virology. 1967 Apr;31(4):633–42.
32. Zwart MP, Elena SF. Modeling multipartite virus evolution: the genome formula facilitates rapid adaptation to heterogeneous environments†. Virus Evol. 2020 Jan 1;6(1).

33. Nee S. Mutualism, parasitism and competition in the evolution of coviruses. Philos Trans R Soc Lond B Biol Sci. 2000 Nov 29;355(1403):1607–13.
34. Iranzo J, Manrubia SC. Evolutionary dynamics of genome segmentation in multipartite viruses. Proceedings of the Royal Society B: Biological Sciences. 2012 Sep 22;279(1743):3812–9.
35. Gallet R, Fabre F, Thébaud G, Sofonea MT, Sicard A, Blanc S, et al. Small Bottleneck Size in a Highly Multipartite Virus during a Complete Infection Cycle. J Virol. 2018 Jul 15;92(14).
36. Di Mattia J, Torralba B, Yvon M, Zeddam JL, Blanc S, Michalakis Y. Nonconcomitant host-to-host transmission of multipartite virus genome segments may lead to complete genome reconstitution. Proceedings of the National Academy of Sciences. 2022 Aug 9;119(32).
37. Sicard A, Pirolles E, Gallet R, Vernerey MS, Yvon M, Urbino C, et al. A multicellular way of life for a multipartite virus. Elife. 2019 Mar 12;8.
38. Xiao YX, Li D, Wu YJ, Liu SS, Pan LL. Constant ratio between the genomic components of bipartite begomoviruses during infection and transmission. Virol J. 2023 Aug 21;20(1):186.
39. Park H, Denha S, Higgs PG. Evolution of Bipartite and Segmented Viruses from Monopartite Viruses. Viruses. 2023 May 10;15(5):1135.
40. Lucía-Sanz A, Manrubia S. Multipartite viruses: adaptive trick or evolutionary treat? NPJ Syst Biol Appl. 2017 Nov 9;3(1):34.
41. Labonté JM, Suttle CA. Previously unknown and highly divergent ssDNA viruses populate the oceans. ISME J. 2013 Nov 11;7(11):2169–77.
42. Creasy A, Rosario K, Leigh B, Dishaw L, Breitbart M. Unprecedented Diversity of ssDNA Phages from the Family Microviridae Detected within the Gut of a Protochordate Model Organism (Ciona robusta). Viruses. 2018 Jul 31;10(8):404.
43. Malathi VG, Renuka Devi P. ssDNA viruses: key players in global virome. Virusdisease. 2019 Mar 19;30(1):3–12.
44. Wawrzyniak P, Płucienniczak G, Bartosik D. The Different Faces of Rolling-Circle Replication and Its Multifunctional Initiator Proteins. Front Microbiol. 2017 Nov 30;8.
45. Zhao L, Rosario K, Breitbart M, Duffy S. Eukaryotic Circular Rep-Encoding Single-Stranded DNA (CRESS DNA) Viruses: Ubiquitous Viruses With Small Genomes and a Diverse Host Range. In 2019. p. 71–133.
46. Tisza MJ, Pastrana D V, Welch NL, Stewart B, Peretti A, Starrett GJ, et al. Discovery of several thousand highly diverse circular DNA viruses. Elife. 2020 Feb 4;9.
47. Rosario K, Dayaram A, Marinov M, Ware J, Kraberger S, Stainton D, et al. Diverse circular ssDNA viruses discovered in dragonflies (Odonata: Epiprocta). Journal of General Virology. 2012 Dec 1;93(12):2668–81.
48. Kazlauskas D, Varsani A, Koonin E V., Krupovic M. Multiple origins of prokaryotic and eukaryotic single-stranded DNA viruses from bacterial and archaeal plasmids. Nat Commun. 2019 Jul 31;10(1):3425.
49. Saunders K, Bedford ID, Yahara T, Stanley J. The earliest recorded plant virus disease. Nature. 2003 Apr;422(6934):831–831.
50. Inoue-Nagata AK, Lima MF, Gilbertson RL. A review of geminivirus diseases in vegetables and other crops in Brazil: current status and approaches for management. Hortic Bras. 2016 Mar;34(1):8–18.

51. Varma A, Malathi VG. Emerging geminivirus problems: A serious threat to crop production. Annals of Applied Biology. 2003 Apr 16;142(2):145–64.
52. Oberemok V V., Gal'chinsky N V., Useinov RZ, Novikov IA, Puzanova Y V., Filatov RI, et al. Four Most Pathogenic Superfamilies of Insect Pests of Suborder Sternorrhyncha: Invisible Superplunderers of Plant Vitality. Insects. 2023 May 13;14(5):462.
53. Varsani A, Navas-Castillo J, Moriones E, Hernández-Zepeda C, Idris A, Brown JK, et al. Establishment of three new genera in the family Geminiviridae: Becurtovirus, Eragrovirus and Turncurtovirus. Arch Virol. 2014 Aug 22;159(8):2193–203.
54. Torres-Herrera SI, Romero-Osorio A, Moreno-Valenzuela O, Pastor-Palacios G, Cardenas-Conejo Y, Ramírez-Prado JH, et al. A Lineage of Begomoviruses Encode Rep and AC4 Proteins of Enigmatic Ancestry: Hints on the Evolution of Geminiviruses in the New World. Viruses. 2019 Jul 13;11(7):644.
55. Lozano G, Trenado HP, Fiallo-Olivé E, Chirinos D, Geraud-Pouey F, Briddon RW, et al. Characterization of Non-coding DNA Satellites Associated with Sweepoviruses (Genus Begomovirus, Geminiviridae) – Definition of a Distinct Class of Begomovirus-Associated Satellites. Front Microbiol. 2016 Feb 17;7.
56. Gnanasekaran P, KishoreKumar R, Bhattacharyya D, Vinoth Kumar R, Chakraborty S. Multifaceted role of geminivirus associated betasatellite in pathogenesis. Mol Plant Pathol. 2019 Jul 18;20(7):1019–33.
57. Malathi VG, Renukadevi P, Chakraborty S, Biswas KK, Roy A, Sivalingam PN, et al. Begomoviruses and Their Satellites Occurring in India: Distribution, Diversity and Pathogenesis. In: A Century of Plant Virology in India. Singapore: Springer Singapore; 2017. p. 75–177.
58. Varma A, Mandal B, Singh MK. Global Emergence and Spread of Whitefly (Bemisia tabaci) Transmitted Geminiviruses. In: The Whitefly, Bemisia tabaci (Homoptera: Aleyrodidae) Interaction with Geminivirus-Infected Host Plants. Dordrecht: Springer Netherlands; 2011. p. 205–92.
59. Ilyas M, Qazi J, Mansoor S, Briddon RW. Genetic diversity and phylogeography of begomoviruses infecting legumes in Pakistan. Journal of General Virology. 2010;91(8):2091–101.
60. Prajapat R, Marwal A, Gaur RK. Begomovirus associated with alternative host weeds: a critical appraisal. Archives Of Phytopathology And Plant Protection. 2014 Jan 20;47(2):157–70.
61. He YZ, Wang YM, Yin TY, Fiallo-Olivé E, Liu YQ, Hanley-Bowdoin L, et al. A plant DNA virus replicates in the salivary glands of its insect vector via recruitment of host DNA synthesis machinery. Proceedings of the National Academy of Sciences. 2020 Jul 21;117(29):16928–37.
62. Qureshi MA, Lal A, Nawaz-ul-Rehman MS, Vo TTB, Sanjaya GNPW, Ho PT, et al. Emergence of Asian endemic begomoviruses as a pandemic threat. Front Plant Sci. 2022 Sep 28;13.
63. Saeed ST, Samad A. Emerging threats of begomoviruses to the cultivation of medicinal and aromatic crops and their management strategies. Virusdisease. 2017 Mar 4;28(1):1–17.
64. Moriones E, Idris A, Briddon RW, Zerbini FM, Martin DP, Martin DP. Capulavirus and Grablovirus : two new genera in the family Geminiviridae. 2017;1819–31.

65. Roumagnac P, Lett JM, Fiallo-Olivé E, Navas-Castillo J, Zerbini FM, Martin DP, et al. Establishment of five new genera in the family Geminiviridae: Citlodavirus, Maldovirus, Mulcrilevirus, Opunvirus, and Topilevirus. Arch Virol. 2022 Feb 27;167(2):695–710.
66. Hernandez C, Brown JK. First Report of a New Curtovirus Species, Spinach severe curly top virus, in Commercial Spinach Plants (*Spinacia oleracea*) from South-Central Arizona. Plant Dis. 2010 Jul;94(7):917–917.
67. Muhire B, Martin DP, Brown JK, Navas-Castillo J, Moriones E, Zerbini FM, et al. A genome-wide pairwise-identity-based proposal for the classification of viruses in the genus Mastrevirus (family Geminiviridae). Arch Virol. 2013 Jun 23;158(6):1411–24.
68. Shepherd DN, Martin DP, VAN DER WALT E, DENT K, VARSANI A, RYBICKI EP. Maize streak virus: an old and complex 'emerging' pathogen. Mol Plant Pathol. 2010 Jan 3;11(1):1–12.
69. Kvarnheden A, Lindblad M, Lindsten K, Valkonen JPT. Genetic diversity of Wheat dwarf virus. Arch Virol. 2002 Jan 1;147(1):205–16.
70. Kumar J, Kumar J, Singh SP, Tuli R. Association of Satellites with a Mastrevirus in Natural Infection: Complexity of Wheat Dwarf India Virus Disease. J Virol. 2014 Jun 15;88(12):7093–104.
71. Briddon RW, Bedford ID, Tsai JH, MARKHAM PG. Analysis of the Nucleotide Sequence of the Treehopper-Transmitted Geminivirus, Tomato Pseudo-Curly Top Virus, Suggests a Recombinant Origin. Virology. 1996 May;219(2):387–94.
72. Zhang W, Olson NH, Baker TS, Faulkner L, Agbandje-McKenna M, Boulton MI, et al. Structure of the Maize Streak Virus Geminate Particle. Virology. 2001 Jan;279(2):471–7.
73. Hipp K, Grimm C, Jeske H, Böttcher B. Near-Atomic Resolution Structure of a Plant Geminivirus Determined by Electron Cryomicroscopy. Structure. 2017 Aug;25(8):1303-1309.e3.
74. Hesketh EL, Saunders K, Fisher C, Potze J, Stanley J, Lomonossoff GP, et al. The 3.3 Å structure of a plant geminivirus using cryo-EM. Nat Commun. 2018 Dec 1;9(1).
75. Xu X, Zhang Q, Hong J, Li Z, Zhang X, Zhou X. Cryo-EM Structure of a Begomovirus Geminate Particle. Int J Mol Sci. 2019 Apr 8;20(7):1738.
76. Goodman RM, Shock TL, Haber S, Browning KS, Bowers GR. The composition of bean golden mosaic virus and its single-stranded DNA genome. Virology. 1980 Oct;106(1):168–72.
77. Hamilton WDO, Bisaro DM, Coutts RHA, Buck KW. Demonstration of the bipartite nature of the genome of a single-stranded DNA plant virus by infection with the cloned DNA components. Nucleic Acids Res. 1983;11(21):7387–96.
78. Fondong VN. Geminivirus protein structure and function Review Geminivirus protein structure and function. 2018;(October).
79. Morinaga T, Ikegami M, Miura K. The Nucleotide Sequence and Genome Structure of Mung Bean Yellow Mosaic Geminivirus. Microbiol Immunol. 1993 Jun 14;37(6):471–6.
80. Sánchez-Durán MA, Dallas MB, Ascencio-Ibañez JT, Reyes MI, Arroyo-Mateos M, Ruiz-Albert J, et al. Interaction between Geminivirus Replication Protein and the SUMO-Conjugating Enzyme Is Required for Viral Infection. J Virol. 2011 Oct;85(19):9789–800.
81. Kong LJ. A geminivirus replication protein interacts with the retinoblastoma protein through a novel domain to determine symptoms and tissue specificity of infection in plants. EMBO J. 2000 Jul 3;19(13):3485–95.

82. Luque A, Sanz-Burgos AP, Ramirez-Parra E, Castellano MM, Gutierrez C. Interaction of Geminivirus Rep Protein with Replication Factor C and Its Potential Role during Geminivirus DNA Replication. Virology. 2002 Oct;302(1):83–94.
83. Bagewadi B, Chen S, Lal SK, Choudhury NR, Mukherjee SK. PCNA Interacts with Indian Mung Bean Yellow Mosaic Virus Rep and Downregulates Rep Activity. J Virol. 2004 Nov;78(21):11890–903.
84. Koonin E V., Ilyina T V. Geminivirus replication proteins are related to prokaryotic plasmid rolling circle DNA replication initiator proteins. Journal of General Virology. 1992 Oct 1;73(10):2763–6.
85. Castillo AG, Collinet D, Deret S, Kashoggi A, Bejarano ER. Dual interaction of plant PCNA with geminivirus replication accessory protein (Ren) and viral replication protein (Rep). Virology. 2003 Aug;312(2):381–94.
86. Wu M, Wei H, Tan H, Pan S, Liu Q, Bejarano ER, et al. Plant DNA polymerases α and δ mediate replication of geminiviruses. Nat Commun. 2021 May 13;12(1):2780.
87. Kushwaha NK, Bhardwaj M, Chakraborty S. The replication initiator protein of a geminivirus interacts with host monoubiquitination machinery and stimulates transcription of the viral genome. PLoS Pathog. 2017 Aug 31;13(8):e1006587.
88. Babu KSD, Manoharan P, Pandi G. Computational studies on Begomoviral AC2/C2 proteins. Bioinformation. 2018 Jun 30;14(06):294–303.
89. Liu L, Chung HY, Lacatus G, Baliji S, Ruan J, Sunter G. Altered expression of Arabidopsis genes in response to a multifunctional geminivirus pathogenicity protein. BMC Plant Biol. 2014 Dec 18;14(1):302.
90. Castillo-González C, Liu X, Huang C, Zhao C, Ma Z, Hu T, et al. Geminivirus-encoded TrAP suppressor inhibits the histone methyltransferase SUVH4/KYP to counter host defense. Elife. 2015 Sep 7;4.
91. Rajeswaran R, Sunitha S, Shivaprasad P V., Pooggin MM, Hohn T, Veluthambi K. The Mungbean Yellow Mosaic Begomovirus Transcriptional Activator Protein Transactivates the Viral Promoter-Driven Transgene and Causes Toxicity in Transgenic Tobacco Plants. Molecular Plant-Microbe Interactions®. 2007 Dec;20(12):1545–54.
92. Sun R, Han J, Zheng L, Qu F. The AC2 Protein of a Bipartite Geminivirus Stimulates the Transcription of the BV1 Gene through Abscisic Acid Responsive Promoter Elements. Viruses. 2020 Dec 7;12(12):1403.
93. Lozano-Duran R, Bejarano ER. Geminivirus C2 protein might be the key player for geminiviral co-option of SCF-mediated ubiquitination. Plant Signal Behav. 2011 Jul 28;6(7):999–1001.
94. Guerrero J, Regedanz E, Lu L, Ruan J, Bisaro DM, Sunter G. Manipulation of the Plant Host by the Geminivirus AC2/C2 Protein, a Central Player in the Infection Cycle. Front Plant Sci. 2020 May 19;11.
95. Settlage SB, Miller AB, Hanley-Bowdoin L. Interactions between geminivirus replication proteins. J Virol. 1996 Oct;70(10):6790–5.
96. Pedersen TJ, Hanley-Bowdoin L. Molecular characterization of the AL3 protein encoded by a bipartite geminivirus. Virology. 1994 Aug 1;202(2):1070–5.
97. Pasumarthy KK, Mukherjee SK, Choudhury NR. The presence of tomato leaf curl Kerala virus AC3 protein enhances viral DNA replication and modulates virus induced gene-silencing mechanism in tomato plants. Virol J. 2011 Dec 18;8(1):178.

98. Wijaya NF, Nova B, Jamsari J. Geminivirus replication enhancer (REn/C3): In silico structure and characterization. In 2023. p. 050001.
99. Mei Y, Wang Y, Zhou X. Broad functional landscape of geminivirus-encoded C4/AC4 protein. Crop Health. 2023 Oct 13;1(1):9.
100. Fondong VN. The diverse roles of the multifunctional C4/AC4 protein in geminivirus infection. In: Geminivirus : Detection, Diagnosis and Management. Elsevier; 2022. p. 309–22.
101. Rojas MR, Jiang H, Salati R, Xoconostle-Cázares B, Sudarshana MR, Lucas WJ, et al. Functional Analysis of Proteins Involved in Movement of the Monopartite Begomovirus, Tomato Yellow Leaf Curl Virus. Virology. 2001 Dec;291(1):110–25.
102. Frischmuth S, Kleinow T, Aberle HJ, Wege C, H&#65533;lser D, Jeske H. Yeast two-hybrid systems confirm the membrane- association and oligomerization of BC1 but do not detect an interaction of the movement proteins BC1 and BV1 of Abutilon mosaic geminivirus. Arch Virol. 2004 Dec 21;149(12):2349–64.
103. Kleinow T, Holeiter G, Nischang M, Stein M, Karayavuz M, Wege C, et al. Post-translational modifications of Abutilon mosaic virus movement protein (BC1) in fission yeast. Virus Res. 2008 Jan;131(1):86–94.
104. Yu N, Wang J, Yu N, Zheng X, Zhou Q, Liu Z. Bioinformatics Analysis of the Interaction between Coat Protein and Nuclear Shuttle Protein in <i>Babuvirus</i> Am J Plant Sci. 2019;10(04):622–30.
105. Zhou Y, Rojas MR, Park MR, Seo YS, Lucas WJ, Gilbertson RL. Histone H3 Interacts and Colocalizes with the Nuclear Shuttle Protein and the Movement Protein of a Geminivirus. J Virol. 2011 Nov 15;85(22):11821–32.
106. Happle A, Jeske H, Kleinow T. Dynamic subcellular distribution of begomoviral nuclear shuttle and movement proteins. Virology. 2021 Oct;562:158–75.
107. Martins LGC, Raimundo GAS, Ribeiro NGA, Silva JCF, Euclydes NC, Loriato VAP, et al. A Begomovirus Nuclear Shuttle Protein-Interacting Immune Hub: Hijacking Host Transport Activities and Suppressing Incompatible Functions. Front Plant Sci. 2020 Apr 8;11.
108. Gupta N, Reddy K, Gnanasekaran P, Zhai Y, Chakraborty S, Pappu HR. Functional characterization of a new ORF βV1 encoded by radish leaf curl betasatellite. Front Plant Sci. 2022 Sep 20;13.
109. Chiu CW, Li YR, Lin CY, Yeh HH, Liu MJ. Translation initiation landscape profiling reveals hidden open-reading frames required for the pathogenesis of tomato yellow leaf curl Thailand virus. Plant Cell. 2022 Apr 26;34(5):1804–21.
110. Gong P, Tan H, Zhao S, Li H, Liu H, Ma Y, et al. Geminiviruses encode additional small proteins with specific subcellular localizations and virulence function. Nat Commun. 2021 Jul 13;12(1):4278.
111. Zhao S, Gong P, Ren Y, Liu H, Li H, Li F, et al. The novel C5 protein from tomato yellow leaf curl virus is a virulence factor and suppressor of gene silencing. Stress Biology. 2022 Dec 2;2(1):19.
112. Sunter G, Bisaro DM. Transcription map of the B genome component of tomato golden mosaic virus and comparison with A component transcripts. Virology. 1989 Dec;173(2):647–55.
113. Schalk HJ, Matzeit V, Schiller B, Schell J, Gronenborn B. Wheat dwarf virus, a geminivirus of graminaceous plants needs splicing for replication. EMBO J. 1989 Feb;8(2):359–64.

114. Qiu Y, Zhang S, Yu H, Xuan Z, Yang L, Zhan B, et al. Identification and Characterization of Two Novel Geminiviruses Associated with Paper Mulberry (*Broussonetia papyrifera*) Leaf Curl Disease. Plant Dis. 2020 Nov;104(11):3010–8.
115. Borah BK, Zarreen F, Baruah G, Dasgupta I. Insights into the control of geminiviral promoters. Virology. 2016 Aug;495:101–11.
116. Groning BR, Hayes RJ, Buck KW. Simultaneous regulation of tomato golden mosaic virus coat protein and AL1 gene expression: expression of the AL4 gene may contribute to suppression of the AL1 gene. Journal of General Virology. 1994 Apr 1;75(4):721–6.
117. Eagle PA, Orozco BM, Hanley-Bowdoin L. A DNA sequence required for geminivirus replication also mediates transcriptional regulation. Plant Cell. 1994 Aug;6(8):1157–70.
118. Horváth G V., Pettkó-Szandtner A, Nikovics K, Bilgin M, Boulton M, Davies JW, et al. Prediction of functional regions of the maize streak virus replication-associated proteins by protein-protein interaction analysis. Plant Mol Biol. 1998;38(5):699–712.
119. Eagle PA, Hanley-Bowdoin L. cis elements that contribute to geminivirus transcriptional regulation and the efficiency of DNA replication. J Virol. 1997 Sep;71(9):6947–55.
120. Haley A, Zhan X, Richardson K, Head K, Morris B. Regulation of the activities of African cassava mosaic virus promoters by the AC1, AC2, and AC3 gene products. Virology. 1992 Jun;188(2):905–9.
121. Trinks D, Rajeswaran R, Shivaprasad P V., Akbergenov R, Oakeley EJ, Veluthambi K, et al. Suppression of RNA Silencing by a Geminivirus Nuclear Protein, AC2, Correlates with Transactivation of Host Genes. J Virol. 2005 Feb 15;79(4):2517–27.
122. Hanley-Bowdoin L, Settlage SB, Orozco BM, Nagar S, Robertson D. Geminiviruses: Models for Plant DNA Replication, Transcription, and Cell Cycle Regulation. CRC Crit Rev Plant Sci. 1999 Jan 24;18(1):71–106.
123. Frey PM, Schärer-Hernández NG, Fütterer J, Potrykus I, Puonti-Kaerlas J. Simultaneous Analysis of the Bidirectional African Cassava Mosaic Virus Promoter Activity Using Two Different Luciferase Genes. Virus Genes. 2001;22(2):231–42.
124. Sunitha S, Mahajan N, Veluthambi K. The TrAP/REn monodirectional promoter of Mungbean yellow mosaic geminivirus (MYMV) displays root-specific expression in transgenic tobacco. Plant Cell, Tissue and Organ Culture (PCTOC). 2012 Jun 26;109(3):535–45.
125. Sharma N, Ruhel R. Rolling Circle Replication and Transcription Processes in Geminiviruses. In: Geminiviruses. Cham: Springer International Publishing; 2019. p. 17–38.
126. Rizvi I, Choudhury NR, Tuteja N. Insights into the functional characteristics of geminivirus rolling-circle replication initiator protein and its interaction with host factors affecting viral DNA replication. Arch Virol. 2015 Feb 2;160(2):375–87.
127. Wu M, Bejarano ER, Castillo AG, Lozano-Durán R. Geminivirus DNA replication in plants. In: Geminivirus : Detection, Diagnosis and Management. Elsevier; 2022. p. 323–46.
128. Preiss W, Jeske H. Multitasking in Replication Is Common among Geminiviruses. J Virol. 2003 Mar;77(5):2972–80.
129. Stenger DC, Revington GN, Stevenson MC, Bisaro DM. Replicational release of geminivirus genomes from tandemly repeated copies: evidence for rolling-circle replication of a plant viral DNA. Proceedings of the National Academy of Sciences. 1991 Sep 15;88(18):8029–33.

130. Jeske H. DNA forms indicate rolling circle and recombination-dependent replication of Abutilon mosaic virus. EMBO J. 2001 Nov 1;20(21):6158–67.
131. Saunders K, Lucy A, Stanley J. RNA-primed complementary-sense DNA synthesis of the geminivirus African cassava mosaic virus. Nucleic Acids Res. 1992;20(23):6311–5.
132. Steinfeldt T, Finsterbusch T, Mankertz A. Demonstration of Nicking/Joining Activity at the Origin of DNA Replication Associated with the Rep and Rep′ Proteins of Porcine Circovirus Type 1. J Virol. 2006 Jul;80(13):6225–34.
133. Laufs J, Traut W, Heyraud F, Matzeit V, Rogers SG, Schell J, et al. In vitro cleavage and joining at the viral origin of replication by the replication initiator protein of tomato yellow leaf curl virus. Proceedings of the National Academy of Sciences. 1995 Apr 25;92(9):3879–83.
134. Johne R, Müller H, Rector A, van Ranst M, Stevens H. Rolling-circle amplification of viral DNA genomes using phi29 polymerase. Trends Microbiol. 2009 May;17(5):205–11.
135. Settlage SB, See RG, Hanley-Bowdoin L. Geminivirus C3 Protein: Replication Enhancement and Protein Interactions. J Virol. 2005 Aug;79(15):9885–95.
136. Jeske H. Geminiviruses. In 2009. p. 185–226.
137. Symington LS. Role of RAD52 Epistasis Group Genes in Homologous Recombination and Double-Strand Break Repair. Microbiology and Molecular Biology Reviews. 2002 Dec;66(4):630–70.
138. Sung P, Krejci L, Van Komen S, Sehorn MG. Rad51 Recombinase and Recombination Mediators. Journal of Biological Chemistry. 2003 Oct;278(44):42729–32.
139. Gafni Y, Epel BL. The role of host and viral proteins in intra- and inter-cellular trafficking of geminiviruses. Physiol Mol Plant Pathol. 2002 May;60(5):231–41.
140. Harrison BD, Swanson MM, Fargette D. Begomovirus coat protein: serology, variation and functions. Physiol Mol Plant Pathol. 2002 May;60(5):257–71.
141. Hehnle S, Wege C, Jeske H. Interaction of DNA with the Movement Proteins of Geminiviruses Revisited. J Virol. 2004 Jul 15;78(14):7698–706.
142. Saeed M, Zafar Y, Randles JW, Rezaian MA. A monopartite begomovirus-associated DNA β satellite substitutes for the DNA B of a bipartite begomovirus to permit systemic infection. Journal of General Virology. 2007 Oct 1;88(10):2881–9.
143. Reagan BC, Burch-Smith TM. Viruses Reveal the Secrets of Plasmodesmal Cell Biology. Molecular Plant-Microbe Interactions®. 2020 Jan;33(1):26–39.
144. Noueiry AO, Lucas WJ, Gilbertson RL. Two proteins of a plant DNA virus coordinate nuclear and plasmodesmal transport. Cell. 1994 Mar;76(5):925–32.
145. Zhao S, Gong P, Liu J, Liu H, Lozano-Durán R, Zhou X, et al. Geminivirus C5 proteins mediate formation of virus complexes at plasmodesmata for viral intercellular movement. Plant Physiol. 2023 Aug 31;193(1):322–38.
146. Rojas MR, Jiang H, Salati R, Xoconostle-Cázares B, Sudarshana MR, Lucas WJ, et al. Functional Analysis of Proteins Involved in Movement of the Monopartite Begomovirus, Tomato Yellow Leaf Curl Virus. Virology. 2001 Dec;291(1):110–25.
147. Liu H, Boulton MI, Oparka KJ, Davies JW. Interaction of the movement and coat proteins of Maize streak virus: implications for the transport of viral DNA. Journal of General Virology. 2001 Jan 1;82(1):35–44.
148. Breves SS, Silva FA, Euclydes NC, Saia TFF, Jean-Baptiste J, Andrade Neto ER, et al. Begomovirus–Host Interactions: Viral Proteins Orchestrating Intra and Intercellular

Transport of Viral DNA While Suppressing Host Defense Mechanisms. Viruses. 2023 Jul 21;15(7):1593.
149. Makeshkumar T, Senthil Alias Sankar M. Recent developments in the diagnosis of geminiviruses. In: Geminivirus : Detection, Diagnosis and Management. Elsevier; 2022. p. 33–42.
150. Liu J, Wang X. Plant diseases and pests detection based on deep learning: a review. Plant Methods. 2021 Dec 24;17(1):22.
151. Rubio L, Galipienso L, Ferriol I. Detection of Plant Viruses and Disease Management: Relevance of Genetic Diversity and Evolution. Front Plant Sci. 2020 Jul 17;11.
152. Fang Y, Ramasamy R. Current and Prospective Methods for Plant Disease Detection. Biosensors (Basel). 2015 Aug 6;5(3):537–61.
153. Mehetre GT, Leo VV, Singh G, Sorokan A, Maksimov I, Yadav MK, et al. Current Developments and Challenges in Plant Viral Diagnostics: A Systematic Review. Viruses. 2021 Mar 5;13(3):412.
154. Boonham N, Kreuze J, Winter S, van der Vlugt R, Bergervoet J, Tomlinson J, et al. Methods in virus diagnostics: From ELISA to next generation sequencing. Virus Res. 2014 Jun;186:20–31.
155. Villamor DE V., Ho T, Al Rwahnih M, Martin RR, Tzanetakis IE. High Throughput Sequencing For Plant Virus Detection and Discovery. Phytopathology. 2019 May;109(5):716–25.
156. Mahlein AK, Oerke EC, Steiner U, Dehne HW. Recent advances in sensing plant diseases for precision crop protection. Eur J Plant Pathol. 2012 May 27;133(1):197–209.
157. Mahlein AK. Plant Disease Detection by Imaging Sensors – Parallels and Specific Demands for Precision Agriculture and Plant Phenotyping. Plant Dis. 2016 Feb;100(2):241–51.
158. Martinelli F, Scalenghe R, Davino S, Panno S, Scuderi G, Ruisi P, et al. Advanced methods of plant disease detection. A review. Agron Sustain Dev. 2015 Jan 11;35(1):1–25.
159. Attaluri S, Dharavath R. Novel plant disease detection techniques-a brief review. Mol Biol Rep. 2023 Nov 12;50(11):9677–90.
160. Zanoli L, Spoto G. Isothermal Amplification Methods for the Detection of Nucleic Acids in Microfluidic Devices. Biosensors (Basel). 2012 Dec 27;3(1):18–43.
161. Bouguettaya A, Zarzour H, Kechida A, Taberkit AM. Deep learning techniques to classify agricultural crops through UAV imagery: a review. Neural Comput Appl. 2022 Jun 5;34(12):9511–36.
162. Yao J, Tran SN, Sawyer S, Garg S. Machine learning for leaf disease classification: data, techniques and applications. Artif Intell Rev. 2023 Dec 18;56(S3):3571–616.
163. Hassan SM, Maji AK, Jasiński M, Leonowicz Z, Jasińska E. Identification of Plant-Leaf Diseases Using CNN and Transfer-Learning Approach. Electronics (Basel). 2021 Jun 9;10(12):1388.
164. Jadhav SB, Udupi VR, Patil SB. Identification of plant diseases using convolutional neural networks. International Journal of Information Technology. 2021 Dec 7;13(6):2461–70.
165. Donoso A, Valenzuela S. In-field molecular diagnosis of plant pathogens: recent trends and future perspectives. Plant Pathol. 2018 Sep 17;67(7):1451–61.
166. Kalimuthu K, Arivalagan J, Mohan M, Samuel Selvan Christyraj JR, Arockiaraj J, Muthusamy R, et al. Point of care diagnosis of plant virus: Current trends and prospects. Mol Cell Probes. 2022 Feb;61:101779.

167. Martínez-Culebras PV, FONT I, JORDÁ C. A rapid PCR method to discriminate between Tomato yellow leaf curl virus isolates. Annals of Applied Biology. 2001 Oct 16;139(2):251–7.
168. Kumar P, Oraon PK, Yadav P, Roy A, Goel S, Reddy MK, et al. Random distribution of nucleotide polymorphism throughout the genome of tomato-infecting begomovirus species occurring in India: implication in PCR based diagnosis. Virusdisease. 2022 Sep 10;33(3):270–83.
169. Londoño MA, Harmon CL, Polston JE. Evaluation of recombinase polymerase amplification for detection of begomoviruses by plant diagnostic clinics. Virol J. 2016 Dec 22;13(1):48.
170. Seepiban C, Charoenvilaisiri S, Warin N, Bhunchoth A, Phironrit N, Phuangrat B, et al. Development and application of triple antibody sandwich enzyme-linked immunosorbent assays for begomovirus detection using monoclonal antibodies against Tomato yellow leaf curl Thailand virus. Virol J. 2017 Dec 30;14(1):99.
171. Mahas A, Hassan N, Aman R, Marsic T, Wang Q, Ali Z, et al. LAMP-Coupled CRISPR–Cas12a Module for Rapid and Sensitive Detection of Plant DNA Viruses. Viruses. 2021 Mar 12;13(3):466.
172. Lavanya R, Arun V. Detection of Begomovirus in chilli and tomato plants using functionalized gold nanoparticles. Sci Rep. 2021 Jul 9;11(1):14203.
173. Schubert J, Habekuß A, Kazmaier K, Jeske H. Surveying cereal-infecting geminiviruses in Germany—Diagnostics and direct sequencing using rolling circle amplification. Virus Res. 2007 Jul;127(1):61–70.
174. Rodríguez-Negrete EA, Morales-Aguilar JJ, Domínguez-Duran G, Torres-Devora G, Camacho-Beltrán E, Leyva-López NE, et al. High-Throughput Sequencing Reveals Differential Begomovirus Species Diversity in Non-Cultivated Plants in Northern-Pacific Mexico. Viruses. 2019 Jun 29;11(7):594.
175. AlHudaib KA, Almaghasla MI, El-Ganainy SM, Arshad M, Drou N, Sattar MN. High-Throughput Sequencing Identified Distinct Bipartite and Monopartite Begomovirus Variants Associated with DNA-Satellites from Tomato and Muskmelon Plants in Saudi Arabia. Plants. 2022 Dec 20;12(1):6.
176. Guevara-Rivera EA, Rodríguez-Negrete EA, Lozano-Durán R, Bejarano ER, Torres-Calderón AM, Arce-Leal ÁP, et al. From Metagenomics to Ecogenomics: NGS-Based Approaches for Discovery of New Circular DNA Single-Stranded Viral Species. In 2024. p. 103–17.
177. Idris A, Al-Saleh M, Piatek M, Al-Shahwan I, Ali S, Brown J. Viral Metagenomics: Analysis of Begomoviruses by Illumina High-Throughput Sequencing. Viruses. 2014 Mar 12;6(3):1219–36.
178. Bornancini VA, Irazoqui JM, Flores CR, Vaghi Medina CG, Amadio AF, López Lambertini PM. Reconstruction and Characterization of Full-Length Begomovirus and Alphasatellite Genomes Infecting Pepper through Metagenomics. Viruses. 2020 Feb 11;12(2):202.
179. Avedi EK, Adediji AO, Kilalo DC, Olubayo FM, Macharia I, Ateka EM, et al. Metagenomic analyses and genetic diversity of Tomato leaf curl Arusha virus affecting tomato plants in Kenya. Virol J. 2021 Dec 6;18(1):2.
180. Hossain R, Ispizua Yamati FR, Barreto A, Savian F, Varrelmann M, Mahlein AK, et al. Elucidation of turnip yellows virus (TuYV) spectral reflectance pattern in Nicotiana

benthamiana by non-imaging sensor technology. Journal of Plant Diseases and Protection. 2023 Feb 14;130(1):35–43.

181. Peng Y, Dallas MM, Ascencio-Ibáñez JT, Hoyer JS, Legg J, Hanley-Bowdoin L, et al. Early detection of plant virus infection using multispectral imaging and spatial–spectral machine learning. Sci Rep. 2022 Feb 24;12(1):3113.
182. Prabhakar M, Prasad YG, Desai S, Thirupathi M, Gopika K, Rao GR, et al. Hyperspectral remote sensing of yellow mosaic severity and associated pigment losses in Vigna mungo using multinomial logistic regression models. Crop Protection. 2013 Mar;45:132–40.
183. Raji SN, Subhash N, Ravi V, Saravanan R, Mohanan CN, MakeshKumar T, et al. Detection and Classification of Mosaic Virus Disease in Cassava Plants by Proximal Sensing of Photochemical Reflectance Index. Journal of the Indian Society of Remote Sensing. 2016 Dec 12;44(6):875–83.
184. Feng Z, Ding X, Zhang H, He L, Duan J, Ma X, et al. Spectroscopic detection of wheat yellow mosaic virus infection based on invariant shape spectral processing and machine learning. Ecol Indic. 2023 Oct;154:110750.
185. Uke A, Khin S, Kitaura K, Ugaki M, Natsuaki KT. Combination of an image-posting system and molecular diagnosis for detecting Sri Lankan cassava mosaic virus. Trop Plant Pathol. 2019 Jun 20;44(3):238–43.
186. Burlyaeva M, Vishnyakova M, Gurkina M, Kozlov K, Ting C ruei LC ti, Schafleitner R, et al. Collections of Mungbean [Vigna radiata) (L .) R . Wilczek] and urdbean [V . mungo (L .) Hepper] in Vavilov Institute (VIR): traits diversity and trends in the breeding process over the last 100 years. Genet Resour Crop Evol [Internet]. 2019;66(4):767–81. Available from: https://doi.org/10.1007/s10722-019-00760-2
187. Kang YJ, Kim SK, Kim MY, Lestari P, Kim KH, Ha BK, et al. Genome sequence of mungbean and insights into evolution within Vigna species. Nat Commun. 2014 Nov 11;5.
188. Yu W, Zhang G, Wang W, Jiang C, Cao L. Identification and comparison of proteomic and peptide profiles of mung bean seeds and sprouts. BMC Chem [Internet]. 2020;1–12. Available from: https://doi.org/10.1186/s13065-020-00700-7
189. Keatinge JDH, Easdown WJ, Yang RY, Chadha ML, Shanmugasundaram S. Overcoming chronic malnutrition in a future warming world: the key importance of mungbean and vegetable soybean. Euphytica. 2011 Jul 4;180(1):129–41.
190. Hou D, Yousaf L, Xue Y, Hu J, Wu J, Hu X, et al. Mung bean (Vigna radiata L.): Bioactive polyphenols, polysaccharides, peptides, and health benefits. Vol. 11, Nutrients. MDPI AG; 2019.
191. Batzer JC, Singh A, Rairdin A, Chiteri K, Mueller DS. Mungbean: A Preview of Disease Management Challenges for an Alternative U.S. Cash Crop. J Integr Pest Manag. 2022 Jan 1;13(1).
192. Schafleitner R, Nair RM, Rathore A, Wang Y wei, Lin C yu, Chu S hui, et al. The AVRDC – The World Vegetable Center mungbean (Vigna radiata) core and mini core collections. BMC Genomics. 2015 Dec 29;16(1):344.
193. Karthikeyan A, Shobhana VG, Sudha M, Raveendran M, Senthil N, Pandiyan M, et al. Mungbean yellow mosaic virus (MYMV): a threat to green gram (Vigna radiata) production in Asia. Int J Pest Manag. 2014;60(4):314–24.
194. Nair RM, Pandey AK, War AR, Hanumantharao B, Shwe T, Alam AKMM, et al. Biotic and Abiotic Constraints in Mungbean Production—Progress in Genetic Improvement. Vol. 10, Frontiers in Plant Science. Frontiers Media S.A.; 2019.

195. Pandey AK, Burlakoti RR, Kenyon L, Nair RM. Perspectives and Challenges for Sustainable Management of Fungal Diseases of Mungbean [Vigna radiata (L.) R. Wilczek var. radiata]: A Review. Front Environ Sci. 2018 Jun 19;6.
196. Nariani TK. Yellow mosaic of mung (Phaseolus aureus L.). Indian Phytopathol. 1960;13(1).
197. Varsani A, Shepherd DN, Dent K, Monjane AL, Rybicki EP, Martin DP. A highly divergent South African geminivirus species illuminates the ancient evolutionary history of this family. Virol J. 2009 Dec 25;6(1):36.
198. Mansoor S, Briddon RW, Zafar Y, Stanley J. Geminivirus disease complexes : an emerging threat. 2003;8(3):128–34.
199. Markham PG, Bedford ID, Liu S, Pinner MS. The transmission of geminiviruses by *Bemisia tabaci*. Pestic Sci. 1994 Oct;42(2):123–8.
200. Czosnek H, Hariton-Shalev A, Sobol I, Gorovits R, Ghanim M. The incredible journey of Begomoviruses in their whitefly vector. Vol. 9, Viruses. MDPI AG; 2017.
201. Malathi VC, John P. Mungbean yellow mosaic viruses. Desk encyclopedia of plant and fungal virology. 2009;217–26.
202. Mohan S, Sheeba A, Murugan E, Ibrahim SM. Screening of Mungbean germplasm for resistance to Mungbean Yellow Mosaic virus under natural condition. Indian J Sci Technol. 2014;7(7):891–6.
203. Tilak V, Manoj C V, Kishore KP. New record of mungbean yellow mosaic India virus in Desmodium laxiflorum and association of bhendi yellow vein mosaic betasatellite in Abelmoschus moschatus in Andhra Pradesh , India. Virusdisease [Internet]. 2022;33(1):119–21. Available from: https://doi.org/10.1007/s13337-021-00749-5
204. Naimuddin K. Identification of Mungbean yellow mosaic India virus infecting Vigna mungo var . silvestris L . 2011;94–100.
205. Kamaal N, Akram M. Yellow mosaic of mungbean and urdbean : current status and future strategies Yellow mosaic of mungbean and urdbean : current status and future strategies. 2016;(January).
206. Shahid MS, Shafiq M, Ilyas M, Raza A, Al-Sadrani MN, Al-Sadi AM, et al. Frequent occurrence of Mungbean yellow mosaic India virus in tomato leaf curl disease affected tomato in Oman. Sci Rep. 2019 Nov 12;9(1):16634.
207. Reddy BVB, Obaiah S, Prasanthi L, Sivaprasad Y, Sujitha A, Reddy BVB, et al. Archives of Phytopathology and Plant Protection with yellow mosaic disease of blackgram (Vigna mungo L .) in Andhra Pradesh , India. Archives of Phytopathology and Plant Protection [Internet]. 2015;48(4):347–55. Available from: http://dx.doi.org/10.1080/03235408.2014.888874
208. Maruthi MN, Manjunatha B, Rekha AR, Govindappa MR, Colvin J, Muniyappa V. Dolichos yellow mosaic virus belongs to a distinct lineage of Old World begomoviruses; its biological and molecular properties. Annals of Applied Biology. 2006 Oct 2;149(2):187–95.
209. Thongmeearkom P. Nuclear Ultrastructural Changes and Aggregates of Viruslike Particles in Mungbean Cells Affected by Mungbean Yellow Mosaic Disease. Phytopathology. 1981;71(1):41.
210. Honda Y, Iwaki M, Saito Y, Thongmeearkom P, Kittisak K, Deema N. Mechanical transmission, purification, and some properties of white-fly-borne mung bean yellow mosaic virus in Thailand. Plant Dis. 1983;

211. Mandal B, Varma A, Malathi VG. Systemic Infection of Vigna mungo Using the Cloned DNAs of the Blackgram Isolate of Mungbean Yellow Mosaic Geminivirus through Agroinoculation and Transmission of the Progeny Virus by Whiteflies. Journal of Phytopathology. 1997 Dec;145(11–12):505–10.
212. Fauquet CM, Briddon RW, Brown JK, Moriones E, Stanley J, Zerbini M, et al. Geminivirus strain demarcation and nomenclature. Arch Virol. 2008 Apr;153(4):783–821.
213. Gilbertson RL, Rojas M, Natwick E. Development of Integrated Pest Management (IPM) Strategies for Whitefly (Bemisia tabaci)-Transmissible Geminiviruses. In: The Whitefly, Bemisia tabaci (Homoptera: Aleyrodidae) Interaction with Geminivirus-Infected Host Plants. Dordrecht: Springer Netherlands; 2011. p. 323–56.
214. Singh CM, Singh P, Pratap A, Pandey R, Purwar S, Vibha, et al. Breeding for Enhancing Legumovirus Resistance in Mungbean: Current Understanding and Future Directions. Agronomy. 2019 Oct 10;9(10):622.
215. Saggaf MH, Ndunguru J, Tairo F, Sseruwagi P, Ascencio-Ibáñez JT, Kilalo D, et al. Immunohistochemical localization of Cassava brown streak virus and its morphological effect on cassava leaves. Physiol Mol Plant Pathol. 2019 Jan;105:67–76.
216. Bashir M, Jamali AR, Ahmad Z. Genetic resistance in mungbean and mashbean germplasm against mungbean yellow mosaic begomovirus. Mycopath. 2006;4(2):1–4.
217. R. Selvi., A.R. Muthiah., N. Manivannan., T.S. Raveendran., A. Manickam., R. Samiyappan. Tagging of RAPD Marker for MYMV Resistance in Mungbean (Vigna radiata (L.) Wilczek). Asian J Plant Sci. 2006 Feb 15;5(2):277–80.
218. Shivaprasad P V., Thillaichidambaram P, Balaji V, Veluthambi K. Expression of full-length and truncated Rep genes from Mungbean yellow mosaic virus-Vigna inhibits viral replication in transgenic tobacco. Virus Genes. 2006 Dec;33(3):365–74.
219. Laosatit K, Somta P, Chen X, Srinives P. Genomic Approaches to Biotic Stresses. In 2020. p. 133–67.
220. Rahman A, Akanda A, Alam AA. Relationship of Whitefly Population Build up with the Spread of TYLCV on Eight Tomato Varieties. Journal of Agriculture & Rural Development. 1970 Jan 1;4(1):67–74.
221. Alam AKMM, Somta P, Jompuk C, Chatwachirawong P, Srinives P. Evaluation of Mungbean Genotypes Based on Yield Stability and Reaction to Mungbean Yellow Mosaic Virus Disease. Plant Pathol J. 2014 Sep 1;30(3):261–8.
222. Subedi S, Neupane S, Ghimire TN. Screening of mungbean and black gram genotypes as sources of genetic resistance against Mungbean Yellow Mosaic Disease. J Agric Sci (Belihuloya). 2016;14:148–55.
223. Prathyusha VB, Swathi E, Divya D, Reddy BVB, Bentur JS, Chalam VC, et al. Field and agroinoculation screening of national collection of urd bean (Vigna mungo) germplasm accessions for new sources of mung bean yellow mosaic virus (MYMV) resistance. 3 Biotech. 2023 Jun 16;13(6):194.
224. Dharajiya DT, Tiwari KK, Ravindrababu Y. Identification of resistant sources of mungbean [Vigna radiata (L.) Wilczek] against mungbean yellow mosaic virus (MYMV) by field evaluation and linked molecular markers. Vegetos. 2021 Dec 15;34(4):814–21.
225. Nair RM, Götz M, Winter S, Giri RR, Boddepalli VN, Sirari A, et al. Identification of mungbean lines with tolerance or resistance to yellow mosaic in fields in India where different begomovirus species and different Bemisia tabaci cryptic species predominate. Eur J Plant Pathol. 2017 Oct 24;149(2):349–65.

226. Choudhary A, Choudhary S, Singh M, Yadav VL, Moond V. Screening of Mung Bean Genotypes against Yellow Mosaic Virus (YMV) Resistance. International Journal of Environment and Climate Change. 2023 Feb 23;13(2):109–14.
227. Bhanu AN. Screening Mungbean [Vigna radiata (L.) Wilczek] Genotypes for Mungbean Yellow Mosaic Virus Resistance under Natural Condition. Advances in Plants & Agriculture Research. 2017 Nov 9;7(6).
228. Mantesh M, tesh V, Pankaja NS. Validation of the Modes of Transmission of Mungbean Yellow Mosaic Virus (MYMV) in Mungbean [Vigna radiata (L.) Wilczek]. Int J Curr Microbiol Appl Sci. 2019 Nov 20;8(11):950–7.
229. Monde G, Walangululu J, Bragard C. Screening cassava for resistance to cassava mosaic disease by grafting and whitefly inoculation. Archives Of Phytopathology And Plant Protection. 2012 Nov;45(18):2189–201.
230. Akhtar KP, Hussain M, Khan AI, Ahsanul Haq M, Mohsin Iqbal M. Influence of plant age, whitefly population and cultivar resistance on infection of cotton plants by cotton leaf curl virus (CLCuV) in Pakistan. Field Crops Res. 2004 Feb;86(1):15–21.
231. G R Hithesh, K D Shah, M C Keerthi, B B Kabaria. Screening of Mungbean Genotypes Against Whitefly <i>Bemisia tabaci</i> (Genn.) And Thrips <i>Megalurothrips distalis</i> (Karny). Indian Journal of Entomology. 2022 Aug 29;1–4.
232. Akhtar KP, Sarwar G, Abbas G, Asghar MJ, Sarwar N, Shah TM. Screening of mungbean germplasm against mungbean yellow mosaic India virus and its vector Bemisia tabaci. Crop Protection [Internet]. 2011;30(9):1202–9. Available from: http://dx.doi.org/10.1016/j.cropro.2011.05.012
233. Rogers SG, Bisaro DM, Horsch RB, Fraley RT, Hoffmann NL, Brand L, et al. Tomato golden mosaic virus A component DNA replicates autonomously in transgenic plants. Cell. 1986 May;45(4):593–600.
234. Grimsley N, Hohn B, Hohn T, Walden R. "Agroinfection," an alternative route for viral infection of plants by using the Ti plasmid. Proceedings of the National Academy of Sciences. 1986 May;83(10):3282–6.
235. Grimsley N, Hohn T, Davies JW, Hohn B. Agrobacterium-mediated delivery of infectious maize streak virus into maize plants. Nature. 1987 Jan;325(6100):177–9.
236. Peyret H, Lomonossoff GP. When plant virology met *Agrobacterium* : the rise of the deconstructed clones. Plant Biotechnol J. 2015 Oct 12;13(8):1121–35.
237. Leiser RM, Ziegler-Graff V, Reutenauer A, Herrbach E, Lemaire O, Guilley H, et al. Agroinfection as an alternative to insects for infecting plants with beet western yellows luteovirus. Proc Natl Acad Sci U S A. 1992 Oct 1;89(19):9136–40.
238. Ascencio-Ibáñez JT, Dallas MM, Hanley-Bowdoin L. Begomovirus Inoculation in Arabidopsis and Cassava. In 2024. p. 71–9.
239. Vaghchhipawala Z, Rojas CM, Senthil-Kumar M, Mysore KS. Agroinoculation and Agroinfiltration: Simple Tools for Complex Gene Function Analyses. In 2011. p. 65–76.
240. Yan H xue, Fu D qi, Zhu B zhong, Liu H ping, Shen X ying, Luo Y bo. Sprout vacuum-infiltration: a simple and efficient agroinoculation method for virus-induced gene silencing in diverse solanaceous species. Plant Cell Rep. 2012 Sep 21;31(9):1713–22.
241. Kaur M, Manchanda P, Kalia A, Ahmed FK, Nepovimova E, Kuca K, et al. Agroinfiltration Mediated Scalable Transient Gene Expression in Genome Edited Crop Plants. Int J Mol Sci. 2021 Oct 8;22(19):10882.

242. Doyle JJ, Doyle JL. A rapid DNA isolation from small amount of fresh leaf tissue. Phytochem Bull. 1987;19:11–5.
243. Dellaporta SL, Wood J, Hicks JB. A plant DNA minipreparation: Version II. Plant Mol Biol Report. 1983 Sep;1(4):19–21.
244. Briddon RW, Prescott AG, Lunness P, Chamberlin LCL, Markham PG. Rapid production of full-length, infectious geminivirus clones by abutting primer PCR (AbP-PCR). J Virol Methods. 1993 Jun;43(1):7–20.
245. Johne R, Mu H, Rector A, Ranst M Van, Stevens H. Rolling-circle amplification of viral DNA genomes using phi29 polymerase. 2009;(April):205–11.
246. Wu CY, Lai YC, Lin NS, Hsu YH, Tsai HT, Liao JY, et al. A simplified method of constructing infectious clones of begomovirus employing limited restriction enzyme digestion of products of rolling circle amplification. J Virol Methods. 2008 Feb;147(2):355–9.
247. Ferreira P de T de O, Lemos TO, Nagata T, Inoue-Nagata AK. One-step cloning approach for construction of agroinfectious begomovirus clones. J Virol Methods. 2008 Feb;147(2):351–4.
248. Trenado HP, Orílio AF, Márquez-Martín B, Moriones E, Navas-Castillo J. Sweepoviruses Cause Disease in Sweet Potato and Related Ipomoea spp.: Fulfilling Koch's Postulates for a Divergent Group in the Genus Begomovirus. PLoS One. 2011 Nov 2;6(11):e27329.
249. Inoue-Nagata AK, Albuquerque LC, Rocha WB, Nagata T. A simple method for cloning the complete begomovirus genome using the bacteriophage φ29 DNA polymerase. J Virol Methods. 2004 Mar;116(2):209–11.
250. Wise AA, Liu Z, Binns AN. Three Methods for the Introduction of Foreign DNA into <i>Agrobacterium</i> In: Agrobacterium Protocols. New Jersey: Humana Press; 2006. p. 43–54.
251. Chincinska IA. Leaf infiltration in plant science: old method, new possibilities. Plant Methods. 2021 Jul 28;17(1):83.
252. Biswas KK, Varma A. Agroinoculation: a method of screening germplasm resistance to mungbean yellow mosaic geminivirus. Indian Phytopathol. 2001;
253. Sudha M, Karthikeyan A, Nagarajan P, Raveendran M, Senthil N, Pandiyan M, et al. Screening of mungbean (Vigna radiata) germplasm for resistance to Mungbean yellow mosaic virus using agroinoculation. Canadian Journal of Plant Pathology. 2013 Jul;35(3):424–30.
254. Taylor P, Sudha M, Karthikeyan A, Nagarajan P, Raveendran M, Senthil N, et al. Screening of mungbean (Vigna radiata) germplasm for resistance to Mungbean yellow mosaic virus using agroinoculation Screening of mungbean (Vigna radiata) germplasm for resistance to Mungbean yellow mosaic virus using agroinoculation. 2013;(November 2014):37–41.
255. Danforth D, Sciences P, Louis S, Lafayette W. Infectivity analysis of two variable DNA B components of Mungbean yellow mosaic virus-Vigna in Vigna mungo and Vigna radiata. 2004;29(3).
256. Chaithanya BH, Reddy BVB, Prasanthi L, Devi RSJ, Manjula K, Naidu GM. Construction of Full-length Dimer Clones of Yellow Mosaic Virus and Screening of Blackgram Germplasm using Agroinoculation. LEGUME RESEARCH - AN INTERNATIONAL JOURNAL. 2022 Jan 18;(Of).

257. Naimuddin K, Akram M, Sanjeev G. Identification of Mungbean yellow mosaic India virus infecting Vigna mungo var. silvestris L. Phytopathol Mediterr [Internet]. 2011;50(1):94–100. Available from: http://www.jstor.org/stable/26458681
258. Kanzaki S. Highly Efficient Agroinoculation Method for Tomato Plants with Tomato Yellow Leaf Curl Kanchanaburi Virus. 2017;86(4):479–86.
259. Li F, Qiao R, Yang X, Gong P, Zhou X. Occurrence, distribution, and management of tomato yellow leaf curl virus in China. Vol. 4, Phytopathology Research. BioMed Central Ltd; 2022.
260. Koeda S, Homma K, Tanaka Y, Kesumawati E, Zakaria S, Kanzaki S. Highly Efficient Agroinoculation Method for Tomato Plants with <i>Tomato Yellow Leaf Curl Kanchanaburi Virus</i> Hort J. 2017;86(4):479–86.
261. Pico B, Ferriol M, Diez MJ, Vinals FN. Agroinoculation methods to screen wild Lycopersicon for resistance to Tomato yellow leaf curl virus. Journal of Plant Pathology. 2001;215–20.
262. Usharani KS, Surendranath B, Haq QMR, Malathi VG. Infectivity analysis of a soybean isolate of Mungbean yellow mosaic India virus by agroinoculation. Journal of General Plant Pathology. 2005 Jun 17;71(3):230–7.
263. Hayes RJ, Coutts RHA, Buck KW. Agroinfection of Nicotiana spp. with Cloned DNA of Tomato Golden Mosaic Virus. Journal of General Virology. 1988 Jul 1;69(7):1487–96.
264. Wang J, Turina M, Stewart LR, Lindbo JA, Falk BW. Agroinoculation of the Crinivirus, Lettuce infectious yellows virus, for systemic plant infection. Virology. 2009 Sep;392(1):131–6.
265. Cruz FCStA, Boulton MI, Hull R, Azzam O. International Rice Research Institute, Los Baños, Philippines. Journal of Phytopathology. 1999 Dec 25;147(11–12):653–9.
266. Zottini M, Barizza E, Costa A, Formentin E, Ruberti C, Carimi F, et al. Agroinfiltration of grapevine leaves for fast transient assays of gene expression and for long-term production of stable transformed cells. Plant Cell Rep. 2008 May 7;27(5):845–53.
267. Klinkenberg FA, Ellwood S, Stanley J. Fate of African Cassava Mosaic Virus Coat Protein Deletion Mutants after Agroinoculation. Journal of General Virology. 1989 Jul 1;70(7):1837–44.
268. Saeed M, Behjatnia SAA, Mansoor S, Zafar Y, Hasnain S, Rezaian MA. A Single Complementary-Sense Transcript of a Geminiviral DNA β Satellite Is Determinant of Pathogenicity. Molecular Plant-Microbe Interactions®. 2005 Jan;18(1):7–14.
269. Pan LL, Chi Y, Liu C, Fan YY, Liu SS. Mutations in the coat protein of a begomovirus result in altered transmission by different species of whitefly vectors. Virus Evol. 2020 Jan 1;6(1).
270. Wroblewski T, Tomczak A, Michelmore R. Optimization of Agrobacterium -mediated transient assays of gene expression in lettuce, tomato and Arabidopsis. Plant Biotechnol J. 2005 Mar 3;3(2):259–73.
271. Yan H xue, Fu D qi, Zhu B zhong, Liu H ping, Shen X ying, Luo Y bo. Sprout vacuum-infiltration: a simple and efficient agroinoculation method for virus-induced gene silencing in diverse solanaceous species. Plant Cell Rep. 2012 Sep 21;31(9):1713–22.
272. Ryu C, Anand A, Kang L, Mysore KS. Agrodrench: a novel and effective agroinoculation method for virus-induced gene silencing in roots and diverse Solanaceous species. The Plant Journal. 2004 Oct 14;40(2):322–31.

273. Courdavault V, Besseau S, Oudin A, Papon N, O'Connor SE. Virus-Induced Gene Silencing: Hush Genes to Make Them Talk. Trends Plant Sci. 2020 Jul;25(7):714–5.
274. Zulfiqar S, Farooq MA, Zhao T, Wang P, Tabusam J, Wang Y, et al. Virus-Induced Gene Silencing (VIGS): A Powerful Tool for Crop Improvement and Its Advancement towards Epigenetics. Int J Mol Sci. 2023 Mar 15;24(6):5608.
275. Ramegowda V, Mysore KS, Senthil-Kumar M. Virus-induced gene silencing is a versatile tool for unraveling the functional relevance of multiple abiotic-stress-responsive genes in crop plants. Front Plant Sci. 2014 Jul 8;5.
276. Vanitharani R, Chellappan P, Fauquet CM. Short interfering RNA-mediated interference of gene expression and viral DNA accumulation in cultured plant cells. Proceedings of the National Academy of Sciences. 2003 Aug 5;100(16):9632–6.
277. Bonfim K, Faria JC, Nogueira EOPL, Mendes ÉA, Aragão FJL. RNAi-Mediated Resistance to Bean golden mosaic virus in Genetically Engineered Common Bean (Phaseolus vulgaris). Molecular Plant-Microbe Interactions®. 2007 Jun;20(6):717–26.
278. Malathi P, Muzammil SA, Krishnaveni D, Balachandran SM, Mangrauthia SK. Coat protein 3 of Rice tungro spherical virus is the key target gene for development of RNAi mediated tungro disease resistance in rice. Agri Gene. 2019 Jun;12:100084.
279. Patil BL. Genetic engineering for virus resistance in plants: principles and methods. In: Genes, Genetics and Transgenics for Virus Resistance in Plants. Caister Academic Press; 2018.
280. Sanford JC, Johnston SA. The concept of parasite-derived resistance—Deriving resistance genes from the parasite's own genome. J Theor Biol. 1985 Mar;113(2):395–405.
281. Tricoll DM, Carney KJ, Russell PF, McMaster JR, Groff DW, Hadden KC, et al. Field Evaluation of Transgenic Squash Containing Single or Multiple Virus Coat Protein Gene Constructs for Resistance to Cucumber Mosaic Virus, Watermelon Mosaic Virus 2 and Zucchini Yellow Mosaic Virus. Nat Biotechnol. 1995 Dec 1;13(12):1458–65.
282. Beachy RN, Loesch-Fries S, Tumer NE. Coat Protein-Mediated Resistance Against Virus Infection. Annu Rev Phytopathol. 1990 Sep;28(1):451–72.
283. Baltes NJ, Hummel AW, Konecna E, Cegan R, Bruns AN, Bisaro DM, et al. Conferring resistance to geminiviruses with the CRISPR–Cas prokaryotic immune system. Nat Plants. 2015 Sep 28;1(10):15145.
284. Ali Z, Abulfaraj A, Idris A, Ali S, Tashkandi M, Mahfouz MM. CRISPR/Cas9-mediated viral interference in plants. Genome Biol. 2015 Dec 11;16(1):238.
285. Zaidi SS e A, Mansoor S, Ali Z, Tashkandi M, Mahfouz MM. Engineering Plants for Geminivirus Resistance with CRISPR/Cas9 System. Trends Plant Sci. 2016 Apr;21(4):279–81.
286. Tashkandi M, Ali Z, Aljedaani F, Shami A, Mahfouz MM. Engineering resistance against *Tomato yellow leaf curl virus* via the CRISPR/Cas9 system in tomato. Plant Signal Behav. 2018 Oct 3;13(10):e1525996.
287. Karkute SG, Singh AK, Gupta OP, Singh PM, Singh B. CRISPR/Cas9 Mediated Genome Engineering for Improvement of Horticultural Crops. Front Plant Sci. 2017 Sep 22;8.
288. Kumar S, Tanti B, Patil BL, Mukherjee SK, Sahoo L. RNAi-derived transgenic resistance to Mungbean yellow mosaic India virus in cowpea. 2017;1–20.
289. Kumar V, Saumik S, Supriya B. RNAi mediated broad-spectrum transgenic resistance in Nicotiana benthamiana to chilli-infecting begomoviruses. Plant Cell Rep. 2015;1389–99.

290. Aragão FJL, Faria JC. First transgenic geminivirus-resistant plant in the field. Nat Biotechnol. 2009 Dec;27(12):1086–8.
291. Tzean Y, Chang HH, Tu TC, Hou BH, Chen HM, Chiu YS, et al. Engineering Plant Resistance to Tomato Yellow Leaf Curl Thailand Virus Using a Phloem-Specific Promoter Expressing Hairpin RNA. Molecular Plant-Microbe Interactions®. 2020 Jan;33(1):87–97.
292. Kumari A, Hada A, Subramanyam K, Theboral J, Misra S, Ganapathi A, et al. RNAi-mediated resistance to yellow mosaic viruses in soybean targeting coat protein gene. Acta Physiol Plant. 2018 Feb 17;40(2):32.
293. Sharma VK, Basu S, Chakraborty S. RNAi mediated broad-spectrum transgenic resistance in Nicotiana benthamiana to chilli-infecting begomoviruses. Plant Cell Rep. 2015 Aug 28;34(8):1389–99.
294. Leibman D, Prakash S, Wolf D, Zelcer A, Anfoka G, Haviv S, et al. Immunity to tomato yellow leaf curl virus in transgenic tomato is associated with accumulation of transgene small RNA. Arch Virol. 2015 Nov 9;160(11):2727–39.
295. Ntui VO, Kong K, Khan RS, Igawa T, Janavi GJ, Rabindran R, et al. Resistance to Sri Lankan Cassava Mosaic Virus (SLCMV) in Genetically Engineered Cassava cv. KU50 through RNA Silencing. PLoS One. 2015 Apr 22;10(4):e0120551.
296. Loriato VAP, Martins LGC, Euclydes NC, Reis PAB, Duarte CEM, Fontes EPB. Engineering resistance against geminiviruses: A review of suppressed natural defenses and the use of RNAi and the CRISPR/Cas system. Plant Science. 2020 Mar;292:110410.
297. Barrangou R, Birmingham A, Wiemann S, Beijersbergen RL, Hornung V, Smith A van B. Advances in CRISPR-Cas9 genome engineering: lessons learned from RNA interference. Nucleic Acids Res. 2015 Apr 20;43(7):3407–19.
298. Mehta D, Stürchler A, Anjanappa RB, Zaidi SS e A, Hirsch-Hoffmann M, Gruissem W, et al. Linking CRISPR-Cas9 interference in cassava to the evolution of editing-resistant geminiviruses. Genome Biol. 2019 Dec 25;20(1):80.
299. Andow DA, Zwahlen C. Assessing environmental risks of transgenic plants. Ecol Lett. 2006 Feb 22;9(2):196–214.
300. Ahmad S, Shahzad R, Jamil S, Tabassum J, Chaudhary MAM, Atif RM, et al. Regulatory aspects, risk assessment, and toxicity associated with RNAi and CRISPR methods. In: CRISPR and RNAi Systems. Elsevier; 2021. p. 687–721.
301. Goberna MF, Whelan AI, Godoy P, Lewi DM. Genomic Editing: The Evolution in Regulatory Management Accompanying Scientific Progress. Front Bioeng Biotechnol. 2022 Feb 21;10.
302. Touzdjian Pinheiro Kohlrausch Távora F, de Assis dos Santos Diniz F, de Moraes Rêgo-Machado C, Chagas Freitas N, Barbosa Monteiro Arraes F, Chumbinho de Andrade E, et al. CRISPR/Cas- and Topical RNAi-Based Technologies for Crop Management and Improvement: Reviewing the Risk Assessment and Challenges Towards a More Sustainable Agriculture. Front Bioeng Biotechnol. 2022 Jun 28;10.
303. Dalakouras A, Wassenegger M, Dadami E, Ganopoulos I, Pappas ML, Papadopoulou K. Genetically Modified Organism-Free RNA Interference: Exogenous Application of RNA Molecules in Plants. Plant Physiol. 2020 Jan;182(1):38–50.
304. Dubrovina AS, Kiselev K V. Exogenous RNAs for Gene Regulation and Plant Resistance. Int J Mol Sci. 2019 May 8;20(9):2282.
305. Fagard M, Boutet S, Morel JB, Bellini C, Vaucheret H. AGO1, QDE-2, and RDE-1 are related proteins required for post-transcriptional gene silencing in plants, quelling in fungi,

and RNA interference in animals. Proceedings of the National Academy of Sciences. 2000 Oct 10;97(21):11650–4.
306. Eckardt NA. RNA Goes Mobile. Plant Cell. 2002 Jul;14(7):1433–6.
307. Waterhouse PM, Wang MB, Lough T. Gene silencing as an adaptive defence against viruses. Nature. 2001 Jun 14;411(6839):834–42.
308. Agrawal N, Dasaradhi PVN, Mohmmed A, Malhotra P, Bhatnagar RK, Mukherjee SK. RNA Interference: Biology, Mechanism, and Applications. Microbiology and Molecular Biology Reviews. 2003 Dec;67(4):657–85.
309. Wilson RC, Doudna JA. Molecular Mechanisms of RNA Interference. Annu Rev Biophys. 2013 May 6;42(1):217–39.
310. Hannon GJ. RNA interference. Nature. 2002 Jul;418(6894):244–51.
311. El-Sappah AH, Yan K, Huang Q, Islam MdM, Li Q, Wang Y, et al. Comprehensive Mechanism of Gene Silencing and Its Role in Plant Growth and Development. Front Plant Sci. 2021 Sep 7;12.
312. Tomari Y, Zamore PD. Perspective: machines for RNAi. Genes Dev. 2005 Mar 1;19(5):517–29.
313. Baulcombe D. RNA silencing. Trends Biochem Sci. 2005 Jun;30(6):290–3.
314. Akbar S, Wei Y, Zhang MQ. RNA Interference: Promising Approach to Combat Plant Viruses. Int J Mol Sci. 2022 May 10;23(10):5312.
315. Zeng Y, Cullen BR. RNA interference in human cells is restricted to the cytoplasm. RNA. 2002 Jul;8(7):S1355838202020071.
316. Elbashir SM, Lendeckel W, Tuschl T. RNA interference is mediated by 21- and 22-nucleotide RNAs. Genes Dev. 2001 Jan 15;15(2):188–200.
317. Zamore PD, Tuschl T, Sharp PA, Bartel DP. RNAi. Cell. 2000 Mar;101(1):25–33.
318. Martinez J, Tuschl T. RISC is a 5′ phosphomonoester-producing RNA endonuclease. Genes Dev. 2004 May 1;18(9):975–80.
319. Haley B, Zamore PD. Kinetic analysis of the RNAi enzyme complex. Nat Struct Mol Biol. 2004 Jul 30;11(7):599–606.
320. Wassenegger M, Krczal G. Nomenclature and functions of RNA-directed RNA polymerases. Trends Plant Sci. 2006 Mar;11(3):142–51.
321. Dalmay T, Hamilton A, Rudd S, Angell S, Baulcombe DC. An RNA-Dependent RNA Polymerase Gene in Arabidopsis Is Required for Posttranscriptional Gene Silencing Mediated by a Transgene but Not by a Virus. Cell. 2000 May;101(5):543–53.
322. Waterhouse PM, Helliwell CA. Exploring plant genomes by RNA-induced gene silencing. Nat Rev Genet. 2003 Jan;4(1):29–38.
323. Rössner C, Lotz D, Becker A. VIGS Goes Viral: How VIGS Transforms Our Understanding of Plant Science. Annu Rev Plant Biol. 2022 May 20;73(1):703–28.
324. Burch-Smith TM, Anderson JC, Martin GB, Dinesh-Kumar SP. Applications and advantages of virus-induced gene silencing for gene function studies in plants. The Plant Journal. 2004 Sep 16;39(5):734–46.
325. Ruiz MT, Voinnet O, Baulcombe DC. Initiation and Maintenance of Virus-Induced Gene Silencing. Plant Cell. 1998 Jun;10(6):937–46.
326. Valentine T, Shaw J, Blok VC, Phillips MS, Oparka KJ, Lacomme C. Efficient Virus-Induced Gene Silencing in Roots Using a Modified Tobacco Rattle Virus Vector. Plant Physiol. 2004 Dec 1;136(4):3999–4009.

327. Ratcliff F, Martin-Hernandez AM, Baulcombe DC. Technical Advance: Tobacco rattle virus as a vector for analysis of gene function by silencing. The Plant Journal. 2001 Jan 18;25(2):237–45.
328. Senthil-Kumar M, Mysore KS. New dimensions for VIGS in plant functional genomics. Trends Plant Sci. 2011 Dec;16(12):656–65.
329. Liu Y, Schiff M, Dinesh-Kumar SP. Virus-induced gene silencing in tomato. The Plant Journal. 2002 Sep 5;31(6):777–86.
330. Nowara D, Gay A, Lacomme C, Shaw J, Ridout C, Douchkov D, et al. HIGS: Host-Induced Gene Silencing in the Obligate Biotrophic Fungal Pathogen *Blumeria graminis* . Plant Cell. 2010 Oct 27;22(9):3130–41.
331. Huang G, Allen R, Davis EL, Baum TJ, Hussey RS. Engineering broad root-knot resistance in transgenic plants by RNAi silencing of a conserved and essential root-knot nematode parasitism gene. Proceedings of the National Academy of Sciences. 2006 Sep 26;103(39):14302–6.
332. Waterhouse PM, Graham MW, Wang MB. Virus resistance and gene silencing in plants can be induced by simultaneous expression of sense and antisense RNA. Proceedings of the National Academy of Sciences. 1998 Nov 10;95(23):13959–64.
333. Rodríguez-Negrete EA, Carrillo-Tripp J, Rivera-Bustamante RF. RNA Silencing against Geminivirus: Complementary Action of Posttranscriptional Gene Silencing and Transcriptional Gene Silencing in Host Recovery. J Virol. 2009 Feb;83(3):1332–40.
334. Pliego C, Nowara D, Bonciani G, Gheorghe DM, Xu R, Surana P, et al. Host-Induced Gene Silencing in Barley Powdery Mildew Reveals a Class of Ribonuclease-Like Effectors. Molecular Plant-Microbe Interactions®. 2013 Jun;26(6):633–42.
335. Wu J, Yin S, Lin L, Liu D, Ren S, Zhang W, et al. Host-induced gene silencing of multiple pathogenic factors of Sclerotinia sclerotiorum confers resistance to Sclerotinia rot in Brassica napus. Crop J. 2022 Jun;10(3):661–71.
336. Nowara D, Gay A, Lacomme C, Shaw J, Ridout C, Douchkov D, et al. HIGS: Host-Induced Gene Silencing in the Obligate Biotrophic Fungal Pathogen *Blumeria graminis* . Plant Cell. 2010 Oct 27;22(9):3130–41.
337. Sang H, Kim JI. Advanced strategies to control plant pathogenic fungi by host-induced gene silencing (HIGS) and spray-induced gene silencing (SIGS). Plant Biotechnol Rep. 2020 Feb 25;14(1):1–8.
338. Wang M, Dean RA. Host induced gene silencing of Magnaporthe oryzae by targeting pathogenicity and development genes to control rice blast disease. Front Plant Sci. 2022 Aug 11;13.
339. Raruang Y, Omolehin O, Hu D, Wei Q, Han ZQ, Rajasekaran K, et al. Host Induced Gene Silencing Targeting Aspergillus flavus aflM Reduced Aflatoxin Contamination in Transgenic Maize Under Field Conditions. Front Microbiol. 2020 Apr 28;11.
340. Koch A, Kumar N, Weber L, Keller H, Imani J, Kogel KH. Host-induced gene silencing of cytochrome P450 lanosterol C14α-demethylase–encoding genes confers strong resistance to *Fusarium* species. Proceedings of the National Academy of Sciences. 2013 Nov 26;110(48):19324–9.
341. Mamta, Reddy KRK, Rajam M V. Targeting chitinase gene of Helicoverpa armigera by host-induced RNA interference confers insect resistance in tobacco and tomato. Plant Mol Biol. 2016 Feb 10;90(3):281–92.

342. Qi T, Guo J, Peng H, Liu P, Kang Z, Guo J. Host-Induced Gene Silencing: A Powerful Strategy to Control Diseases of Wheat and Barley. Int J Mol Sci. 2019 Jan 8;20(1):206.
343. Koch A, Wassenegger M. Host-induced gene silencing – mechanisms and applications. New Phytologist. 2021 Jul 2;231(1):54–9.
344. Zand Karimi H, Innes RW. Molecular mechanisms underlying host-induced gene silencing. Plant Cell. 2022 Aug 25;34(9):3183–99.
345. Hou Y, Ma W. Natural Host-Induced Gene Silencing Offers New Opportunities to Engineer Disease Resistance. Trends Microbiol. 2020 Feb;28(2):109–17.
346. Ghag SB. Host induced gene silencing, an emerging science to engineer crop resistance against harmful plant pathogens. Physiol Mol Plant Pathol. 2017 Dec;100:242–54.
347. Wesley SV, Helliwell CA, Smith NA, Wang M, Rouse DT, Liu Q, et al. Construct design for efficient, effective and high-throughput gene silencing in plants. The Plant Journal. 2001 Sep 23;27(6):581–90.
348. Seemanpillai M, Dry I, Randles J, Rezaian A. Transcriptional Silencing of Geminiviral Promoter-Driven Transgenes Following Homologous Virus Infection. Molecular Plant-Microbe Interactions®. 2003 May;16(5):429–38.
349. Ribeiro SG, Lohuis H, Goldbach R, Prins M. Tomato Chlorotic Mottle Virus Is a Target of RNA Silencing but the Presence of Specific Short Interfering RNAs Does Not Guarantee Resistance in Transgenic Plants. J Virol. 2007 Feb 15;81(4):1563–73.
350. Bonfim K, Faria JC, Nogueira EOPL, Mendes ÉA, Aragão FJL. RNAi-Mediated Resistance to *Bean golden mosaic virus* in Genetically Engineered Common Bean (*Phaseolus vulgaris*). Molecular Plant-Microbe Interactions®. 2007 Jun;20(6):717–26.
351. Aragão FJL, Faria JC. First transgenic geminivirus-resistant plant in the field. Nat Biotechnol. 2009 Dec;27(12):1086–8.
352. Ammara U e, Mansoor S, Saeed M, Amin I, Briddon RW, Al-Sadi AM. RNA interference-based resistance in transgenic tomato plants against Tomato yellow leaf curl virus-Oman (TYLCV-OM) and its associated betasatellite. Virol J. 2015 Dec 4;12(1):38.
353. Patil BL, Bagewadi B, Yadav JS, Fauquet CM. Mapping and identification of cassava mosaic geminivirus DNA-A and DNA-B genome sequences for efficient siRNA expression and RNAi based virus resistance by transient agro-infiltration studies. Virus Res. 2016 Feb;213:109–15.
354. Medina-Hernández D, Rivera-Bustamante R, Tenllado F, Holguín-Peña R. Effects and Effectiveness of Two RNAi Constructs for Resistance to Pepper golden mosaic virus in Nicotiana benthamiana Plants. Viruses. 2013 Nov 28;5(12):2931–45.
355. Tenllado F, Barajas D, Vargas M, Atencio FA, González-Jara P, Díaz-Ruíz JR. Transient Expression of Homologous Hairpin RNA Causes Interference with Plant Virus Infection and Is Overcome by a Virus Encoded Suppressor of Gene Silencing. Molecular Plant-Microbe Interactions®. 2003 Feb;16(2):149–58.
356. Whangbo JS, Hunter CP. Environmental RNA interference. Trends in Genetics. 2008 Jun;24(6):297–305.
357. Wang M, Weiberg A, Lin FM, Thomma BPHJ, Huang HD, Jin H. Bidirectional cross-kingdom RNAi and fungal uptake of external RNAs confer plant protection. Nat Plants. 2016 Sep 19;2(10):16151.
358. Koch A, Biedenkopf D, Furch A, Weber L, Rossbach O, Abdellatef E, et al. An RNAi-Based Control of Fusarium graminearum Infections Through Spraying of Long dsRNAs

Involves a Plant Passage and Is Controlled by the Fungal Silencing Machinery. PLoS Pathog. 2016 Oct 13;12(10):e1005901.
359. Wang M, Jin H. Spray-Induced Gene Silencing: a Powerful Innovative Strategy for Crop Protection. Trends Microbiol. 2017 Jan;25(1):4–6.
360. Hough J, Howard JD, Brown S, Portwood DE, Kilby PM, Dickman MJ. Strategies for the production of dsRNA biocontrols as alternatives to chemical pesticides. Front Bioeng Biotechnol. 2022 Oct 10;10.
361. Romeis J, Widmer F. Assessing the Risks of Topically Applied dsRNA-Based Products to Non-target Arthropods. Front Plant Sci. 2020 Jun 4;11.
362. Bennett M, Deikman J, Hendrix B, Iandolino A. Barriers to Efficient Foliar Uptake of dsRNA and Molecular Barriers to dsRNA Activity in Plant Cells. Front Plant Sci. 2020 Jun 12;11.
363. Mitter N, Worrall EA, Robinson KE, Xu ZP, Carroll BJ. Induction of virus resistance by exogenous application of double-stranded RNA. Curr Opin Virol. 2017 Oct;26:49–55.
364. Rank AP, Koch A. Lab-to-Field Transition of RNA Spray Applications – How Far Are We? Front Plant Sci. 2021 Oct 15;12.
365. Das PR, Sherif SM. Application of Exogenous dsRNAs-induced RNAi in Agriculture: Challenges and Triumphs. Front Plant Sci. 2020 Jun 25;11.
366. Cagliari D, Dias NP, Galdeano DM, dos Santos EÁ, Smagghe G, Zotti MJ. Management of Pest Insects and Plant Diseases by Non-Transformative RNAi. Front Plant Sci. 2019 Oct 25;10.
367. Worrall EA, Bravo-Cazar A, Nilon AT, Fletcher SJ, Robinson KE, Carr JP, et al. Exogenous Application of RNAi-Inducing Double-Stranded RNA Inhibits Aphid-Mediated Transmission of a Plant Virus. Front Plant Sci. 2019 Mar 15;10.
368. Rêgo-Machado CM, Inoue-Nagata AK, Nakasu EYT. Topical application of dsRNA for plant virus control: a review. Trop Plant Pathol. 2022 Oct 20;48(1):11–22.
369. Dalakouras A, Wassenegger M, McMillan JN, Cardoza V, Maegele I, Dadami E, et al. Induction of Silencing in Plants by High-Pressure Spraying of In vitro-Synthesized Small RNAs. Front Plant Sci. 2016 Aug 30;07.
370. Tenllado F, Martínez-García B, Vargas M, Díaz-Ruíz J. Crude extracts of bacterially expressed dsRNA can be used to protect plants against virus infections. BMC Biotechnol. 2003;3(1):3.
371. Timmons L, Court DL, Fire A. Ingestion of bacterially expressed dsRNAs can produce specific and potent genetic interference in Caenorhabditis elegans. Gene. 2001 Jan;263(1–2):103–12.
372. Hoang BTL, Fletcher SJ, Brosnan CA, Ghodke AB, Manzie N, Mitter N. RNAi as a Foliar Spray: Efficiency and Challenges to Field Applications. Int J Mol Sci. 2022 Jun 14;23(12):6639.
373. Mitter N, Worrall EA, Robinson KE, Li P, Jain RG, Taochy C, et al. Clay nanosheets for topical delivery of RNAi for sustained protection against plant viruses. Nat Plants. 2017 Jan 9;3(2):16207.
374. Worrall EA, Bravo-Cazar A, Nilon AT, Fletcher SJ, Robinson KE, Carr JP, et al. Exogenous Application of RNAi-Inducing Double-Stranded RNA Inhibits Aphid-Mediated Transmission of a Plant Virus. Front Plant Sci. 2019 Mar 15;10.
375. Yoon J, Fang M, Lee D, Park M, Kim KH, Shin C. Double-stranded RNA confers resistance to pepper mottle virus in Nicotiana benthamiana. Appl Biol Chem. 2021 Dec 7;64(1):1.

376. Konakalla NC, Kaldis A, Berbati M, Masarapu H, Voloudakis AE. Exogenous application of double-stranded RNA molecules from TMV p126 and CP genes confers resistance against TMV in tobacco. Planta. 2016 Oct 25;244(4):961–9.
377. Tenllado F, Díaz-Ruíz JR. Double-Stranded RNA-Mediated Interference with Plant Virus Infection. J Virol. 2001 Dec 15;75(24):12288–97.
378. Delgado-Martín J, Ruiz L, Janssen D, Velasco L. Exogenous Application of dsRNA for the Control of Viruses in Cucurbits. Front Plant Sci. 2022 Jun 27;13.
379. Kaldis A, Berbati M, Melita O, Reppa C, Holeva M, Otten P, et al. Exogenously applied dsRNA molecules deriving from the *Zucchini yellow mosaic virus* (ZYMV) genome move systemically and protect cucurbits against ZYMV. Mol Plant Pathol. 2018 Apr 31;19(4):883–95.
380. Machado CMR, Nakasu EYT, Silva JMF, Lucinda N, Nagata T, Nagata AKI. siRNA biogenesis and advances in topically applied dsRNA for controlling virus infections in tomato plants. Sci Rep [Internet]. 2020;1–13. Available from: https://doi.org/10.1038/s41598-020-79360-5
381. Holeva MC, Sklavounos A, Rajeswaran R, Pooggin MM, Voloudakis AE. Topical Application of Double-Stranded RNA Targeting 2b and CP Genes of Cucumber mosaic virus Protects Plants against Local and Systemic Viral Infection. Plants. 2021 May 12;10(5):963.
382. Namgial T, Kaldis A, Chakraborty S, Voloudakis A. Topical application of double-stranded RNA molecules containing sequences of Tomato leaf curl virus and Cucumber mosaic virus confers protection against the cognate viruses. Physiol Mol Plant Pathol. 2019 Dec;108:101432.
383. Melita O, Kaldis A, Berbeti M, Reppa C, Holeva M, Lapidot M, et al. Topical application of double-stranded RNA molecules deriving from Tomato yellow leaf curl virus reduces cognate virus infection in tomato. Biol Plant. 2021 May 12;65:100–10.
384. Singh OW, Gupta D, Joshi B, Roy A, Mukherjee SK, Mandal B. Spray application of a cocktail of dsRNAs reduces infection of chilli leaf curl virus in Nicotiana benthamiana. Journal of Plant Diseases and Protection. 2022 Apr 1;129(2):433–8.
385. Rego-Machado CM, Nakasu EYT, Silva JMF, Lucinda N, Nagata T, Inoue-Nagata AK. siRNA biogenesis and advances in topically applied dsRNA for controlling virus infections in tomato plants. Sci Rep. 2020 Dec 17;10(1):22277.
386. Aski M, Dikshit HK, Singh D, Prasad L, Kumari J. Scientific Cultivation of Mungbean for Nutritional Security in India [Internet]. 2015. Available from: www.popularkheti.info
387. Lovejot K, Jadhav MS, Senthil N, Bharthi N, Malathi VG, Nagarajan P. Molecular cloning and characterization of Yellow Mosaic Virus from mungbean from northern region of Tamilnadu indicates association of Mungbean Yellow Mosaic India Virus DNA A with ... Molecular Cloning and Characterization of Yellow Mosaic Virus from Mun. 2015;(October).
388. Kumar S, Stecher G, Li M, Knyaz C, Tamura K. MEGA X : Molecular Evolutionary Genetics Analysis across Computing Platforms. 2018;35(6):1547–9.
389. Martin DP, Murrell B, Golden M, Khoosal A, Muhire B. RDP4 : Detection and analysis of recombination patterns in virus genomes. 2015;1(1):1–5.
390. Posada D, Crandall KA. Evaluation of methods for detecting recombination from DNA sequences : Computer simulations. 2001;98(24).

391. Rozas J, Ferrer-mata A, S JC, Guirao-rico S, Librado P, Ramos-onsins E, et al. DnaSP 6 : DNA Sequence Polymorphism Analysis of Large Data Sets. 2017;34(12):3299–302.
392. Noris E, Miozzi L. Real-time pcr protocols for the quantification of the begomovirus tomato yellow leaf curlsardinia virus in tomato plants and in its insect vector. Methods in Molecular Biology. 2015;1236:61–72.
393. Brown JK, Zerbini FM, Navas-Castillo J, Moriones E, Ramos-Sobrinho R, Silva JCF, et al. Revision of Begomovirus taxonomy based on pairwise sequence comparisons. Arch Virol. 2015 Jun 1;160(6):1593–619.
394. Aski M, Dikshit HK, Singh D, Prasad L, Kumari J. Popular Kheti. 2015;2(2):18–27.
395. Alam AKMM, Somta P. Identification and confirmation of quantitative trait loci controlling resistance to mungbean yellow mosaic disease in mungbean [Vigna radiata (L .) Wilczek]. 2014;1497–506.
396. Greengram I. " Management of Mungbean Yellow Mosaic Virus " Management of Mungbean Yellow Mosaic Virus Infecting Greengram ." 2018;402.
397. Karthikeyan AS, Vanitharani R, Balaji V, Anuradha S, Thillaichidambaram P, Shivaprasad P V, et al. Analysis of an isolate of Mungbean yellow mosaic virus (MYMV) with a highly variable DNA B component Brief Report. 2004;132575:1643–52.
398. Lovejot K, Jadhav MS, Senthil N, Bharthi N, Malathi VG, Nagarajan P. Molecular cloning and characterization of Yellow Mosaic Virus from mungbean from northern region of Tamilnadu indicates association of Mungbean Yellow Mosaic India Virus DNA A with ... Molecular Cloning and Characterization of Yellow Mosaic Virus from Mun. 2015;(October).
399. Bag MK, Gautam NK, Prasad T v, Pandey S, Dutta M, Roy A. Evaluation of an Indian collection of black gram germplasm and identi fi cation of resistance sources to Mungbean yellow mosaic virus. Crop Protection [Internet]. 2014;61:92–101. Available from: http://dx.doi.org/10.1016/j.cropro.2014.03.021
400. Kumar S, Tanti B, Mukherjee SK, Sahoo L. Biocatalysis and Agricultural Biotechnology Molecular characterization and infectivity of Mungbean Yellow Mosaic India virus associated with yellow mosaic disease of cowpea and mungbean. Biocatal Agric Biotechnol [Internet]. 2017;11(July):183–91. Available from: http://dx.doi.org/10.1016/j.bcab.2017.07.004
401. Banerjee A, Umbrey Y, Yadav RM, Roy S. Molecular evidence of an isolate of mungbean yellow mosaic India virus with a recombinant DNA B component occurring on mungbean from mid-hills of Meghalaya , India. Virusdisease [Internet]. 2018;29(1):68–74. Available from: https://doi.org/10.1007/s13337-018-0429-5
402. Nair RM, Götz M, Winter S, Giri RR, Boddepalli VN, Sirari A, et al. Identification of mungbean lines with tolerance or resistance to yellow mosaic in fields in India where different begomovirus species and different Bemisia tabaci cryptic species predominate. 2017;349–65.
403. Lyons DM, Lauring AS. Evidence for the selective basis of transition-to-transversion substitution bias in two RNA viruses. Mol Biol Evol. 2017 Dec 1;34(12):3205–15.
404. Lucía-sanz A, Manrubia S. Multipartite viruses : adaptive trick or evolutionary treat ? 2017;(April).
405. Nawaz-ul-rehman MS, Fauquet CM. Evolution of geminiviruses and their satellites. FEBS Lett [Internet]. 2009;583(12):1825–32. Available from: http://dx.doi.org/10.1016/j.febslet.2009.05.045

406. Sanjuán R, Domingo-Calap P. Genetic Diversity and Evolution of Viral Populations. Encyclopedia of Virology. 2021. p. 53–61.
407. Wang Y, Qin Y, Wang S, Zhang D, Tian Y, Zhao F. Species and genetic variability of sweet potato viruses in China. Phytopathology Research [Internet]. 2021; Available from: https://doi.org/10.1186/s42483-021-00097-8
408. Li F, Qiao R, Yang X, Gong P, Zhou X. Occurrence , distribution , and management of tomato yellow leaf curl virus in China. Phytopathology Research [Internet]. 2022;1–12. Available from: https://doi.org/10.1186/s42483-022-00133-1
409. Ramesh S v, Chouhan BS, Gupta GK, Husain SM, Chand S. Genomic sequence characterization of Begomovirus infecting soybean and molecular evolutionary genomics of Legume yellow mosaic viruses (LYMVs). 2017;10(02):88–96.
410. Suman S, Sharma VK, Kumar H, Shahi VK. Re-evaluation of the Mungbean [Vigna radiata (L .) Wilczek] Genotypes for Resistance to Mungbean Yellow Mosaic Virus (MYMV) under Screen-House Conditions. 2018;7(04):2821–9.
411. Sai CB, Nagarajan P, Raveendran M, Rabindran R, R KBJ, Senthil N. Understanding the inheritance of mungbean yellow mosaic virus (MYMV) resistance in mungbean (Vigna radiata L . Wilczek). 2017;(3).
412. Basavaraj S, Ramesh S. Identification of stable sources of resistance to mungbean yellow mosaic virus (MYMV) disease in mungbean [Vigna radiata (L .) Wilczek]. 2019;(May).
413. Sudha M, Karthikeyan A, Nagarajan P, Raveendran M, Senthil N, Angappan K, et al. Screening of mungbean (Vigna radiata) germplasm for resistance to Mungbean yellow mosaic virus using agroinoculation Screening of mungbean (Vigna radiata) germplasm for resistance to Mungbean yellow mosaic virus using agroinoculation. 2013;0661.
414. Ma Z, Zhang H, Ding M, Zhang Z, Yang X, Zhou X. Molecular characterization and pathogenicity of an infectious cDNA clone of tomato brown rugose fruit virus. Phytopathology Research [Internet]. 2021;3(1):14. Available from: https://doi.org/10.1186/s42483-021-00091-0
415. Kumar S, Dhobale KV, Das M, Sahoo L. Plant Sciences. 2021;10(12):4416–31.
416. Jacob SS, Vanitharani R, Karthikeyan AS, Chinchore Y, Thillaichidambaram P, Veluthambi K. Mungbean yellow mosaic virus -Vi Agroinfection by Codelivery of DNA A and DNA B From One Agrobacterium Strain. 17(18).
417. Paul PC, Biswas MK, Mandal D, Pal P, Pathology P, Bengal W. STUDIES ON HOST RESISTANCE OF MUNGBEAN AGAINST MUNGBEAN YELLOW MOSAIC VIRUS IN THE AGRO-ECOLOGICAL CONDITION OF LATERITIC ZONE OF WEST BENGAL. 2013;8(2):583–7.
418. Bhanu AN, Singh MN, Srivastava K. Screening mungbean [Vigna radiata (L .) wilczek] genotypes for mungbean yellow mosaic virus resistance under natural condition. 2017;(Table 1):417–20.
419. Schneeberger C, Speiser P, Kury F, Zeulinger R. Quantitative Detection of Reverse Transcriptase-PCR Products by Means of a Novel and Sensitive DNA Stain.
420. Shafiq M, Iqbal Z, Ali I, Abbas Q, Mansoor S, Briddon RW, et al. Real-time quantitative PCR assay for the quantification of virus and satellites causing leaf curl disease in cotton in Pakistan. J Virol Methods. 2017 Oct 1;248:54–60.
421. Ramesh S v, Shivakumar M, Ramteke R, Bhatia VS, Chouhan BS, Goyal S, et al. Quanti fi cation of a legume begomovirus to evaluate soybean genotypes for resistance to yellow

mosaic disease. J Virol Methods [Internet]. 2019;268(January 2018):24–31. Available from: https://doi.org/10.1016/j.jviromet.2019.03.002

422. Shanmugasundaram S, Keatinge Jacqueline D' JDH, Hughes A, Keatinge JDH, D' J. The Mungbean Transformation Diversifying Crops, Defeating Malnutrition [Internet]. 2009. Available from: www.ifpri.org/millionsfed
423. Settlage SB, See RG, Hanley-Bowdoin L. Geminivirus C3 Protein: Replication Enhancement and Protein Interactions. J Virol. 2005 Aug;79(15):9885–95.
424. Chen K, Khatabi B, Fondong VN. The AC4 Protein of a Cassava Geminivirus Is Required for Virus Infection. Molecular Plant-Microbe Interactions®. 2019 Jul;32(7):865–75.
425. Carluccio AV, Prigigallo MI, Rosas-diaz T, Lozano- R, Stavolone L. S-acylation mediates Mungbean yellow mosaic virus AC4 localization to the plasma membrane and in turns gene silencing suppression. 2018;1–26.
426. Ochagav E, Seguin J, Malpica-l N, Hohn T, Lecca MR, Rosabel P, et al. Field Trial and Molecular Characterization of RNAi-Transgenic Tomato Plants That Exhibit Resistance to Tomato Yellow Leaf Curl Geminivirus. 2016;29(3):197–209.
427. Kamesh Krishnamoorthy K, Malathi VG, Renukadevi P, Kumar SM, Raveendran M, Sudha M, et al. Exogenous delivery of dsRNA for management of mungbean yellow mosaic virus on blackgram. Planta. 2023 Nov 7;258(5):94.
428. Jiang H, Li K, Gai J. Optimizing RNAi-Target by Nicotiana benthamiana -Soybean Mosaic Virus System Drives Broad Resistance to Soybean Mosaic Virus in Soybean. 2021;12(November):1–13.
429. Timmons L, Court DL, Fire A. Ingestion of bacterially expressed dsRNAs can produce specific and potent genetic interference in Caenorhabditis elegans. Gene. 2001 Jan;263(1–2):103–12.
430. Tenllado F, Martínez-garcía B, Vargas M, Díaz-ruíz JR. protect plants against virus infections. 2003;11:1–11.
431. Washington O, Dipinte S, Bhawana G, Anirban J, Sunil R, Mukherjee K. Spray application of a cocktail of dsRNAs reduces infection of chilli leaf curl virus in Nicotiana benthamiana. Journal of Plant Diseases and Protection [Internet]. 2021;(0123456789). Available from: https://doi.org/10.1007/s41348-021-00549-5
432. Peng J, Xia Z, Chen L, Shi M, Pu J, Guo J, et al. Rapid and efficient isolation of high-quality small RNAs from recalcitrant plant species rich in polyphenols and polysaccharides. PLoS One. 2014 May 1;9(5).
433. Noris E, Miozzi L. Real-time pcr protocols for the quantification of the begomovirus tomato yellow leaf curlsardinia virus in tomato plants and in its insect vector. Methods in Molecular Biology. 2015;1236:61–72.
434. Simón A, Ruiz L, Velasco L, Janssen D. Absolute Quantification of Tomato leaf curl New Delhi virus Spain strain, ToLCNDV-ES: Virus Accumulation in a Host-Specific Manner. Plant Dis. 2018 Jan;102(1):165–71.
435. Worrall EA, Bravo-cazar A, Nilon AT, Fletcher SJ. Exogenous Application of RNA Inhibits Aphid-Mediated Transmission of a Plant Virus. 2019;10(March).
436. Vadlamudi T, Patil BL, Kaldis A, Sai Gopal DVR, Mishra R, Berbati M, et al. DsRNA-mediated protection against two isolates of Papaya ringspot virus through topical application of dsRNA in papaya. J Virol Methods. 2020 Jan;275:113750.
437. Tabein S, Jansen M, Noris E, Vaira AM, Marian D, Behjatnia SAA, et al. The Induction of an Effective dsRNA-Mediated Resistance Against Tomato Spotted Wilt Virus by

Exogenous Application of Double-Stranded RNA Largely Depends on the Selection of the Viral RNA Target Region. Front Plant Sci. 2020 Nov 26;11.

438. Gupta D, Singh OW, Basavaraj YB, Roy A. Direct Foliar Application of dsRNA Derived From the Full-Length Gene of NSs of Groundnut Bud Necrosis Virus Limits Virus Accumulation and Symptom Expression. 2021;12(December):1–12.
439. Konakalla NC, Bag S, Deraniyagala AS, Culbreath AK, Pappu HR. Induction of Plant Resistance in Tobacco (Nicotiana tabacum) against Tomato Spotted Wilt Orthotospovirus through Foliar Application of dsRNA. Viruses. 2021 Apr 12;13(4):662.
440. Ramesh S V, Shivakumar M, Praveen S, Chouhan BS, Chand S. Expression of short hairpin RNA (shRNA) targeting AC2 gene of Mungbean yellow mosaic India virus (MYMIV) reduces the viral titre in soybean. 3 Biotech [Internet]. 2019;9(9):1–9. Available from: https://doi.org/10.1007/s13205-019-1865-7
441. Fuentes A, Carlos N, Ruiz Y, Callard D, Sánchez Y, Ochagavía ME, et al. Field Trial and Molecular Characterization of RNAi-Transgenic Tomato Plants That Exhibit Resistance to Tomato Yellow Leaf Curl Geminivirus. Molecular Plant-Microbe Interactions®. 2016 Mar;29(3):197–209.
442. Ammara U e, Mansoor S, Saeed M, Amin I, Briddon RW, Al-Sadi AM. RNA interference-based resistance in transgenic tomato plants against Tomato yellow leaf curl virus-Oman (TYLCV-OM) and its associated betasatellite. Virol J. 2015 Dec 4;12(1):38.
443. Sharma VK, Basu S, Chakraborty S. RNAi mediated broad-spectrum transgenic resistance in Nicotiana benthamiana to chilli-infecting begomoviruses. Plant Cell Rep. 2015 Aug 28;34(8):1389–99.
444. Kumari A, Hada A, Subramanyam K, Theboral J, Misra S, Ganapathi A, et al. RNAi-mediated resistance to yellow mosaic viruses in soybean targeting coat protein gene. Acta Physiol Plant. 2018 Feb 17;40(2):32.
445. Vanderschuren H, Alder A, Zhang P, Gruissem W. Dose-dependent RNAi-mediated geminivirus resistance in the tropical root crop cassava. Plant Mol Biol. 2009 Jun 20;70(3):265–72.
446. Niehl A, Soininen M, Poranen MM, Heinlein M. Synthetic biology approach for plant protection using ds <scp>RNA</scp>. Plant Biotechnol J. 2018 Sep 25;16(9):1679–87.
447. Papi L. Double-stranded RNA production and the kinetics of recombinant Escherichia coli HT115 in fed-batch culture. 2018;20:10–3.
448. Voloudakis AE, Holeva MC, Sarin LP, Bamford DH, Vargas M, Poranen MM, et al. Efficient Double-Stranded RNA Production Methods for Utilization in Plant Virus Control. In 2015. p. 255–74.
449. Dubrovina AS, Kiselev K V. Exogenous RNAs for Gene Regulation and Plant Resistance. Int J Mol Sci. 2019 May 8;20(9):2282.
450. Dalakouras A, Jarausch W, Buchholz G, Bassler A, Braun M, Manthey T, et al. Delivery of Hairpin RNAs and Small RNAs Into Woody and Herbaceous Plants by Trunk Injection and Petiole Absorption. Front Plant Sci. 2018 Aug 24;9.
451. Dalakouras A, Wassenegger M, Dadami E, Ganopoulos I, Pappas ML, Papadopoulou K. Genetically Modified Organism-Free RNA Interference: Exogenous Application of RNA Molecules in Plants. Plant Physiol. 2020 Jan;182(1):38–50.
452. Meister G, Tuschl T. Mechanisms of gene silencing by double-stranded RNA. Nature. 2004 Sep 15;431(7006):343–9.

453. Koch A, Biedenkopf D, Furch A, Weber L, Rossbach O, Abdellatef E, et al. An RNAi-Based Control of Fusarium graminearum Infections Through Spraying of Long dsRNAs Involves a Plant Passage and Is Controlled by the Fungal Silencing Machinery. PLoS Pathog. 2016 Oct 13;12(10):e1005901.
454. Sangwan A, Gupta D, Singh OW, Roy A, Mukherjee SK, Mandal B, et al. Size variations of mesoporous silica nanoparticle control uptake efficiency and delivery of AC2-derived dsRNA for protection against tomato leaf curl New Delhi virus. Plant Cell Rep. 2023 Oct 24;42(10):1571–87.
455. Worrall EA, Hamid A, Mody KT, Mitter N, Pappu HR. Nanotechnology for Plant Disease Management. 2018;1–24.
456. Mitter N, Worrall EA, Robinson KE, Li P, Jain RG, Taochy C. Clay nanosheets for topical delivery of RNAi for sustained protection against plant viruses. Nat Plants [Internet]. 2017;(January). Available from: http://dx.doi.org/10.1038/nplants.2016.207
457. Hanley-bowdoin L, Settlage SB, Orozco BM, Robertson D, Settlage SB, Orozco BM, et al. Critical Reviews in Plant Sciences Geminiviruses : Models for Plant DNA Replication , Transcription , and Cell Cycle Regulation Geminiviruses : Models for Plant DNA Replication , Transcription , and Cell Cycle Regulation. Vol. 2689. 2010.
458. Yadava P, Suyal G, Mukherjee SK. Begomovirus DNA replication and pathogenicity. 2010;98(3).
459. Chasan R. Geminiviruses: A Twin Approach to Replication. Plant Cell. 1995 Jun;7(6):659.
460. Benitez-Alfonso Y, Faulkner C, Ritzenthaler C, Maule AJ. Plasmodesmata: Gateways to Local and Systemic Virus Infection. Molecular Plant-Microbe Interactions®. 2010 Nov;23(11):1403–12.
461. Sattelmacher B. The apoplast and its significance for plant mineral nutrition. Vol. 149, New Phytologist. 2001. p. 167–92.
462. Sakurai N. Dynamic Function and Regulation of Apoplast in the Plant Body. Vol. 111, Journal of Plant Research. 1998.
463. Woith E, Fuhrmann G, Melzig MF. Extracellular Vesicles—Connecting Kingdoms. Int J Mol Sci. 2019 Nov 14;20(22):5695.
464. Cui Y, Gao J, He Y, Jiang L. Plant extracellular vesicles. Protoplasma. 2020 Jan 30;257(1):3–12.
465. Delaunois B, Colby T, Belloy N, Conreux A, Harzen A, Baillieul F, et al. Large-scale proteomic analysis of the grapevine leaf apoplastic fluid reveals mainly stress-related proteins and cell wall modifying enzymes. BMC Plant Biol. 2013 Dec 8;13(1):24.
466. Rutter BD, Innes RW. Extracellular vesicles isolated from the leaf apoplast carry stress-response proteins. Plant Physiol. 2017 Jan 1;173(1):728–41.
467. Cai Q, He B, Wang S, Fletcher S, Niu D, Mitter N, et al. Message in a Bubble : Shuttling Small RNAs and Proteins Between Cells and Interacting Organisms Using Extracellular Vesicles. 2021;
468. Cai Q, Qiao L, Wang M, He B, Lin FM, Palmquist J, et al. Plants send small RNAs in extracellular vesicles to fungal pathogen to silence virulence genes [Internet]. Vol. 360, Science. 2018. Available from: https://www.science.org
469. Sharova EI, Medvedev SS, Demidchik V V. Ascorbate in the Apoplast: Metabolism and Functions. Vol. 67, Russian Journal of Plant Physiology. Pleiades Publishing; 2020. p. 207–20.

470. Wang Y, Wang Y. Trick or treat: Microbial pathogens evolved apoplastic effectors modulating plant susceptibility to infection. Vol. 31, Molecular Plant-Microbe Interactions. American Phytopathological Society; 2018. p. 6–12.
471. García G, Clemente-Moreno MJ, Díaz-Vivancos P, García M, Hernández JA. The apoplastic and symplastic antioxidant system in onion: Response to long-term salt stress. Antioxidants. 2020 Jan 1;9(1).
472. Diaz-Vivancos P, Rubio M, Mesonero V, Periago PM, Ros Barceló A, Martínez-Gómez P, et al. The apoplastic antioxidant system in Prunus: Response to long-term plum pox virus infection. J Exp Bot. 2006 Nov;57(14):3813–24.
473. Podgórska A, Burian M, Szal B. Extra-cellular but extra-ordinarily important for cells: Apoplastic reactive oxygen species metabolism. Vol. 8, Frontiers in Plant Science. Frontiers Media S.A.; 2017.
474. Blomster T, Salojärvi J, Sipari N, Brosché M, Ahlfors R, Keinänen M, et al. Apoplastic reactive oxygen species transiently decrease auxin signaling and cause stress-induced morphogenic response in Arabidopsis. Plant Physiol. 2011;157(4):1866–83.
475. Wang Y, Wang Y, Wang Y. Apoplastic Proteases: Powerful Weapons against Pathogen Infection in Plants. Vol. 1, Plant Communications. Cell Press; 2020.
476. Jashni MK, Mehrabi R, Collemare J, Mesarich CH, de Wit PJGM. The battle in the apoplast: Further insights into the roles of proteases and their inhibitors in plant–pathogen interactions. Front Plant Sci. 2015 Aug 3;6(AUG).
477. Farvardin A, González-hernández AI, Llorens E, García-agustín P, Scalschi L, Vicedo B. The apoplast: A key player in plant survival. Vol. 9, Antioxidants. MDPI; 2020. p. 1–26.
478. Du Y, Stegmann M, Misas Villamil JC. The apoplast as battleground for plant-microbe interactions. New Phytologist. 2016 Jan 1;209(1):34–8.
479. Delaunois B, Jeandet P, ClÃ©ment C, Baillieul F, Dorey S, Cordelier S. Uncovering plant-pathogen crosstalk through apoplastic proteomic studies. Front Plant Sci. 2014 Jun 3;5.
480. Dora S, Terrett OM, Sánchez-Rodríguez C. Plant-microbe interactions in the apoplast: Communication at the plant cell wall. Vol. 34, Plant Cell. American Society of Plant Biologists; 2022. p. 1532–50.
481. Pechanova O, Hsu CY, Adams JP, Pechan T, Vandervelde L, Drnevich J, et al. Apoplast proteome reveals that extracellular matrix contributes to multistress response in poplar. BMC Genomics. 2010 Nov 29;11(1).
482. Martínez-González AP, Ardila HD, Martínez-Peralta ST, Melgarejo-Muñoz LM, Castillejo-Sánchez MA, Jorrín-Novo J V. What proteomic analysis of the apoplast tells us about plant–pathogen interactions. Vol. 67, Plant Pathology. Blackwell Publishing Ltd; 2018. p. 1647–68.
483. Borniego ML, Molina MC, Guiamét JJ, Martinez DE. Physiological and Proteomic Changes in the Apoplast Accompany Leaf Senescence in Arabidopsis. Front Plant Sci. 2020 Jan 8;10.
484. Agrawal GK, Jwa NS, Lebrun MH, Job D, Rakwal R. Plant secretome: Unlocking secrets of the secreted proteins. Proteomics. 2010 Feb;10(4):799–827.
485. Lohaus G, Pennewiss K, Sattelmacher B, Hussmann M, Hermann Muehling K. Is the infiltration-centrifugation technique appropriate for the isolation of apoplastic fluid? A critical evaluation with different plant species. Physiol Plant. 2001 Apr;111(4):457–65.
486. Rutter BD, Innes RW. Extracellular vesicles isolated from the leaf apoplast carry stress-response proteins. Plant Physiol. 2017 Jan 1;173(1):728–41.

487. O'Leary BM, Rico A, McCraw S, Fones HN, Preston GM. The infiltration-centrifugation technique for extraction of apoplastic fluid from plant leaves using Phaseolus vulgaris as an example. Journal of Visualized Experiments. 2014 Dec 19;(94).
488. Maravi DK, Kumar S, Sahoo L. NMR - Based Metabolomic Profiling of Mungbean Infected with Mungbean Yellow Mosaic India Virus. Appl Biochem Biotechnol [Internet]. 2022;(0123456789). Available from: https://doi.org/10.1007/s12010-022-04074-5
489. Chen L, Wu J, Li Z, Liu Q, Zhao X, Yang H. Metabolomic analysis of energy regulated germination and sprouting of organic mung bean (Vigna radiata) using NMR spectroscopy. Food Chem. 2019 Jul 15;286:87–97.
490. Deborde C, Moing A, Roch L, Jacob D, Rolin D, Giraudeau P. Progress in Nuclear Magnetic Resonance Spectroscopy Plant metabolism as studied by NMR spectroscopy. Prog Nucl Magn Reson Spectrosc [Internet]. 2017;102–103:61–97. Available from: https://doi.org/10.1016/j.pnmrs.2017.05.001
491. Emwas A hamid, Roy R, Mckay RT, Tenori L, Saccenti E, Gowda GAN, et al. NMR Spectroscopy for Metabolomics Research. 2019;
492. Bueno PCP, Lopes NP. Metabolomics to Characterize Adaptive and Signaling Responses in Legume Crops under Abiotic Stresses. ACS Omega. 2020;5(4):1752–63.
493. Choi YH, Kim HK, Linthorst HJM, Hollander JG, Lefeber AWM, Erkelens C, et al. NMR Metabolomics to Revisit the Tobacco Mosaic Virus Infection in Nicotiana tabacum Leaves. 2006;742–8.
494. Ren Z, Fang M, Muhae G, Din U, Gao H, Yang Y. Metabolomics analysis of grains of wheat infected and noninfected with Tilletia controversa Kühn. Sci Rep [Internet]. 2021;(0123456789):1–9. Available from: https://doi.org/10.1038/s41598-021-98283-3
495. Villa-ruano N, Zepeda-vallejo LG, Hern CJ, Ramirez-estrada K, Zamudio-lucero S, Hidalgo- D, et al. Bean cultivars (Phaseolus vulgaris L .) under the spotlight of NMR metabolomics. 2021;150(July).
496. Farag MA, El-din MGS, Selim MA, Owis AI. Nuclear Magnetic Resonance Metabolomics Approach for the Analysis of Major Legume Sprouts Coupled to Chemometrics. 2021;1–28.
497. Rosenblum ES, Tjeerdema RS. NMR-Based Metabolomics : A Powerful Approach for Characterizing the Effects of Environmental Stressors on Organism Health. 2003;37(21):4982–9.
498. Mozumder NHMR, Lee YR, Hwang KH, Lee MS, Kim EH. Characterization of tea leaf metabolites dependent on tea (Camellia sinensis) plant age through 1 H NMR - based metabolomics. Appl Biol Chem [Internet]. 2020; Available from: https://doi.org/10.1186/s13765-020-0492-7
499. Li Q, Zhao C, Zhang Y, Du H, Xu T, Xu X. H NMR-Based Metabolomics Coupled With Molecular Docking Reveal the Anti-Diabetic Effects and Potential Active Components of Berberis vernae on Type 2 Diabetic Rats. 2020;11(June):1–14.
500. Spada S, Rudqvist NP, Wennerberg E. Isolation of DNA from exosomes. In: Methods in Enzymology. Academic Press Inc.; 2020. p. 173–83.
501. Huang Y, Wang S, Cai Q, Jin H. Effective methods for isolation and purification of extracellular vesicles from plants. J Integr Plant Biol. 2021 Dec 28;63(12):2020–30.
502. Szatanek R, Baj-Krzyworzeka M, Zimoch J, Lekka M, Siedlar M, Baran J. The Methods of Choice for Extracellular Vesicles (EVs) Characterization. Int J Mol Sci. 2017 May 29;18(6):1153.

503. Rutter B, Rutter K, Innes R. Isolation and Quantification of Plant Extracellular Vesicles. Bio Protoc. 2017;7(17).
504. Liu G, Kang G, Wang S, Huang Y, Cai Q. Extracellular Vesicles: Emerging Players in Plant Defense Against Pathogens. Vol. 12, Frontiers in Plant Science. Frontiers Media S.A.; 2021.
505. Hoen EN, Cremer T, Gallo RC, Margolis LB. Extracellular vesicles and viruses: Are they close relatives? Vol. 113, Proceedings of the National Academy of Sciences of the United States of America. National Academy of Sciences; 2016. p. 9155–61.
506. Chen Q, Liu Y, Ren J, Zhong P, Chen M, Jia D, et al. Exosomes mediate horizontal transmission of viral pathogens from insect vectors to plant phloem. Elife. 2021 Jul 2;10.
507. Cao X, Liu J, Pang J, Kondo H, Chi S, Zhang J, et al. Common but Nonpersistent Acquisitions of Plant Viruses by Plant-Associated Fungi. Viruses. 2022 Oct 17;14(10):2279.
508. Andika IB, Tian M, Bian R, Cao X, Luo M, Kondo H, et al. Cross-Kingdom Interactions Between Plant and Fungal Viruses. Annu Rev Virol. 2023 Sep 29;10(1):119–38.
509. Yu X, Li B, Fu Y, Xie J, Cheng J, Ghabrial SA, et al. Extracellular transmission of a DNA mycovirus and its use as a natural fungicide. Proceedings of the National Academy of Sciences. 2013 Jan 22;110(4):1452–7.
510. Wang S. Extracellular Vesicles : Emerging Players in Plant Defense Against Pathogens. 2021;12(September).
511. Gilbertson RL, Sudarshana M, Jiang H, Rojas MR, Lucas WJ. Limitations on Geminivirus Genome Size Imposed by Plasmodesmata and Virus-Encoded Movement Protein: Insights into DNA Trafficking. Plant Cell. 2003 Nov;15(11):2578–91.
512. Zhang SC, Ghosh R, Jeske H. Subcellular targeting domains of Abutilon mosaic geminivirus movement protein BC1. Arch Virol. 2002 Nov 1;147(12):2349–63.
513. Zhang SC, Wege C, Jeske H. Movement Proteins (BC1 and BV1) of Abutilon Mosaic Geminivirus Are Cotransported in and between Cells of Sink but Not of Source Leaves as Detected by Green Fluorescent Protein Tagging. Virology. 2001 Nov;290(2):249–60.
514. Aberle HJ, Rütz ML, Karayavuz M, Frischmuth S, Wege C, Hülser D, et al. Localizing the movement proteins of Abutilon mosaic geminivirus in yeast by subcellular fractionation and freeze-fracture immuno-labelling. Arch Virol. 2002 Jan 1;147(1):103–17.
515. Frischmuth S, Wege C, Hülser D, Jeske H. The movement protein BC1 promotes redirection of the nuclear shuttle protein BV1 of Abutilon mosaic geminivirus to the plasma membrane in fission yeast. Protoplasma. 2007 Mar 19;230(1–2):117–23.
516. da Silva PRA, Vidal MS, Soares C de P, Polese V, Tadra-Sfeir MZ, De Souza EM, et al. Sugarcane apoplast fluid modulates the global transcriptional profile of the diazotrophic bacteria Paraburkholderia tropica strain Ppe8. PLoS One. 2018 Dec 1;13(12).
517. Floerl S, Majcherczyk A, Possienke M, Feussner K, Tappe H, Gatz C, et al. Verticillium longisporum infection affects the leaf apoplastic proteome, metabolome, and cell wall properties in Arabidopsis thaliana. PLoS One. 2012 Feb 20;7(2).
518. Zhou L, Bokhari SA, Dong CJ, Liu JY. Comparative proteomics analysis of the root apoplasts of rice seedlings in response to hydrogen peroxide. PLoS One. 2011;6(2).
519. Song Y, Zhang C, Ge W, Zhang Y, Burlingame AL, Guo Y. Identification of NaCl stress-responsive apoplastic proteins in rice shoot stems by 2D-DIGE. J Proteomics. 2011 Jun 10;74(7):1045–67.

520. Ceballos-Laita L, Gutierrez-Carbonell E, Lattanzio G, Vázquez S, Contreras-Moreira B, Abadía A, et al. Protein profile of Beta vulgaris leaf apoplastic fluid and changes induced by Fe deficiency and Fe resupply. Front Plant Sci. 2015 Mar 18;6(MAR).
521. Fecht-Christoffers MM, Braun HP, Lemaitre-Guillier C, VanDorsselaer A, Horst WJ. Effect of Manganese Toxicity on the Proteome of the Leaf Apoplast in Cowpea. Plant Physiol. 2003;133(4):1935–46.
522. Baker CJ, Kovalskaya NY, Mock NM, Owens RA, Deahl KL, Whitaker BD, et al. An internal standard technique for improved quantitative analysis of apoplastic metabolites in tomato leaves. Physiol Mol Plant Pathol. 2012 Apr;78:31–7.
523. Green KA, Berry D, Feussner K, Eaton CJ, Ram A, Mesarich CH, et al. Lolium perenne apoplast metabolomics for identification of novel metabolites produced by the symbiotic fungus Epichloë festucae. New Phytologist. 2020 Jul 1;227(2):559–71.
524. Baker CJ, Smith JM, Yarberry AJ, Rice C. Induction of apoplast phenolics in pepper (Capsicum annuum) leaves in response to pathogenic bacteria. Physiol Mol Plant Pathol. 2020 Jan 1;109.
525. Asis CA, Shimizu T, Khan MK, Akao S, Shimizu T, Akao S, et al. Organic acid and sugar contents in sugarcane stem apoplast solution and their role as carbon source for endophytic diazotrophs. Soil Sci Plant Nutr. 2003 Dec 1;49(6):915–20.
526. Santamaría-Hernando S, López-Maroto Á, Galvez-Roldán C, Munar-Palmer M, Monteagudo-Cascales E, Rodríguez-Herva JJ, et al. Pseudomonas syringae pv. tomato infection of tomato plants is mediated by GABA and l-Pro chemoperception. Mol Plant Pathol. 2022 Oct 1;23(10):1433–45.
527. Baker CJ, Mock NM, Smith JM, Aver'yanov AA. The dynamics of apoplast phenolics in tobacco leaves following inoculation with bacteria. Front Plant Sci. 2015 Aug 20;6(AUG).
528. Figueiredo J, Cavaco AR, Guerra-Guimarães L, Leclercq C, Renaut J, Cunha J, et al. An apoplastic fluid extraction method for the characterization of grapevine leaves proteome and metabolome from a single sample. Physiol Plant. 2021 Mar 1;171(3):343–57.
529. Führs H, Götze S, Specht A, Erban A, Gallien S, Heintz D, et al. Characterization of leaf apoplastic peroxidases and metabolites in Vigna unguiculata in response to toxic manganese supply and silicon. J Exp Bot. 2009;60(6):1663–78.
530. Witzel K, Shahzad M, Matros A, Mock HP, Mühling KH. Comparative evaluation of extraction methods for apoplastic proteins from maize leaves. Plant Methods. 2011 Dec 22;7(1).
531. Kim HK, Choi YH, Verpoorte R. NMR-based metabolomic analysis of plants. Vol. 5, Nature Protocols. 2010. p. 536–49.
532. Emwas AH, Roy R, McKay RT, Tenori L, Saccenti E, Nagana Gowda GA, et al. Nmr spectroscopy for metabolomics research. Vol. 9, Metabolites. MDPI AG; 2019.
533. Murti RH, Afifah EN, Nuringtyas TR. Metabolomic Response of Tomatoes (Solanum lycopersicum L.) against Bacterial Wilt (Ralstonia solanacearum) Using 1H-NMR Spectroscopy. Plants. 2021 Jun 3;10(6):1143.
534. Choi YH, Kim HK, Linthorst HJM, Hollander JG, Lefeber AWM, Erkelens C, et al. NMR metabolomics to revisit the tobacco mosaic virus infection in Nicotiana tabacum leaves. J Nat Prod. 2006 May;69(5):742–8.
535. Villa-Ruano N, Velásquez-Valle R, Zepeda-Vallejo LG, Pérez-Hernández N, Velázquez-Ponce M, Arcos-Adame VM, et al. 1H NMR-based metabolomic profiling for identification

of metabolites in Capsicum annuum cv. mirasol infected by beet mild curly top virus (BMCTV). Food Research International. 2018 Apr 1;106:870–7.

536. More P, Agarwal P, Agarwal PK. The Jatropha leaf curl Gujarat virus on infection in Jatropha regulates the sugar and tricarboxylic acid cycle metabolic pathways. 3 Biotech [Internet]. 2022;12(10):1–13. Available from: https://doi.org/10.1007/s13205-022-03306-z
537. Rossouw LT, Madala NE, Tugizimana F, Steenkamp PA, Esterhuizen LL, Dubery IA. Deciphering the resistance mechanism of tomato plants against whitefly-mediated tomato curly stunt virus infection through ultra-high- performance liquid chromatography coupled to mass spectrometry (Uhplc-ms)-based metabolomics approaches. Metabolites. 2019 Apr 1;9(4).
538. Zhang Z, He H, Yan M, Zhao C, Lei C, Li J, et al. Widely targeted analysis of metabolomic changes of Cucumis sativus induced by cucurbit chlorotic yellows virus. BMC Plant Biol. 2022 Dec 1;22(1).
539. Maravi DK, Kumar S, Sahoo L. NMR-Based Metabolomic Profiling of Mungbean Infected with Mungbean Yellow Mosaic India Virus. Appl Biochem Biotechnol. 2022 Dec 1;194(12):5808–26.
540. Knaggs AR. The biosynthesis of shikimate metabolites. Nat Prod Rep. 2003 Jan 21;20(1):119–36.
541. Kumar N, Goel N. Phenolic acids: Natural versatile molecules with promising therapeutic applications. Biotechnology Reports. 2019 Dec;24:e00370.
542. Montenegro-Landívar MF, Tapia-Quirós P, Vecino X, Reig M, Valderrama C, Granados M, et al. Polyphenols and their potential role to fight viral diseases: An overview. Science of The Total Environment. 2021 Dec;801:149719.
543. Dehghanian Z, Habibi K, Dehghanian M, Aliyar S, Asgari Lajayer B, Astatkie T, et al. Reinforcing the bulwark: unravelling the efficient applications of plant phenolics and tannins against environmental stresses. Heliyon. 2022 Mar;8(3):e09094.
544. Šamec D, Karalija E, Šola I, Vujčić Bok V, Salopek-Sondi B. The Role of Polyphenols in Abiotic Stress Response: The Influence of Molecular Structure. Plants. 2021 Jan 8;10(1):118.
545. Divekar PA, Narayana S, Divekar BA, Kumar R, Gadratagi BG, Ray A, et al. Plant Secondary Metabolites as Defense Tools against Herbivores for Sustainable Crop Protection. Int J Mol Sci. 2022 Feb 28;23(5):2690.
546. López-Gresa MP, Torres C, Campos L, Lisón P, Rodrigo I, Bellés JM, et al. Identification of defence metabolites in tomato plants infected by the bacterial pathogen Pseudomonas syringae. Environ Exp Bot. 2011 Dec;74:216–28.
547. Hammerschmidt R. Chlorogenic acid: A versatile defense compound. Physiol Mol Plant Pathol. 2014 Oct;88:iii–iv.
548. Mhlongo MI, Piater LA, Madala NE, Steenkamp PA, Dubery IA. Phenylpropanoid Defences in Nicotiana tabacum Cells: Overlapping Metabolomes Indicate Common Aspects to Priming Responses Induced by Lipopolysaccharides, Chitosan and Flagellin-22. PLoS One. 2016 Mar 15;11(3):e0151350.
549. Ahmad N, Xu Y, Zang F, Li D, Liu Z. The evolutionary trajectories of specialized metabolites towards antiviral defense system in plants. Molecular Horticulture. 2024 Jan 12;4(1):2.
550. Villarino M, Sandín-España P, Melgarejo P, De Cal A. High Chlorogenic and Neochlorogenic Acid Levels in Immature Peaches Reduce Monilinia laxa Infection by

Interfering with Fungal Melanin Biosynthesis. J Agric Food Chem. 2011 Apr 13;59(7):3205–13.

551. Li Y, Chen M, Wang S, Ning J, Ding X, Chu Z. AtMYB11 regulates caffeoylquinic acid and flavonol synthesis in tomato and tobacco. Plant Cell, Tissue and Organ Culture (PCTOC). 2015 Aug 7;122(2):309–19.
552. Baker CJ, Mock NM, Smith JM, Aver'yanov AA. The dynamics of apoplast phenolics in tobacco leaves following inoculation with bacteria. Front Plant Sci. 2015 Aug 20;6.
553. Baker CJ, Whitaker BD, Mock NM, Rice CP, Roberts DP, Deahl KL, et al. Differential induction of redox sensitive extracellular phenolic amides in potato. Physiol Mol Plant Pathol. 2008 Nov;73(4–5):109–15.
554. Singh YJ, Grewal SK, Gill RK. Proline metabolism and phenylpropanoid pathway act independently in conferring resistance against yellow mosaic virus infection in black gram. Physiol Mol Plant Pathol. 2021 Dec;116:101713.
555. Dasgupta U, Mishra GP, Dikshit HK, Mishra DC, Bosamia T, Roy A, et al. Comparative RNA-Seq analysis unfolds a complex regulatory network imparting yellow mosaic disease resistance in mungbean [Vigna radiata (L.) R. Wilczek]. PLoS One. 2021 Jan 12;16(1):e0244593.
556. Tauzin AS, Giardina T. Sucrose and invertases, a part of the plant defense response to the biotic stresses. Front Plant Sci. 2014 Jun 23;5.
557. Cho YH, Yoo SD. Signaling Role of Fructose Mediated by FINS1/FBP in Arabidopsis thaliana. PLoS Genet. 2011 Jan 6;7(1):e1001263.
558. Shalitin D, Wolf S. Cucumber mosaic virus infection affects sugar transport in melon plants. Plant Physiol. 2000 Jun;123(2):597–604.
559. Aidlin Harari O, Dekel A, Wintraube D, Vainer Y, Mozes-Koch R, Yakir E, et al. A sucrose-specific receptor in Bemisia tabaci and its putative role in phloem feeding. iScience. 2023 May;26(5):106752.
560. Luna E, Pastor V, Robert J, Flors V, Mauch-Mani B, Ton J. Callose Deposition: A Multifaceted Plant Defense Response. Molecular Plant-Microbe Interactions®. 2011 Feb;24(2):183–93.
561. O'Leary BM, Neale HC, Geilfus CM, Jackson RW, Arnold DL, Preston GM. Early changes in apoplast composition associated with defence and disease in interactions between Phaseolus vulgaris and the halo blight pathogen Pseudomonas syringae Pv. phaseolicola. Plant Cell Environ. 2016 Oct 1;39(10):2172–84.
562. Galili G. The aspartate-family pathway of plants. Plant Signal Behav. 2011 Feb 28;6(2):192–5.
563. Mattioli R, Palombi N, Funck D, Trovato M. Proline Accumulation in Pollen Grains as Potential Target for Improved Yield Stability Under Salt Stress. Front Plant Sci. 2020 Oct 28;11.
564. Fabro G, Kovács I, Pavet V, Szabados L, Alvarez ME. Proline Accumulation and AtP5CS2 Gene Activation Are Induced by Plant-Pathogen Incompatible Interactions in Arabidopsis. Molecular Plant-Microbe Interactions®. 2004 Apr;17(4):343–50.

APPENDICES

Appendix A

TR-1: AC4/AC1:

CCTCATCTCCATGTTCTGCTTCAATTCGAAGGAAAGTTGCAAACGAAGAACGAAAGGTTCTTCGACCTGGTTTCCCCAA
CCAGATCAGCACATTACCATCCGAACGTTCAGGCAGCTAAAAGCGCATCAGATGTTAAGTCATACATGGACAAAGACG
GAGACGTCCTTGACCATGGAAGTTTCCAAGTCGATGGCAGATCAGCTAGAGGAGGTAAACAGTCTGCCAACGACGCT
TATGC

TR-2: AC2/AC3/AC1:

TTCTCCTCCGTCGATCAAAGCGCAACACAAGGTTGCCAAGAAGCGAGCAATTCGACGCTCTCGAATTGATTTAAGCTGT
GGGTGTAGTTATTACATCCATATCAACTGCCGTAACTATGGATTTTCGCACCGGGGACAACATCACTGCAGCTCAACTC
AGGAATGGCGTCTTTATTTGGGAGGTGCGAAATCCCCTCTCTTTCAAGATCATGCAGCACCGTCAGATTCAAGCAGGG
TCC

Fig. 1. The nucleotide sequence of TR-1 and TR-2 is depicted.
Two selected target regions (TRs), TR-1 and TR-2, for RNA interference (RNAi) induction in mungbean against Mungbean Yellow Mosaic India Virus (MYMIV).

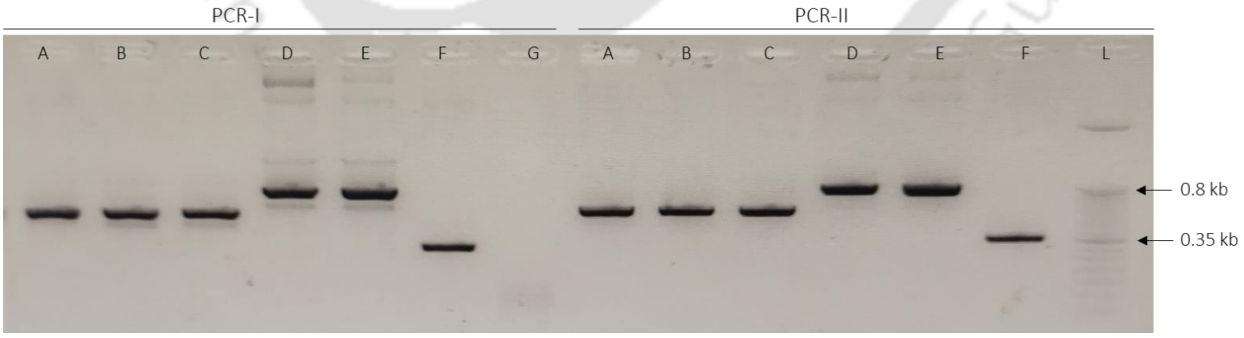

Fig 2. PCR confirmatory analysis of three hpRNAi constructs in sense and antisense orientation in pKannibal backbone.
PCR analysis using two different primers set: A: hpTR-1_pKannibal; B: hpTR-2_pKannibal clone I; C: hpTR-2_pKannibal clone II; D: hpTR-1+2_pKannibal clone I; E: hpTR-1+2_pKannibal clone II; F: Empty pKannibal; G: Negative control; L: 50 bp DNA ladder.

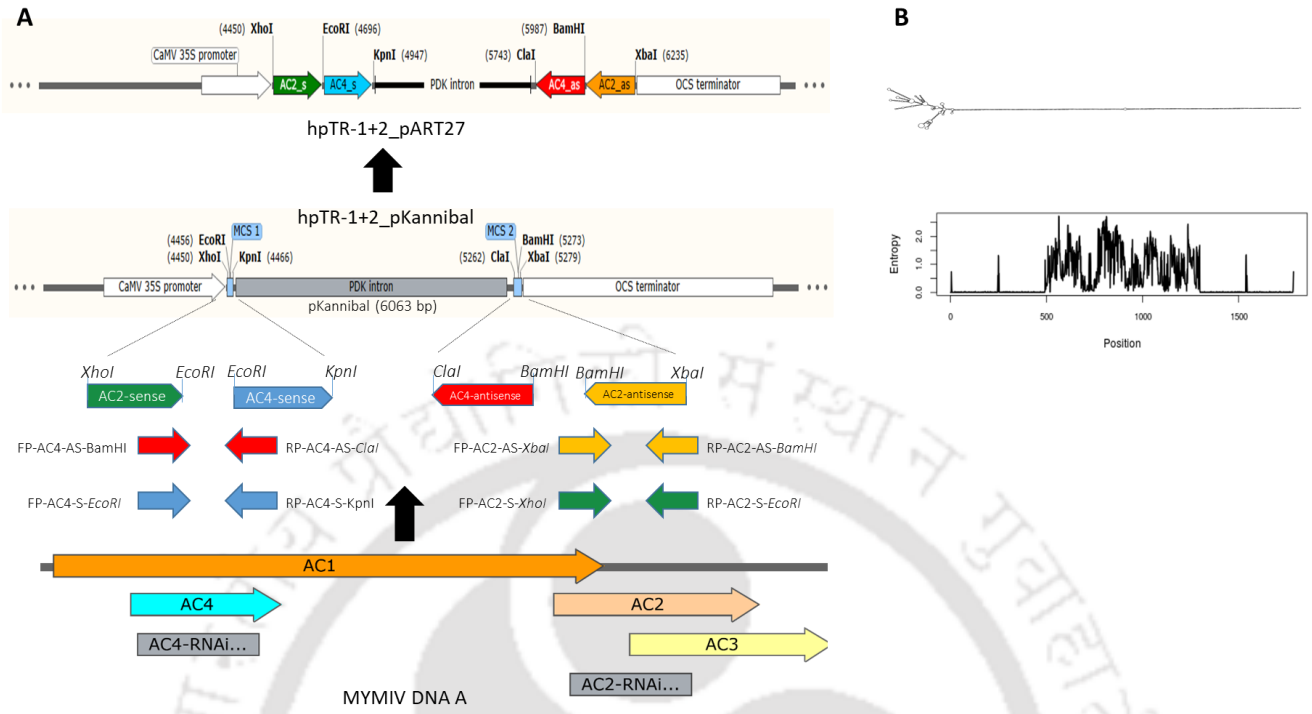

Fig 3. Schematic representation of hpRNAi clone preparation and hpRNA structure prediction.

A) Construction of hpRNAi cassette, example: hpTR-1+2_pART27 clone preparation is demonstrated; **B**) Schematic representation of predicted dsRNA secondary structure of hpTR-1+2, results have been computed using RNAfold 2.4.18.

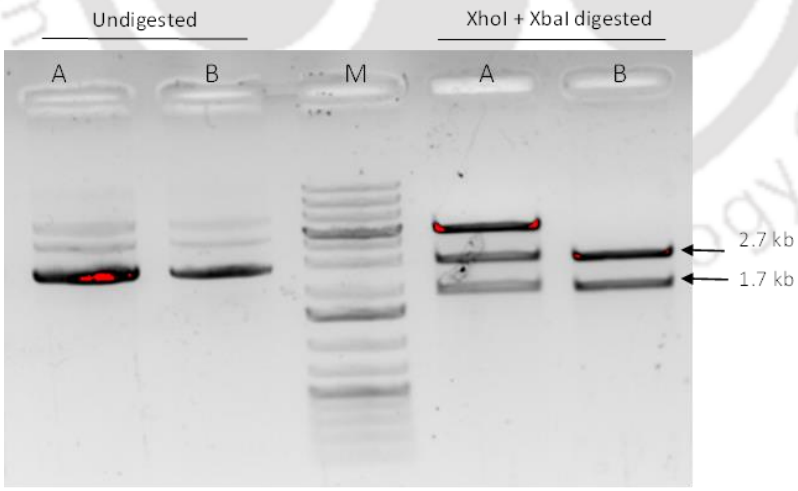

Fig. 4 Restriction Digestion based confirmation of hpRNA_L4440 recombinant clones. Analysis carried out using two enzymes i.e., XhoI and XbaI. A: hpTR-1+2_L4440 clone-I, B: hpTR-1+2_L4440 clone-II, Lane M: 100bp DNA ladder. Appearance of two bands (2.7 kb and 1.7 kb) upon double digestion confirms both sense and antisense fragments are present in L4440 vector backbone.

Appendix B

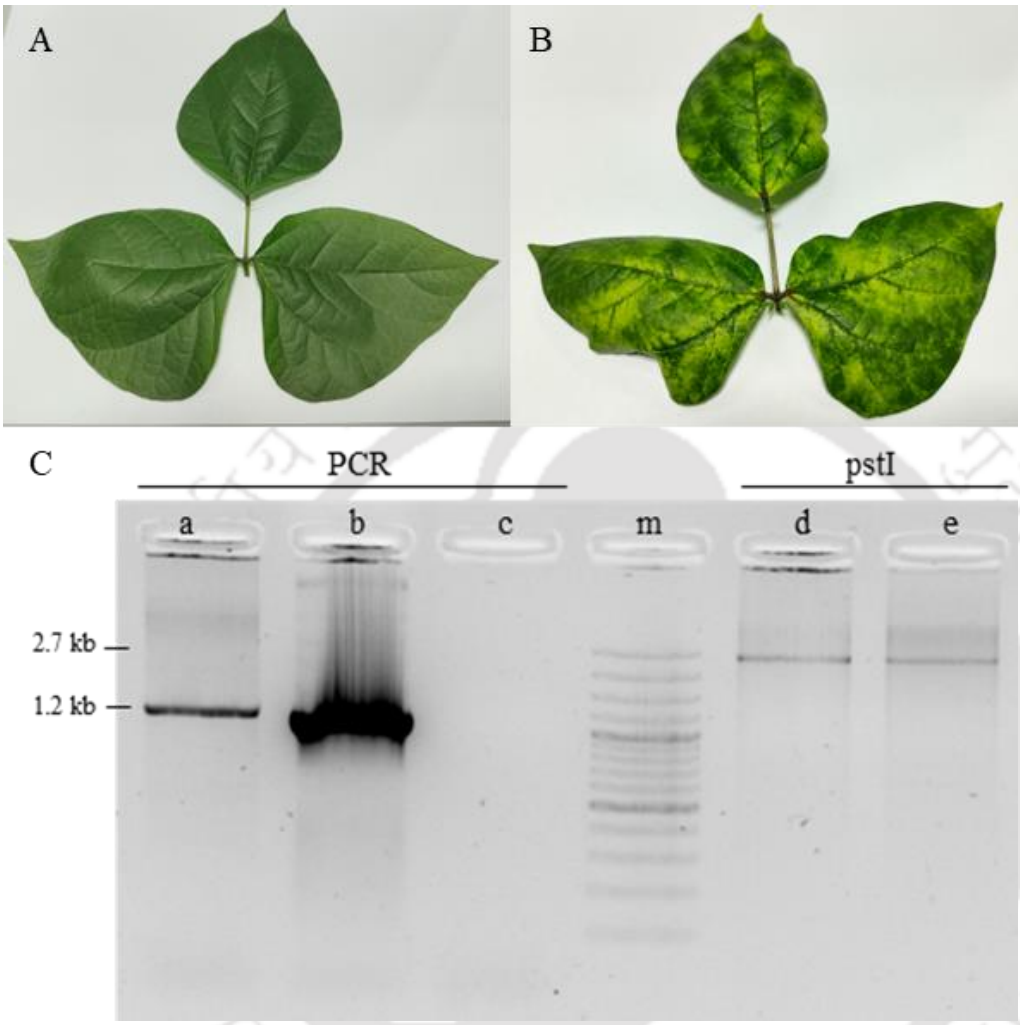

Fig. 1 Representative images of mungbean leaves and molecular analysis of MYMIV infected and uninfected leaf samples:
A. Healthy mungbean trifoliate, **B**. Symptomatic MYMIV-infected leaf, **C.** PCR analysis of infected (a), positive control (b), and uninfected (c). Restriction digestion (unique cutter, PstI) of RCA product of infected (d) and positive control (e) along with DNA ladder (m).

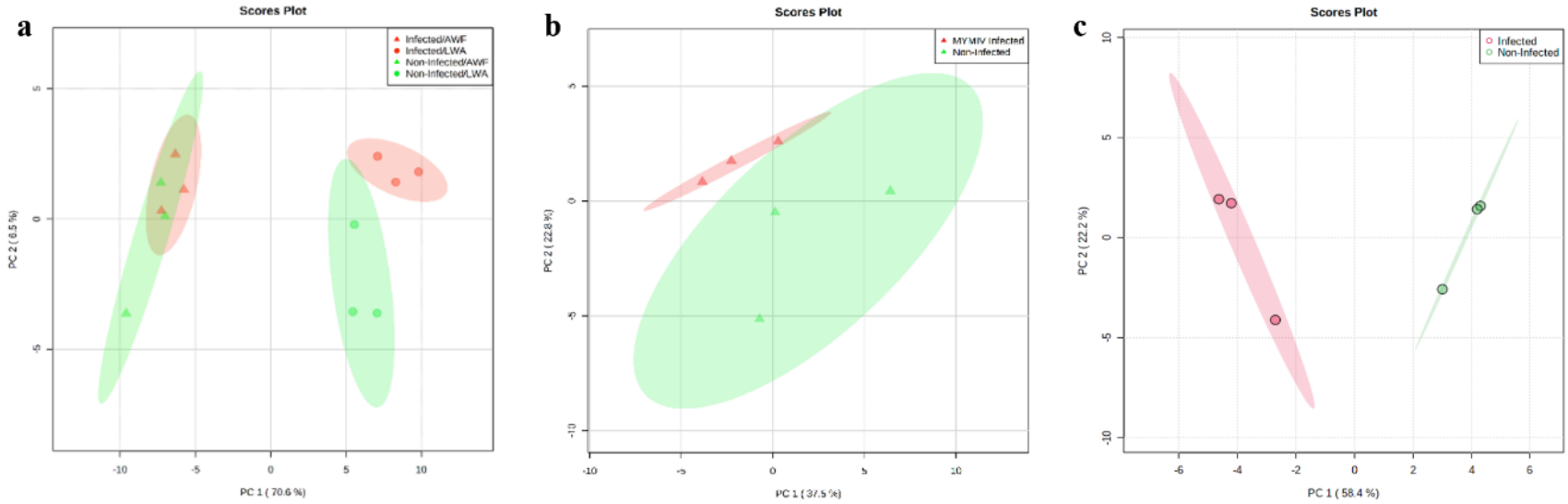

Fig. 2 PCA scores plot between MYMIV-infected and uninfected:
a) PCA score plot of apoplast and symplast fractions combined; b) PCA score plot of apoplast fractions; c) PCA score plot of symplast fractions.

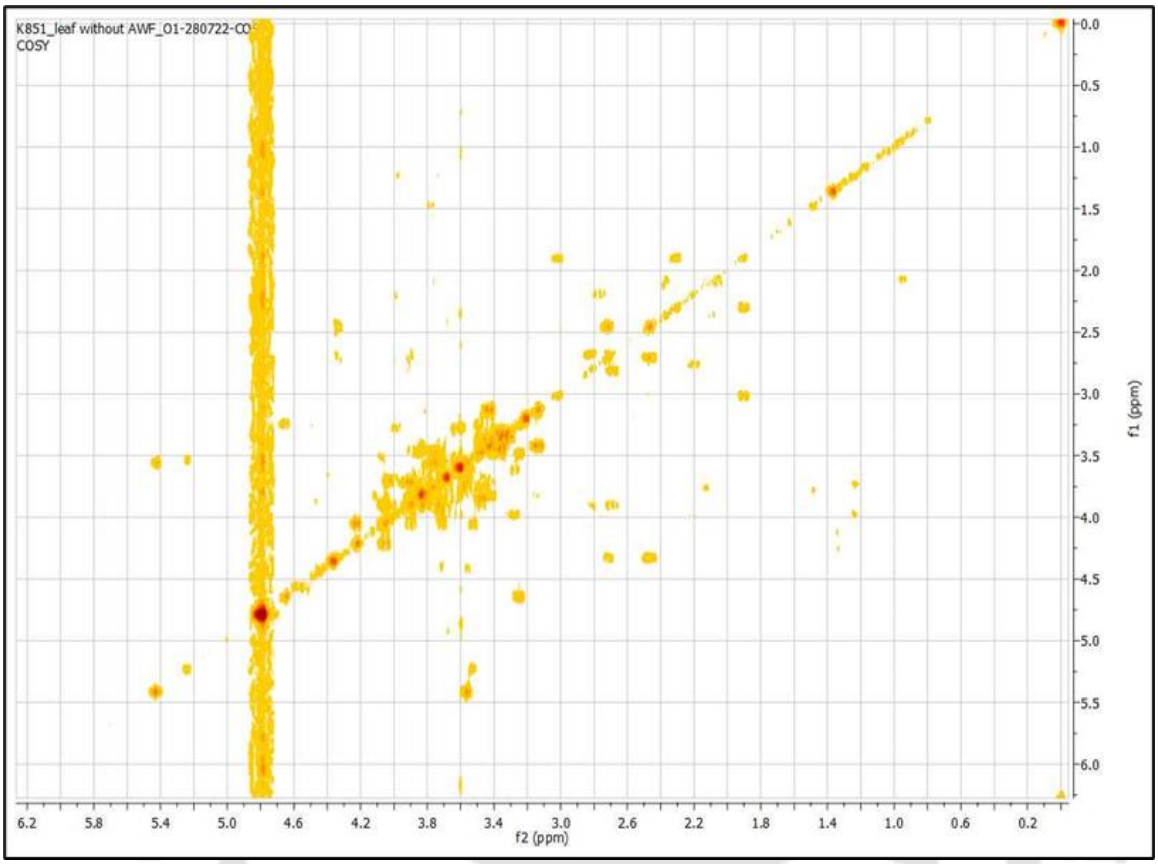

Fig. 3 1H-1H COSY spectrum of a representative aqueous extract of symplast fraction from MYMIV-infected mungbean cv. K851.

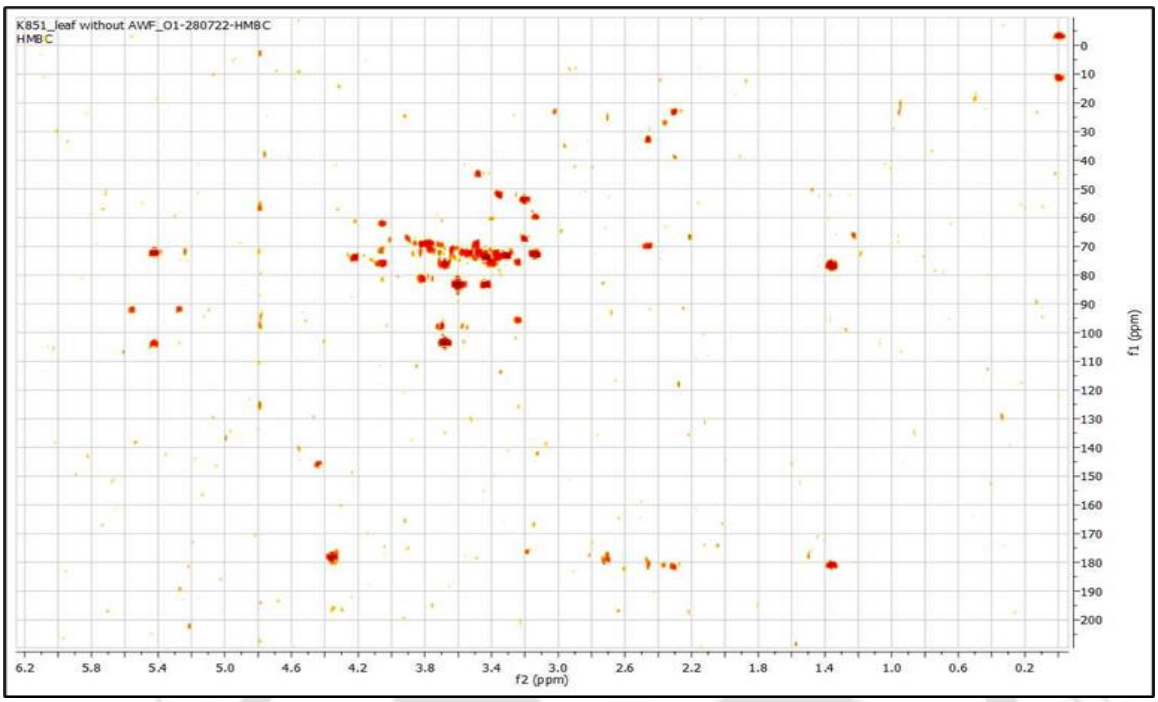

Fig. 4 1H-13C HMBC spectrum of a representative aqueous extract of symplast fraction from MYMIV-infected mungbean cv. K851.

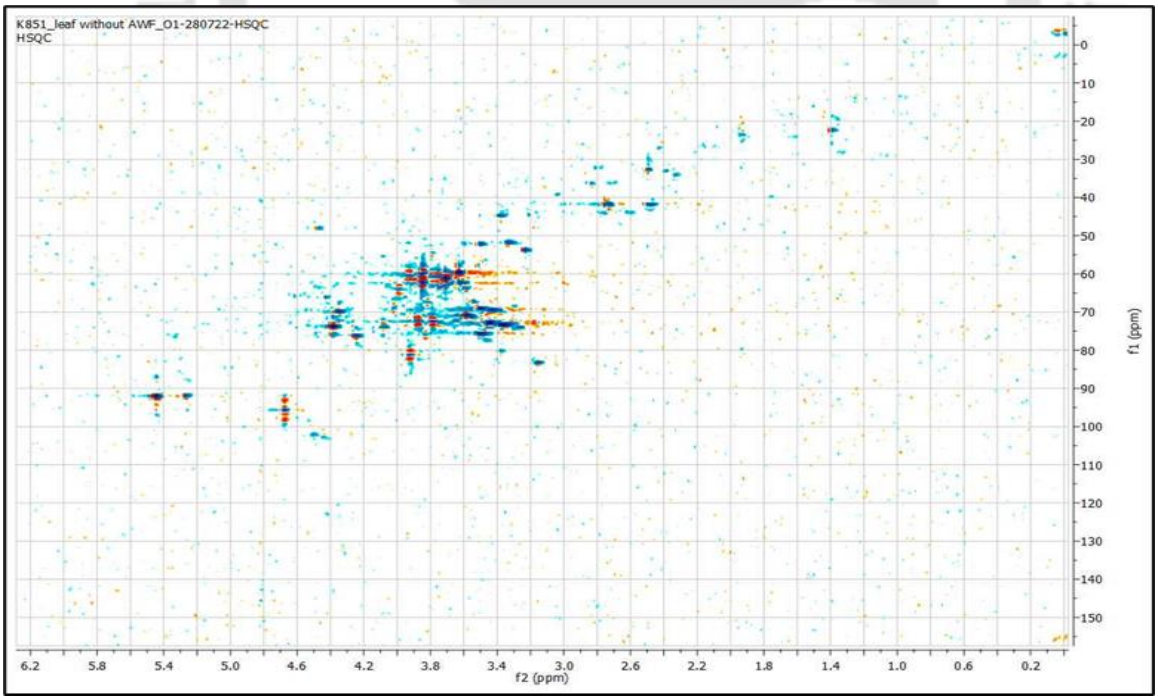

Fig. 5 1H-13C HSQC spectrum of a representative aqueous extract of symplast from MYMIV-infected mungbean cv. K851.

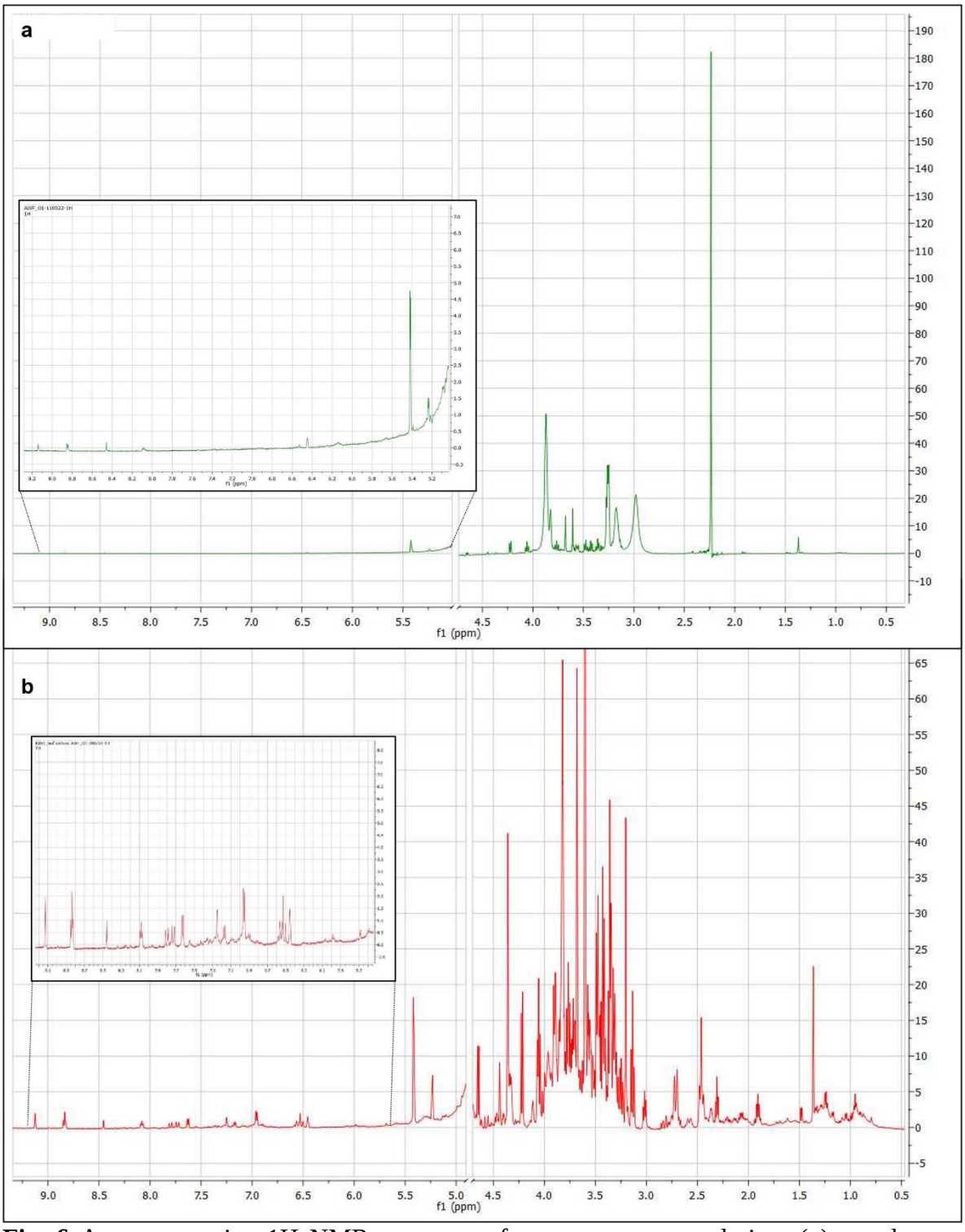

Fig. 6 A representative 1H NMR spectrum of aqueous extract solution. (**a**) apoplast and (**b**) symplast from MYMIV-infected mungbean leaf.

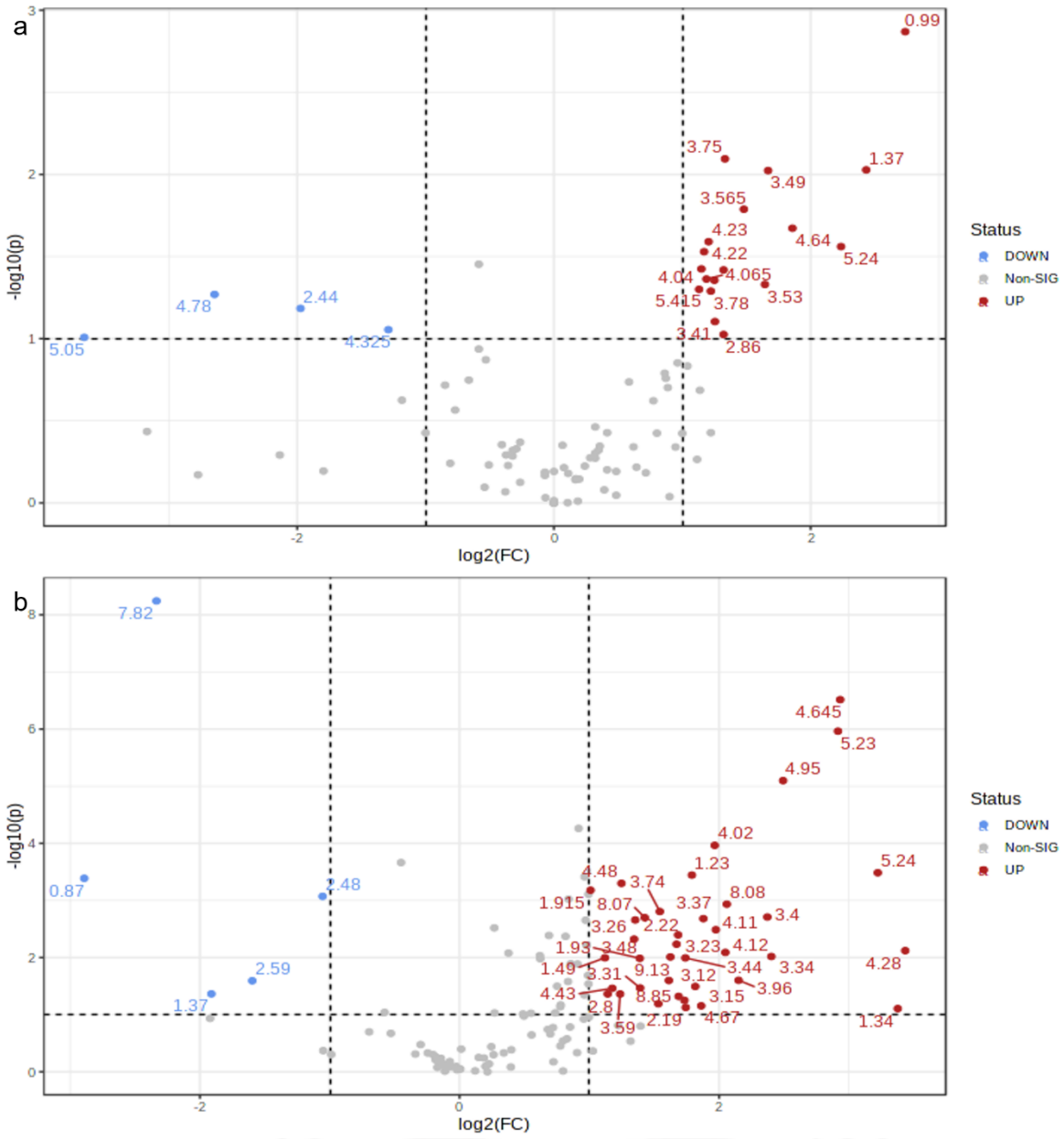

Fig. 7 Important metabolite signal identified by volcano plot which is described by both fold change threshold (x) 2 and t-test threshold (y) 0.1.

The red circles represent features above the threshold. The further its position away from the (0,0), the more significant the feature is: **a**) AWF sample group of uninfected and MYMIV-infected; **b**) LWA sample group of uninfected and MYMIV-infected.

Research Output: Conferences/Workshops

Conferences:

- **Kiran Vilas Dhobale** and L. Sahoo, "Begomovirus cell-to-cell movement via apoplast". 8th International Conference on Advanced Nanomaterials and Nanotechnology- ICANN 2023, 29 Nov-01 Dec 2023, Indian Institute of Technology Guwahati, India.
- **Kiran Vilas Dhobale** and L. Sahoo, "Identification & characterization of mungbean infecting viruses in India and quantification of viral DNA in agroinoculated host and non-host plant". North-East Research Conclave- Sustainable Science and Technology, 20-22 May 2022, Indian Institute of Technology Guwahati, India.
- **Kiran Vilas Dhobale** and L. Sahoo, "Molecular identification and characterization of mungbean infecting begomoviruses from various hotspots in India.". Assam Botany Congress (ABC-02) and International Conference on Plant Science. 3-5 December 2021, Botanical Society of Assam, Guwahati Department of Botany, Cachar College, Silchar, Assam.
- **Kiran Vilas Dhobale** and L. Sahoo, "Identification and characterization of mungbean infecting begomoviruses from various hotspots in India". International Conference on Biotechnology for Environment Health (ICBEH). 25-27 November 2021, Vellore Institute of Technology (VIT), India.
- **Kiran Vilas Dhobale** and L. Sahoo, "Molecular Identification of Mungbean infecting Begomoviruses from Various Hotspots in India". International Symposium on Advances in Plant Biotechnology and Genome Editing" APBGE-2021 & 42nd Meeting of Plant Tissue Culture Association (India). 8-10 April 2021, ICAR-Indian Institute of Agricultural Biotechnology, Ranchi, India.

Workshops:

- Secrets to Writing A Brilliant Statement of Purpose, 9th March 2022, Students Academic Board, IIT Guwahati.
- International Online STTP on "Computational Techniques Applications in Bioinformatics", 13-25 September 2021, Department of Information Technology in Collaboration with Student Chapters of IEEE Computer Society and Association for Computing Machinery, MVSR Engineering College, Hyderabad, Telangana, India.
- One Day International Virtual Conference on "Recent trends in Plant Genetics and Genomics", VIT School of Agricultural Innovations & Advanced Learning (VAIAL), India.
- Evolution and spread of SARS-Cov-2 as a part of webinar series, "Progress and Prospects in Biolog 2020" 19th July 2020, Dept. of Zoology, university of Calcutta, India.
- International Day of Light (IDL-2020), 16th May 2020, IEEE Photonics society and SPIE students' chapters, Dept. of Physics, IIT Guwahati.

Research Output: Publications

From thesis work:

- **Dhobale, K.V.** and Sahoo, L. (2024). Hairpin-RNA Spray Confers Resistance to Mungbean Yellow Mosaic India Virus in Mungbean. bioRxiv, doi: https://doi.org/10.1101/2024.03.15.585278. *(Pre-print)*.

- **Dhobale, K.V.,** Sahoo, L. (2024). Identification of mungbean yellow mosaic India virus and susceptibility-related metabolites in the apoplast of mung bean leaves. *Plant Cell Rep*., https://doi.org/10.1007/s00299-024-03247-2.

- **Dhobale, K.V.,** Murugan, B., Deb, R., Sahoo, L. (2023). Molecular Epidemiology of Begomoviruses Infecting Mungbean from Yellow Mosaic Disease Hotspot Regions of India. *Appl Biochemistry and Biotechnology*. https://doi.org/10.1007/s12010-023-04402-3. IF: 3.0.

From collaborative work:

- Banerjee, A., Chah, C. N., Dhal, M. K., Madhu, K., **Dhobale, K. V.**, Rattan, B., Katiyar, V., and Sekharan, S., (2024), Microenvironment of Landfill-Mined Soil-Like Fractions (LMSF): Evaluating the Polymer Composting Potential Using Metagenomics and Geoenvironmental Characterization. *Int J Environ Res*, https://doi.org/10.1007/s41742-024-00598-2. IF: 3.2

- Rattan, B., Banerjee, A., **Dhobale, K.V.,** Garg, A., Sahoo, L. and Sreedeep, S., (2024). Examining the soil bacterial community under the combined influence of water-absorbing polymer and plant subjected to drought stress. *Plant and Soil*, doi: https://doi.org/10.1007/s11104-024-06658-y. IF: 4.9.

- Rattan, B., **Dhobale, K.V.**, et al. (2022). Influence of inorganic and organic fertilizers on the performance of water-absorbing polymer amended soils from the perspective of sustainable water use efficiency. *Soil and Tillage Research.* doi: https://doi.org/10.1016/j.still.2022.105449. IF: 6.5.

- Kumar, S., **Dhobale, K.V.**, et al. (2021). Molecular characterization and infectivity analysis of MYMIV mungbean isolate in various genotypes of mungbean and cowpea. *Annals of Plant Sciences*. Volume 10, Issue 12 pp. 4416-4431. IF: 5.0.